

Mitigation of the risk of progressive collapse
in steel and composite building frames
under exceptional events

D2-2

FAILNOMORE

D2-2: Design and critical analysis of the worked examples

Revised, 2022

List of contributors:

Politehnica University Timisoara

Florea DINU, Ioan MARGINEAN, Dominiq JAKAB and Dan DUBINA

Feldmann + Weynand GmbH

Freddy Wertz and Klaus Weynand

ArcelorMittal Belval & Differdange S.A.

Renata OBIALA, Miguel CANDEIAS, Marion CHARLIER and Omer ANWAAR



This project has received funding from the Research Fund for Coal and Steel under grant agreement No 899371

 steelconstruct.com/eu-projects/failnomore/

 linkedin.com/company/failnomore/

 researchgate.net/project/FAILNOMORE...

Contents

1	Introduction.....	5
2	Description of the structures and actions	6
2.1	Description of the structures. Geometry and structural systems.....	7
2.2	Actions, combination of actions	8
2.3	Design requirements and output.....	9
3	Steel Structure in Seismic area	10
3.1	Description of the design and main outputs	10
3.1.1	Connections	13
3.1.2	Modal Analysis.....	15
3.2	Verifications for identified actions.....	17
3.2.1	Blast	17
3.2.2	Internal explosions.....	25
3.2.3	Seismic	30
3.3	Verifications for unidentified actions	33
3.3.1	Alternate load path method	33
3.4	Final design outputs and remarks.....	43
4	Composite Structure in Seismic area (UPT)	44
4.1	Description of the design and main outputs	44
4.1.1	Connections	47
4.2	Verifications for identified actions.....	48
4.2.1	Impact.....	48
4.3	Verifications for unidentified actions	54
4.3.1	ALPM.....	54
4.4	Final design outputs and remarks.....	57
5	Steel Structure in Non-Seismic area (F+W).....	58
5.1	Description of the design and main outputs	58
5.1.1	Design checks.....	58
5.1.2	Members.....	58
5.1.3	Connections	65
5.1.4	Remarks	66
5.2	Verifications for identified actions.....	67
5.2.1	Seismic (prescriptive approach).....	67
5.3	Verifications for unidentified actions	68
5.3.1	Prescriptive approach	68
5.3.2	ALPM: Full numerical approach	74
5.3.3	ALPM : Analytical approach	89

5.3.4	Segmentation (prescriptive approach)	100
5.4	Final design outputs and remarks.....	100
6	Composite Structure in Non-Seismic area (AM)	101
6.1	Description of the design and main outputs	101
6.1.1	Connections	103
6.2	Verifications for identified actions.....	104
6.2.1	Impact	104
6.2.2	Blast	107
6.2.3	Localised fire	112
6.3	Verifications for unidentified actions	117
6.3.1	ALPM.....	117
6.3.2	Key element	124
6.4	Final design outputs and remarks.....	127
7	Explicit modelling of accidental actions (identified threat) vs. notional column removal (unidentified threat)	128
8	Remarks and conclusions	130
8.1	Structures in non-seismic area	130
8.2	Structures in seismic area	131
8.3	Simplified vs. advanced approaches.....	131
A.1	Definition of structural blast loads	132
A.1.1	Charts to determine the blast parameters	132
A.2	Tabular tools for response estimation SDOF systems	132
A.2.1	Transformation factors for Beams and One-way Slabs	132
A.2.2	Maximum deflection and maximum response time of elasto-plastic SDOF systems	135
A.2.3	Pressure-impulse charts for deformations	137
A.3	Detailed calculation of SS/NS structure.....	138
A.3.1	Joint B1	138
A.3.2	Joint C2w	142
A.3.3	Joint D3s	146
A.3.4	Joint 3-3 (column splice):.....	150
A.3.5	Joint C2w - redesigned.....	153
A.3.6	Joint D3s – redesigned	157
A.3.7	Indirect affected columns verification - numerical approach (scenario 1)	161
A.3.8	A1s/ A2 connection verification - numerical approach (scenario 1).....	164
A.3.9	A1s/ A2 connection verification - numerical approach (scenario 1).....	170
A.3.10	Redesign column verifications – numerical model – scenario 1.....	174
A.3.11	B1/ B3 connection verification - numerical approach ()	177
A.3.12	C2w connection verification - numerical approach (scenario1)	181

A.3.13	C3w connection verification - numerical approach (scenario1)	185
A.3.14	Modified C3w connection verification - numerical approach	189
A.3.15	A1s/ A2 connection verification - numerical approach (scenario 2).....	193
A.3.16	Moment verification for connections (analytical approach)	197
A.3.16.1	Joint B1/B3.....	197
A.3.16.2	Joint C2 / C3	199
A.3.1	Moment verification for redesigned connections (analytical approach).....	201
A.3.1.1	Joint B1/B3:.....	201
A.3.1.2	Joint C2/C3:.....	203
	References	205

1 Introduction

This document represents a detailed report of the design and robustness verifications of 4 different structures which are the worked examples of the FAILNOMORE project.

The purpose of the project “Mitigation of the risk of progressive collapse in steel and composite building frames”- FAILNOMORE, is to consolidate the knowledge developed in the aforementioned research and transform it into practical recommendations and guidelines. The set of practical and user-friendly design guidelines for mitigating the risk of progressive collapse is focused on steel and composite structures subjected to exceptional events such as impact, explosions, fire, seismic, referring also to available normative documents, in order to propose a commonly agreed European design methodology. The project was funded for 24 months (starting from July 2020) by the Research Fund for Coal and Steel (RFCS) under grant agreement No 899371.

The FAILNOMORE project partners are:

- University of Liège (ULG) – Belgium
- University of Coimbra (UC) – Portugal
- Imperial College London (IC) – UK
- University of Stuttgart (USTUTT) – Germany
- University of Trento (UNITN) – Italy
- Politehnica University Timisoara (UPT) – Romania
- Czech Technical University of Prague (CVUT) – Czech Republic
- Rzeszow University of Technology (PRZ) – Poland
- Technical University of Delft (TUD) – The Netherlands
- Universitat Politècnica de Catalunya (UPC) – Spain
- INSA de Rennes (INSAR) – France
- European Convention for Constructional Steelwork (ECCS) – Europe
- Feldmann+ Weyand GmbH (F+W) – Germany
- ArcelorMittal Belval & Differdange S.A. (AM) – Luxembourg

The worked examples design and computations have been developed in Workpackage 2, *Task 2-2: Preparation of commented worked examples* (see Figure 1) and are part of dissemination materials which will be available in 10 languages (English, Portuguese, German, Italian, Romanian, Czech, Polish, Dutch, Spanish and French).

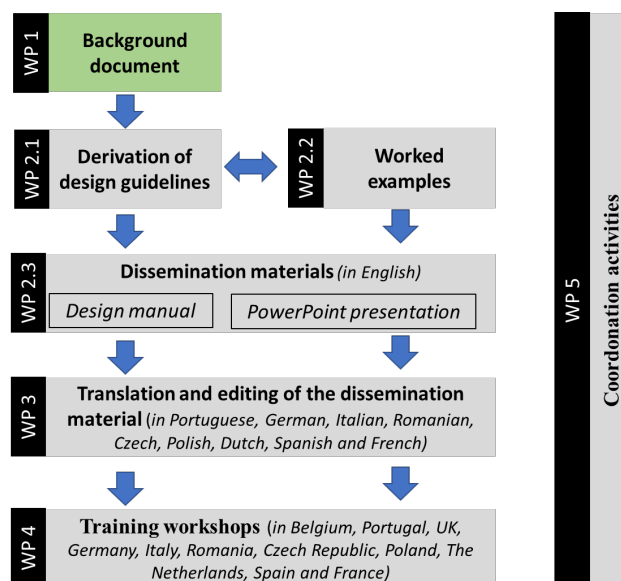


Figure 1. Research strategy adopted in the FAILNOMORE project to prepare the dissemination materials

The objective of these worked examples is to develop case studies acting as examples of good practice. The four worked examples were predesigned starting from commonly agreed building geometry and design assumptions. The types of structures and approaches for checking the robustness of the structures is presented in the next section.

2 Description of the structures and actions

The four structural configurations selected for the present study are presented in Table 1. Two structures are initially designed for the persistent design situation (non-seismic region) and two for persistent and seismic design situations (seismic region) using the present drafts of the Eurocodes.

Table 1. Types of structures

Reference name	Type of structure
SS/S	Steel Structure in Seismic area
CS/S	Composite Structure in Seismic area
SS/NS	Steel Structure in Non-Seismic area
CS/NS*	Composite Structure in Non-Seismic area
* The structure has two variations – one with steel columns and one with composite columns. In both cases the floor beams and slabs are designed as composite.	

The design and computations for the SS/S and CS/S structures are performed by the Politehnica University Timisoara (UPT), while for SS/NS structure by the Feldmann+ Weynand GmbH (F+W), and respectively the CS/NS by ArcelorMittal Belval & Differdange S.A. (AM).

The response of structures under accidental loading is assessed using two main approaches. First category includes verifications with different levels of sophistication against five accidental actions (Table 2). The verifications require the evaluation of the threat first, so they are called threat dependent methods. These methods corresponds to a certain threat level, so they may not cover the exposure against higher threat intensities or other unspecified threats. Second category includes verifications against unidentified actions, which do not require the characterization of the threat, so the methods are threat independent (Table 3). This category contains more general approaches and can be more appropriate in providing the structural robustness, especially when the threats and exposure are hard to define. In the following, the application of these methods is detailed. Where appropriate, the result of the analysis may indicate a redesign of the structure or the application of a more sophisticated approach. The selection of the scenarios for accidental action verifications was made considering the following:

- Each scenario is applied at least one time to verify one of the structures
- Where relevant, the same scenario is applied for more than one structure, to allow direct comparisons between the results

Table 2 and Table 3 also present the numbers for the worked examples as they appear in *D2-3: Technically complete draft of the design manual in English*.

For ease of use, the initial design and the verification for accidental actions is done structure by structure, considering each structure as an independent worked example (W.E.). Comments and comparisons between accidental scenarios and implications in design are done at the end of each example. A special section is also included to provide comments and remarks in regard of the role of initial design (seismic vs. non-seismic, steel vs composite) and the impact of different accidental actions on the structural robustness.

Table 2. Types of approaches for identified actions and their application.

	Identified actions									
	Impact			External explosion		Internal explosion		Localised fire	Seismic	
Structure	Equivalent static approach	Simplified dynamic approach	Full dynamic approach	Equivalent SDOF approach	Full dynamic approach	Equivalent static approach	Dynamic approach (TNT equiv. method)	Localised fire models	Prescriptive method	Advanced numerical analysis (multi-hazard)
SS/S				I.2.2/ SS/S	I.2.3/ SS/S	I.3.1/ SS/S	I.3.2/ SS/S			I.5.2/ SS/S
CS/S	I.1.1/ CS/S	I.1.2/ CS/S	I.1.3/ CS/S							
SS/NS									I.5.1/ SS/NS	
CS/NS	I.1.4/ CS/NS			I.2.1/ CS/NS				I.4.1/ CS/NS		

Table 3. Types of approaches for unidentified actions and their application

	Unidentified actions					
	Alternate load path method (ALPM)				Key element	Segmentation
Structure	Prescriptive approach (Tying method)	Analytical approach	Simplified prediction of dynamic response	Full numerical approach	Normative approach	Weak segment borders / Strong segment borders
SS/S	II.1.1/ SS/S		II.4.2/ SS/S	II.4.3/ SS/S		
CS/S	II.1.2/ CS/S			II.4.4/ CS/S		
SS/NS	II.1.3/ SS/NS	II.4.1/ SS/NS		II.4.5/ SS/NS		II.3.1/ SS/NS
CS/NS	II.1.4/ CS/NS			II.4.6/ CS/NS	II.2.1/ CS/NS	

2.1 Description of the structures. Geometry and structural systems

The geometry of the structures is shown in Figure 2 and consist of:

- Non-Seismic area:
 - 6 storeys of 4.0 m height each
 - 6 bays of 8.0 m in the Y direction
 - 3 bays of 12.0 m in the X direction
- Seismic area:
 - 6 storeys of 4.0 m height each
 - 6 bays of 8.0 m in the longitudinal direction
 - 3 bays of 12.0 m in the transversal direction - internal
 - 6 bays of 6.0 m in the transversal direction - perimeter

The main structural system is made of:

- Non-Seismic area (Figure 2a):
 - An internal V-braced core to resist lateral loads from wind
 - Main beams and secondary beams to resist gravity loads

- Seismic area (Figure 2b):
 - A dual system made of an internal V-braced core and perimeter moment resisting frames to resist lateral loads from wind and earthquakes
 - Main beams and secondary beams to resist gravity loads

More details about the structural systems are given in the next sections.

The initial design used S355 steel and C30/37 concrete. Additionally, in case of the structures in seismic areas, S460 steel grade was used for the non-dissipative beams in the braced frame. H and circular hollow sections were used for steel elements. The joints were designed according to the EN 1993-1-8 provisions, with additional requirements for seismic resistant systems in terms of minimum capacity (see EN 1998-2). More details about the structural systems are given in the next sections.

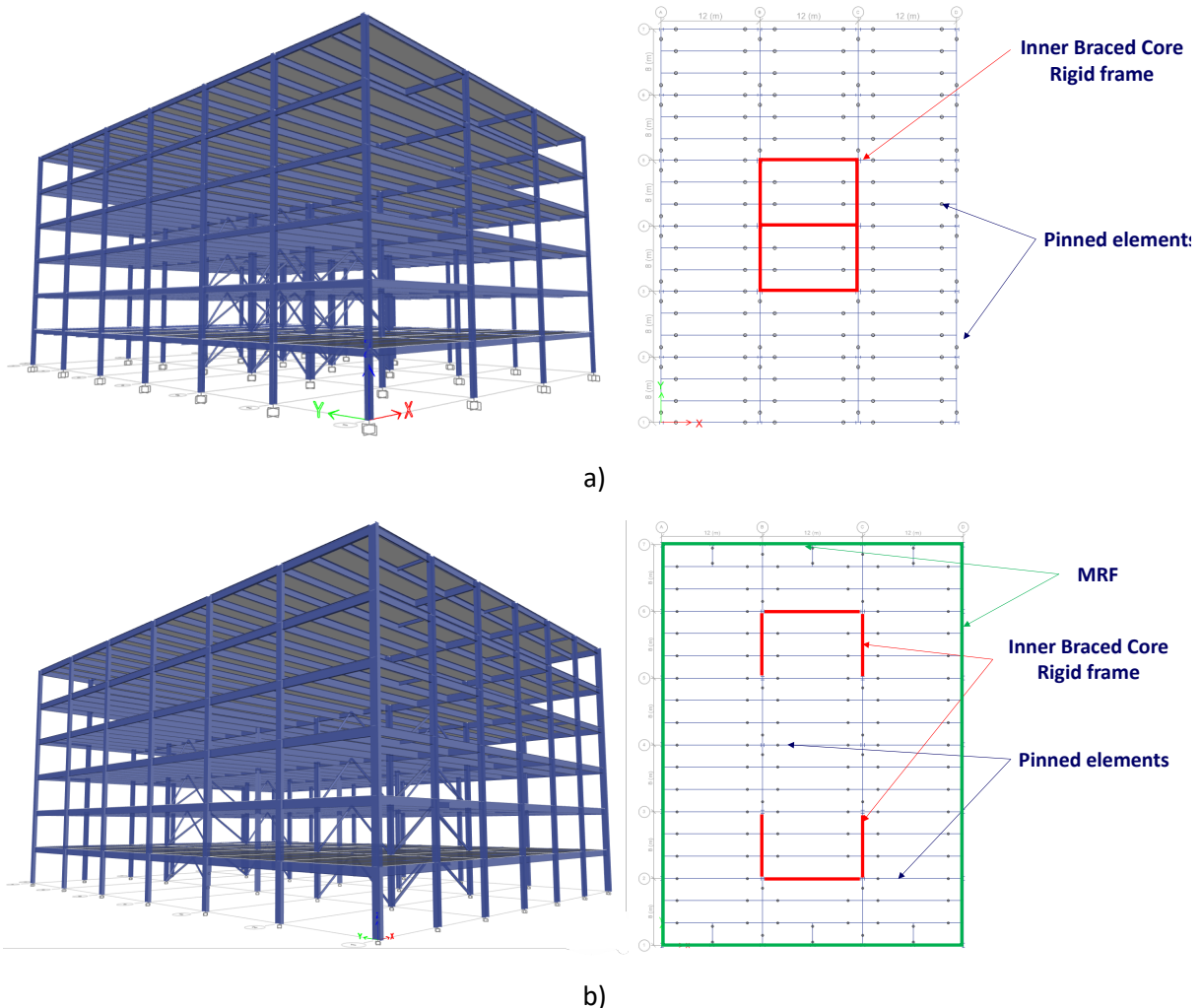


Figure 2. Presentation of the structural systems: a) non-seismic structures; b) seismic structures

2.2 Actions, combination of actions

The actions that were used in the design of each structural typology are presented in Table 11. Combination of actions for Ultimate limit state ULS and Serviceability limit state SLS were done using EN 1990 “Eurocode: Basis of Structural Design”. Additionally, Damage limitation limit state DL, according to EN 1998 “Design of structures for earthquake resistance”, was considered for SS/S and CS/S cases.

Table 4. Evaluation of actions

Loads	Structures		
	UPT (SS/S + CS/S)	AMBD (CS/NS)	F+W (SS/NS)
	Location		
	Timiș, RO	Luxembourg	Aachen, DE
Dead load	- Floors: $g_k = 5 \text{ kN/m}^2$ - Façade (supported by the perimeter beams): $g_k = 4 \text{ kN/m}$		
Live load	- Live load for office buildings: $q_k = 3 \text{ kN/m}^2$ - construction load $q_k = 1 \text{ kN/m}^2$ (general floors and roof).		
WIND			
Wind speed	$v_{b,0} = 25 \text{ m/s}$	$v_{b,0} = 24 \text{ m/s}$	$v_{b,0} = 25 \text{ m/s}$
Equiv. wind pressure	$q_b = 0.4 \text{ kN/m}^2$	$q_b = 0.36 \text{ kN/m}^2$	$q_b = 0.9 \text{ kN/m}^2$ *
Terrain category	III	III	"Binnenland"*
Snow load	$s_k = 1.5 \text{ kN/m}^2$	$s_k = 0.5 \text{ kN/m}^2$	$s_k = 0.85 \text{ kN/m}^2$ **
Seismic load			
Elastic response spectrum	Type 1		
Ground type	B		
Design ground acceleration, a_g	0.25 g		
Behavior factor, q	q = 4.8 (dual frame CBF+MRF)		
* Simplified wind pressure acc. to DIN EN 1991-1-4/NA Tab. NA.B.3 as commonly used in Germany. This replaces the concept of terrain category. "Binnenland" can be translated with "inland region" or "interior region" and is used to be distinguished from island and coastal regions.			
** Snow zone 2 acc. to DIN EN 1991-1-3/NA			

2.3 Design requirements and output

The structural analysis was done using 3D models and linear elastic procedure. Additionally, for seismic resistant systems SS/S and CS/S the seismic response and plastic mechanism was checked by means of non-linear static analysis procedure (push-over analysis), using N2 method. The local and global checks include the following verifications:

- ULS verifications: results are presented using utilization ratios (UF).
- SLS verifications, which were based on the following admissibility criteria:
 1. Allowable deflection for secondary beams: $L/250$
 2. Allowable deflection for main beams: $L/350$
 3. Top displacement under wind: $H/500$.

Additionally, for the seismic resistant structure the following verifications were performed:

1. Damage limitation requirement: Interstorey drift limit at 0.75% H_{st} , where H_{st} is the story height (buildings with ductile non-structural elements);
2. Second order effects: $\theta \leq 0.2$;
3. Verification of dissipative members and connections in CBF and MRF;
4. Verification of non-dissipative members and connections in CBF and MRF.

3 Steel Structure in Seismic area

3.1 Description of the design and main outputs

The output of the design for SS/S is presented in Table 5 to Table 7.

The cross sections for the different categories of beams and UF for strength (including buckling resistance where appropriate) and stiffness are presented in Table 5.

Table 6 presents the cross sections for the different categories of columns and the utilization ratios for strength (including buckling resistance). The UF for columns of the Lateral Load Resisting System LLRS refer to maximum demand between combinations with wind or seismic action. To note that columns are designed for seismic loads corresponding to non-dissipative elements (amplified seismic action—see chapter 6.6.3 from EC8).

The SLS verification for the wind action is presented in Table 9. The ratio between the lateral top displacement and the acceptable limit has a maximum value of approximately 0.1.

Regarding the specific verifications for the structures in seismic zone, Table 10 presents the interstorey drift check at Damage limitation state. As it may be observed, the structure successfully fulfils the limitation to 0.75%, having the largest value of 0.24%. The structure has also been checked at ULS in terms of interstorey drift limitation. Similarly to Damage limitation state, an interstorey drift verification was done according to the relation 3-1, presented below.

$$d_r^{ULS} = c \cdot q \cdot d_{re} \leq d_{r,a}^{ULS} \quad 3-1$$

where:

- c is the amplification factor (considered 1 since $T_1 \geq T_C$)
- q – behaviour factor
- d_{re} – relative displacement obtained from static calculation.

The acceptable limit for this verification is 2.5% H_{st} . As presented in Table 11, all values are below this limit, the largest being 0.49%.

In addition, the results for the verification of the second-order effects are provided in Table 46. As it may be observed, the largest value for θ is 0.096. Consequently, as it is mentioned in EC8, the effect of the second order effects may be neglected, having a value smaller than 0.1.

The seismic loading for the design of the non-dissipative elements takes in account the utilization factor of the braces. Consequently, having an UF of 0.462 for the most stressed brace, an overstrength factor of $1/0.462 = 2.16$ was obtained. Considering also the strain hardening effect by 1.1 and 1.25 factors, the total overstrength factor considered for the design of the non-dissipative elements was $\Omega_T = 3.0$.

Finally, the contribution of the perimeter MRF was checked. In (RFCS 2017), is mentioned that the duality should be checked by verifying that the MRFs should be able to resist at least 25% from the seismic force. Considering the equilibrium of a simple frame and the plastic hinges form at the ends of the beam, the capacity of a MRF is twice the plastic capacity of the beam divided by the story height. The necessary flexural resistance of the beam may be determined using 3-2 which is presented below.

$$M_{pl,b} = \frac{F_y^{MRF}}{2} \cdot \frac{H}{n} \quad 3-2$$

where:

- F_y^{MRF} - capacity of the frame
- H -storey height
- n – number of beams.

For the verification, in the above formula the capacity of the frame is replaced with 0.25 from the story seismic force and n with 12 since there are 6 beams per frame and 2 frames per direction. As presented in, Table 13 in both directions the necessary flexural capacity is smaller than the efficient one, hence the duality condition is checked.

Table 5. Utilization factors for beams – SS/S

Case	Element	Direction ¹	Storey	Section	Utilization factor	
					Strength	Deflection ²
SS/S	Perimeter beams	X	1-6	IPE550	0.278	0.023
		Y	1-6	IPE600	0.302	0.153
	Interior beams	X	1-6	IPE550	0.546	0.85
		Y	1-6	IPE550	0.909	0.928
	⁴ Inner core beams	X	1-3	³ H800	0.936	-
			4-5	HEM800	0.953	-
			6	HEM700	0.789	-
		Y	1-3	HEM500	0.859	-
			4-6	HEB500	0.878	-

¹See Figure 2 for the orientation of the axes
²Deflection verification criterion: L/250 for secondary beams, L/350 for main beams
³H800 is a built-up section, having the same height as regular HEM800, with b = 380mm, t_f = 50 mm, and t_w = 30 mm.
⁴S460 steel grade used for the inner core beams.

Table 6. Sections and utilization factors for columns – SS/S

Case	Element	Section	Utilization factor
SS/S	Corner columns	HE550B	0.49
	Perimeter columns	HE500B	0.71
	Inner Core columns	HD400X463	0.95

Table 7. Sections and utilization factors for braces – SS/S

Case	Element	Direction	Storey	Section	Utilization factor
SS/S	Brace	Y	1-3	HEA320	0.41
			4	HEA260	0.43
			5	HEA220	0.46
			6	HEA200	0.39
		X	1-3	HEB340	0.41
			4-5	HEA320	0.27
			6	HEA260	0.26

It may be observed that, for SS/S case, the condition for homogeneity (25% maximum difference between UF elements on elevation) was fulfilled for most elements. The difference between the most stressed and least stressed braced is 16% in case of Y direction. However, on X direction on the last two stories the condition was not fulfilled due to the requirement of using Class 1 section for high ductility class.

Table 8 presents the slenderness verification requirement according to the seismic design. It may be observed that all the braces fulfilled the condition, the maximum value 0.76 is lower than the admissible limit of 2.0.

Table 8. Slenderness check – SS/S

Case	Direction	Storey	Section	A [mm ²]	f _y [MPa]	I [mm ⁴]	L _{cr} [mm]	N _{cr} [kN]	λ [-]
SS/S	X	6	HEA260	8680	275	36680000	3605500	5848.1	0.638877
		5-4	HEA320	12400	275	36950000	3605500	5891.2	0.76081
		1-3	HEB340	17090	275	96900000	3605500	15449.4	0.551546
	Y	6	HEA200	2570	275	13360000	2828500	3461.1	0.653809
		5	HEA220	3030	275	19950000	2828500	5168.3	0.584921
		4	HEA260	3310	275	36680000	2828500	9502.5	0.501197
		1-3	HEA320	3710	275	69850000	2828500	18095.6	0.434101

Table 9. SLS check for LLRS against wind action – SS/S

Case	Direction	Top displacement [mm]
SS/S	X	4.62
	Y	3.2

Table 10. Interstorey drifts SS/S – DL

Case	Storey	Direction	Drift [%]
SS/S	6	X	0.171
	5		0.209
	4		0.244
	3		0.222
	2		0.224
	1		0.183
	6	Y	0.190
	5		0.241
	4		0.238
	3		0.203
	2		0.193
	1		0.148

Table 11. Interstorey drifts for SS/S - ULS

Case	Storey	Direction	Drift [%]
SS/S	6	X	0.343
	5		0.419
	4		0.486
	3		0.440
	2		0.445
	1		0.364
	6	Y	0.380
	5		0.482
	4		0.476
	3		0.406
	2		0.385
	1		0.297

Table 12. Second order effects – SS/S

Case	Storey	h	P _x	V _x	d _x	θ _x	Case	Storey	h	P _y	V _y	d _y	θ _y
		[mm]	[kN]	[kN]	[mm]	[rad]			[mm]	[kN]	[kN]	[mm]	[rad]
SS/S	6	4000	10867	1753	60.77	0.094	SS/S	6	4000	10867	1881	59.12	0.085
	5	4000	21734	2983	52.77	0.096		5	4000	21734	3176	50.10	0.086
	4	4000	32602	3912	42.80	0.089		4	4000	32602	4094	38.57	0.077
	3	4000	43469	4628	31.02	0.073		3	4000	43469	4810	27.01	0.061
	2	4000	54336	5193	20.18	0.053		2	4000	54336	5376	17.01	0.043
	1	4000	65203	5524	9.09	0.027		1	4000	65203	5707	7.42	0.021

Table 13. Contribution of the MRF frames for the LLRS – SS/S

Case	Story label	Direction	V _i [kN]	0.25 V _i [kN]	n	M _{Rd,nec} [kNm]	W _{nec} [mm ³]	Section	W _{eff} [mm ³]	M _{Rd,eff} [kNm]
SS/S	6	x	1752.5	438.1	12	73.0	205695.6	IPE550	2787000	989.4
	5		2983.3	745.8	12	124.3	350149.8	IPE550	2787000	989.4
	4		3911.9	978.0	12	163.0	459139.5	IPE550	2787000	989.4
	3		4628.3	1157.1	12	192.8	543229.7	IPE550	2787000	989.4
	2		5192.7	1298.2	12	216.4	609469.1	IPE550	2787000	989.4
	1		5523.6	1380.9	12	230.2	648313.6	IPE550	2787000	989.4
	6	x	1881.3	470.3	12	78.4	220813.2	IPE600	35112000	12464.8
	5		3176.0	794.0	12	132.3	372765.1	IPE600	35112000	12464.8
	4		4094.4	1023.6	12	170.6	480560.5	IPE600	35112000	12464.8
	3		4810.2	1202.5	12	200.4	564574.4	IPE600	35112000	12464.8
	2		5376.1	1344.0	12	224.0	630999.7	IPE600	35112000	12464.8
	1		5707.5	1426.9	12	237.8	669894.1	IPE600	35112000	12464.8

3.1.1 Connections

The typology of connections which are of interest for the worked example are the following:

- Beam-to-column connections for MRFs (of LLRS)
- Beam-to-beam and beam-to-column connections for gravitational load resisting system

In case of the beam-to-column connections for MRFs, prequalified seismic moment resisting connections were adopted (see EqualJoints project). From the four typologies investigated and prequalified, the extended end-plate connection was preferred. The summary of the results for the moment resisting connections may be found in Table 14. The connections were designed as equal strength connections, as it may be inferred from the ratio between the connection flexural resistance and the flexural capacity of the beam having an approximate value of 1.

Table 14. Results of moment resisting connections at ULS – SS/S

Position	Connection type	Moment resistance (kNm)	Shear resistance (kN)	Failure mode in flexure	UF*	$\frac{M_{Rd}}{M_{pl,b}}$
A/1, A/7 IPE600-HEB550	Extended end plate	1173	1516	End plate in bending	0.29	0.94
A/1, A/7, A/2-6 IPE600-HEB500	Extended end plate	1169	1387	End plate in bending	0.26	0.94
1/A - 1/D IPE550-HEB500	Extended end plate	957	1409	End plate in bending	0.15	0.97

Note:
* Utilisation factor is defined for ULS, persistent design situation, only

Figure 3 presents the view of a moment resisting connection (joint connecting the corner column HEB550 with the beam IPE600 in frames A/1, A/7).

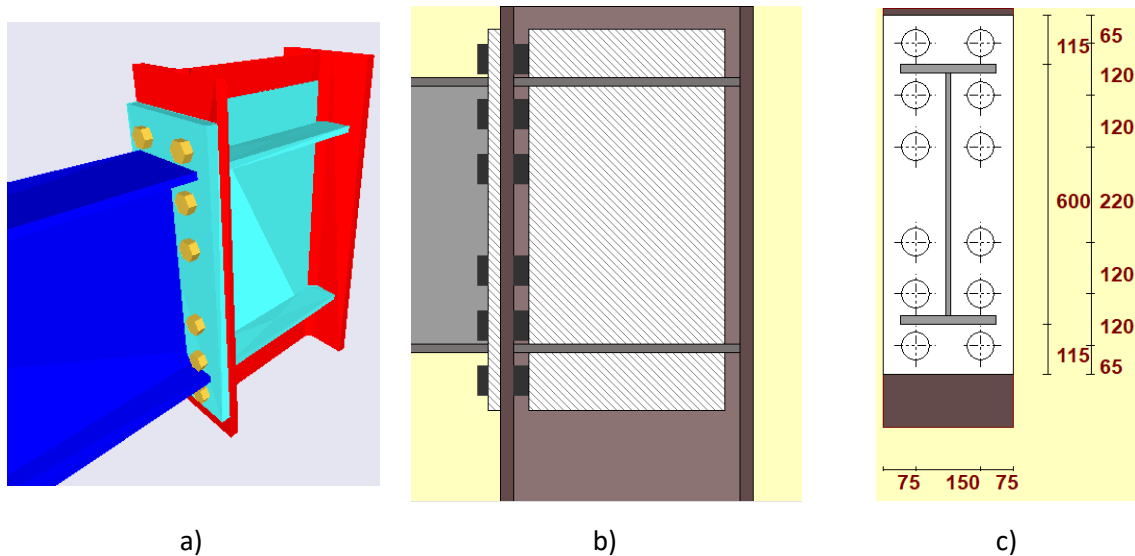


Figure 3 Configuration of a moment resisting joint – frames A/1, A/7 – SS/S: a) 3D view of the joint, b) side view of the joint, c) front view of the joint

The properties of the elements (plates and bolts) used for the connection are detailed in Table 15.

Table 15 Properties of the elements of a moment resisting connection – SS/S

Element	Height [mm]	Width [mm]	Thickness [mm]	Material
End plate	830	300	28	S355
Stiffener (continuity plates)	492	104	20	S355
Supplementary web plate	830	462	10	S355

M36 Gr. 10.9 bolts were used to connect the elements of the joint. The welds used are full penetration welds according to the recommendations given in the pre-normative design recommendations (see EqualJointsPlus project).

For the other elements (beam-to-beam as well as beam-to-column except the MRFs and the braced core) pinned connections were used. As typology, pinned connection with cleats were used for SS/S. The summary of the results for the pinned connections is presented in Table 16. The configuration is the same between the joints, only the connecting elements differ.

Table 16. Results of pinned connections at ULS - SS/S

Case	Position	Story	Connection type	Shear resistance (kN)	Failure mode	UF*
SS/S	A/1-7, D/1-7 IPE550-IPE600	1-6	Cleat angle	196	Sec. beam bolts in shear	0.72
	B/1-7, C/1-7 IPE550-IPE550	1-6	Cleat angle	196	Sec. beam bolts in shear	0.72
	B/2, B/5, C/2, C/5 - IPE550-HEM500	1-3	Cleat angle	196	Sec. beam at notch	0.67
	B/2, B/5, C/2, C/5 IPE550-HEB500	4-6	Cleat angle	196	Sec. beam bolts in shear	0.65

Note:
* Utilisation factor is defined for ULS, persistent design situation, only

Figure 4 presents the view of a pinned connections (joint connecting a secondary beam IPE550 with a main beam IPE550 between frames B/1-7 and C/1-7).

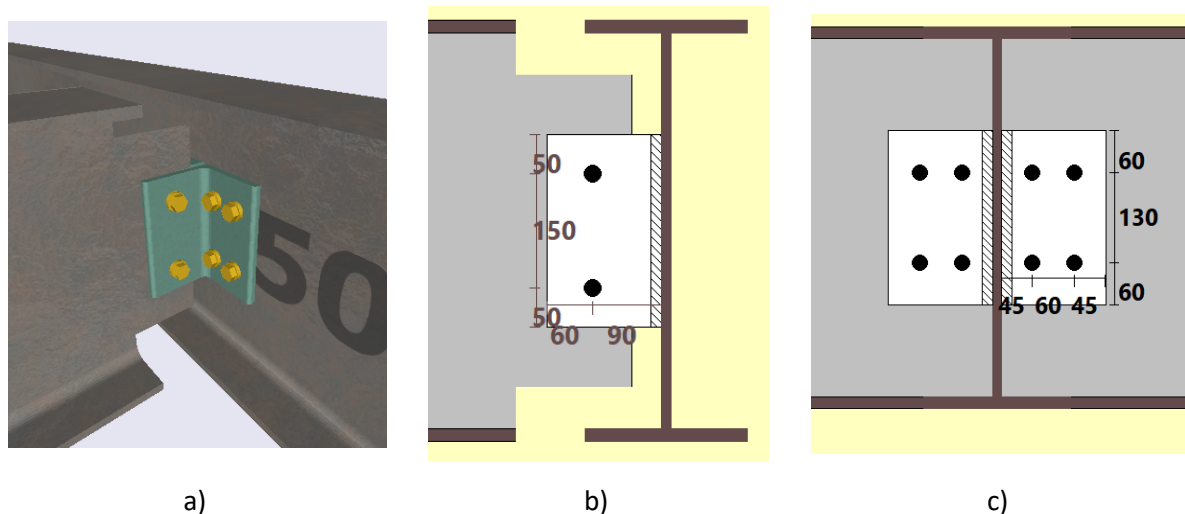


Figure 4 Configuration of pinned joint – frames B/1-7, C/1-7 – SS/S: a) 3D view of the joint, b) side view of the joint, c) front view of the joint

For the connection L150x15 cleats from S355 steel grade have been used. 2 M20 Gr. 10.9 were used for the secondary beam and 8 M20 Gr. 10.9 for the main beam.

3.1.2 Modal Analysis

The structural configurations were mainly designed to cover both seismic and non-seismic areas but keeping similar main structural features to allow for some direct comparisons in the design against accidental actions. Thus, same spans, bays, and storey heights were adopted. However, some adjustments were necessary for seismic resistant structures, i.e.,:

- The position of the braced spans close to the centre of rigidity (Figure 2a) makes the structure sensitive to torsional effects (Figure 5a). For seismic design, this is a feature to avoid, as it may cause collapse or heavy damages during earthquakes. As a result, the braced spans were moved to the exterior (Figure 2b) and additionally, MRFs were added on the perimeter on all sides. This resulted in a better response with first two translational modal shapes (Figure 5b).
- A dual steel frame seismic resistant system requires a minimum of 25% contribution from the MRFs to the total capacity (see EN 1998-2). To fulfil this requirement, the cross-sections of the beams and columns in the MRFs needed to be increased, and additionally, intermediate columns were introduced on the short sides (X) of the perimeter. The spans remained unchanged at the interior.

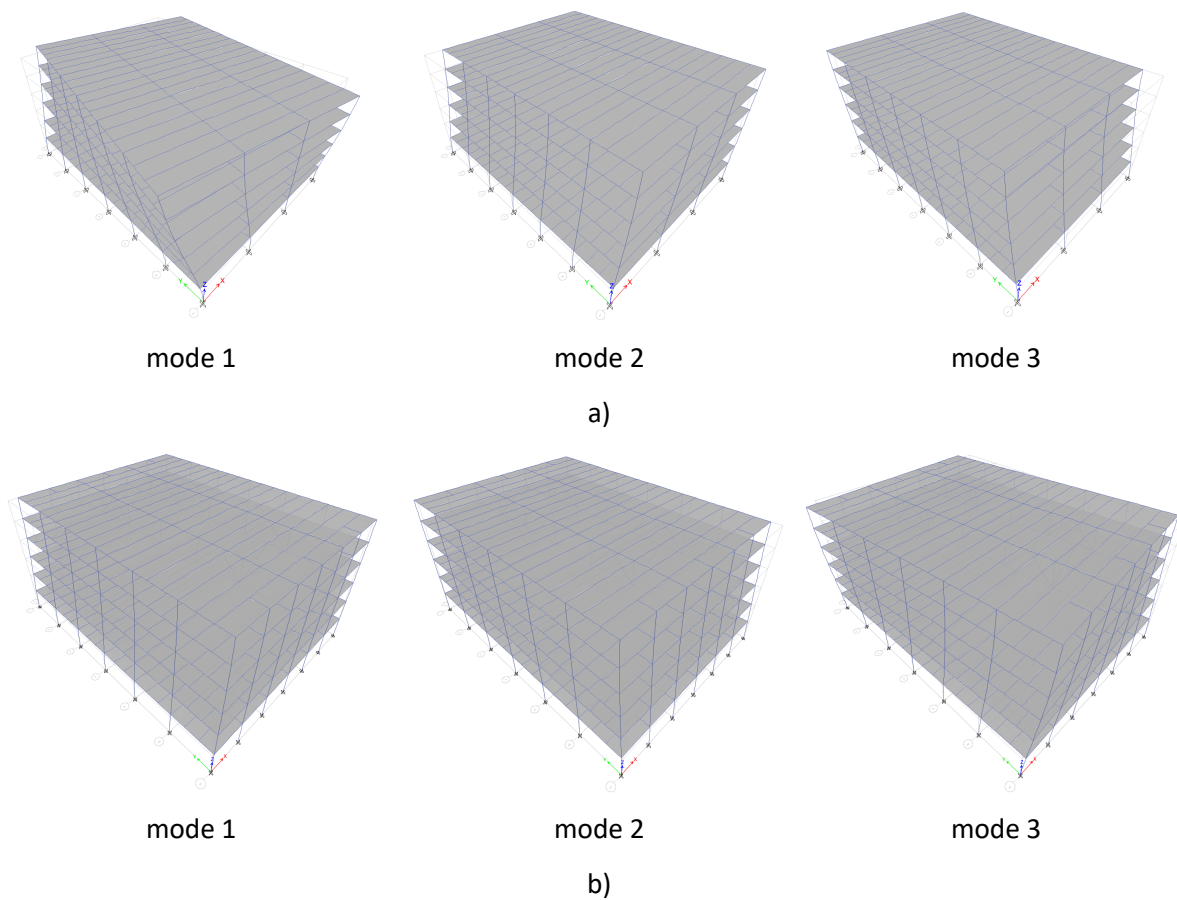


Figure 5. Modal shapes of the seismic resistant systems: a) initial, with a 1st torsional mode; b) after reconfiguration, with mode 1 and 2 translational

The condition that the effective modal mass should sum up to at least 90% of the total effective mass is fulfilled and the values are provided in Table 17 for the SS/S structure. The first mode is translation on X direction, the second is translation on Y direction, and in the third is torsion about Z axis, as presented in Figure 5b. The behaviour of CS/S structure (modal shapes) is very similar and the results are not presented.

Table 17. Modal parameters for SS/S structure

Case	Mode	Period [s]	SumUX	SumUY	SumRZ
Modal	1	0.769	0.7972	0	0
Modal	2	0.729	0.7972	0.7672	0
Modal	3	0.709	0.7972	0.7672	0.8153
Modal	4	0.271	0.9343	0.7672	0.8153
Modal	5	0.256	0.9343	0.9289	0.8153
Modal	6	0.25	0.9343	0.9289	0.9356
Modal	7	0.159	0.9692	0.9289	0.9356
Modal	8	0.147	0.9692	0.9289	0.9701
Modal	9	0.145	0.9692	0.9675	0.9701
Modal	10	0.113	0.9888	0.9675	0.9701
Modal	11	0.105	0.9888	0.9862	0.9701
Modal	12	0.105	0.9888	0.9862	0.9891

3.2 Verifications for identified actions

No example has been considered for impact action for SS/S case according to Table 2. See section 4.2.1 for examples on the structure with composite beams.

3.2.1 Blast

3.2.1.1 Equivalent SDOF approach

This example gives information about the design against blast action due to accidental external explosion using the equivalent single-degree-of-freedom approach. The method evaluates the out-of-plane deflection demand of an element (in this case a column) and compares it with a flexural capacity to assess the damage. The method characterises the blast load by means of a pressure which is applied on the column (considered as equivalent single-degree-of-freedom system).

For this worked example only the blast action is considered, neglecting the gravitational loads.

As blast scenario, the column considered in the analysis is a perimeter column located in the middle of the long façade of the building – see Figure 6. The blast scenario assumes that a car is placed at a standoff distance of 20m from the column and carries an explosive charge equal to 100 kg of TNT (or equivalent). The burst is defined as a free-air burst with a free height from the ground of 1m.

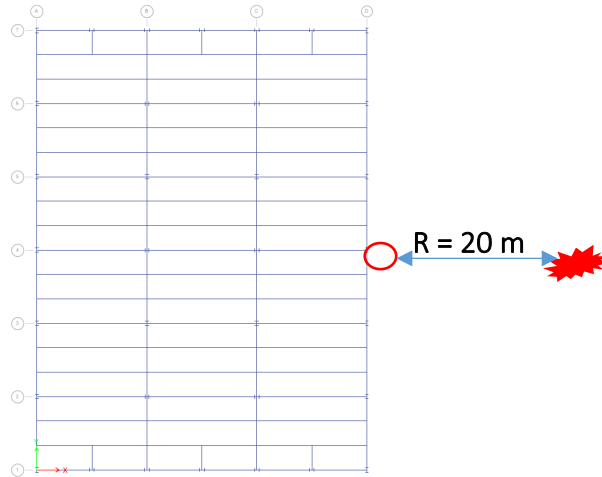


Figure 6. Plan view of the columns under blast load – SS S

As defined in (DoD 2014), the blast scenario previously defined in Figure 6 is characterized by the following blast parameters:

TNT equivalent mass of the explosive charge	$W = 100kg$
Standoff distance	$R = 20m$
Height of the blast	$H_c = 1m$
Scaled distance	$Z = \frac{R}{W^{\frac{1}{3}}} = \frac{20}{100^{\frac{1}{3}}} = 4.309 \frac{m}{kg^{\frac{1}{3}}}$
Distance from blast source	$R_h = \sqrt{R^2 + H_c^2} = \sqrt{20^2 + 1^2} = 20.025m$
Angle of incidence	$\alpha_i = \tan^{-1}\left(\frac{H_c}{W^{\frac{1}{3}}}\right) = \tan^{-1}\left(\frac{1}{100^{\frac{1}{3}}}\right) = 12.158^\circ$

Afterwards, using the previously determined values, the pressure, impulse, durations, velocity and wavelength are computed. Several other tools could be employed as well (i.e., (UN SaferGuard n.d.)) and/or directly from the chart Figure 138. The obtained values are presented below.

Incident pressure	$P_{so} = 56.44 kPa$
Incident impulse	$I_s = 313.71 kPa.ms$
Reflected pressure	$P_r = 137.37 kPa$
Reflected impulse	$I_r = 688.09 kPa.ms$
Time of arrival	$t_a = 30.29 ms$
Positive phase duration	$t_0 = 16.49 ms$
Blast wavelength	$L_w = 0.4 \frac{m}{kg^{\frac{1}{3}}}$
Shock front velocity	$U = 413.93 \frac{m}{s}$

Note If the chart is used, the values for the time intervals, impulses, and wavelength need to be scaled (multiplied with $W^{1/3}$), however the pressures and the shock wave velocity remain unaffected.

The peak dynamic pressure (q_0) and the sound velocity (C_r) and may be obtained using Figure 139 and Figure 140 considering the value of the incident pressure (P_{so}) previously defined.

Sound velocity $C_r = 0.38 \frac{m}{ms}$

Peak dynamic pressure $q = 8.5kPa$

Based on scaled impulses and corresponding pressures, the fictitious positive phase duration and fictitious duration of the reflected wave are computed below. The computation is necessary since the blast wave formulation was initially defined for an infinite surface.

Fictitious positive phase duration $t_{of} = 2 \frac{I_s}{P_{so}} = 2 \times \frac{313.71}{56.44} = 11.12 ms$

Fictitious duration for the reflected wave $t_{rf} = 2 \frac{I_r}{P_r} = 2 \times \frac{688.09}{137.37} = 10.02 ms$

Height of the element $h_s = 4m$

Width of the wall $w_s = 4m$

Drag coefficient $C_D = 1$

Smallest dimensions (height versus wall) $s_d = \min\left(h_s, \frac{w_s}{2}\right) = \min\left(4, \frac{4}{2}\right) = 2m$

Largest dimension (height versus wall) $l_d = \max\left(h_s, \frac{w_s}{2}\right) = \max\left(4, \frac{4}{2}\right) = 4m$

Ratio (smallest / largest) $r_{s,l} = \frac{s_d}{l_d} = \frac{2}{4} = 0.5$

Clearing time $t_c = \frac{4s_d}{(1 + r_{s,l})C_r} = \frac{4 \times 2}{(1 + 0.5) \times 0.38} = 14.04ms$

Peak pressure acting on the wall $P = P_{so} + q.C_D = 56.44 + 8.5 \times 1 = 64.94kPa$

The column will be designed using the reflected pressure and the fictitious duration of the reflected pressure such that the largest impulse is used. The procedure may be used again to determine the negative phase of the of the blast. However, in this case, smaller values for the pressure and impulses will be obtained.

Single degree of freedom approach (SDOF)

For simple structures, a rigorous dynamic analysis can be performed to evaluate the response. For practical design purposes however, approximations need to be made to allow the design with reasonable accuracy. Consequently, an equivalent SDOF system of the column will be used to determine the ductility demand of the column subjected to the pressure previously determined. Firstly, the uniformly distributed load (F_d) and point load (F_p) generated by the blast on the column are computed.

Reflected pressure $P_r = 137.37kPa$

Height of the column $h_c = 3.5m$

Width of the panel in front of the column $w_p = 5m$

Fictitious duration of the reflected wave $t_{rf} = 10.02ms$

Self-weight of the column $G_c = 1.834 \frac{kN}{m}$

Distributed load from the blast on the column $F_d = P_r w_p = 137.37 \times 5 = 686.85 \frac{kN}{m}$

Point load from the blast on the column $F_p = F_d h_c = 686.85 \times 3.5 = 2404 kN$

Note The effective height of the column may be considered less than 4 m since the connection will form a rigid zone.

Since an equivalent static approach is employed, the loading should be amplified by means of DLF. Using Figure 145a, a DLF may be determined function of the t_d/T (ratio between duration of the reflected pressure and the period of vibration of the column). An initial assumption $t_d/T = 2/3$ is taken into account for the computation of the maximum moment.

Dynamic load factor $DLF = 1.4$

The column is fixed at both ends. Using Table 66 for the one-way slab and double fixed element (the case of the column considering the load distribution of the curtain wall), the transformation factors for mass and stiffness may be obtained. Finally, the maximum moment may be obtained.

Loading factor $K_L = 0.64$

Mass factor $K_M = 0.50$

Plastic modulus $W_{pl.c} = 1292 cm^3$

Inertia $I_c = 12620 cm^4$

Dynamic increase factor $DIF = 1.2$

Steel yield strength $f_y = 426 MPa$

Steel elastic modulus $E = 210 GPa$

Column stiffness

$$K_c = \frac{384E \cdot I_c}{5h_c^3} = \frac{384 \times 210 \times 10^6 \times 12620 \times 10^{-8}}{5 \times 3.5^3} = 47472 \frac{kN}{m}$$

Maximum resistant moment

$$M_{Rd} = W_{pl.c} \cdot f_y \cdot DIF = 1292 \times 10^{-6} \times 426 \times 10^3 = 550.4 kNm$$

$$\text{Maximum applied moment } M_{max} = \frac{F_p \cdot h_c}{8} DLF = \frac{2747.4 \times 3.5}{8} \times 1.4 = 1472 kNm$$

$$\text{Effective mass } M_e = \frac{G_c \cdot h_c \cdot K_M}{g} = \frac{1.834 \times 3.5 \times 0.50}{9.81} = 327.3 kg$$

$$\text{Effective stiffness } K_e = K_c K_L = 47471.8 \times 0.64 = 30382 \frac{kN}{m}$$

Natural period of vibration $T_c = 2\pi \sqrt{\frac{M_e}{K_e}} = 2 \times \pi \sqrt{\frac{327.3}{30382}} = 0.0206$

Ratio $\frac{t_{rf}}{T_c} = 0.49$

Note The yielding strength of the steel may be affected by an amplification factor of 1.2 for the strain rate.

The new determined ratio $\frac{t_{rf}}{T_c}$ (or t_d/T) allows for a second, more precise iteration. Afterwards, the maximum resistance is determined.

Second interaction – Dynamic load factor $DLF = 1.6$

Maximum applied moment $M_{max} = \frac{F_p \cdot h_c}{8} DLF = \frac{2747.4 \times 3.5}{8} \times 1.6 = 1683 \text{ kNm}$

Resistance force $R_m = \frac{8(2M_{Rd})}{h_c} = \frac{8 \times 2 \times 550.4}{3.5} = 2516 \text{ kN}$

Dynamic reaction

$$V_m = 0.39R_m + 0.11F_p + G_c \cdot h_c \cdot 0.5$$

$$V_m = 0.39 \times 2516 + 0.11 \times 2747.4 + 1.834 \times 3.5 \times 0.5 = 1248.92 \text{ kN}$$

Ratio $\frac{R_m}{F_p} = 1.05$

The ratio between the maximum resistance and the point load is used to determine the ductility demand – μ using Figure 141 for the maximum out-of-plane displacement and maximum response time.

Ratios $\mu_1 = 1.05 (X_M / X_E)$

$$\mu_2 = 0.82 (t_m / T)$$

Yield displacement $\chi_e = \frac{R_m}{K_e} = \frac{2516}{30382} = 82.82 \text{ mm}$

Maximum displacement $\chi_M = \mu_1 \times \chi_e = 1.05 \times 82.82 = 86.96 \text{ mm}$

Maximum response time $t_m = \mu_2 \times T_c = 0.82 \times 0.0206 = 16.91 \text{ ms}$

To evaluate the performance of a structural system or component, pressure impulse diagrams are used based on several damage limits. Using Figure 146 and Figure 147, class B2 is chosen with the corresponding ductility limit in flexure for element with compact section.

$$\mu_{max} = 1 \quad \text{Compression -> Beam -column with compact section -> B1}$$

Check $\frac{\mu_1}{\mu_{max}} = 1.05$

According to the results, the column can withstand the blast load (the value may be considered admissible), the requirement from class B1 (superficial damage) being fulfilled.

3.2.1.2 Full dynamic approach

This example gives information about the design against blast action due to accidental external explosion using the full dynamic approach. The method considers a numerical model in which the blast load is applied by means of a pressure load.

The current worked example treats the same scenario in terms of geometry, explosive charge, and blast parameters. However, a more complex, full numerical analysis is employed to compare the results and assess the efficiency of the simplified approach.

The following loading are considered for the accidental design situation:

- Permanent loads DL (see Table 4).
- Live loads LL (see Table 4 for SS/S structure).
- Blast action A_{Ed} (see section below)

The following combination of actions is used for the accidental design situation:

$$DL + 0.5 \times LL + A_{Ed}$$

Figure 7 presents the 3D numerical model and the position of the charge.

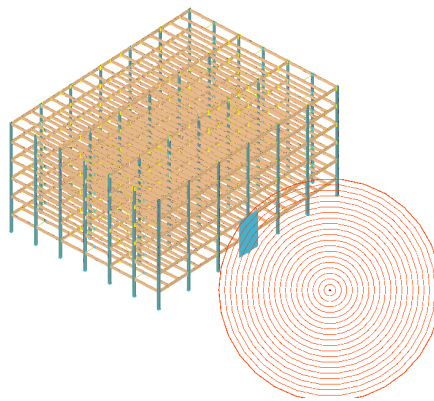


Figure 7. 3D model with the position of the charge

The numerical analysis has been performed in ELS (Extreme Loading for Structures software), using a full 3D model (see Figure 8) where the entire structure has been modelled.

As in the worked example only the blast action is considered, neglecting the gravitational loads.

Model assumptions in AEM

ELS uses a nonlinear solver based on AEM (Tagel-Din and Meguro 2000) and allows the automatic detection and computation of yielding, hardening, failure of materials, separation of elements, contact at impact, buckling/post-buckling, crack propagation, membrane action, and P- Δ effect. In the AEM modelling technique the structural elements are modelled as small solid elements (discretization is made both along the length of the member and of the cross-section) connected by normal and shear springs that follow the constitutive law of the corresponding material (including plastic behaviour, separation, contact). After reaching the separation strain, springs are removed. Then, if the separated elements come in contact, springs are generated at the surface of elements that are forced towards each other (Applied Science International 2021).

Columns and beams were defined as solid objects with a constant I / H shape cross-section. The objects were discretized into small solid elements, generating 25 sets of springs at each surface. Link elements were used to model vertical braces and horizontal ties (anchored to perimeter columns). Beam-to-column connection properties were modelled with 8-node objects for end-plates and individual springs for each bolt. Pinned connections were defined by connecting the secondary beams with the main beams using just the springs representing the bolts. Column bases were considered fixed. Reinforced

concrete (RC) slabs are solid concrete elements with steel springs at the level of the reinforcement. Springs also model connectors, linking the beams to the RC slab.

To take into account the inertial effects, dead and live loads were assigned on the floors using lumped masses, which simulate better inertia effects in comparison to load assignments.

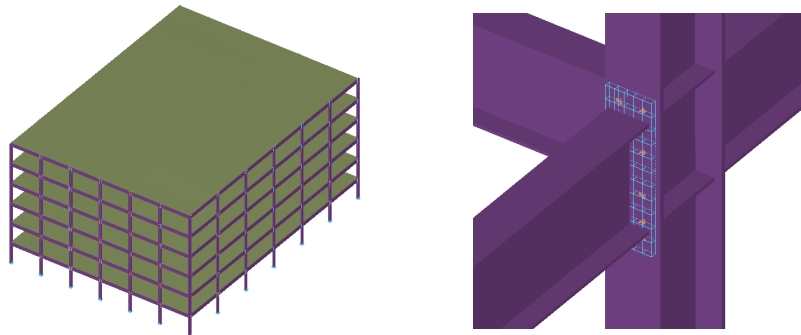


Figure 8. 3D model of the structure (general view and connection detail)

To improve the accuracy of the AEM model, fine meshing was applied on the behaviour of the structural elements and joints which are contributing to the load redistribution capacity. The calibration was done against relevant experimental data from tests on subassemblies and joints (see Figure 9). Thus, Figure 9a shows the force-displacement curves in a column loss scenario from experimental test and using numerical simulation in ELS, while Figure 9b shows the beam-to-column hysteretic and backbone curves from tests on joints. It may be seen the accuracy of the numerical model in reproducing the structural response is adequate.

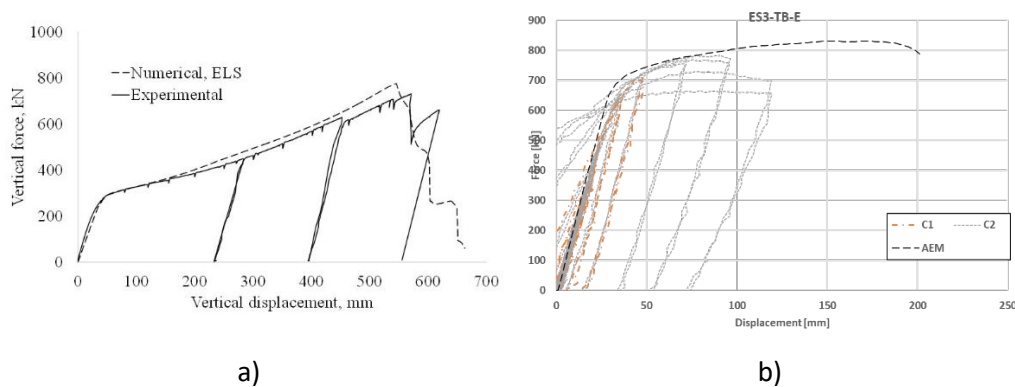


Figure 9. System calibration on CODEC Tests and Connections calibration on Equaljoints Tests: a) force-displacement in a column loss scenario (Dinu et al. 2016); beam-to-column hysteretic and backbone curves (Landolfo et al. 2018)

To account for the tributary area loaded by blast, rigid plates were modelled to transfer the pressure horizontally to the 1st and 2nd storey columns. The blast loading parameters are computed automatically by the integrated blast pressure generator, as presented in Figure 10.

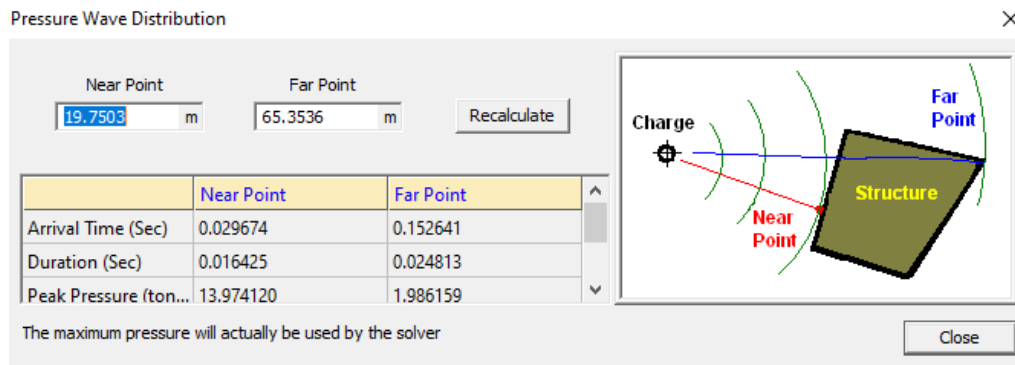


Figure 10. 3D model with the position of the charge

The analysis is performed in two steps:

1st step: the permanent and live loads are applied on the structure in a nonlinear static analysis.

2nd step: the charge is detonated, and the blast load is applied in a nonlinear dynamic analysis. The time step for this analysis is 1e-6 sec.

Only the positive phase of the blast is considered; no reflection from the ground is accounted in the analysis.

The results of the analysis are presented in Figure 11 (left) in terms of maximum horizontal displacement at the mid-height of the column is 24 mm. Additionally, the maximum plastic strain reached is 1%.

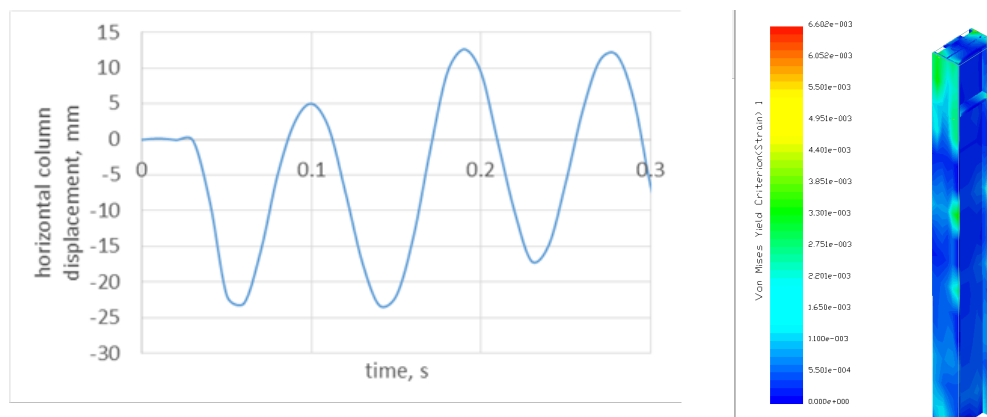


Figure 11. Horizontal deformation vs time at column mid-height (left) and Von Mises strains (right)

The following conclusion may be drawn after comparing the results from the full dynamic approach and the equivalent SDOF approach:

- The displacement in the full nonlinear dynamic analysis is less than the value obtained using tabular method (24 mm vs. 87 mm, see 3.2.1.1)
- Nonlinear analysis can account for distribution of plasticity in the element
- Full 3D model can account for real boundary conditions and interactions between elements
- Full dynamic approach and 3D modelling can account for sequential application of blast pressure on the surface (different arrival times along the column length)

Note that, in case of near field blasts, the effects can be amplified by the uplift pressure against the adjoining floors, which can result in higher dynamic effects and even risk of progressive collapse (Dinu et al. 2018).

3.2.2 Internal explosions

3.2.2.1 Equivalent static approach

This example gives information about the design against internal blast due to accidental internal gas explosion using the equivalent static approach. Using a pressure model function of the venting area and the volume of the enclosure, an equivalent pressure may be determined. Afterwards, a linear elastic analysis is performed to assess the level of damage.

In this worked example the following loading are considered for the accidental design situation:

- Permanent loads DL (see Table 4).
- Live loads LL (see Table 4 for SS/S structure).
- Gas pressure A_{Ed} (see section below)

The following combination of actions is used for the accidental design situation:

$$DL + 0.5 \times LL + A_{Ed}$$

The compartment to be analysed is located at the ground floor. The venting surface is considered on the external wall and is made of glass window, while the other 3 internal walls are made of stronger materials. The column considered for the verification is circled with green in Figure 12.

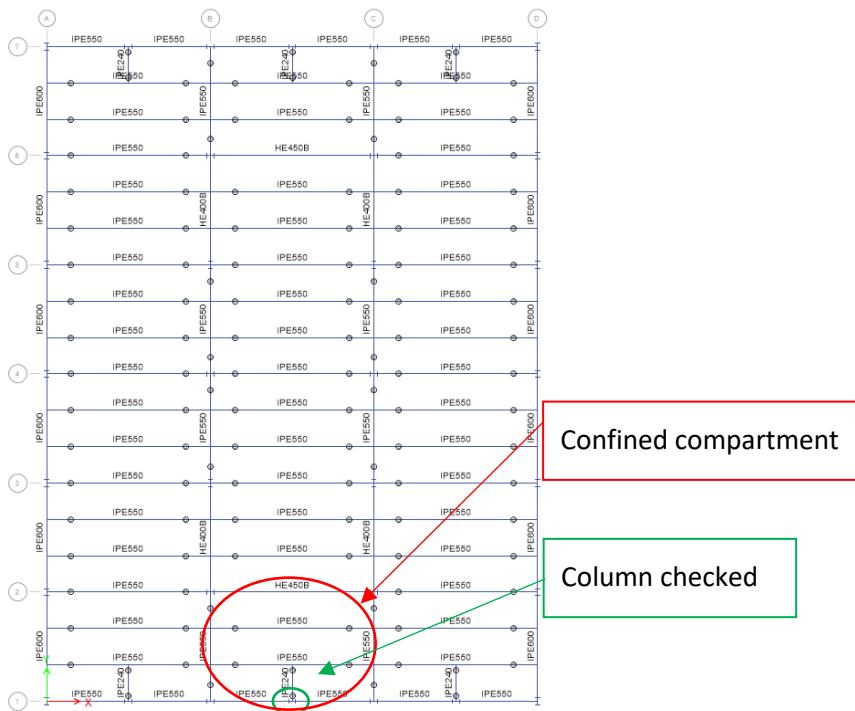


Figure 12. Position of the confined compartment and checked column – SS/S

The venting area and volume of the enclosure were computed (see Table 18) , considering that the glass wall is on the length of the enclosure and on the entire height of the level.

Table 18. Geometry of the compartment – SS/S

L	12	m	length
B	8	m	width
H	4	m	height
A_v	48	m^2	venting area
V	384	m^3	compartment volume
A_v/V	0.125	m^{-1}	ratio venting area to compartment volume

After successfully checking that the pressure model from EN1991-1-7 can be applied for the current example ($V < 1000 \text{ m}^3$ and A_v/V between 0.05 and 0.15), the following equivalent static pressure for the internal gas explosion was obtained:

$$p_d = 3 + p_{stat} \quad (3)$$

or

$$p_d = 3 + \frac{p_{stat}}{2} + \frac{0.04}{(A_v/V)^2} \quad (4)$$

whichever is the greater.

It was assumed that $p_{stat} = 3 \text{ kN/m}^2$, which represents the static uniformly distributed pressure which venting components fail.

Consequently, the design pressure in case of accidental situation is:

$$p_d = 7.06 \text{ kN/m}^2$$

In the following, the pressure was applied as a linear load acting on the height of the column considering a tributary area of 6m.

A linear elastic analysis is made on the full 3D model using SAP2000 software. The section of the elements are those resulted from the initial design (persistent and seismic design situations). The acceptance criteria are given in terms of utilization factors (U.F.) for accidental combinations, only.

The results of the linear static analysis of the column is presented in Table 19.

Table 19. Results of linear static analysis

Section	Axis	Bottom support	N [kNm]	M [kNm]	U.F. [-]
HEB500	Minor	Fixed	612	72	0.279

The column analysed with this approach did not exceed the capacity and does not require redesign. However, since no local damage occurs, more sophisticated approaches may be used to quantify the damage that might appear.

3.2.2.2 Dynamic approach – TNT equivalence method

This example gives information about the design against internal gas explosions, using the dynamic approach - TNT equivalence method.

Note: In D2-3 it was presented a simplified procedure, similar to the one used in case of external blast. However, for this worked example, the effect of the frangibility of the walls, pressure leakage from the compartment etc. are taken into account as prescribed in (DoD 2014).

As in the W.E presented in 3.2.1.1, the same structural configuration and the same enclosure is used. However, in the case of the equivalent TNT method – static approach empirical model (Bjerketvedt, Bakke, and van Wingerden 1997) – gas explosion may be assimilated with a TNT explosion using pressure-distance curves.

The procedure proposed to solve this case is based on the recommendations (DoD 2014). However, the process is quite complex and implies several steps to fully solve the problem, which are highlighted below.

Steps for the procedure:

- A. Determine the impulse reflected on the frangible wall in case of an equivalent TNT explosion
- B. Determine the impulse reflected on the frangible wall considering the frangibility
- C. Determine the pressure that can build up due to the gas explosion, the corresponding impulse and the fictitious duration of gas loading

D. Using the equivalent SDOF approach, use the previously determined pressure and duration of the gas loading to load a column and check with the ductility limit.

For each step there are several sub steps which will be explained.

For the current worked example, since the compartment is included in a multistorey steel frame, the enclosure is considered a containment or 4 wall cubicle with roof. However, the wall on the perimeter frame will be a glass curtain wall, without load bearing capacity. Consequently, it may be considered a frangible wall, being included in the façade. The only condition mentioned in (DoD 2014) is that the wall should have a resistance equal or less than 1.2 kPa. Considering the average wind values in the region of the structure, the wall fits in the category of frangible walls.

Equivalent TNT mass

A mass of 40.31 kg of TNT was obtained considering a volume of 384 m³ for the enclosure.

Computation

Step A

Step A.1 - Establishing the dimensions

H=	4.0	m	height of cubicle
L=	12.0	m	length of cubicle
h=	2.0	m	height of charge point
l=	6.0	m	distance from the side wall
R _A =	4.0	m	distance from the charge to the wall

In the above list, aside from the geometrical characteristics of the enclosure, the meanings for l and R_A are given in Figure 2-51 (DoD 2014) , for a four wall cubicle with roof, the case of the back wall with N = 4 (N -representing the number of reflecting surfaces).

Step A.2 – Charge weight

W = 40.3 kg (without considering an amplification factor of 1.2 for the 40.3 kg)

Step A.3 – Scaled distances

h/H=	0.5	-
l/L=	0.5	-
L/R _A =	3.0	-
L/H=	3	
Z _A =	1.17	m/kg ^{1/3}

Several ratios are computed which will be necessary to determine the reflected pressure and impulse in the next step.

Step A.4 – Pressure and impulse values

With the previously determined scaled distances and ratios, Table 2-3 – UFC 3-340-02 is accessed. Based on h/H, l/L and N, it may be determined the figures which will be used to determine the pressure and impulse. It has to be mentioned that there may be cases for double interpolation for the values obtained from the figures.

Consequently, for ratios h/H and l/L of 0.5 and N = 4, Figure 2-100 will be used to determine the average peak reflected pressure and Figure 2-149 for the scaled average unit reflected impulse. In the figures, the L/R_A and Z_A variables will also be used since multiple graphs are represented for each figure.

The following values were obtained from the figures:

L/H	Pr [kPa]	L/H	$i_r/W^{1/3}$ [$kPa - ms/kg^{1/3}$]
2.5	200	2.5	95
5	250	5	130

Step A.5 – Determine final values for the pressure and the impulse

For the ratio L/H having the value 3, the following values were obtained:

$$P_r = 210 \text{ kPa}$$

$$i_r = 102 \text{ kPa} - \text{ms}/\text{kg}^{1/3}$$

Note: The peak reflected pressure and the average scaled impulse obtained in Step A consider the wall to be rigid. To consider the fragility of the wall, the average scaled impulse will be affected by a reflection factor. This procedure is performed in Step B.

Step B

Step B.1 – Peak reflected pressure and average unit reflected impulse

These two quantities were determined in Step A.5.

Step B.2 – Ratio between unit weight of the wall and the charge

W_f	48.8	kg/m^2	unit weight of the frangible wall
W	40.3	kg	
$W_f/W^{1/6}$	26.36	-	

Step B.3 – Determine Z

The fictitious scaled distance Z corresponding to the average scaled impulse from Step B.1 is determined from Figure 2-7 (DoD 2014). Considering a value of $102 \text{ kPa} - \text{ms}/\text{kg}^{1/3}$ for the scaled impulse, a value of approximately $1.8 \text{ m}/\text{kg}^{1/3}$ is determined for the scaled distance.

Step B.4 – Reflection factor f_r

The reflection factor f_r is determined from Figure 2-150 – (DoD 2014) using the ratio determined in step B.2 and the scaled range determined in step B.3. Consequently, an approximate value of 0.89 is obtained for the reflection factor.

Step B.5 – Average impulse acting on the backwall considering the reflection factor

The average reflected impulse (multiplied with $W^{1/3}$ to have unscaled value) acting on the backwall is obtained by multiplying the value from step 1 with the reflection factor. The value of the peak reflected pressure remains the same. Thus, a fictitious time duration may be computed by dividing twice the value of the average reflected impulse to the value of the peak reflected pressure. The results of the computation are presented below.

I_r	405.3	kPa-ms
P_r	210	kPa
t_0	3.86	Ms

Step C

Step C.1 – Charge weight

This step was already performed in previous steps. Hence, charge of 40.3 kg is used, value already multiplied with 1.2 amplification factor.

Step C.2 – Free volume inside the cubicle

The free volume inside the enclosure is determined by subtracting the volume of all interior equipment, structural elements etc. from the total volume of the containment. For the current case, a factor of 0.75 was used to multiply the total volume to obtain the free volume of the cubicle.

$$V_f = 288 \text{ m}^3$$

Step C.3 – Charge weight to free volume ratio

$$W/V_f = 0.014017 \text{ kg/m}^3$$

Step C.4 – Peak gas pressure

The peak gas pressure that may build up in the enclosure due to the gas explosion is obtained from Figure 2-152 – (DoD 2014) function of the aforementioned ratio.

$$P_g = 5512 \text{ kPa}$$

Step C.5 – Venting area

For this case, the length of venting area was considered the length of entire wall on the perimeter and the width as half of the height of the wall. Consequently, a venting area of 96 m² was obtained.

Step C.6 – Scaled value of the vent area

$$\frac{A}{V_f^{2/3}} = 2.20128 \text{ m}^2/\text{m}^2$$

Step C.7 – Scaled weight of the cover

The cover of the containment is assumed to be a frangible wall, with a unit weight of 48.82 kg/m² as used in Step B.

$$\frac{W_f}{W^{1/3}} = 1.21 \text{ kg}^{2/3}/\text{m}^2$$

Step C.8 – Scaled average reflected impulse

The scaled average reflected impulse is the value determined during step B.5 and divided with the third root of the charge weight. The result of the computation is presented below.

$$\frac{i_r}{W^{1/3}} = 814.62 \text{ kPa} - \text{ms}/\text{kg}^{1/3}$$

Step C.9 – Scaled gas impulse

For the current case, the following parameters are needed:

- Scaled average reflected impulse – determined in Step C.8
- Scaled venting area – determined in Step C.6
- Charge weight to free volume ratio – determined in Step C.3
- Scaled weight of the cover – determined in Step C.7

With these values, Figures 2-153 and 2-154 (DoD 2014) will be used to determine the values of the scaled gas impulse.

Performing a linear interpolation and multiplying with the third root of the charge weight the value of the impulse obtained is presented below.

$$I_g = 10776.8 \text{ kPa-ms}$$

Step C.10 – Fictitious duration of the gas loading

The fictitious duration of the gas loading is determined by dividing twice the value of the impulse obtained in step C.9 to the pressure of the gas determined in step C.4. A final value of 112.12 ms was obtained.

Step D – SDOF approach for a column using the duration of loading and pressure determined in Step C

Since this approach was previously described in section 3.2.1.1, a shorter presentation of the computation performed is hereby shown.

The value of the pressure obtained is 552 kPa. With this value (and assuming a tributary width of 1.0 m for loading the column) a point load of 1930.5 kN was considered on the column. The removal time is determined during step C.10 – 0.112 s.

The removal time to natural period of vibration of the column ratio obtained is 5.44 which yields to a dynamic increase factor of 1.95 for the second iteration. Consequently, for the aforementioned ratio and the resistance to force ratio of 1.30 (, a ductility factor of 2.0 is obtained.

With the ductility factor of 2.0 being less than 3, as specified for class B3 – severe damage – Figure 147. Response limits for hot-rolled structural steel Figure 147, the column fulfils the requirements in case of this action.

It may be concluded that using the static approach, a more detailed analysis of the column was performed. According to the equivalent static approach, the column remained with a ratio less than 1.0, meaning that there was no local damage. However, using this more advanced method, local damage occurs, but it was not considered critical for the structure.

To better assess the level of damage that the structure might be subjected to, a more sophisticated approach could be used i.e., dynamic analysis.

3.2.3 Seismic

3.2.3.1 Advanced numerical analysis (multi-hazard)

This worked example gives information about the design of a steel structure considering multi-hazard events, i.e., column failure after an earthquake using advanced numerical analysis.

The following loading are considered for the accidental design situation:

- Permanent loads DL (see Table 4).
- Live loads LL (see Table 4 for SS/S structure).
- Seismic action A_{Ed} corresponding to ULS (see section below)

The following combination of actions is used for the seismic design situation:

$$DL + 0.3 \times LL + A_{Ed}$$

Note: The combination is used for the nonlinear static analysis (push-over analysis). The column failure is addressed using the column loss approach (ALPM).

After the structure is subjected to an earthquake, a column can be lost, thus making the structure vulnerable to subsequent hazards. In the following, this procedure is applied to verify the capacity of the structure to resist progressive collapse using column loss approach.

Step 1: Seismic analysis – The structure is subjected to a design level earthquake

Step 2: Column loss scenarios: Lost columns are located at A1, A2, A4, B1, B' (Figure 13).

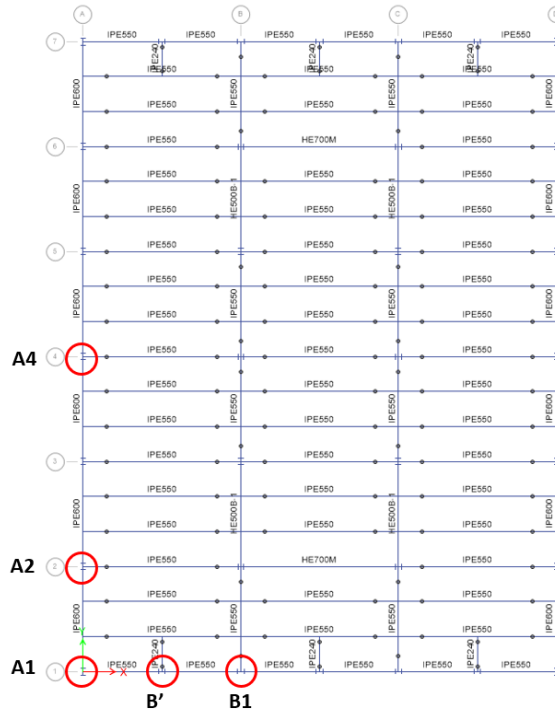


Figure 13. Position of the columns to be removed after earthquake

The seismic analysis is performed using push-over analysis and the damage evaluation is done using the N2 method. After the gravity loads are applied, the structure is subjected to a monotonically increasing pattern of lateral forces, representing the inertial forces which would be experienced by the structure when subjected to ground shaking. Under incrementally increased loads, some structural elements may yield. Consequently, after each plastic hinge is formed, the structure experiences a loss in stiffness and load capacity. To evaluate the seismic demands for ULS, the structure is pushed to its target top displacement D_t . Figure 14 shows the capacity curves for transversal and longitudinal directions and the target points for ULS and DLLS (damage limitation limit state). Figure 15 plastic mechanism at failure for transversal and longitudinal directions. No plastic hinges develop in perimeter moment resisting frames in neither X nor Y direction at ULS, but only in the braced frames.

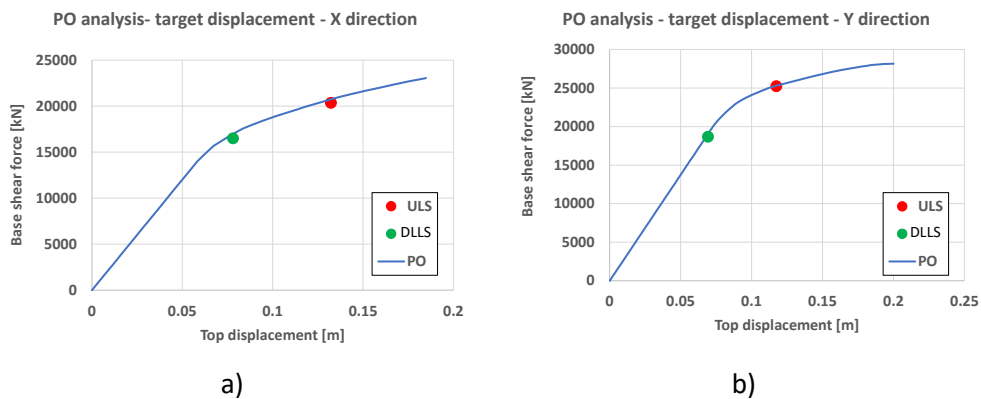


Figure 14. Seismic analysis: a) push-over curve with the position of the target point – X direction; b) push-over curve with the position of the target point – Y direction

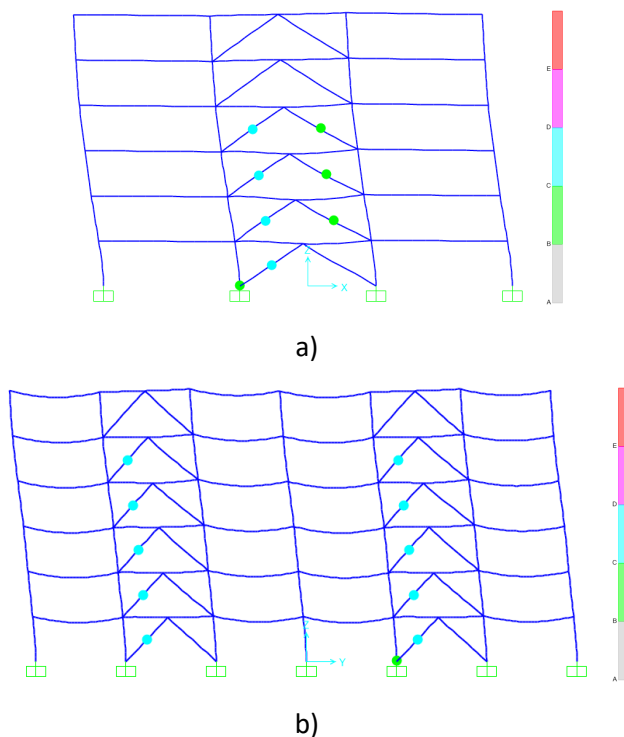
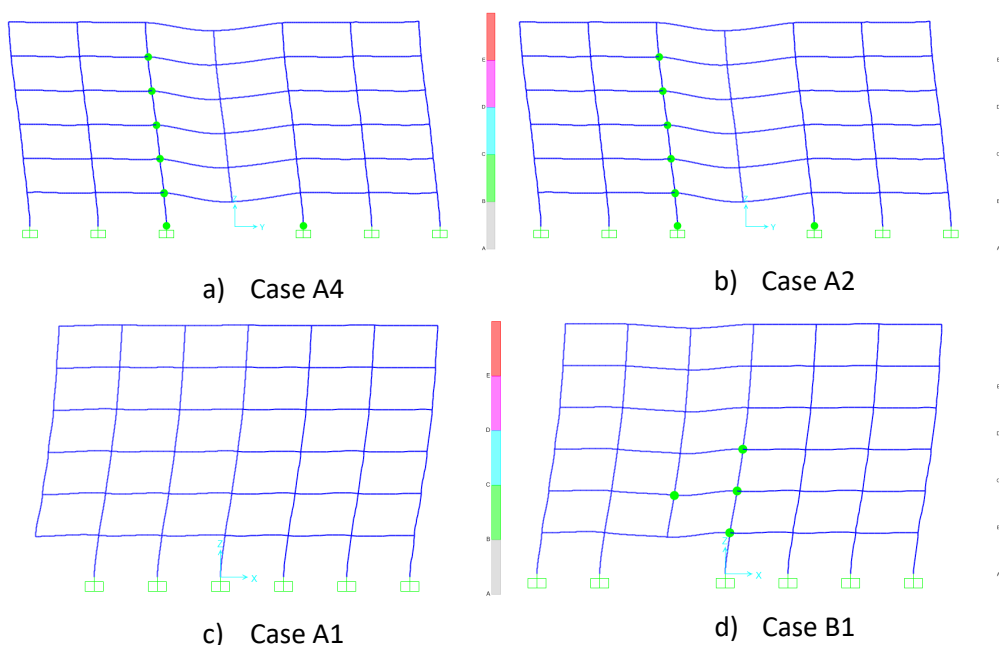
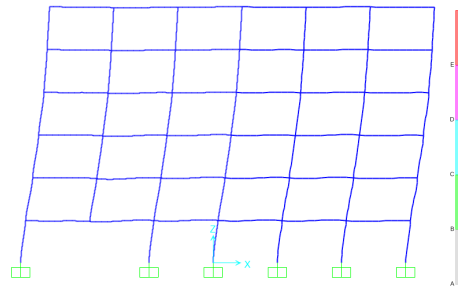


Figure 15. Seismic analysis: a) plastic mechanism at D_t ULS – current transversal frame; b) plastic mechanism at D_t ULS – current longitudinal frame

Five removal scenarios are considered, i.e., perimeter, penultimate, and corner columns located at the ground floor. The scenarios involve columns on the short and long sides of the facade. The assessment of progressive collapse resistance is done using the alternate path (AP) method and nonlinear dynamic procedure (NDP), in accordance with the (DoD 2014) guidelines. The gravity loads are applied in first stage; then, in the second stage, the element is removed almost instantaneously (removal duration of 0.005 seconds).

Below are presented the formation of the plastic mechanisms which occur in perimeter frames in the scenarios mentioned above. For each case, the plastic mechanisms (Figure 16a) to e)) and history of vertical displacement above the removed column Figure 17 are presented.





e) Case B'

Figure 16. Plastic mechanism after column removal for scenarios considered

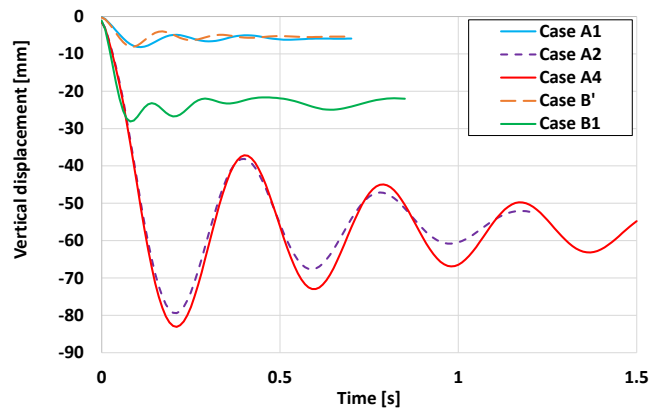


Figure 17. Time history response for column removal scenarios

It may be concluded that the structure has the capacity to resist the progressive collapse even with the loss of a column after an earthquake.

The level of damage in the elements (given by the level of plastic deformation in the plastic hinges) is small.

Other performance objective (e.g., collapse prevention) may be employed to assess the structural behaviour.

3.3 Verifications for unidentified actions

3.3.1 Alternate load path method

3.3.1.1 Prescriptive approach - tying method

This example shows the application of the tying method for beams and their connections (horizontal tying).

The following actions are considered for the accidental design situation:

- Permanent loads DL (see Table 4).
- Live loads LL (see Table 4 for SS/S structure).
- No specific accidental action is taken into account

Figure 18 presents the internal beams (main and secondary) for which the approach is applied.

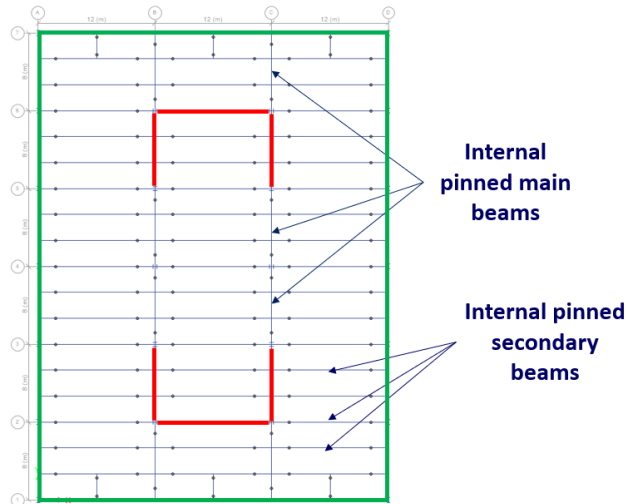


Figure 18. Horizontal ties considered for using prescriptive method – SS/S

Relationships to evaluate horizontal tying forces:

- for internal ties: $T_i = 0.8(g_k + \psi q_k)$ or 75 kN, whichever is greater
- for perimeter ties: $T_p = 0.4(g_k + \psi q_k)$ or 75 kN, whichever is greater

Computation

- internal pinned secondary beams (IPE550, all on short direction, see Figure 19 for joint configuration)

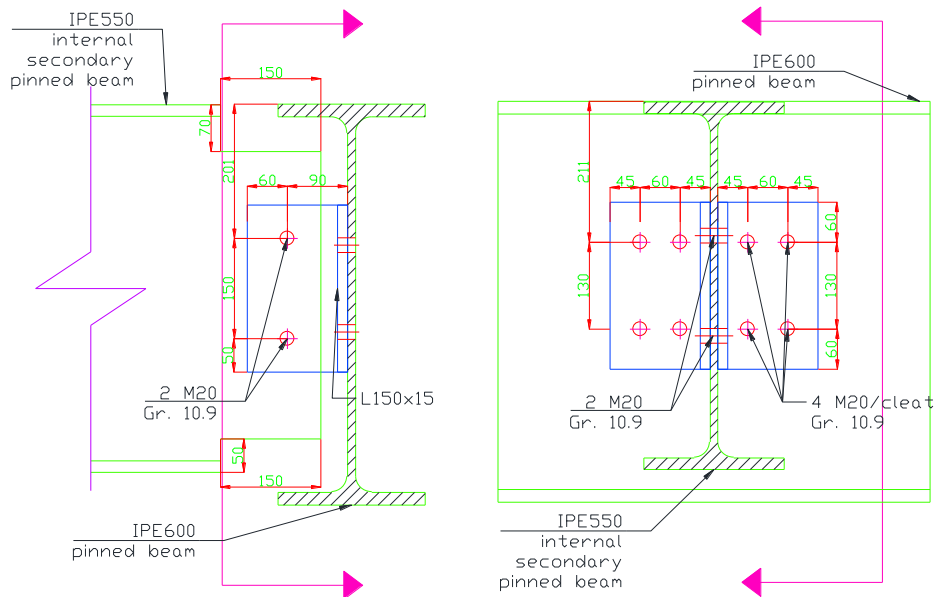


Figure 19. Joint configuration of pinned connection for a secondary beam

Spacing between ties (secondary beams)

$$s = 2.66m$$

Span of the tie

$$L = 12m$$

Design tensile load for internal ties

$$T_i = \max[0.8(g_k + \psi q_k)s.L; 75kN] = \max[0.8(5 + 0.5 \times 3)2.66 \times 12; 75kN] \\ = 166 kN$$

- internal pinned main beams (IPE550, all on long direction, see Figure 20 for joint configuration)

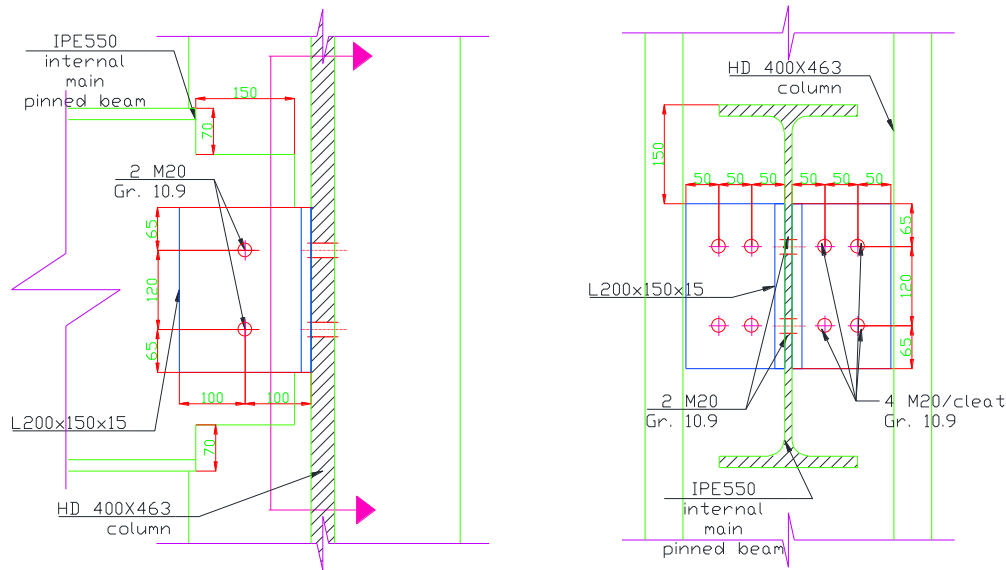


Figure 20. Joint configuration of pinned connection for a main beam

Spacing between ties
(main beams)

$$s = 12m$$

Span of the tie

$$L = 8m$$

Design tensile load for internal ties

$$T_i = \max[0.8(g_k + \Psi \cdot q_k)s \cdot L; 75kN] = \max[0.8(5 + 0.5 \times 3)12 \times 8; 75kN] \\ = 499.2 \text{ kN}$$

The shear resistances and UF for the connections of the internal ties considered for the verification are presented in Table 20.

Table 20 Connection check for tying forces according to the prescriptive method

Element	Tying force (kN)	Shear resistance (kN)	Failure mode	UF (-)
internal pinned secondary beams	166	392	Sec. beam in bearing	0.42
internal pinned main beams	499.2	392	Main. beam bolts in shear	1.27

Note: The capacity of the connection in tension was verified without any verification to the main beam. Care is needed as the main beam web can become the critical component.

In case of the connections for the internal pinned secondary beams, the UF of 0.42 results in an appropriate design.

In case of the connections for the internal pinned main beams, the UF of 1.27 required a redesign of the joint. Consequently, another bolt row (3 rows in total) increased the shear capacity to **588 kN** which gives an UF of **0.85** for the connection – see Figure 21 for the redesigned configuration.

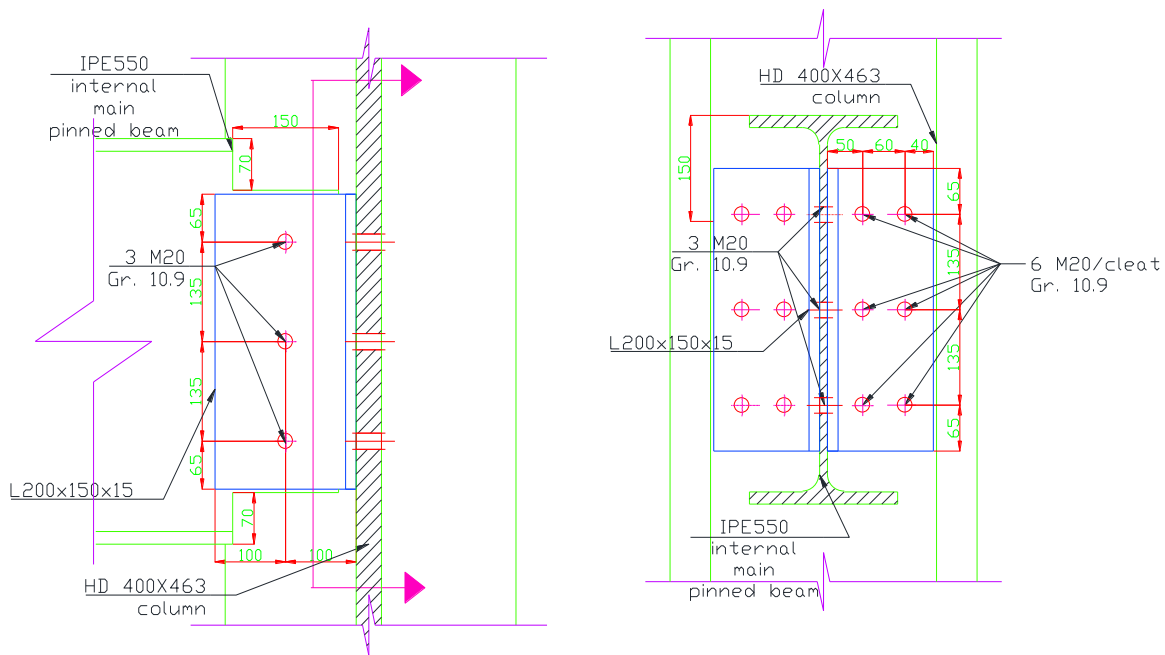


Figure 21. Joint configuration of pinned connection for a main beam

It may be concluded that the design for gravity loads may be insufficient for tying force requirements in case of large tributary areas.

3.3.1.2 Simplified numerical approach

This worked example gives information about the design against unidentified threats using the simplified numerical approach from ALPM.

The following actions are considered for the accidental design situation:

- Permanent loads DL (see Table 4).
- Live loads LL (see Table 4 for SS/S structure).
- No specific accidental action is taken into account

The following combination of actions is used for the accidental design situation:

$$DL + 0.5 \times LL$$

The simplified numerical method adopted for the current worked example allows one to establish the maximum ductility demand and verifying the demand versus capacity ratio. However, for determining the response of the structure for a column removal scenario a nonlinear static analysis was performed. Consequently, considering the energy balance (Izzuddin et al. 2008) between the work done by the loading and the internal energy stored, the pseudo-static response was determined. Analytically, the energy balance was computed as the area under curve using the mathematical approximation with the equivalent trapezoidal shape for the points on the graph. Finally, the energy was normalized to the displacement to obtain the pseudo-static curve.

According to scenario presented in Figure 22, the column considered to be removed is at the ground floor.

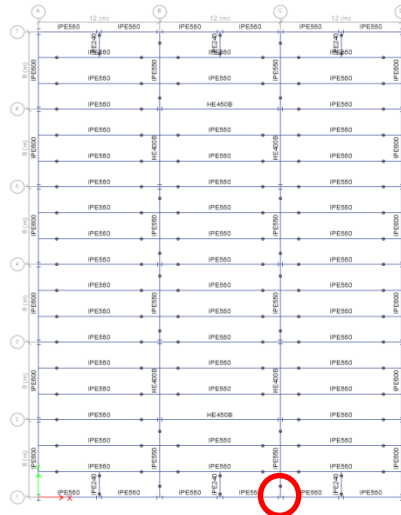


Figure 22. Column removal scenario – ALPM -simplified method – SS/S

For this method, a 3D nonlinear static numerical analysis was performed on the model in SAP2000 software. The gravitational loading was assigned according to the previously mentioned combination. The loading was applied only on the zone connected with the column – first two frames on y direction and first frame in z direction. Furthermore the column displacement was imposed downwards up to reaching failure.

Geometry and material nonlinearities (plastic hinges) were considered in the analysis. The pushdown curve for scenario C1 is curve PD (blue) in Figure 23. On the vertical axis the force has been normalized with gravity load multiplier λ ($\lambda=1$ for an applied load of 1.0 DL + 0.5 LL).

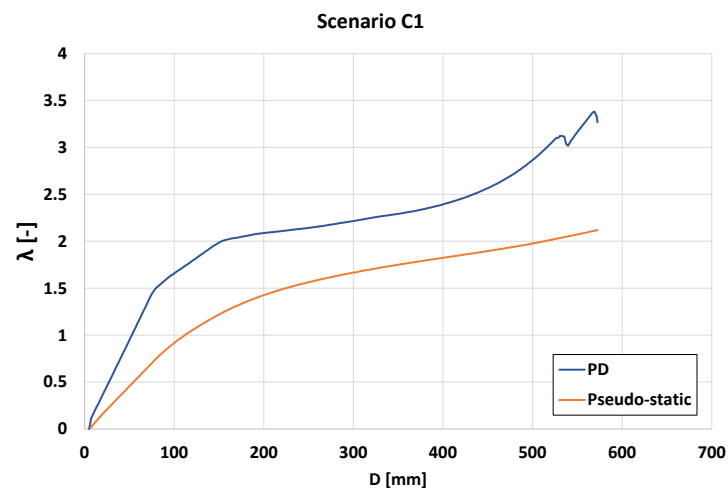


Figure 23 Normalized force multiplier vs. vertical displacement for push-down and pseudo-dynamic curves – ALPM – simplified numerical approach – SS/S

After performing the energy balance (Izzuddin et al. 2008), the pseudo-static curve was determined and plotted comparatively with the pushdown curve – Pseudo-static curve (orange) in Figure 23.

It may be concluded that for the column removal scenario considered, the structure has resistance and ductility capacity to find alternate load paths and not to undergo progressive collapse. The simplified numerical approach starting from a nonlinear static analysis offers a practical assessment of the ductility demand for design against progressive collapse. Compared with the full numerical analysis, the procedure is engineering oriented and may be performed faster. Even though the nonlinear

dynamic analysis allows for more precise results, taking implicitly the dynamic amplification of the loading, the results provided using this method are comparable.

3.3.1.3 Full numerical approach

This worked example gives information about the design against unidentified threats using the ALPM and nonlinear dynamic analysis.

The following actions are considered for the accidental design situation:

- Permanent loads DL (see Table 4).
- Live loads LL (see Table 4 for SS/S structure).
- No specific accidental action is taken into account

The following combination of actions is used for the accidental design situation:

$$DL + 0.5 \times LL$$

Note: This combination is valid for dynamic analysis only, because the dynamic effects caused by the column loss are considered implicitly by means of the removal duration parameter.

The scenarios taken into consideration for column removal are presented in Figure 24.

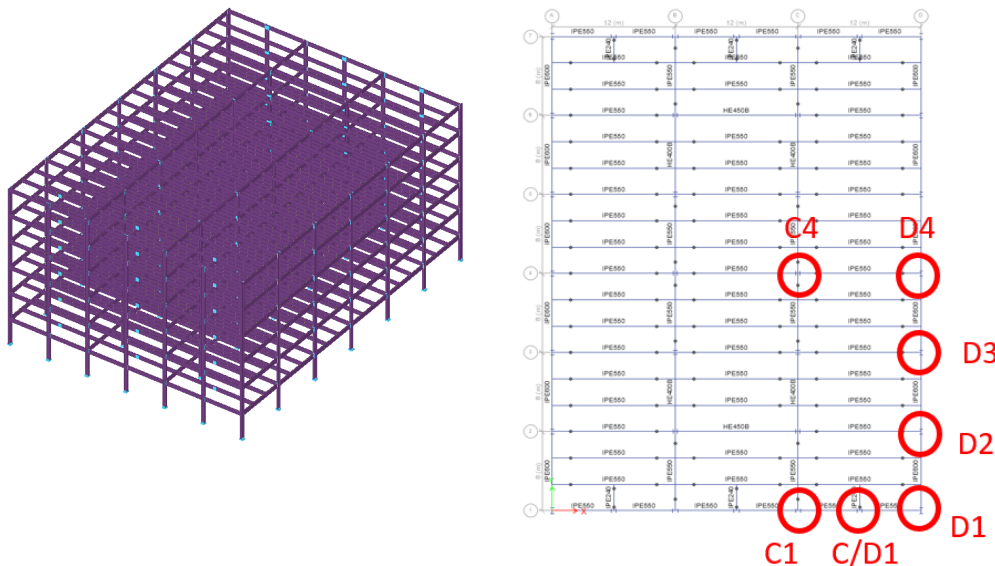


Figure 24. Isometric view of the structure (left) and location of columns to be removed for ALPM – full numerical approach – SS/S

The calculations are made using the ELS (Extreme Loading for Structures software) using the full 3D model of the structure.

Details about the numerical model are given in worked example from section 3.2.1.2. The model has been calibrated against relevant tests. The gravity loads were calculated using the combination of actions defined above and assigned to all floors.

Analysis:

- **1st step:** All gravity loads assigned to the floors using a static analysis
- **2nd step:** Duration of column removal is 0.001 seconds

Figure 25 presents time-history vertical displacement curves for each column removal scenario. As can be seen, for case C4, the column removal causes progressive collapse on the entire affected area - see Figure 26.

For cases C/D1, D1, D2, D3, D4 the structure has the capacity to resist the progressive collapse. Figure 27 presents the deformed shape in case of D2 column removal scenario. The deformations are small

and the resisting mechanism is based on flexural capacity (see Figure 28 and Figure 29), without the initiation of catenary action in beams (see Figure 30).

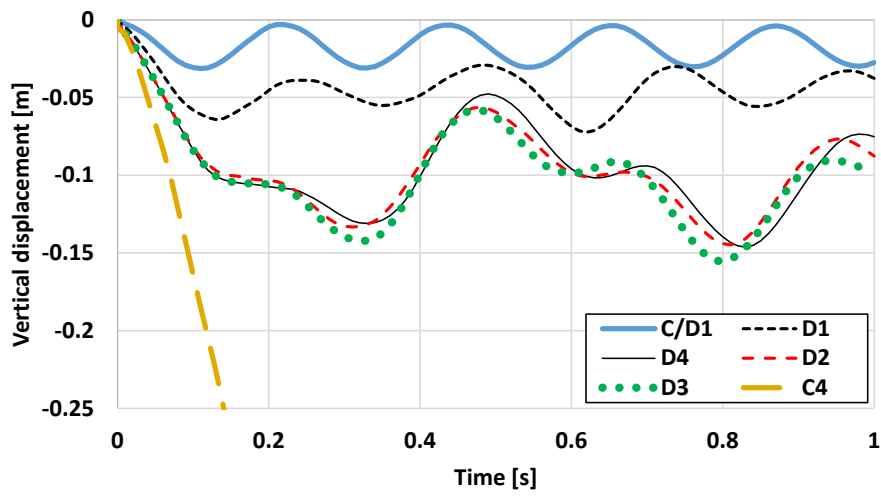


Figure 25. Time-history vertical displacement curves for removed columns

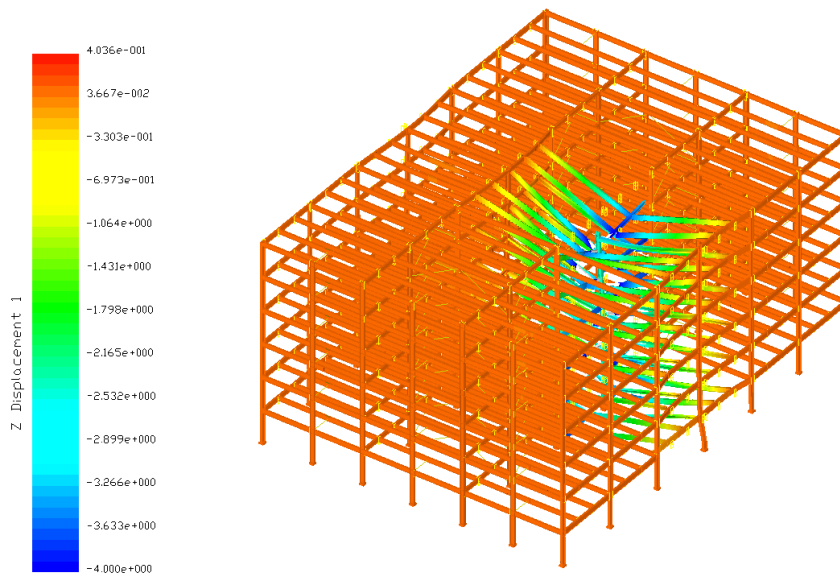


Figure 26. Failure mode after C4 after column removal

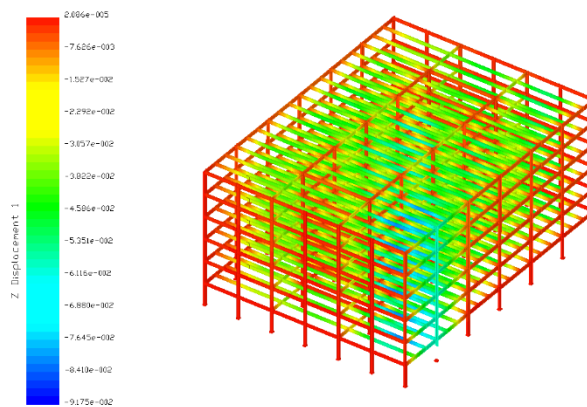


Figure 27. Vertical displacement of the structure in case of D2 column removal scenario

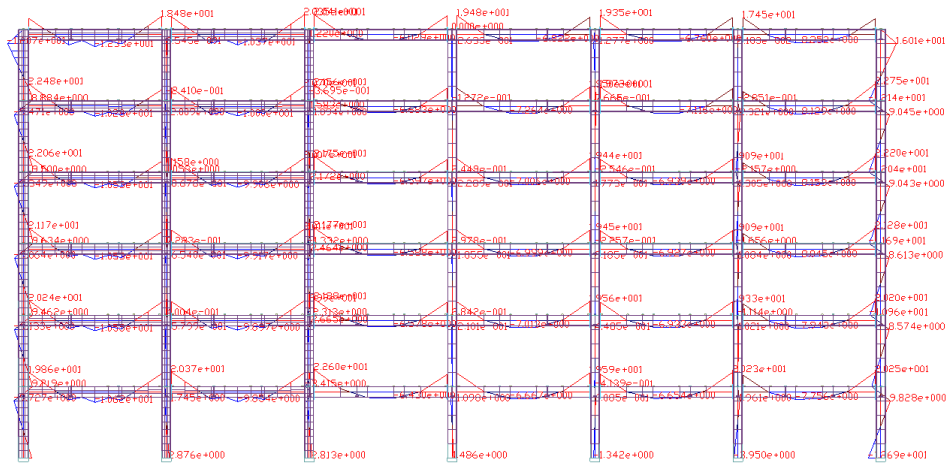


Figure 28. Bending moment diagram before D2 column removal scenario [tonf m].

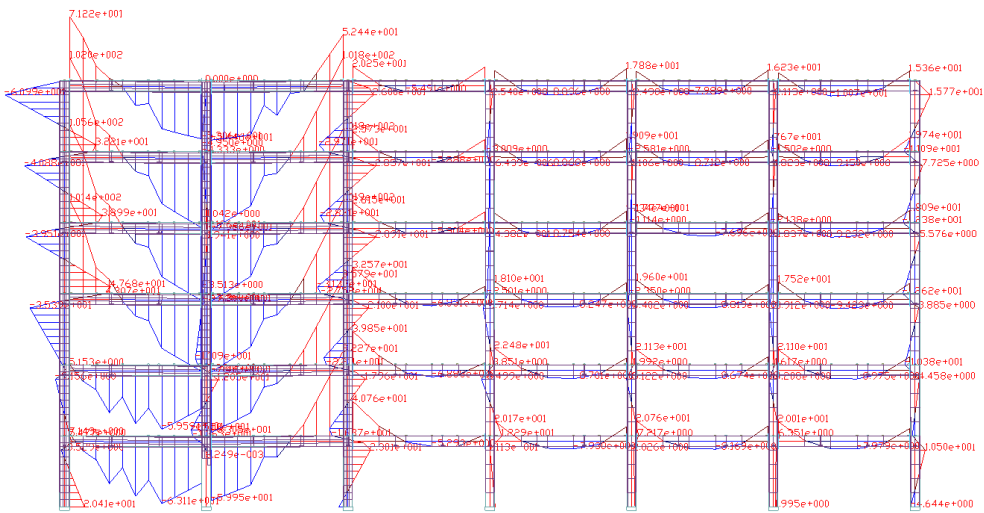


Figure 29. Bending moment diagram after D2 column removal scenario [tonf m].

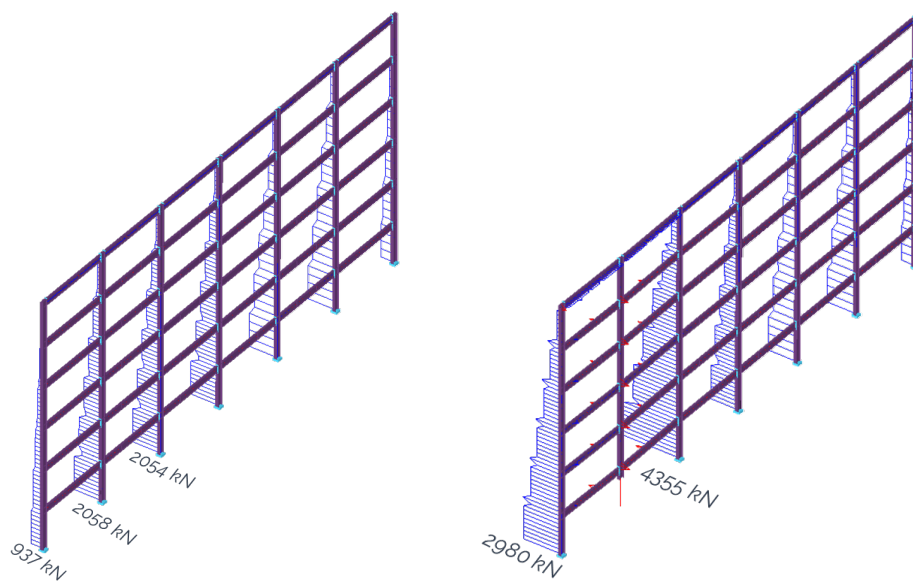


Figure 30. Axial force diagram before and after D2 column removal scenario [tonf].

The results presented above were obtained using the design level of gravity loads: $DL + 0.5 \times LL$ (i.e., $\lambda = 1$). To evaluate the strength reserve against progressive collapse for cases C/D1, D1, D2, D3, D4, the gravity loads were increased by means of the gravity load multiplier, λ . Then, the columns were removed using the same procedure as above.

In the following, only the results for scenario D4 are discussed. As it can be seen from Figure 31, the progressive collapse is initiated for $\lambda = 1.4$ due to the failure of beam-to-column connections for beams IPE600.

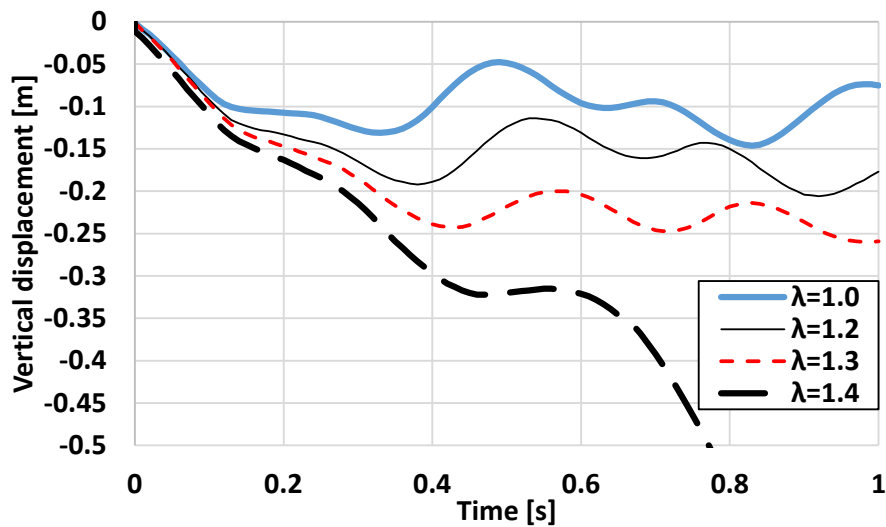


Figure 31. Time-history vertical displacement curves for scenario D4 at different gravity load multiplier λ

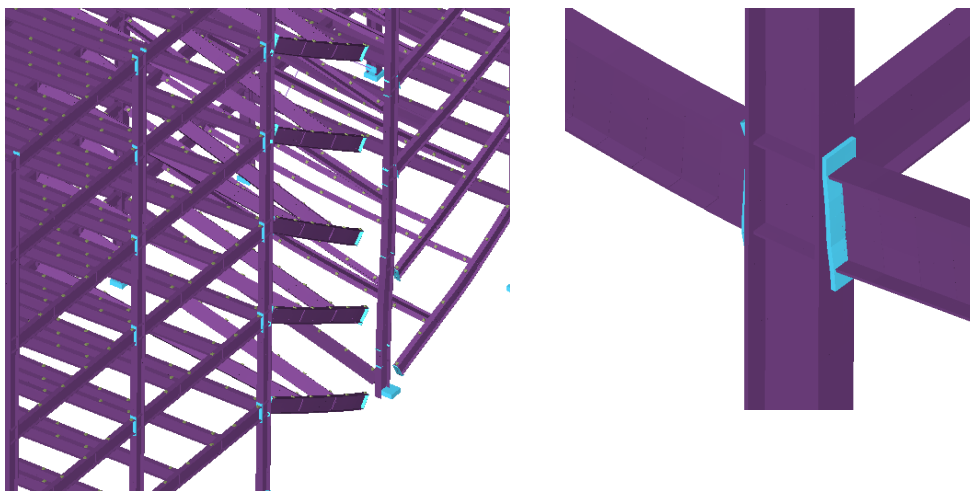


Figure 32. Failure of beam-to-column joint triggers the progressive collapse (scenario D4, $\lambda = 1.4$)

Based on the results obtained, the following remarks can be made :

- In the case of C4 column removal, where all adjacent beams are pinned, computed for shear only, the structure is not able to transfer the loads, thus undergoing progressive collapse.
- All other scenarios result in safe response of the structure (plastic deformations develop but progressive collapse is prevented)
- If higher gravity loads are present on the structure, progressive collapse may also initiate – see case D4, $\lambda = 1.4$. If this is the case, the structure requires redesign.

The redesign can be done using different strategies. The most efficient strategy is based on the activation of the catenary effects. Considering the weak point is the capacity of beam-to-column connection, in the following, the strengthening strategy involves stiffening of the connection by means of vertical ribs on both top and bottom sides of the beam ends.

- Improving the connection typology

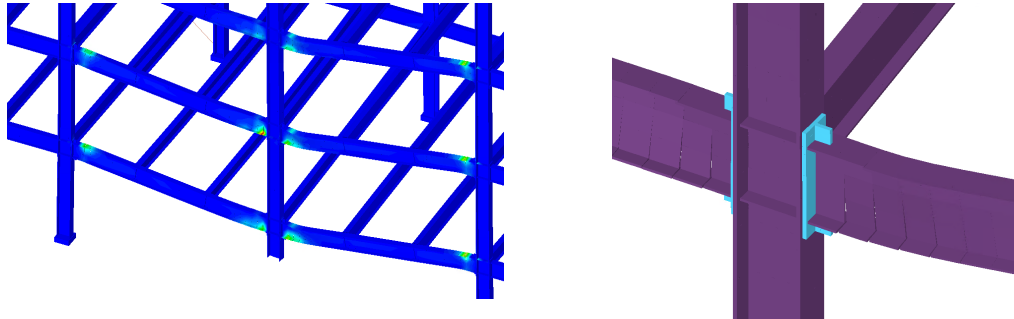


Figure 33 Structure with SEP: stain map on failure mode (left) and detail (right)

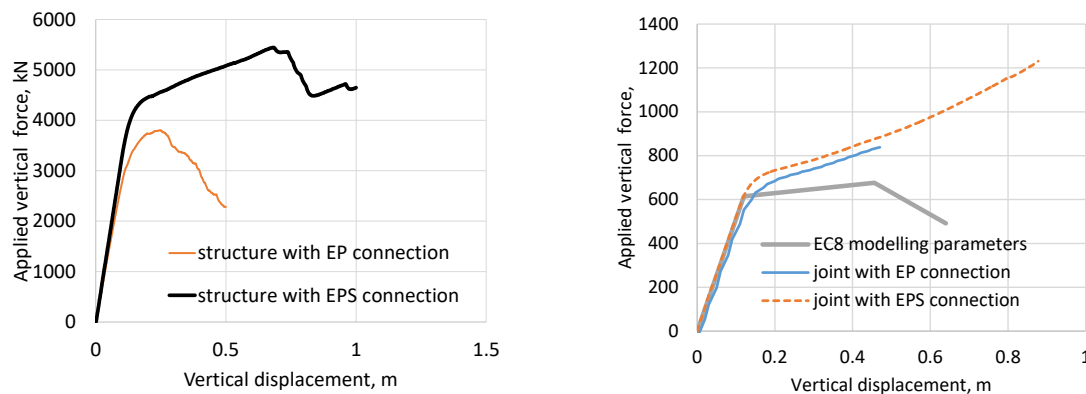


Figure 34 pushdown curves for structure (left) and for one frame with one level (right)

To compare the efficiency of the stiffening technique, push-down analysis is done on structure with EP connection and structure with stiffened connections (EPS).

The analysis assumes the column is removed then the gravity load on the floors is incremented up to the attainment of failure, obtaining the so-called capacity curves. Figure 34 presents comparatively the capacity curves before and after the strengthening of the connection. As seen, the unstiffened end plate connection has a limited deformation capacity and fails before the development of any catenary action in beams.

The stiffened connections have the capacity higher than the beam and the plastic deformation develop in the beam ends rather than in the connection. This allows a significant increase in capacity, partly in flexural, but mostly in catenary.

As seen in charts from Figure 34, column removal situations where adjacent main beams have continuous connections result in limited vertical deflections.

Conclusions

The perimeteral columns have no problems in finding alternate load paths to redistribute the load for a gravity load multiplier of $\lambda=1$, withstanding almost double the load.

The interior column part of the gravity resisting system (connected only by pinned beams) is especially vulnerable. Losing such a column implies progressive collapse of the tributary bays of the column. For columns B4 and C4, redesign of the connections would improve the performance in case of column

loss, or, alternatively, protecting the columns to reduce or eliminate the risk of local damage can be another approach.

3.4 Final design outputs and remarks

The design output (sections and connections) is mostly determined by the seismic requirements, therefore allowing the structure to have significant capacity reserves.

For identified accidental actions, the structure can withstand the analysed scenarios, without triggering progressive collapse, even in case of multi-hazard assessment.

For unidentified accidental actions verifications, the vulnerable scenarios represent column removals from zones which are not part of the seismic lateral resisting system. For these cases, the strengthening of the connection in terms of moment capacity may lead to a solution with more robustness, able to resist progressive collapse.

4 Composite Structure in Seismic area (UPT)

4.1 Description of the design and main outputs

The CS/S case is very similar with SS/S one (same sections are used, except for the interior beams, and similar structural performance was obtained), detailed in section 3, so a shorter description of the design is presented.

The output of the design for CS/S is presented in Table 21 to Table 23. The cross sections for the different categories of beams and UF for strength (including buckling resistance where appropriate) and stiffness are presented in Table 21. Compared to SS/S case, a reduction in cross-section for the interior beams was made, as mentioned in the noted below the same table, owing to the composite effect.

Table 22 presents the cross sections for the different categories of columns and the utilization ratios for strength (including buckling resistance). The UF for columns of the Lateral Load Resisting System LLRS refer to the same conditions as mentioned for SS/S and have a similar value.

Table 23 presents the cross sections for the braces and the utilization ratios for strength (including buckling resistance). It may be inferred that the sections are the same as for SS/S case, with very small differences in case of UF. Consequently, the verification for the slenderness was presented in 3.1 and is not resumed for the current case. Similarly, the total overstrength factor considered for the design of the non-dissipative elements was $\Omega_T = 3.0$, as in the SS/S, owing to the similarity in UF and sections.

The SLS verification for the wind action is presented in As in SS/S case concerning the condition for homogeneity, (25% maximum difference between UF elements on elevation) it was fulfilled for most elements, except the last two stories on X direction due to the requirement of using Class 1 section for high ductility class.

Table 24. The ratio between the lateral top displacement and the acceptable limit has a maximum value of approximately 0.1, as in the case of SS/S.

Table 21. Utilization factors for beams – CS/S

Case	Element	Direction ¹	Storey	Section	Utilization factor	
					Strength	Deflection ³
CS/S	Perimeter beams ²	X	1-6	IPE550	0.278	0.178
		Y	1-6	IPE600	0.302	0.157
	Interior beams ²	X	1-6	IPE400	0.627	0.971
		Y	1-6	IPE450	0.874	0.94
	⁵ Inner core beams	X	1-3	⁴ H800	0.936	-
			4-5	HEM800	0.953	-
			6	HEM700	0.789	-
		Y	1-3	HEM500	0.859	-
			4-5	HEB500	0.878	-

¹See Figure 2 for the orientation of the axes

²Nelson studs d=19mm, h=100 mm / 160 mm – steel beams fully connected to a solid slab of 12cm

³Deflection verification criterion: L/250 for secondary beams, L/350 for main beams

⁴H800 is a built-up section, having the same height as regular HEM800, with b = 380mm, t_f = 50 mm, and t_w = 30 mm.

⁵S460 steel grade used for the inner core beams.

Table 22. Sections and utilization factors for columns – CS/S

Case	Element	Section	Utilization factor
CS/S	Corner columns	HE550B	0.48
	Perimeter columns	HE500B	0.71
	Inner Core columns	HD400X463	0.95

Table 23. Sections and utilization factors for braces – CS/S

Case	Element	Direction	Storey	Section	Utilization factor
CS/S	Brace	Y	1-3	HEA320	0.41
			4	HEA260	0.43
			5	HEA220	0.46
			6	HEA200	0.40
		X	1-3	HEB340	0.41
			4-5	HEA320	0.39
			6	HEA260	0.26

As in SS/S case concerning the condition for homogeneity, (25% maximum difference between UF elements on elevation) it was fulfilled for most elements, except the last two stories on X direction due to the requirement of using Class 1 section for high ductility class.

Table 24. SLS check for LLRS against wind action – CS/S

Case	Direction	Top displacement [mm]
CS/S	X	4.61
	Y	3.16

Regarding the specific verifications for the structures in seismic zone, Table 25 presents the interstorey drift check at Damage limitation state. As it may be observed, the structure successfully fulfils the limitation to 0.75%, having the largest value of 0.24%. The structure has also been checked at ULS in terms of interstorey drift limitation. Similarly to Damage limitation state, an interstorey drift verification was done as in the case of SS/S structure. The acceptable limit for this verification is 2.5% H_{st} , and as presented in Table 26, all values are below this limit, the largest being 0.49%.

Table 25. Interstorey drifts for CS/S – DL

Case	Storey	Direction	Drift [%]
CS/S	6	X	0.172
	5		0.210
	4		0.243
	3		0.220
	2		0.222
	1		0.182
	6	Y	0.190
	5		0.241

Table 26. Interstorey drifts for CS/S - ULS

Case	Storey	Direction	Drift [%]
CS/S	6	X	0.343
	5		0.419
	4		0.486
	3		0.440
	2		0.444
	1		0.364
	6	Y	0.381
	5		0.482

4	0.238	4	0.476
3	0.203	3	0.406
2	0.192	2	0.385
1	0.148	1	0.296

The results for the verification of the second-order effects are provided in Table 27. As it may be observed, the largest value for θ is 0.096, as for SS/S case, and the effect of the second order effects may be neglected, having a value smaller than 0.1. The procedure to evaluate the contribution of the MRF for the dual frame system is detailed in section 3.1. Owing to the similar forces (lateral and vertical used for the assessment of second order effects) and sections, As presented in Table 28, in both directions the necessary flexural capacity is smaller than the efficient one, hence the duality condition is checked for CS/S.

Table 27. Second order effects for CS/S

Case	Storey	h	P_x	V_x	d_x	θ_x	Case	Storey	h	P_y	V_y	d_y	θ_y
		[mm]	[kN]	[kN]	[mm]	[rad]			[mm]	[kN]	[kN]	[mm]	[rad]
CS/S	6	4000	10867	1753	60.73	0.094	CS/S	6	4000	10867	1883	59.11	0.085
	5	4000	21734	2985	52.73	0.096		5	4000	21734	3178	50.08	0.086
	4	4000	32602	3914	42.76	0.089		4	4000	32602	4097	38.54	0.077
	3	4000	43469	4630	30.99	0.073		3	4000	43469	4813	26.98	0.061
	2	4000	54336	5195	20.16	0.053		2	4000	54336	5379	16.98	0.043
	1	4000	65203	5526	9.10	0.027		1	4000	65203	5710	7.40	0.021

Table 28. Contribution of the MRF frames for the LLRS – CS/S

Case	Story label	Direction	V_i [kN]	$0.25 V_i$ [kN]	n	$M_{Rd,nec}$ [kNm]	W_{nec} [mm ³]	Section	W_{eff} [mm ³]	$M_{Rd,eff}$ [kNm]
CS/S	6	X	1753.4	438.3	12	73.1	205796.4	IPE550	2787000	989.4
	5		2984.7	746.2	12	124.4	350314.6	IPE550	2787000	989.4
	4		3913.5	978.4	12	163.1	459332.4	IPE550	2787000	989.4
	3		4630.1	1157.5	12	192.9	543444.7	IPE550	2787000	989.4
	2		5194.7	1298.7	12	216.4	609711.1	IPE550	2787000	989.4
	1		5526.1	1381.5	12	230.3	648600.5	IPE550	2787000	989.4
	6	x	1882.8	470.7	12	78.4	220980.2	IPE600	35112000	12464.8
	5		3178.0	794.5	12	132.4	373009.1	IPE600	35112000	12464.8
	4		4096.9	1024.2	12	170.7	480855.4	IPE600	35112000	12464.8
	3		4813.0	1203.2	12	200.5	564905.2	IPE600	35112000	12464.8
	2		5378.9	1344.7	12	224.1	631327.2	IPE600	35112000	12464.8
	1		5710.0	1427.5	12	237.9	670185.7	IPE600	35112000	12464.8

4.1.1 Connections

The typology of connections which are of interest for the worked example are the following:

- Beam-to-column connections for MRFs (of LLRS)
- Beam-to-beam and beam-to-column connections for gravitational load resisting system

In case of the beam-to-column connections for MRFs, prequalified seismic moment resisting connections were adopted as in SS/S case (see Equal Joints project), choosing the same typology, the extended end-plate connection was preferred. Since no cross-sectional changes were made for the MRFs, the same configurations were used as for SS/S case. Moreover, as the slab is considered totally disconnected from the steel frame in a circular zone around a column (see EN 1998-2), the composite character of beams with slab was disregarded in the calculation of the joint. The summary of the results for the moment resisting connections may be found in Table 14 from section 3.1.1. A typical connection configuration is presented in Figure 3 and the properties of the elements (plates and bolts) are presented in Table 15.

For the other elements (beam-to-beam as well as beam-to-column except the MRFs and the braced core) pinned connections were used as for SS/S case. As typology, pinned connection with cleats were used for CS/S. The summary of the results for the pinned connections is presented in Table 29. The configuration is the same between the joints, only the connecting elements differ.

Table 29. Results of pinned connections at ULS - CS/S

Case	Position	Story	Connection type	Shear resistance (kN)	Failure mode	UF*
CS/S	A/1-7, D/1-7 IPE400-IPE600	1-6	Cleat angle	196	Sec. beam in bearing	0.90
	B/1-7, C/1-7 IPE400-IPE450	1-6	Cleat angle	196	Sec. beam in bearing	0.97
	B/2, B/5, C/2, C/5 - IPE550-HEM500	1-3	Cleat angle	196	Sec. beam at notch	0.74
	B/2, B/5, C/2, C/5 IPE550-HEB500	4-6	Cleat angle	196	Sec. beam at notch	0.84

* Utilisation factor is defined for ULS, persistent design situation, only

Figure 35 presents the view of a pinned connections (joint connecting a secondary beam IPE400 with a main beam IPE550 between frames A/1-7 and D/1-7).

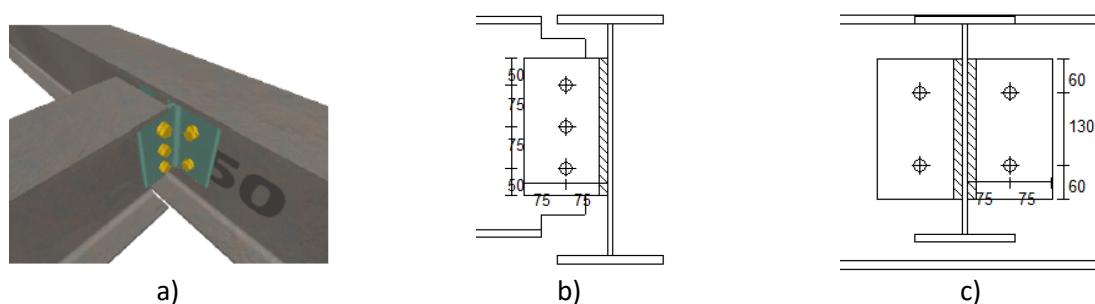


Figure 35 Configuration of pinned joint – frames B/1-7, C/1-7 – CS/S: a) 3D view of the joint, b) side view of the joint, c) front view of the joint

For the connection L150x15 cleats from S355 steel grade have been used. 3 M20 Gr. 10.9 were used for the secondary beam and 4 M20 Gr. 10.9 for the main beam.

4.2 Verifications for identified actions

4.2.1 Impact

4.2.1.1 Equivalent static approach

This example gives information about the design against impact due to accidental collision of a vehicle using an equivalent static approach.

The following actions are considered for the accidental design situation:

- Permanent loads DL (see Table 4)
- Live loads LL (see Table 4 for CS/S structure)
- Impact action A_{Ed} (see section below)

The combination of actions for the accidental design situation is:

$$DL + 0.5 \times LL + A_{Ed}$$

Impact scenarios include perimeter columns along traffic lines. In the example, both long (along vertical traffic lane) and short (along horizontal traffic lane) facades are exposed.

The impact gives rise to a collision force that has components parallel and perpendicular to the direction of travel. In design, the two components can be considered independent.

Impact assumptions:

- Exposed columns: first floor (C1-C5 – see Figure 36 and Figure 37)
- Impact point height: 1.5m
- Impact forces (see Table 30)

Table 30. Impact forces for linear static analysis – CS/S

Case	F_{dx} (kN)	F_{dy} (kN)
C1	1000	500
	500	100
C2	1000	500
C3	1000	500
C4	1000	500
C5	1000	500

The impact loads are calculated using data from Table 4.1 of (EN 1991-1-7 2006), considering the case: *Motorways and country national main roads*.

A **linear elastic analysis** is made on the full 3D model using SAP2000 software. The section of the elements are those resulted from the initial design (persistent and seismic design situations). The acceptance criteria are given in terms of utilization factors (UF) for accidental combinations, only.

Table 31 presents the results for the scenarios considered.

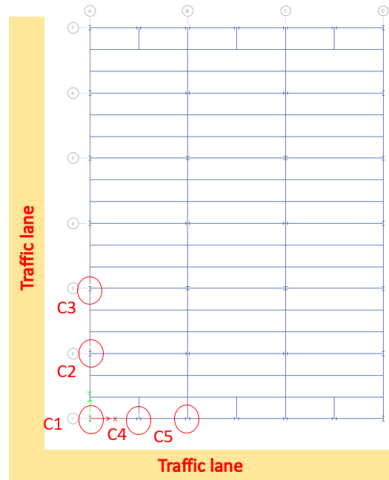


Figure 36. Road layout

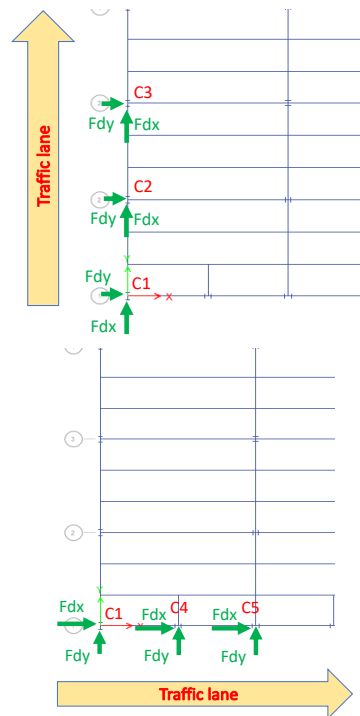


Figure 37. Plan views with direction of impact for each traffic lane

Table 31. Results of linear static analysis – CS/S

Case	Section	Impact force [kN]	Axis	Bottom support	N [kNm]	M [kNm]	U.F. [-]	Critical impact force **[kN]	
C1	HEB550	1000	Major	Fixed	1048	670	0.478	2700	
		500	Minor	Fixed	1053	230	0.656	800	
		500	Major	Fixed	*				
		1000	Minor	Fixed	1074	625	1.313	-	
C2	HEB500	1000	Major	Fixed	2218	677	0.899	1250	
		500	Minor	Fixed	2216	342	1.044	-	
C3	HEB500	1000	Major	Fixed	2229	681	0.9	1250	
		500	Minor	Fixed	2238	342	1.048	-	
C4	HEB500	1000	Major	Fixed	591	755	0.63	1300	
		500	Minor	Fixed	647	339	0.74	700	
C5	HEB500	1000	Major	Fixed	1687	787	0.864	1800	
		500	Minor	Fixed	1696	340	0.954	550	

* The scenario is less demanding as the column was already verified for the same impact load applied according to the weak axis of the section

** Impact force that causes the failure of the column (UF=1).

Based on the results, the following conclusions were drawn:

- Six out of nine impact scenarios satisfy the UF criterion, resulting in a proper design.
- Three out of nine impact scenarios result in capacity exceedance. However, the results may be conservative, as they are obtained using a simplified static analysis. Therefore, for the

verifications that are not fulfilled using this approach, a capacity assessment with more sophisticated approaches may be use instead (see worked example from section 4.2.1.2)

- To mitigate the impact, the hazard may be prevented or eliminated
- In order to improve the design and response to impact load, other measures can be implemented:
 - Higher steel grade for columns
 - Column oriented to obtain maximum impact resistance.

4.2.1.2 Simplified dynamic approach

This example gives information about the design against impact due to accidental collision of a vehicle using simplified dynamic approach.

The following actions are considered for the accidental design situation:

- Permanent loads DL (see Table 4)
- Live loads LL (see Table 4 for CS/S structure)
- Impact action A_{Ed} (see section below)

The combination of actions for the accidental design situation is:

$$DL + 0.5 \times LL + A_{Ed}$$

The impact scenarios include perimeter columns along traffic lanes, as previously defined in worked example from 4.2.1.1. In the current worked example, however, a single scenario is detailed, i.e., column C1 (UF = 1.313), minor axis impact, which has the highest U.F. according to equivalent static approach design – see Table 31, worked example 4.2.1.1 for the forces considered.

A nonlinear dynamic analysis is made on a single column (isolated from the structure) using SAP2000 software.

The impact direction is along the weak axis, similar with the application of force F_{dx} , considering a vehicle speed and mass of $v_r= 90$ km/h and $m=3.5$ tons, respectively.

The column is made from HEB500, S355 steel, and is 4.0 m high. The column has the following boundary conditions:

- the column base is fixed,
- top of the column has all degrees of freedom fixed, except for the vertical displacement, which is unrestrained.

The analysis is performed in two steps:

1st step: vertical nodal load corresponding to the top of the column obtained from the static analysis in the accidental combination ($DL + 0.5 \times LL$) is applied as an axial compressive force using a static analysis.

2nd step: the impact force is applied transversally on the weak axis direction, using a dynamic nonlinear analysis and hard impact approach.

Computation

$$F = v_r \sqrt{k \cdot m}$$

where:

- v_r - impact velocity
- m - impact mass
- K - stiffness of the impact object

The parameters are calculated considering the same type of road (*Motorways and country national main roads*):

- $K= 300$ [kN/m] = 300000 [N/m]

- $v_r = 90 \text{ km/h} = 25 \text{ [m/s]}$
- $m = 3500 \text{ kg}$

This results in:

$$F = v_r \sqrt{k \cdot m} = 25 \sqrt{300000 \cdot 3500} = 810000 \text{ N} = 810 \text{ kN}$$

Note: If the impact force is amplified by the recommended value of DLF (DLF = 1.4), for the proposed vehicle velocity of 80 km/h (Table C1 of EN1991-1-7) the equivalent dynamic impact force, F_{equiv} , calculated above is similar to the one applied in the static analysis (see section worked example from 4.2.1.1):

$$F_{equiv} = 80 / 3.6 \sqrt{300 \cdot 3.5} \cdot 1.4 = 1008 \text{ kN}$$

In the dynamic analysis, the force is applied using a ramp function with instant rise and a duration of: The total duration of the dynamic analysis is one second (larger than the ramp function duration Δt), to verify if the column remains stable after the ramp function ends.

The nonlinear behaviour is modelled using plastic hinges at each column end and at the point of impact using P-M2-M3 interaction. The plastic hinges are modelled using fibres.

The effect of the fast impact loading is considered using a DIF (strain rate effect) applied to the material resistance.

The DIF formulation for hot-rolled steel with yield strength up to 420 N/mm² can be expressed according to (CEB 1988) method.

The strain rate ($\dot{\epsilon}$) is obtained in an iterative procedure. In the first iteration, the ratio between the specific deformation and the time up to the point of yielding is computed based on the analysis results without applying a DIF. Afterwards, the analysis is performed again with the modified material properties by using a DIF, followed by DIF recalculation. If the new DIF values are comparable with the ones from the previous step (convergence), no further iterations are needed.

$$\text{DIF} = \frac{f_{dy}}{f_y} = 1 + \frac{6.0}{f_y} \ln \frac{\dot{\epsilon}}{5 \times 10^{-5}}$$

$$\text{DIF} = \frac{f_{du}}{f_u} = 1 + \frac{7.0}{f_u} \ln \frac{\dot{\epsilon}}{5 \times 10^{-5}}$$

$$\text{DIF}(f_y) = 1.118$$

The column can sustain the impact force, but with incipient plastic deformations at the point of impact (see Figure 39) 0.054% normal strain, 0.073% at the bottom end and 0.036% at the top end of the column.

Figure 38 shows the lateral displacement history of the column at the impact point. The peak horizontal displacement is 29.12 mm, with a residual deflection of 16.47 mm.

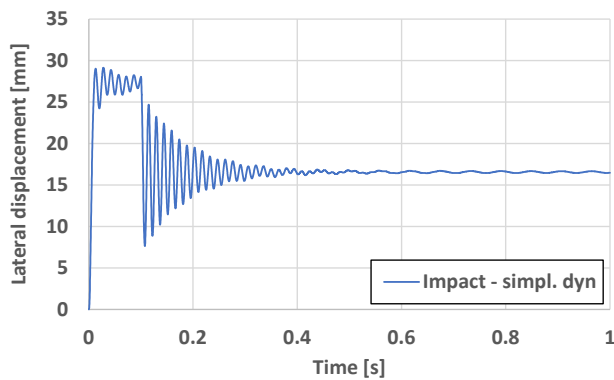


Figure 38. Lateral displacement time history at point of impact – CS S

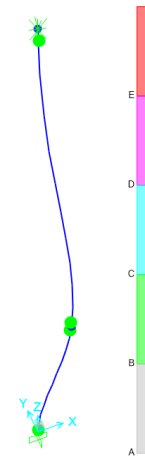


Figure 39. Plastic hinges – CS S

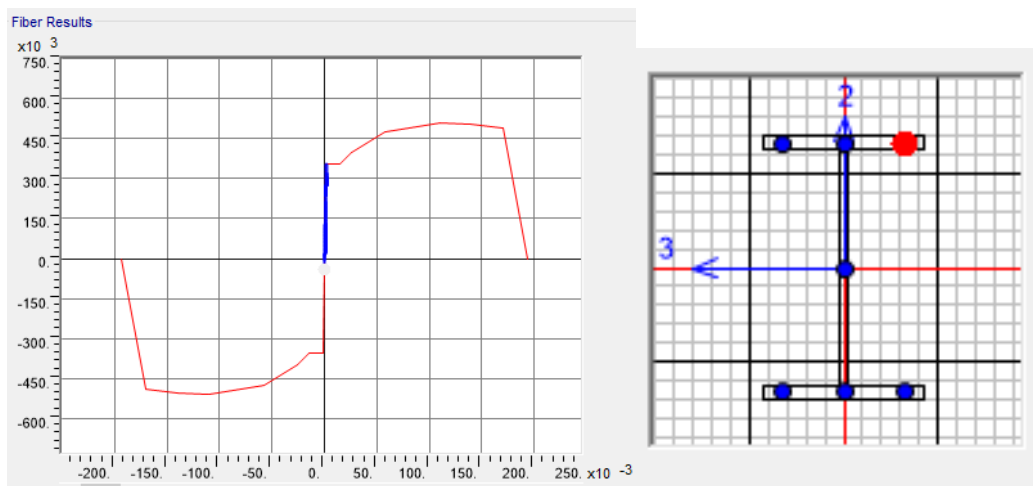


Figure 40. Lateral displacement time history at point of impact – CS S

It may be concluded that the application of equivalent static approach (W.E 4.2.1.1) indicated that the utilisation factor exceeds unity → redesign is needed. However, if plastic deformations are allowed to develop in the column, the design becomes **acceptable** by applying a *simplified dynamic approach* → end of design.

4.2.1.3 Full dynamic approach

This example gives information about the design against impact due to accidental collision of a vehicle using a full dynamic approach.

The following actions are considered for the accidental design situation:

- Permanent loads DL (see Table 4)
- Live loads LL (see Table 4 for CS/S structure)
- Impact action A_{Ed} (see section below)

The combination of actions for the accidental design situation is:

$$DL + 0.5 \times LL + A_{Ed}$$

For definition of impact scenarios, see example W.E 4.2.1.1, with specific details considered in worked example 4.2.1.2.

Impact parameters

The parameters are calculated considering the same type of road (*Motorways and country national main roads*):

- $K = 300 \text{ [kN/m]} = 300000 \text{ [N/m]}$ stiffness of the impact object
- $v_i = 90 \text{ km/h} = 25 \text{ [m/s]}$ impact velocity
- $m = 3500 \text{ kg}$, impact mass

A nonlinear dynamic analysis is made on full 3D model using ELS software.

Modelling criteria in ELS

To analyse a complex structural behaviour, such as an object collision followed by separation of elements and possible collapse, the response of structure after impact with a vehicle was explicitly modelled in ELS.

Details about model assumptions in AEM are provided in the worked example from section 3.2.1.2.

The analysis is performed in two steps.

1st step: the permanent and live load are applied on the structure in a nonlinear static analysis

2nd step: the impact body is colliding with the C2 column in a dynamic nonlinear analysis.

Model Assumptions for impact

The impacting body (i.e., car) is allowed to slide on the horizontal plane only, at a height of 1.5 m, and has mass assigned to account for the weight of 3.5 tones. The initial velocity of the object is 25 m/s. The impact object is composed of a contact plate, a plate with assigned mass, and axial springs between them. The height of the contact zone between the lorry and the column is considered 0.6 m. The stiffness of 300 kN/m is modelled with the help of elastic springs.

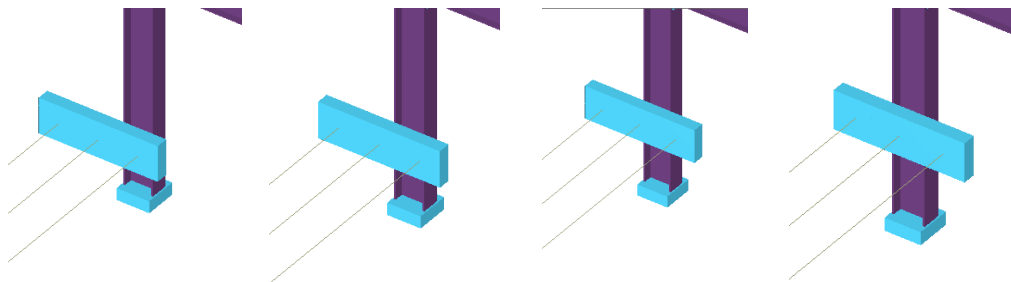


Figure 41. Collision object moving towards

The analysis shows limited plastic deformations, with a maximum lateral deflection of 10.6 mm as presented in Figure 42c.

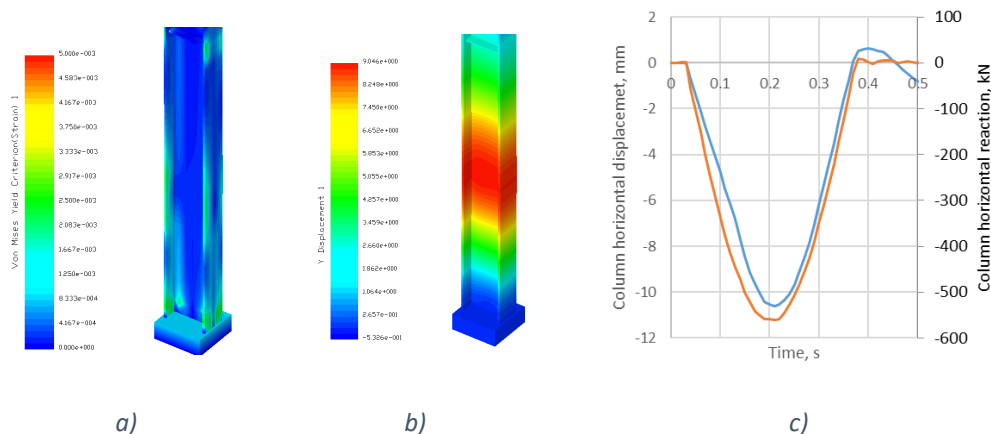


Figure 42. Results for impacted column: a) strains; b) deformations; c) horizontal base reaction force (orange) and horizontal displacement at impact point (blue)

Compared with the worked example from 4.2.1.2, full dynamic approach results in less deformation (as presented in Figure 43), as the restraining provided by the adjacent structure (especially the vertical restraining) is taken into account, and the “real” rise function of the impact force is less steep than the one applied for simplified dynamic approach.

Note that explicit consideration of *impact object-structure* interaction may result in much higher demands than typically considered in simplified dynamic analysis (Dubina, Marginean, and Dinu 2019).

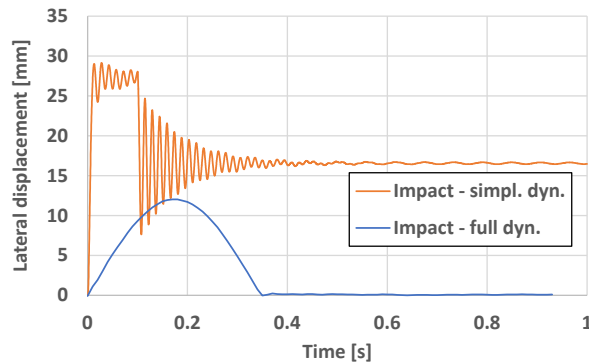


Figure 43. Lateral displacement in time – comparison of dynamic approaches

4.3 Verifications for unidentified actions

4.3.1 ALPM

4.3.1.1 Prescriptive approach – Tying method

This example shows the application of the tying method for beams and their connections (horizontal tying).

The following actions are considered for the accidental design situation:

- Permanent loads DL (see Table 4)
- Live loads LL (see Table 4 for CS/S structure)
- No specific accidental action is taken into account

The verification is performed the same as in case of worked example from section 3.3.1.1, for main beam, but also the longitudinal reinforcement in the effective length of the beam is taken into consideration.

Computation

- internal pinned main beams

Spacing between ties (main beams) $s = 12m$

Span of the tie $L = 8m$

Design tensile load for internal ties

$$T_i = \max[0.8(g_k + \Psi \cdot q_k) \cdot s \cdot L; 75kN] = \max[0.8(5 + 0.5 \times 3)12 \times 8; 75kN] = 499.2 kN$$

The axial force capacity of the main beam connection is the sum of the tension force transferred through the bolts and the tension force transferred through longitudinal reinforcement in the effective width of the reinforced concrete slab.

Results

$$N_u = 392 \text{ kN} + 73 \text{ kN} = 465 > T_i = 499.2 \text{ kN} \rightarrow \text{connection redesign is required.}$$

Therefore, 3 bolts rows M20 10.9 were provided instead of 2, as presented in Figure 21 with the new joint configuration.

$$N_u^* = 661 \text{ kN} > T_i = 499.2 \text{ kN}, \text{UF} = 0.76$$

It may be concluded that all internal main pinned beams and their connections check the verification for required tying forces, with limited changes in the design required.

As previously state in W.E from 3.3.1.1, it may be concluded that the design for gravity loads may be insufficient for tying force requirements in case of large tributary areas.

4.3.1.2 Full numerical approach

This example gives information about the design against unidentified threats using the full numerical approach from ALPM.

The following actions are considered for the accidental design situation:

- Permanent loads DL (see Table 4)
- Live loads LL (see Table 4 for CS/S structure)
- No specific accidental action is considered.

The combination of actions for the accidental design situation is:

$$DL + 0.5 \times LL$$

The same scenarios are used as in the case of W.E from section 3.3.1.3, see Figure 44.

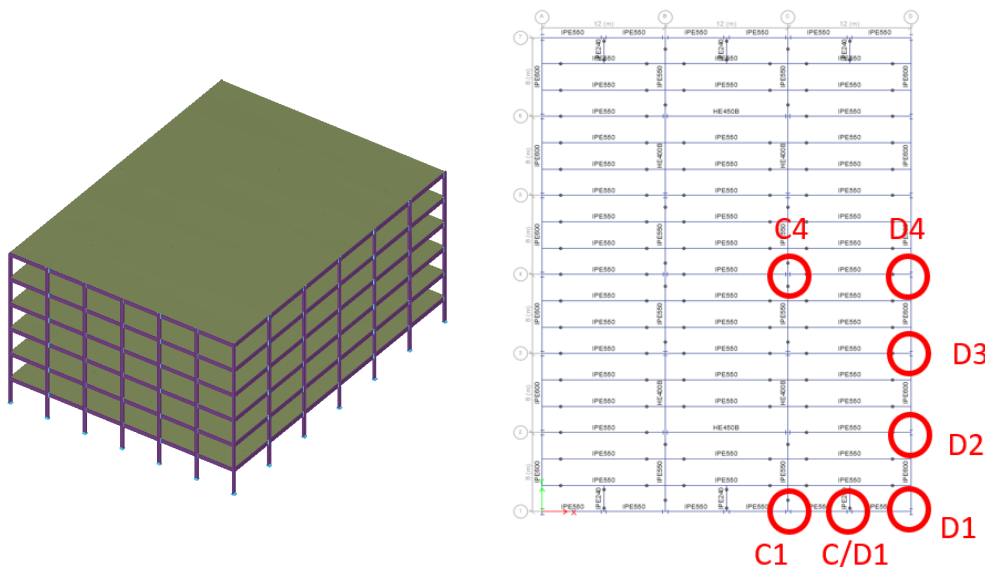


Figure 44. Isometric view of the structure (left) and location of columns to be removed for ALPM – full numerical approach (right)– CS/S

Modelling assumptions and analysis procedure follow the same methods as presented in the 3.2.1.2. The only difference is the addition of the concrete slab (concrete and reinforcement) and the interaction with the steel structure (shear studs) (details are given in Table 5). Note that the steel structure (elements and connections) is the same as in case of the bare steel structure SS/S. Besides the assumptions made for the calibration of the Steel Structure numerical model each Nelson

connector was modelled in the structure with its corresponding shear and tension capacity. The model was calibrated against relevant experimental data (Dinu et al. 2016), see Figure 45

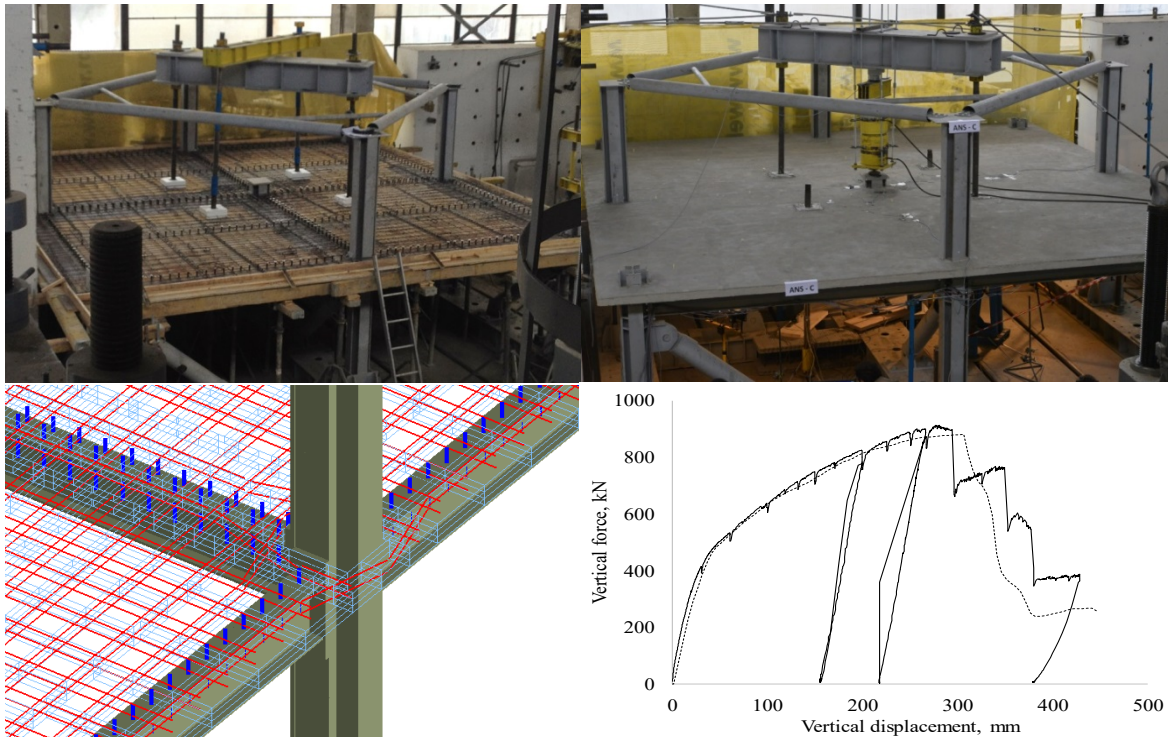
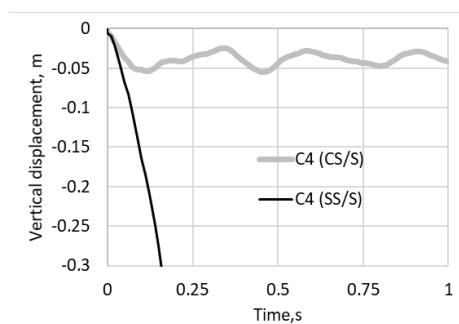
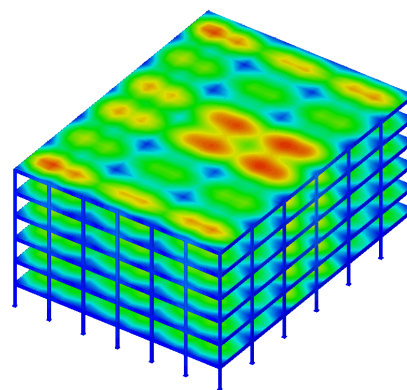


Figure 45. Calibration of model with composite slabs: experimental specimen(top) and numerical model and calibration curves (bottom)

The results of the NDP show that the CS/S structure has the capacity to resist progressive collapse for all removal scenarios, including scenario C4 which proved to be critical for structure SS/S. Figure 46a shows comparatively the force displacement curve CS/S and SS/S for scenario C4 and gravity load multiplier $\lambda = 1$. Figure 46b shows the deformed shape for CS/S. The structure exhibits limited plastic deformation in steel elements and concrete slab in the area affected by the column loss – see Figure 46c,d.



a)



b)

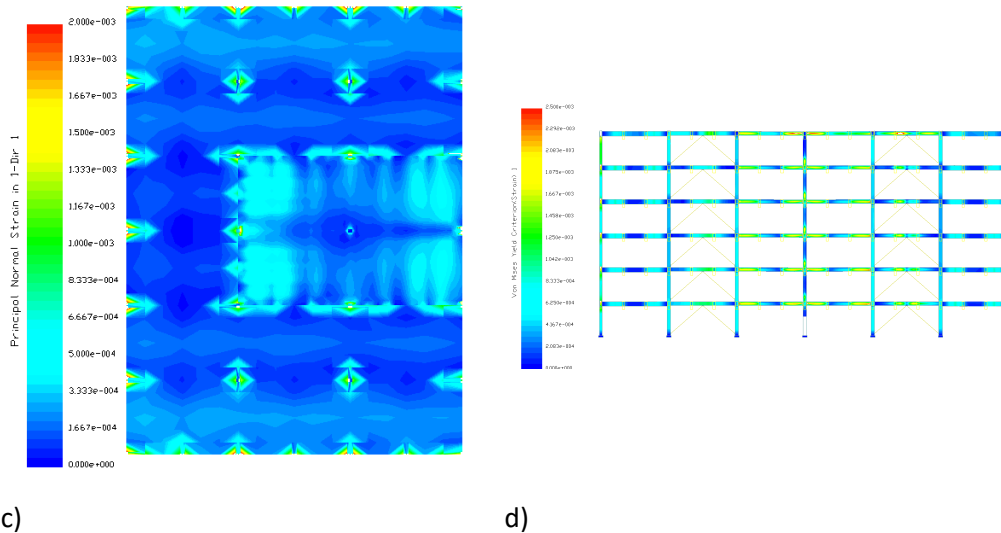


Figure 46. Results for CS/S and scenario C4: a) vertical force vs vertical displacement – CS/S vs SS/S, b) isometric view of the deformed structure, c) current plan view with the deformations in the concrete slab (bottom side), d) deformations in steel elements frame C/3-5

The following conclusions were drawn:

- The interaction between steel frame and concrete slab provides additional capacity to resist the column loss without the development of progressive collapse.
- The steel-concrete interaction is beneficial especially for frames with pinned beam ends as the axial force requirement in beams to allow the development of catenary action can be excessive.

4.4 Final design outputs and remarks

Composite action between steel beams and concrete slab provides additional redistribution capacity and can considerably reduce the local damage and the risk of progressive collapse. The connections are reinforced due to the additional level arm given by the reinforcement of the concrete slab in bending moment, while in tension, the tensile capacity of the reinforcement is added to the tensile capacity of the connection.

Scenarios which would lead to progressive collapse without composite action (i.e. C4 column removal) when modelled with the reinforced concrete slab working together with the steel beams and connection, result in analyses where local damage is contained and is not propagated.

5 Steel Structure in Non-Seismic area (F+W)

5.1 Description of the design and main outputs

5.1.1 Design checks

The structural analysis is performed by means of a 3D model using the SCIA (version 2019) software. An illustration of the model is given in Figure 47. Internal forces and deformations are obtained by carrying a 2nd order analysis.

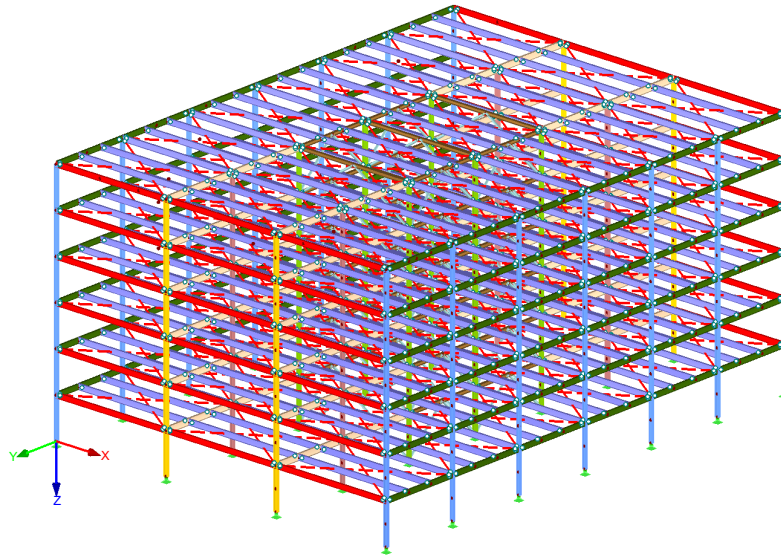


Figure 47. 3D view of the FE model

All checks have been performed according to Eurocode including the German National Annex.

5.1.2 Members

Members cross-sections have been optimized according to ULS/SLS requirements.

Member cross-sections are illustrated in the following figures. ULS and SLS results for the chosen cross-sections are summarized in the following table. Some of the beam cross-sections are required to limit vertical deformations ($L/250$ for rare load case combination).

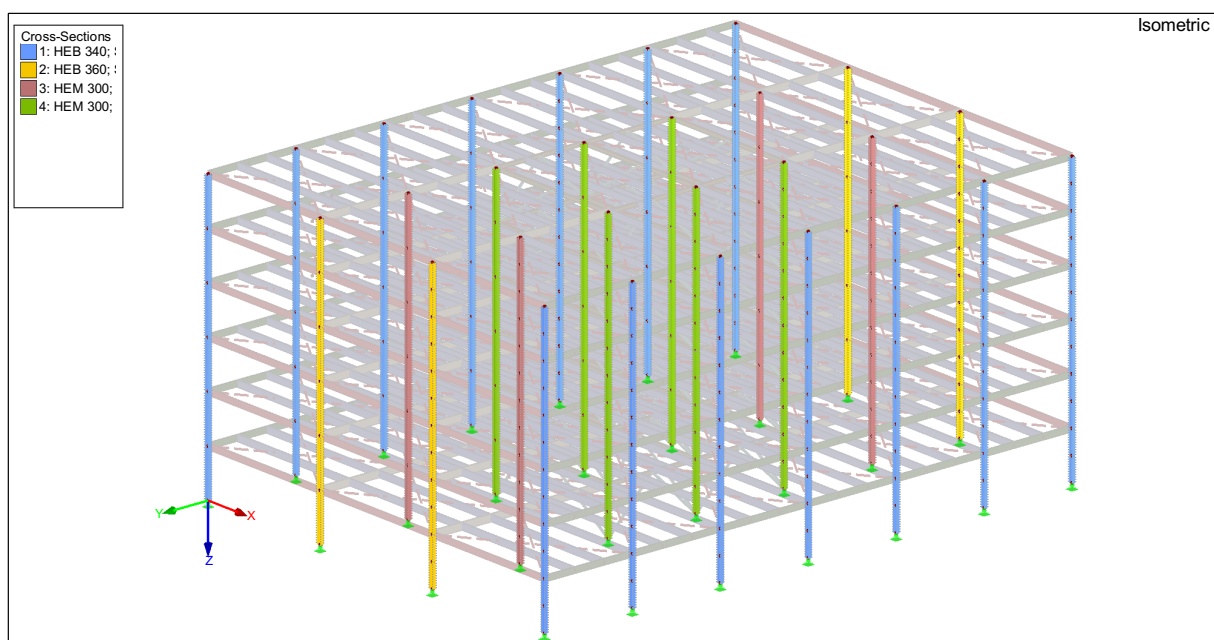


Figure 48. Columns cross-sections

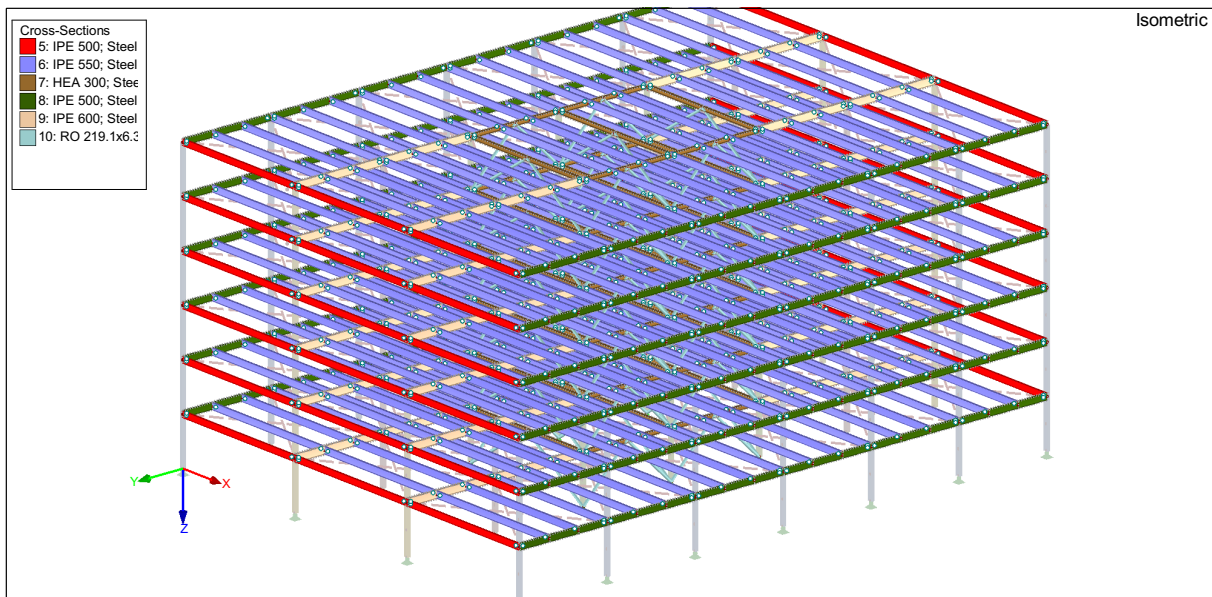


Figure 49. Beams cross-sections

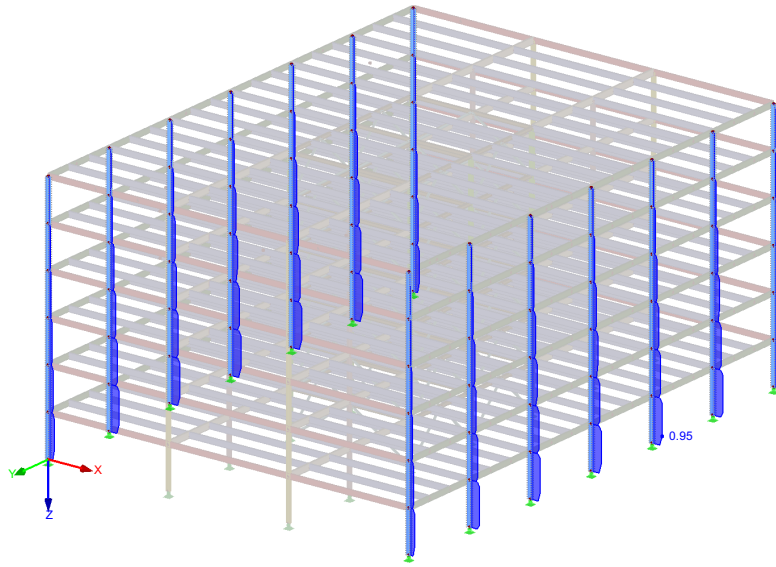
Table 32. ULS utilization factors and SLS deflections

Element	Section	ID	ULS utilization factor	SLS deflection (rare combination)
Columns Y-facades	HEB 340	1	0.95	-
Columns X-facades	HEB 360	2	0.98	-
Inner columns	HEM 300	3	0.95	-
Beams X-facades	IPE500	A	0.52	43.8 mm
Beams Y-facades	IPE500	A	0.77	29.8 mm
Inner X-beams	IPE550	B	0.61	45.9 mm
Inner Y-beams	IPE600	C	0.89	29.1 mm
Inner core beams	HEA300	D	0.90	6.5 mm
Inner core braces	CHS 219.1x6.3	-	0.90	-

Maximal design ratios are also illustrated in the following figures.

STEEL EC3 CA1
Ultimate Limit State: Cross-Section Design, Stability Design, Weld Design, Pressure Design, Plastic Design

Isometric

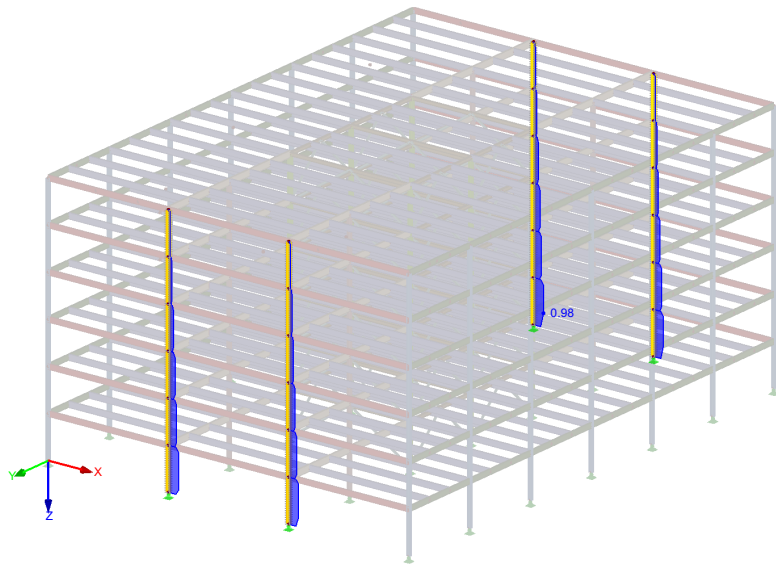


Max Design Ratio: 0.95

Figure 50. Maximum ULS utilization ratio of columns in Y-facades

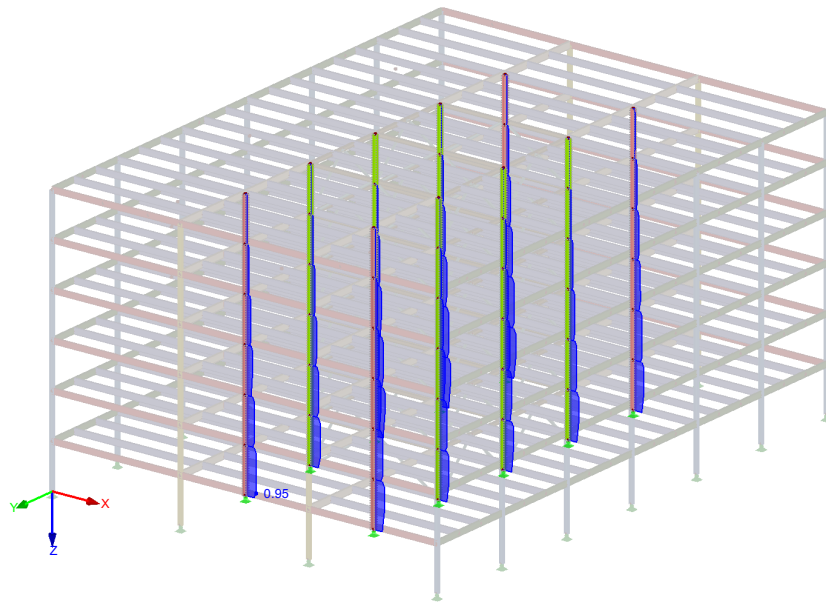
STEEL EC3 CA1
Ultimate Limit State: Cross-Section Design, Stability Design, Weld Design, Pressure Design, Plastic Design

Isometric



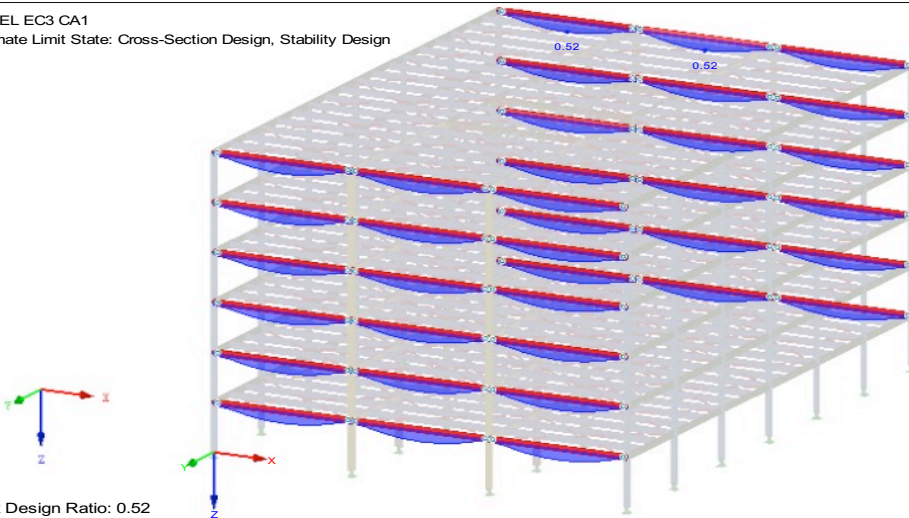
Max Design Ratio: 0.98

Figure 51. Maximum ULS utilization ratio of columns in X-facades



Max Design Ratio: 0.95

Figure 52. Maximum ULS utilization ratio of inner columns



Max Design Ratio: 0.52

Figure 53. Maximum ULS utilization ratio of beams in X-facades

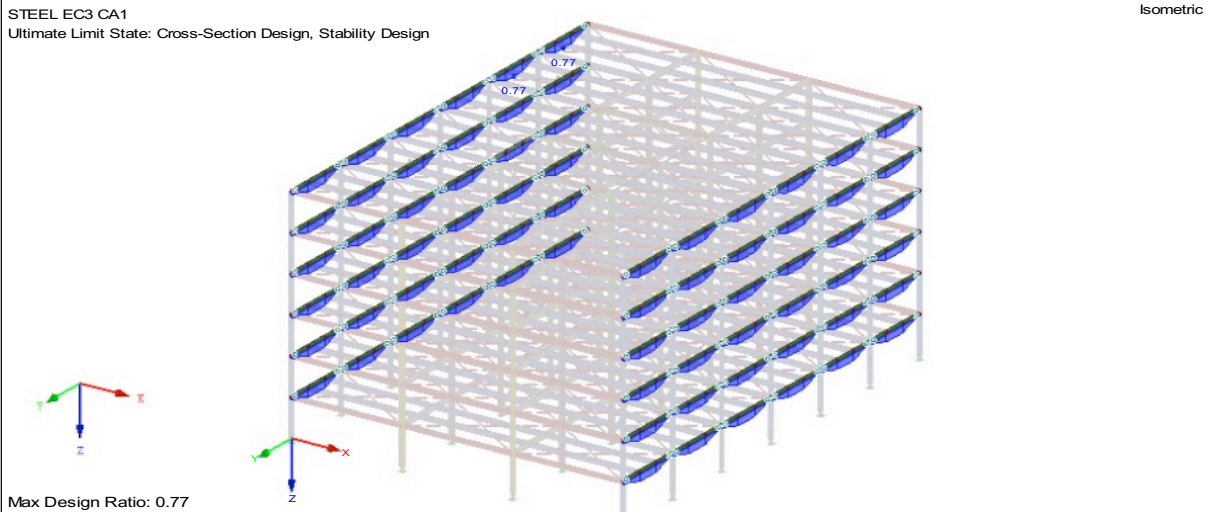


Figure 54. Maximum ULS utilization ratio of beams in Y-facades

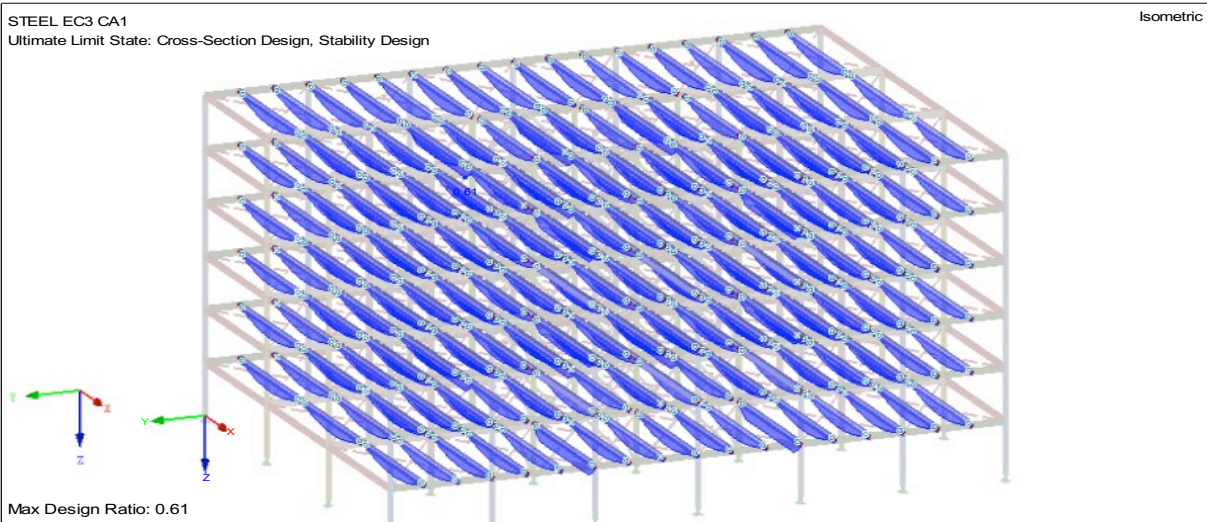


Figure 55. Maximum ULS utilization ratio of inner X-beams

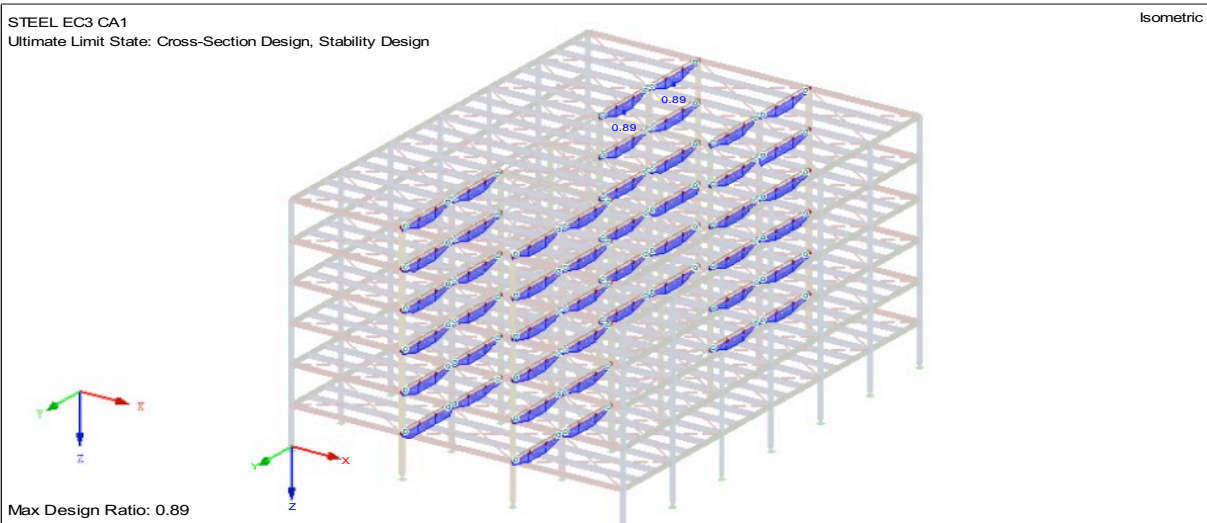


Figure 56. Maximum ULS utilization ratio of inner Y-beams

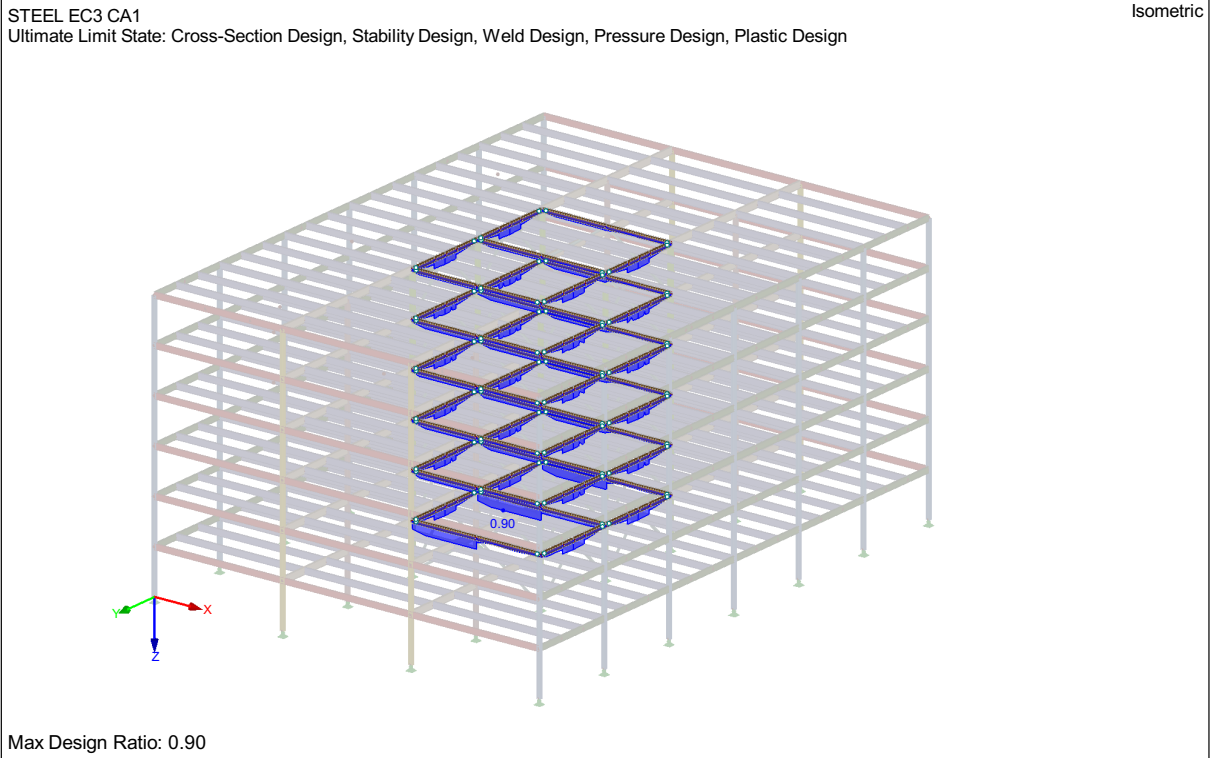


Figure 57. Maximum ULS utilization ratio of inner core beams

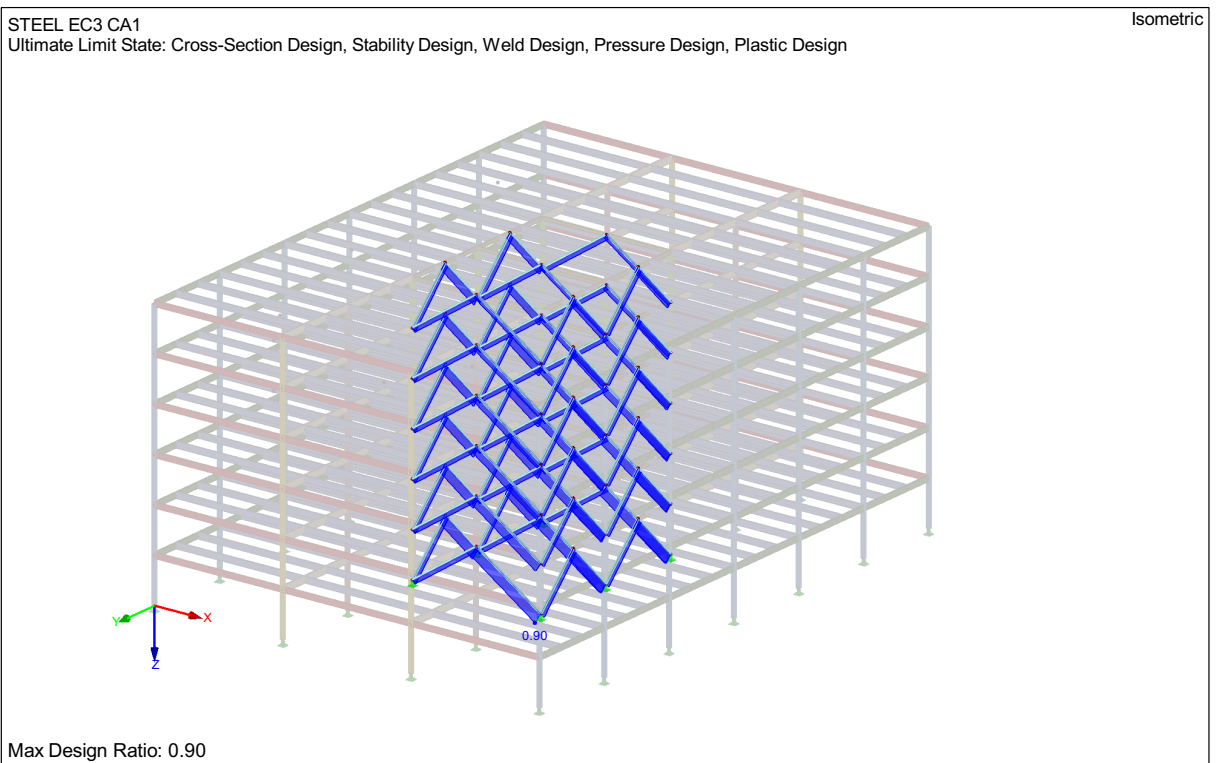


Figure 58. Maximum ULS utilization ratio of inner core braces

Lateral displacements are shown in the following figures.

RC2: GZG - Charakteristisch
Global Deformations u-X [mm]
Result Combinations: Max and Min Values

Against Y-direction

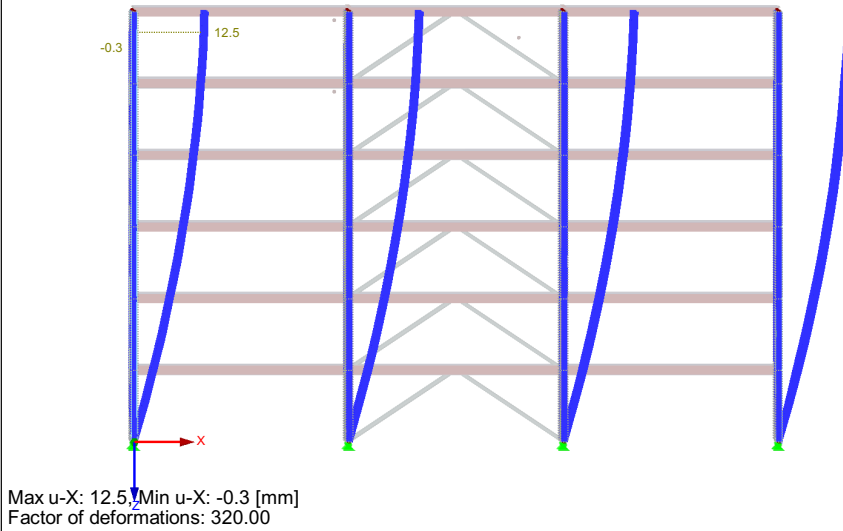


Figure 59. SLS lateral displacement against X-direction

RC2: GZG - Charakteristisch
Global Deformations u-Y [mm]
Result Combinations: Max and Min Values

Against X-direction

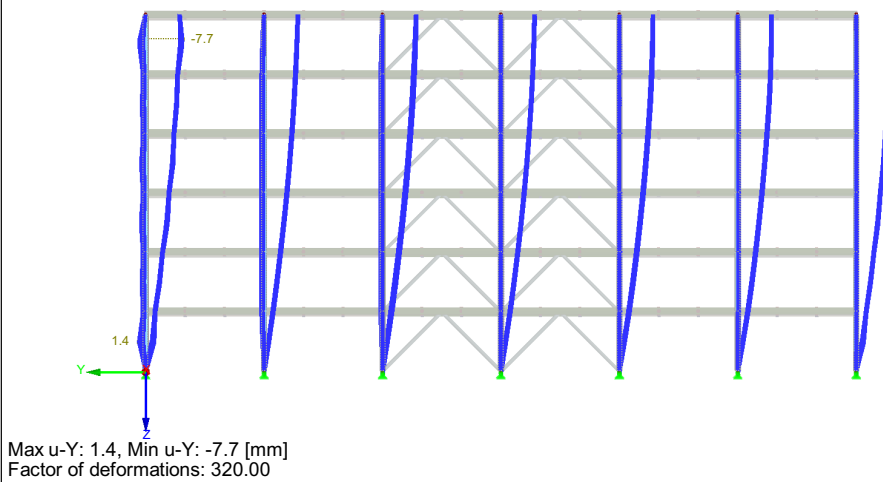


Figure 60. SLS lateral displacement against Y-direction

Notice:

- The buckling length of the columns is defined as 4,0 m.
- LT-buckling of beams is neglected (restrained due to the diaphragms).

5.1.3 Connections

Beam-to-beam as well as beam-to-column joints are pinned fin plate joints. Brace joints as well as column base joints are not detailed here. Column splices are moment resisting end plates joints. Column splice positions is assumed approximately at middle height of the building. The design of column splices is constructive (only compression forces and neglectable bending moments).

The nomenclature of the joints throughout the worked example is based on members IDs in Table 32. Joint names, ULS shear forces and resistances are summarized in the following table. To keep the worked example concise, the individual checks performed at ULS are not detailed here.

Table 33. ULS verifications of joints

Position s = strong axis w = weak axis	ULS load (kN)	Resistance (kN)	Failure mode	UF
A1s / A2	130	196	Fin plate in bearing	0.66
A1w	240	255	Fin plate in bearing	0.94
B1 / B3	180	196	Fin plate in bearing	0.92
C2w / C3w	430	443	Fin plate in bearing	0.97
D3s	60	102	Beam web in bearing	0.59
D3w	90	102	Beam web in bearing	0.88
BA / BC	180	196	Fin plate in bearing	0.92
BD	180	185	Fin plate in bearing	0.97

The joints are illustrated in the following figures. All bolts are 10.9 and plates are S355. Fin plates are 10 mm thick while end plates for column splices are 15 mm thick. Fin plate welds are 6 mm thick while end plates have 5 mm flange welds and 4 mm web welds.

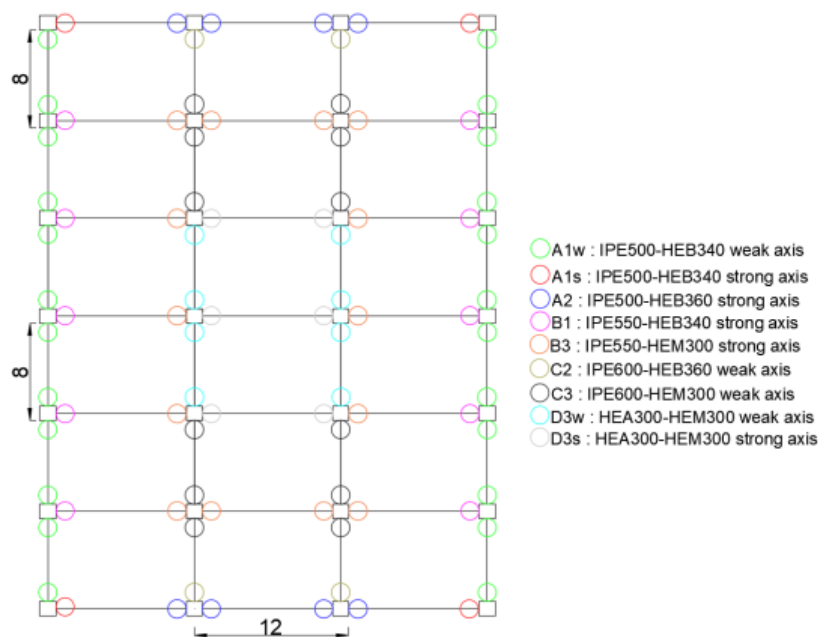


Figure 61. Joint positions

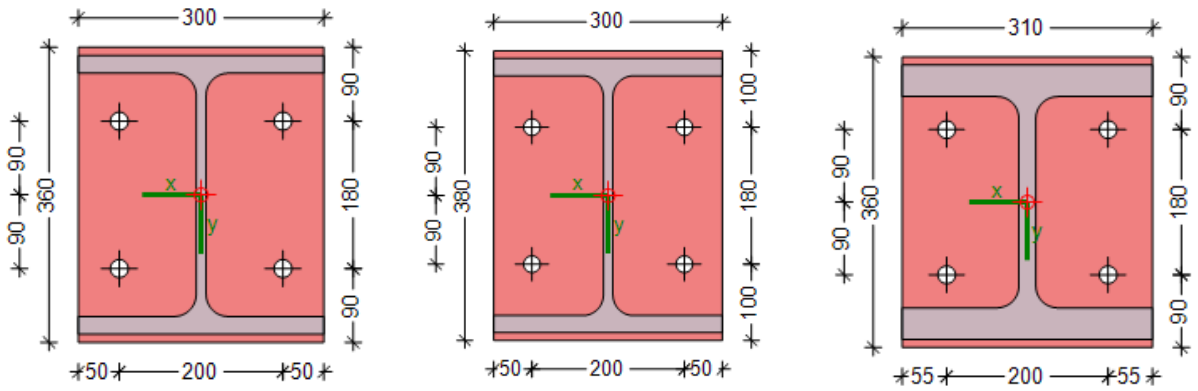


Figure 62. Column splices with 4xM20 (left: 1-1, center: 2-2, right: 3-3)

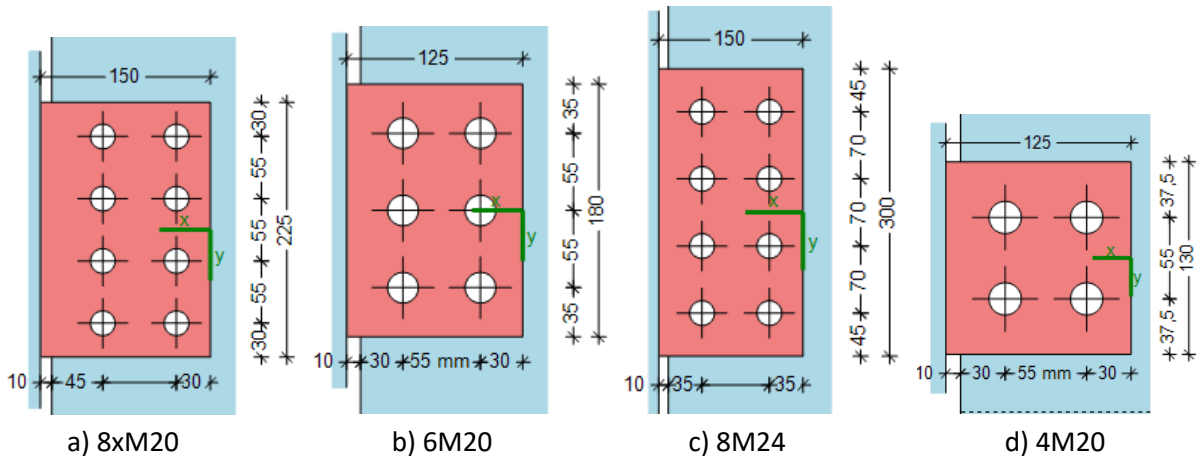


Figure 63. Fin plate beam-to-column joints (a) A-1w, b) A1s, A2, B1, B3, c) C-2w, C-3w, d) D-3s, D-3w)

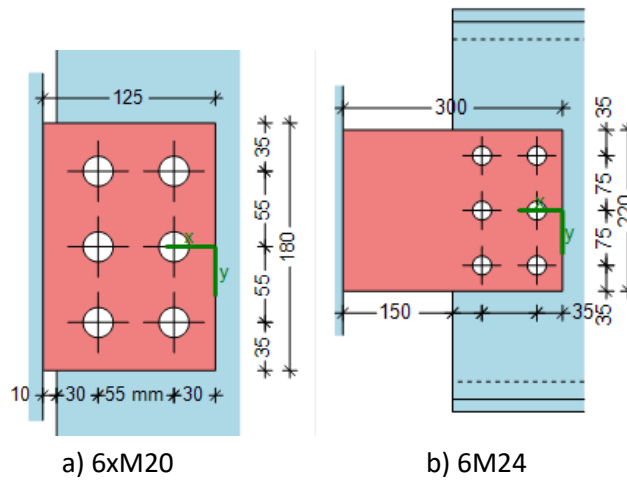


Figure 64. Fin plate beam-to-beam joints (a) B-A, B-C, b) B-D)

The joint design has been performed using the software COP. Notice that the design of such joints is not directly covered by the current version of the Eurocode, so that the verification is based on the ECCS No. 126 (ECCS TC 10 2009) . These verifications also contains ductility requirements for a proper pinned assumption of the joints. All failure mode are here ductile (fin plate or beam web in bearing).

5.1.4 Remarks

Following assumptions have been made for the design of the structure:

- Wind loads have been applied as distributed loads on columns (no surface loads), reference areas are shown on the Figure 65.

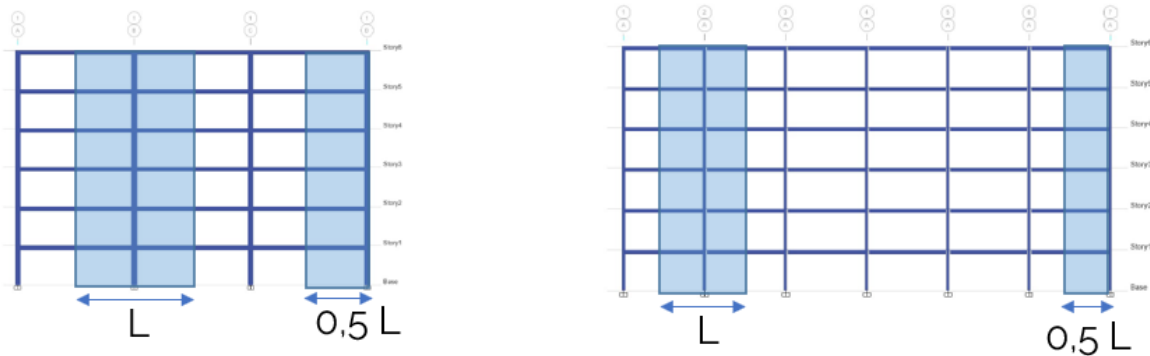


Figure 65. Wind loads as distributed loads on column

- No lateral-torsional buckling for beams has been considered as beam upper flanges are restrained by the slab.
- In order to model the diaphragms, pinned coupling elements (infinite stiffness) are defined in each deck.

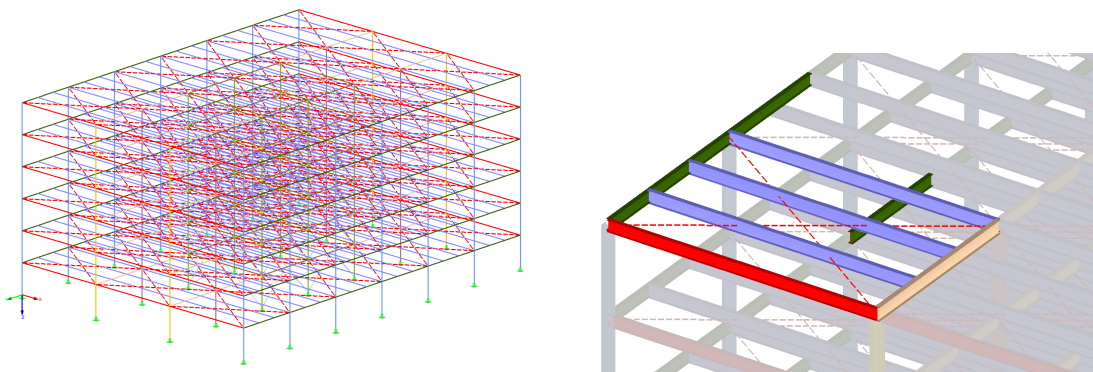


Figure 66. Diaphragm modelling using stiff coupling elements

5.2 Verifications for identified actions

5.2.1 Seismic (prescriptive approach)

The structure in this worked example has been firstly designed for non-seismic design conditions at two limit states (ULS, SLS). No particular calculations have been conducted with respect to the seismic action. In practice, there are simplified rules in the German norm allowing the practitioner to neglect the seismic action under some conditions if a wind design has been performed. This is mainly valid for low-rise buildings to optimize engineering costs.

Here, we don't consider the seismic action as accidental action but as an exceptional one. In this scenario, the earthquake is much stronger than the one defined in the code. The structure is therefore not directly designed to withstand such forces. Based on the prescriptive approach, we can however mitigate effects of the hazard:

- Due to the symmetrical arrangement in plan and the regularity in elevation, the structure stiffness is well balanced which offers a favourable response to the seismic action.
- Equal floor heights also contribute to the good behaviour of the structure in case of earthquake.

- To increase the overall ductility of the structure, HEA300 beams can be changed to HEB300, as HEA300 S355 profiles are class 3 and HEB300 S355 are class 1. All the other members are already class 1 profiles.
- To optimize the structure response, the originally designed pinned joints could be replaced by ductile semi-rigid joints. This would allow to delay the formation of plastic hinges in the joints such that the postcritical behaviour of the structure could be enhanced.

5.3 Verifications for unidentified actions

According to DIN EN 1991-1-7 A.4, the building belongs to consequence class 2b, as it is an office building with between 4 and 15 storeys. This requires horizontal and vertical ties, as well as to consider the eventuality of column loss scenarios.

In the following, exceptional events will be considered. As the occurrence of such events is very small, those will be considered in combination with the accidental load case combination according to DIN EN 1990 Equ 6.11a with ψ_1 for live loads and ψ_2 for climatic loads, such that the accidental combination becomes :

$$1.0 \times \text{dead load} + 0.5 \text{ live load}$$

5.3.1 Prescriptive approach

5.3.1.1 Tying forces

Tying forces are determined according to DIN EN 1991-1-7 as following:

$$T_i = 0.8(g_k + \psi q_k)sL \quad \text{or} \quad 75 \text{ kN, whichever is greater} \quad (34)$$

$$T_p = 0.4(g_k + \psi q_k)sL \quad \text{or} \quad 75 \text{ kN, whichever is greater} \quad (35)$$

In this approach, only surface loads are taken into account. As we have also line loads (facade loads), these are taken into account here by converting them into surface loads for external ties.

Horizontal tying forces are detailed in Table 34. Note that only members along frames are defined as ties here, so that beam-to-beam joints are not subjected to tying forces.

Table 34. Horizontal tying forces according to the prescriptive approach

External tie		Internal tie	
s	8 m	s	8 m
L	12 m	L	12 m
ψ	0,5	ψ	0,5
g_k	5 kN/m ²	g_k	5 kN/m ²
q_k	3 kN/m ²	q_k	3 kN/m ²
g_k facade	4 kN/m		
g_k facade equ.	0,5 kN/m ²		
T_e	268,8 kN	T_i	499,2 kN

Vertical tying forces are detailed in the following table.

Table 35. Vertical tying forces according to the prescriptive approach

External tie (HEB360)		Internal tie (HEM300)	
s	8 m	s	8 m
L	12 m	L	12 m
ψ	0,5	ψ	0,5
g_k	5 kN/m ²	g_k	5 kN/m ²
q_k	3 kN/m ²	q_k	3 kN/m ²
g_{IPE600}	1,22 kN/m	g_{IPE600}	1,22 kN/m
g_{IPE500}	0,907 kN/m	g_{IPE550}	1,06 kN/m
g_{IPE550}	1,06 kN/m	g_{HEM300}	2,38 kN/m
g_{HEB360}	1,42 kN/m	h	4 m
h	4 m	n IPE550	4
n IPE550	1,5		
g_k facade	4 kN/m		
T_e	400,5 kN	T_i	694,2 kN

5.3.1.2 Verifications of members

The prescriptive approach only provides tension forces for tying members. In this worked example, we combine these forces with the internal forces (bending moments for members and shear forces for joints) coming from the exceptional load case combination.

The verification of members has been carried out according to DIN EN 1993-1-1. Details about the verification are given in Table 36.

Table 36. Member verifications for horizontal tying forces according to the prescriptive approach

Internal ties									
	N_{Ed} (kN)	M_{Ed} (kNm)	Class	W_y (cm ³)	$N_{pl,Rd}$ (kN)	M_{Rd} (kNm)	η_N	η_M	η_{M-N}
IPE550	499,2	327	1	2787	4757	989,4	0,10	0,33	0,33
IPE600	499,2	610	1	3512	5538	1246,8	0,09	0,49	0,49
HEA300	499,2	96	3	1260	3994	447,3	0,12	0,21	0,34
External ties									
	N_{Ed} (kN)	M_{Ed} (kNm)	Class	W_y (cm ³)	$N_{pl,Rd}$ (kN)	M_{Rd} (kNm)	η_N	η_M	η_{M-N}
IPE500	268,8	242	1	2194	4118	778,9	0,07	0,31	0,31

For the internal HEA300 members, an elastic M-N interaction had to be performed as the cross section is class 3.

Table 37. Member verifications for vertical tying forces according to the prescriptive approach

Internal ties									
	N_{Ed} (kN)	M_{Ed} (kNm)	Class	W_y (cm ³)	$N_{pl,Rd}$ (kN)	M_{Rd} (kNm)	η_N	η_M	η_{M-N}
HEM300	694,2	0	1	4078	10760,05	1447,7	0,06	0,00	0,06
External ties									
	N_{Ed} (kN)	M_{Ed} (kNm)	Class	W_y (cm ³)	$N_{pl,Rd}$ (kN)	M_{Rd} (kNm)	η_N	η_M	η_{M-N}
HEB360	400,5	0	1	2683	6411,3	952,5	0,06	0,00	0,06

All verifications are fulfilled.

5.3.1.3 Verification of joints

Fin plate joints verifications are carried out according to ECCS No. 126 (ECCS TC 10 2009). For bolts in shear and plates in bearing due to horizontal tying is considered. Results are given in Table 38.

Table 38. Joints verifications for tying forces according to the prescriptive approach

Position s = strong axis w = weak axis	Tying force (kN)	Failure mode	UF
A1s / A2	268.8	Fin plate in bearing	0.63
A1w	268.8	Column web in bending	0.73
B1 / B3	499.2	Fin plate in bearing	1.16
C2w	499.2	Column web in bending	1.15
C3w	499.2	Fin plate in bearing	0.67
D3s/D3w	499.2	Beam web in bearing	2.02
D3w	90	Beam web in bearing	0.88
1-1 / 2-2	400.5	End plate in bending	0.88
3-3	694.2	End plate in bending	1.31

For the connections which do not satisfy the verifications, to see the failure modes, the detailed calculation of joints B1 (main results in Figure 67 and details given in A.3.1), C2w (main results in Figure 68 and details given in A.3.2), D3s (main results in Figure 69 and details given in A.3.3), and 3-3 (main results in Figure 70 and details given in A.3.4) is provided. The verification of the other joints is performed in the same manner but is not detailed here.

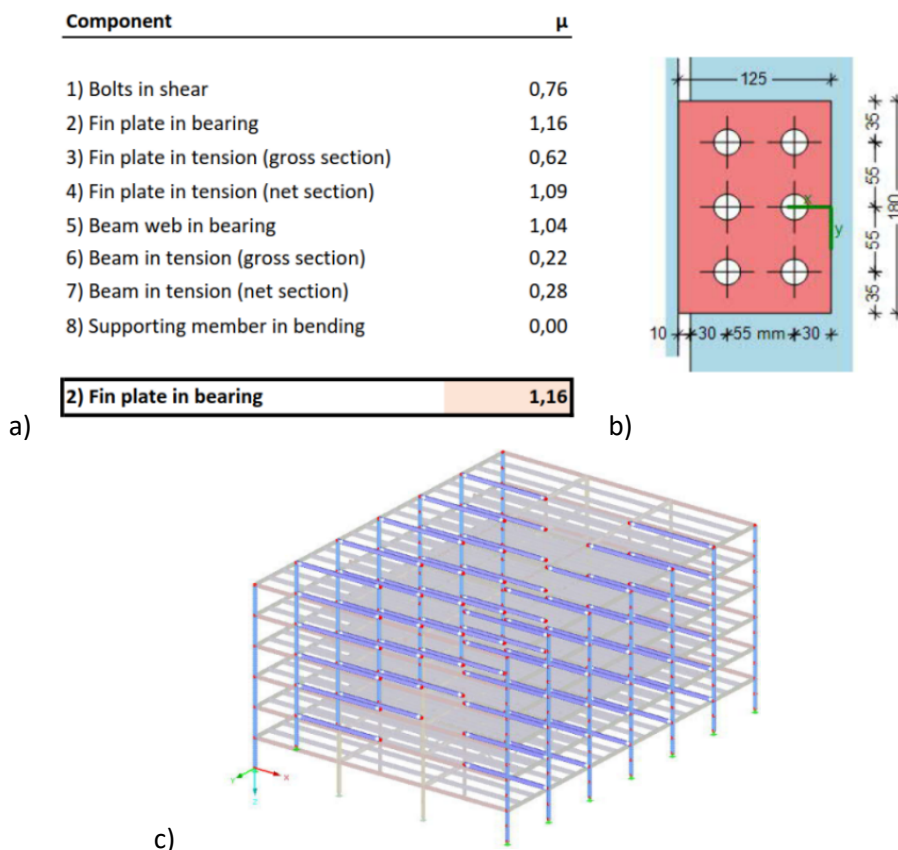


Figure 67. Joint B1: a) capacity ratios for components of connection; b) connection geometry; c) location in the structure

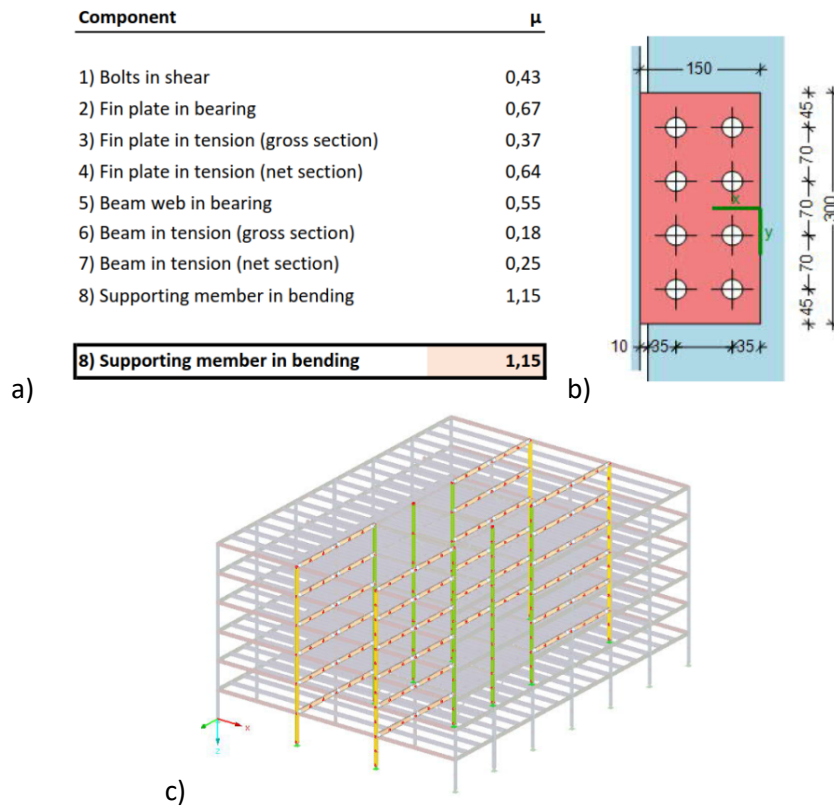


Figure 68. Joint C2w: a) capacity ratios for components of connection; b) connection geometry; c) location in the structure

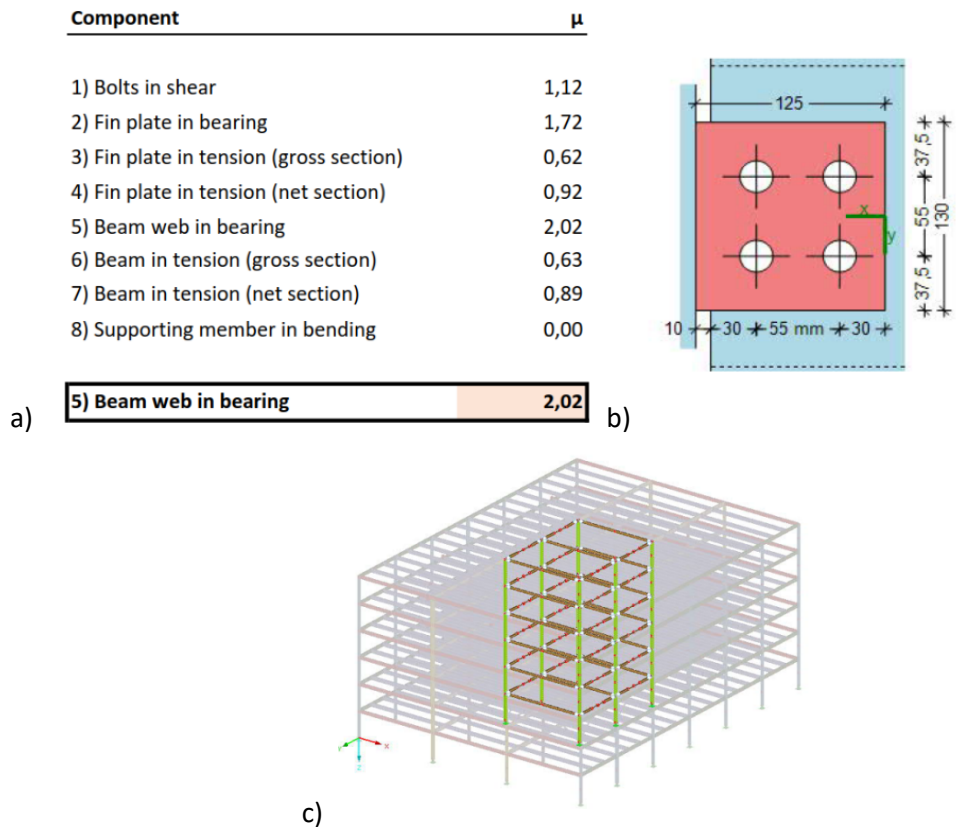


Figure 69. Joint D3s: a) capacity ratios for components of connection; b) connection geometry; c) location in the structure

Rows resistances from COP

Bolt row 1	End plate in bending	$F_{EPB,1,Rd}$	286 kN
	Beam web in tension	$F_{BWT,1,Rd}$	3729 kN
	End plate in bending (2)	$F_{EPB,1,Rd}$	286 kN
	Beam web in tension (2)	$F_{BWT,1,Rd}$	3729 kN
	Effective tension resistance	$F_{t1,Rd}$	286 kN
	Lever arm	h_1	240,5 mm
Bolt row 2	End plate in bending	$F_{EPB,2,Rd}$	286 kN
	Beam web in tension	$F_{BWT,2,Rd}$	3729 kN
	End plate in bending (2)	$F_{EPB,2,Rd}$	286 kN
	Beam web in tension (2)	$F_{BWT,2,Rd}$	3729 kN
	Effective tension resistance	$F_{t2,Rd}$	222,3 kN
	Lever arm	h_2	60,5 mm

1) Rows resistance

The total tension resistance of the joint (no bending force applied) is equal to the sum of the contribution of each bolt row.

$$F_{T,Rd} = 508,3 \text{ kN}$$

$$F_{Ed} = 694,2 \text{ kN}$$

$$\mu = 1,37$$

Figure 70. Capacity ratios for components of connection from joint 3-3 (column splice)

Joints B1, B3, C2w, D3s, D3w and 3-3 don't have a sufficient resistance to withstand tying forces according to the prescriptive approach.

Notice that for double sided beam-to-column configurations, the component "column web in bending" is considered as not activated, in other words not relevant for the verification. This is why joints C2w and C3w have different resistances.

5.3.1.4 Redesign of the structure

Members do not need to be modified to withstand tying forces according to the prescriptive approach.

Redesigned joints B1, B3, C2w, D3s, D3w and 3-3 are commented in the following:

- **B1/B3** : slight modification of fin plate geometry
- **C2w** : welded column web plate added
- **D3s/D3w** : 2 bolts added and modification of the fin plate geometry
- **3-3** : M24 bolts (instead of M20) and 20 mm end plate instead of 15 mm

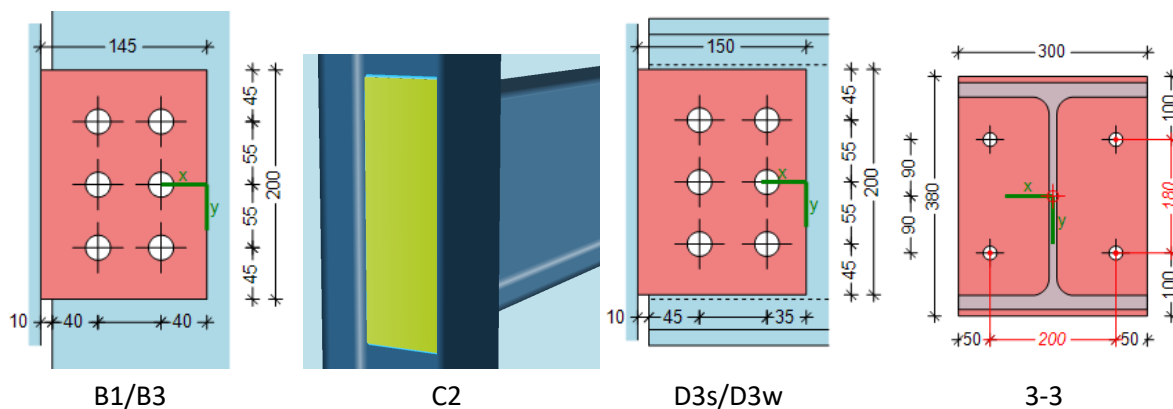


Figure 71. Redesigned joints to fulfill tying forces verifications according to the prescriptive approach

Updated utilization factors for these joints are summarized in Table 39.

Table 39. Redesigned joints verifications for tying forces according to the prescriptive approach

Position s = strong axis w = weak axis	Tying force (kN)	Failure mode	UF
B1 / B3	499.2	Fin plate in tension (net)	0.93
C2w	499.2	Column web in bending	0.88
D3s/D3w	499.2	Beam web in tension (net)	1.03
3-3	694.2	End plate in bending	0.83

The check of the D3s/D3w joints is exceeded by 3%. We choose to accept this small exceedance as it is usually done in practice. A solution to fulfil this check could be to replace the HEA300 with HEB300 beams. This might be also a good thing for the postcritical behaviour in case of column loss as HEB300 S355 are class 1 profiles while HEA300 are class 3.

As an example, the detailed verification of redesigned joints C2w and D3s are illustrated in the following. Figure 72 and Figure 73 illustrate the main verifications outcome, while in A.3.5 and A.3.6 full reports are given.

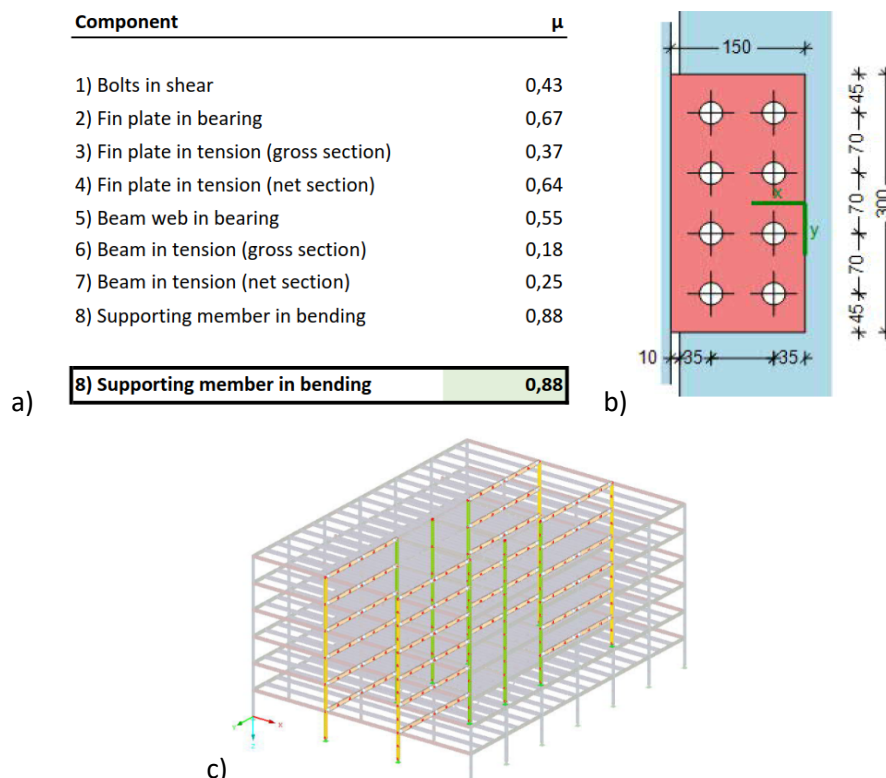


Figure 72. Redesigned joint C2w: a) capacity ratios for components of connection; b) connection geometry; c) location in the structure

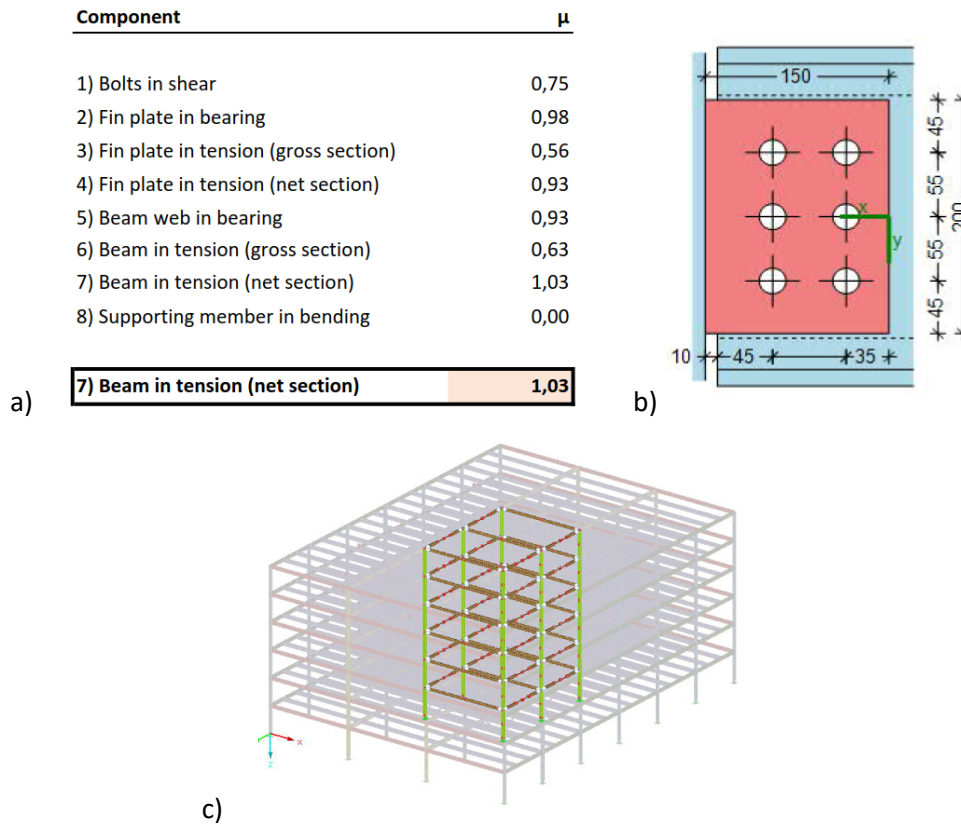


Figure 73. Redesigned joint D3s: a) capacity ratios for components of connection; b) connection geometry; c) location in the structure

5.3.2 ALPM: Full numerical approach

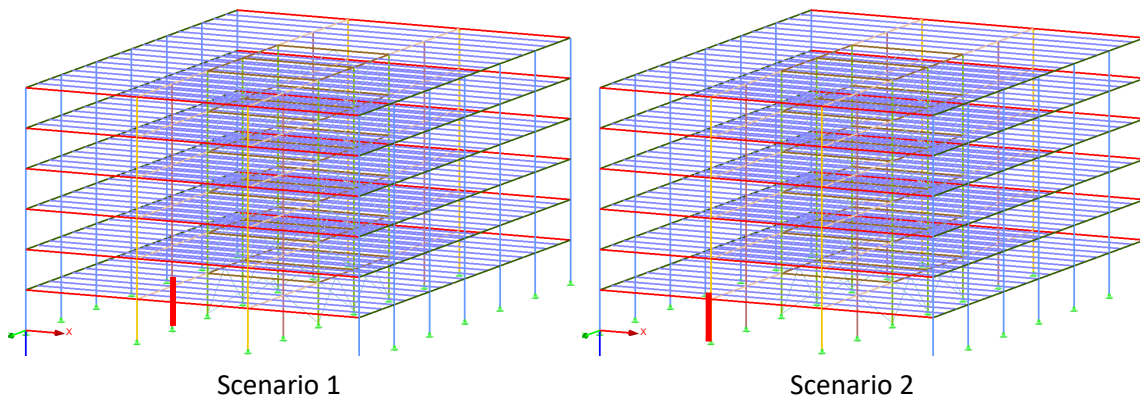
The full numerical approach will be addressed using the finite element model developed for the ULS/SLS design of the structure. The aim is to remove a column and let membrane effects develop in the ties in a first step and then verify if the ties (members and joints) can withstand these tensile forces.

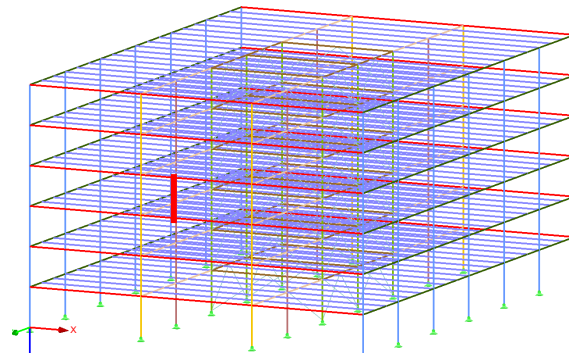
5.3.2.1 Scenarios

We consider 3 possible different column loss scenarios for this worked example:

- **Scenario 1:** Inner column loss at floor 0
- **Scenario 2:** Facade column loss at floor 0
- **Scenario 3:** Inner column loss above column splice

Those 3 scenarios are illustrated on the following figures (lost column marked in red).





Scenario 3

Figure 74. Investigated column loss scenarios in the numerical approach

Notice that those are not the only scenarios to consider for a complete numerical approach of the robustness design. It is up to the engineer to define which scenarios might be possible in reality and which of them are the most relevant for the robustness design of the structure.

5.3.2.2 Methodology and assumptions

The FE analysis will be performed using a Newton-Raphson algorithm (also known as 3rd order analysis) allowing the integration of large deformations. As this can lead to lateral-torsional buckling of the beams for which no instability can occur in reality as they are maintained by the diaphragms, we prevent this instability to occur by fictively increasing the torsional inertia of the beam members.

Even though plastic deformations due to a column loss are expected, material non linearities are not taken into account in the analysis. In practice, many practitioners use similar FE software without the possibility to take into account material non linearities. It also leads to more complex inputs and requires higher expertise in finite element modelling, what is not always the case for standard engineering offices.

In order to ensure convergence of the algorithm, the column loss scenario is modeled as follows:

- First, the structure is analysed without any column loss under the accidental load case combination. From this, the actual compression force in column to be lost is known.
- Then at the upper node of the column to be lost, this force is applied and the column is removed, so that this force replaces the column.
- The last step simulates the column loss: A force of same magnitude in opposite direction is gradually applied at the same node. Load steps of 0.025 are used to ensure convergence. At the end of the analysis, the statical system corresponds to a complete column loss. Note that dynamical effects of the column loss are not considered in this worked example.

To avoid any composite action between diaphragms and the steel structure but keep the diaphragm effect (infinitely rigid decks), diaphragm models have to be modified for column loss scenarios. These are shown in the Figure 75.

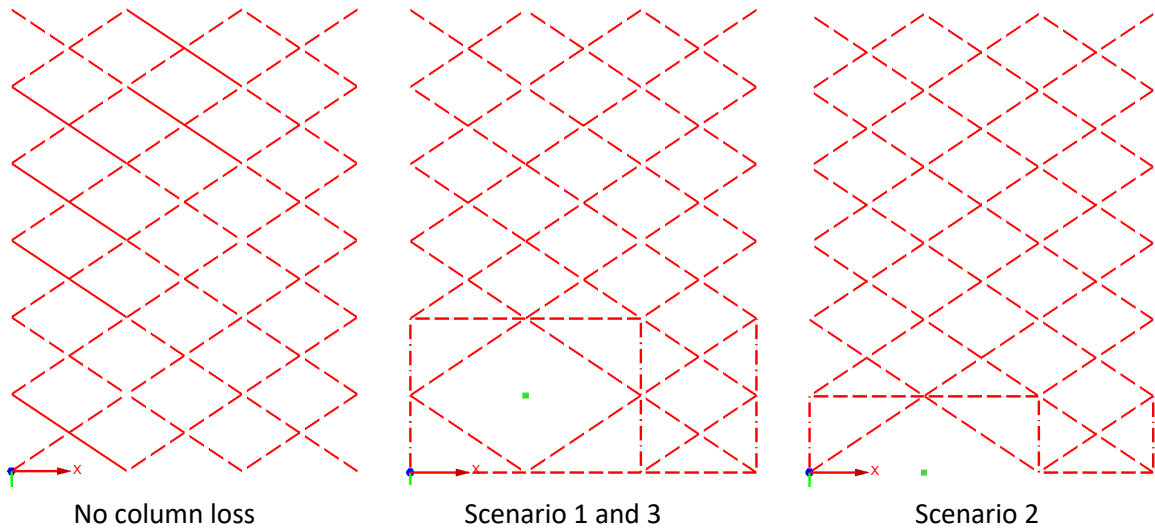


Figure 75. Coupling elements pattern for diaphragm modelling in various column loss scenarios

5.3.2.3 Forces and deformations

Results of all considered column loss scenarios are illustrated in the following figures.

- **Scenario 1** : Inner column loss at floor 0

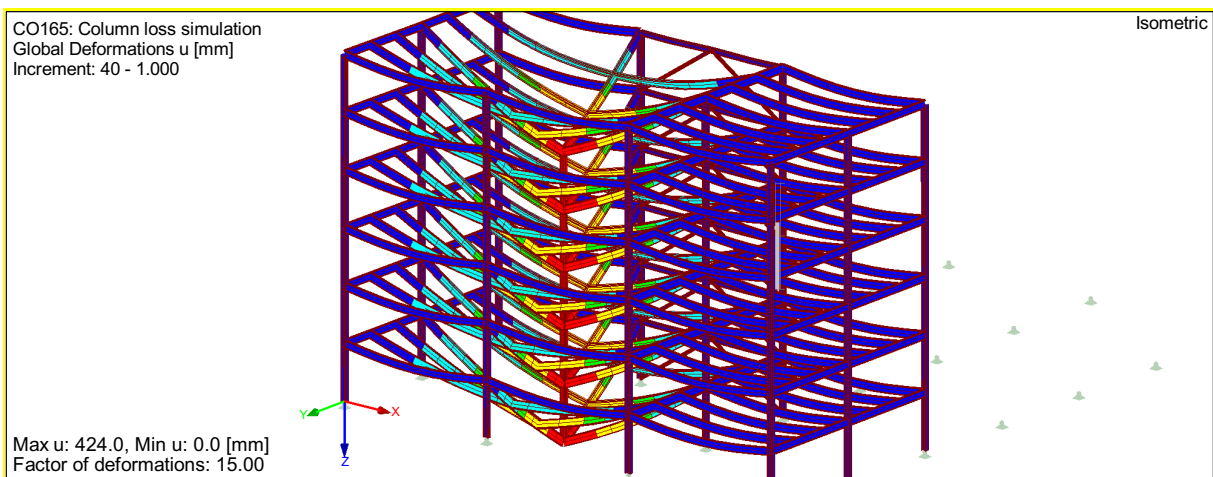


Figure 76. Deformed system (directly affected part) after column loss (scenario 1)

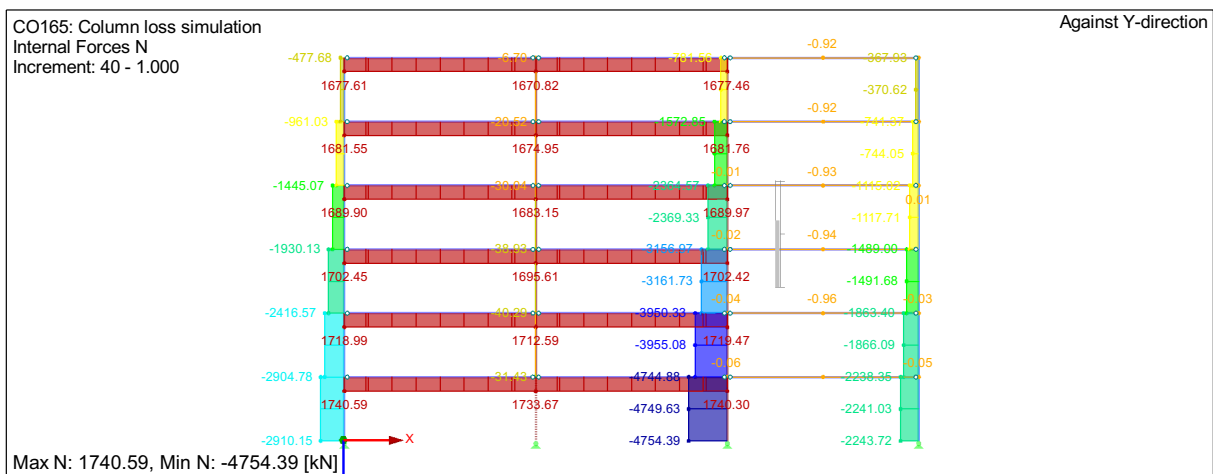


Figure 77. Normal internal forces in IPE550 frame after column loss (scenario 1)

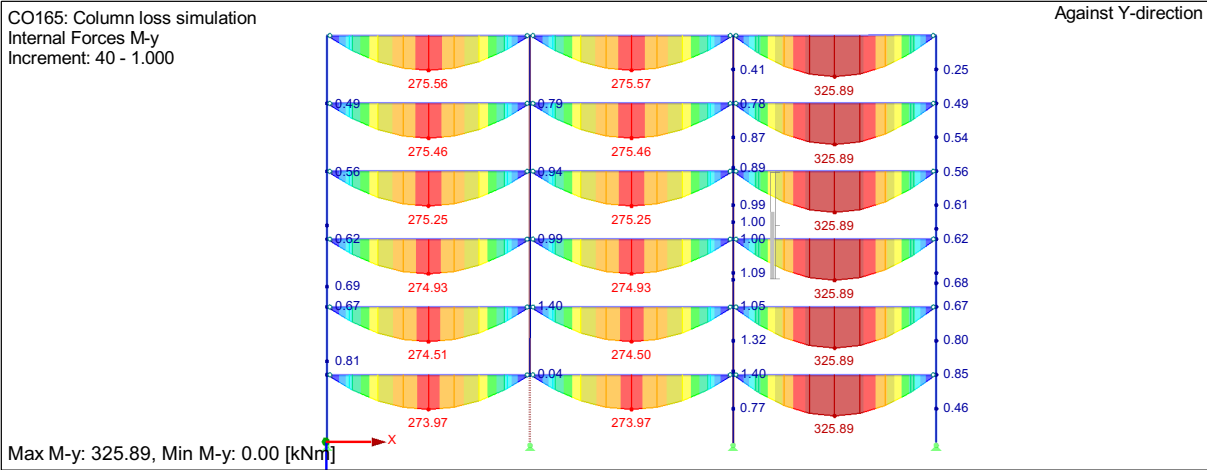


Figure 78. Bending moments in IPE550 frame after column loss (scenario 1)

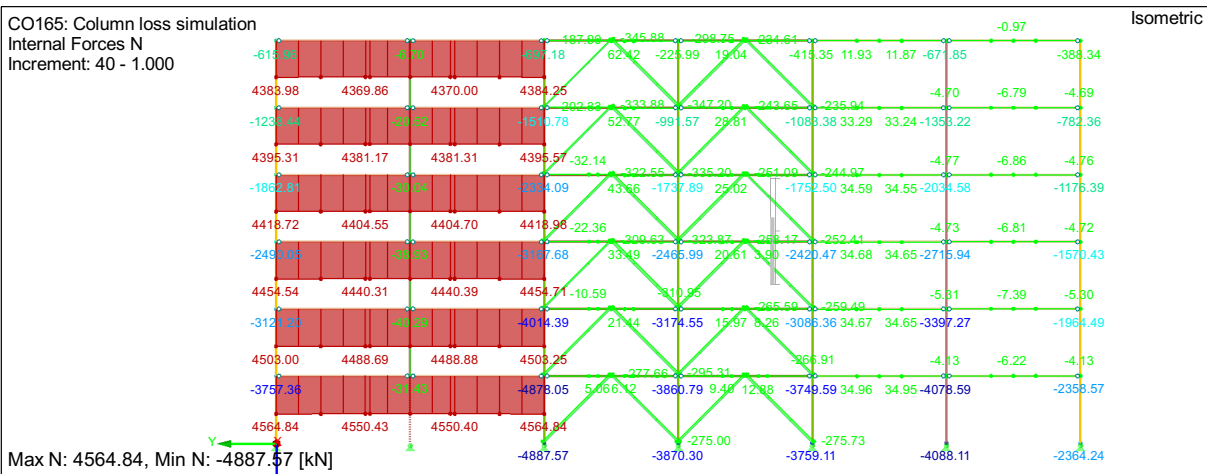


Figure 79. Normal internal forces in IPE600 frame after column loss (scenario 1)

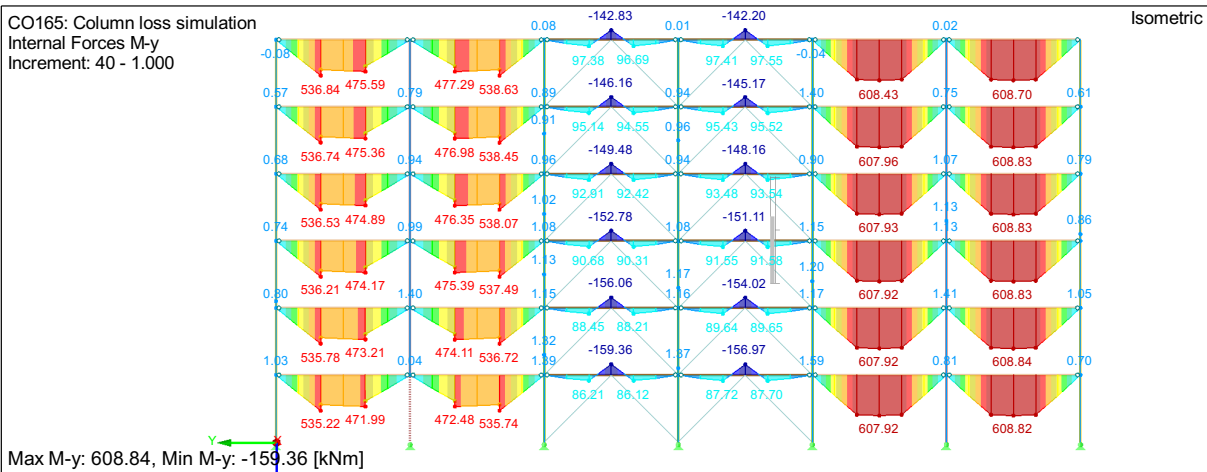


Figure 80. Bending moments in IPE600 frame after column loss (scenario 1)

- Scenario 2 : Facade column loss at floor 0

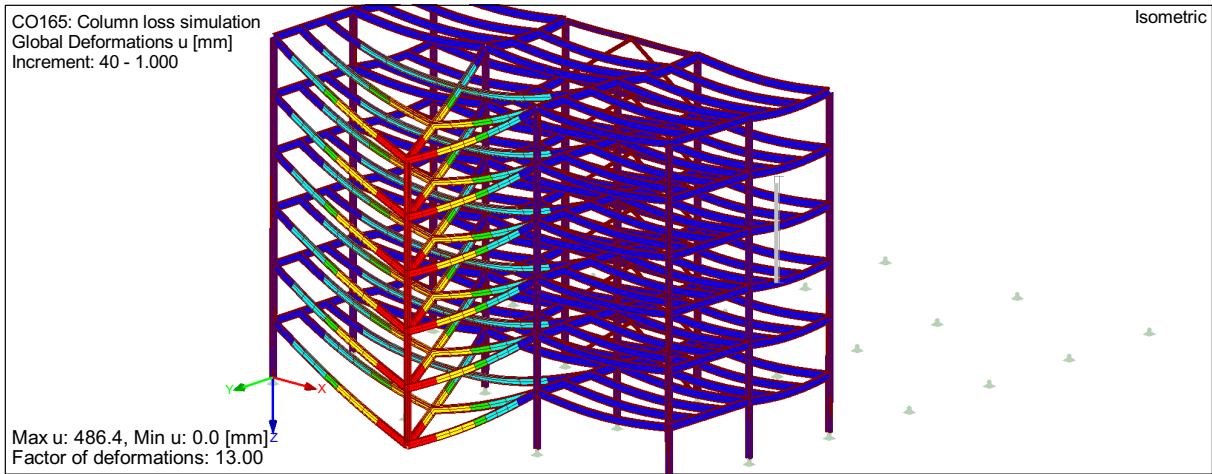


Figure 81. Deformed system (directly affected part) after column loss (scenario 2)

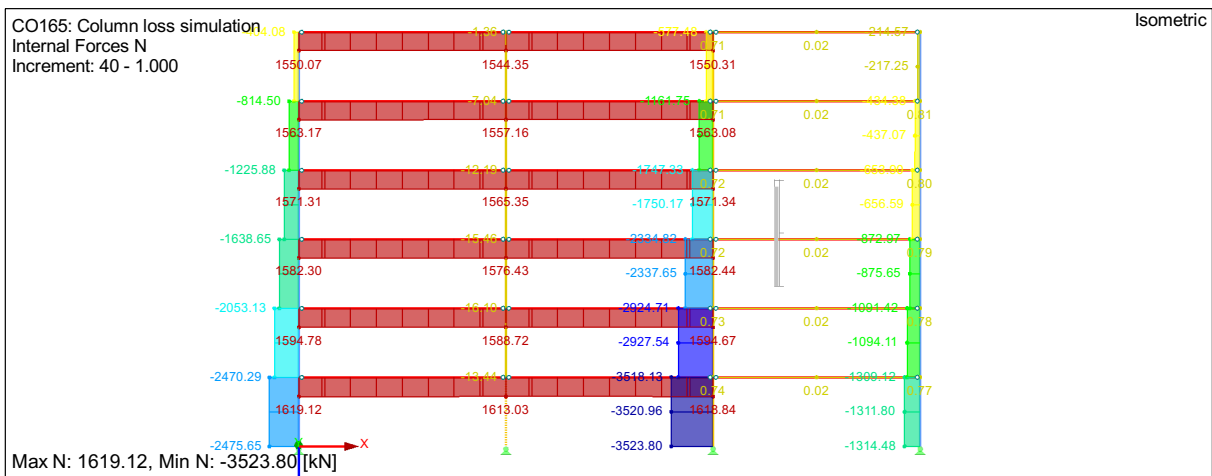


Figure 82. Normal internal forces in IPE500 frame after column loss (scenario 2)

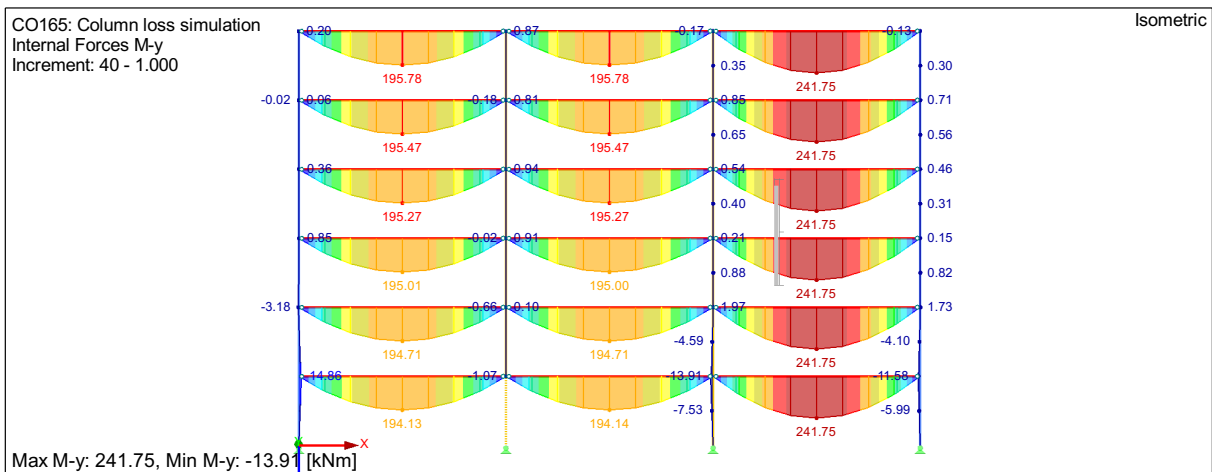


Figure 83. Bending moments in IPE500 frame after column loss (scenario 2)

- **Scenario 3** : Inner column loss above column splice

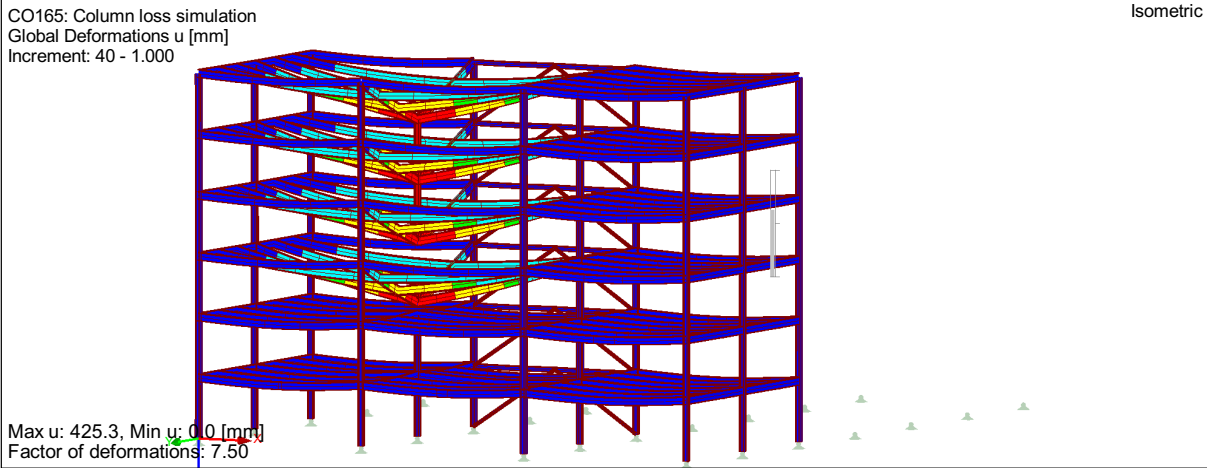


Figure 84. Deformed system (directly affected part) after column loss (scenario 3)

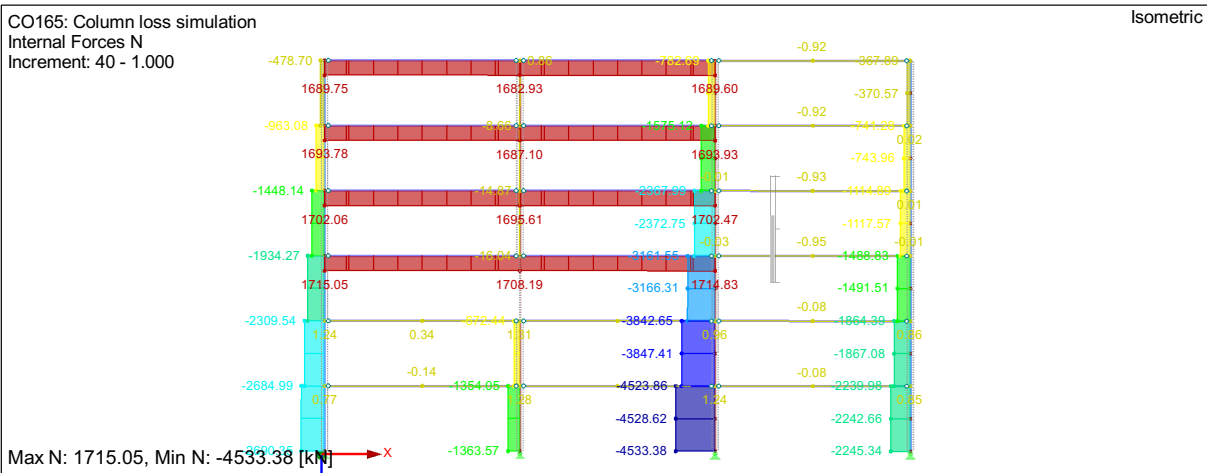


Figure 85. Normal internal forces in IPE550 frame after column loss (scenario 3)

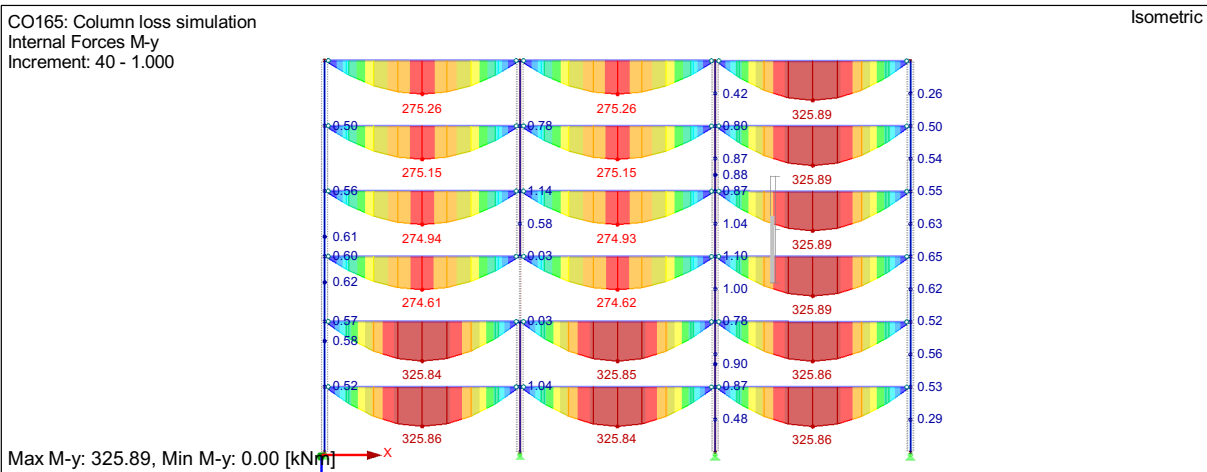


Figure 86. Bending moments in IPE550 frame after column loss (scenario 3)

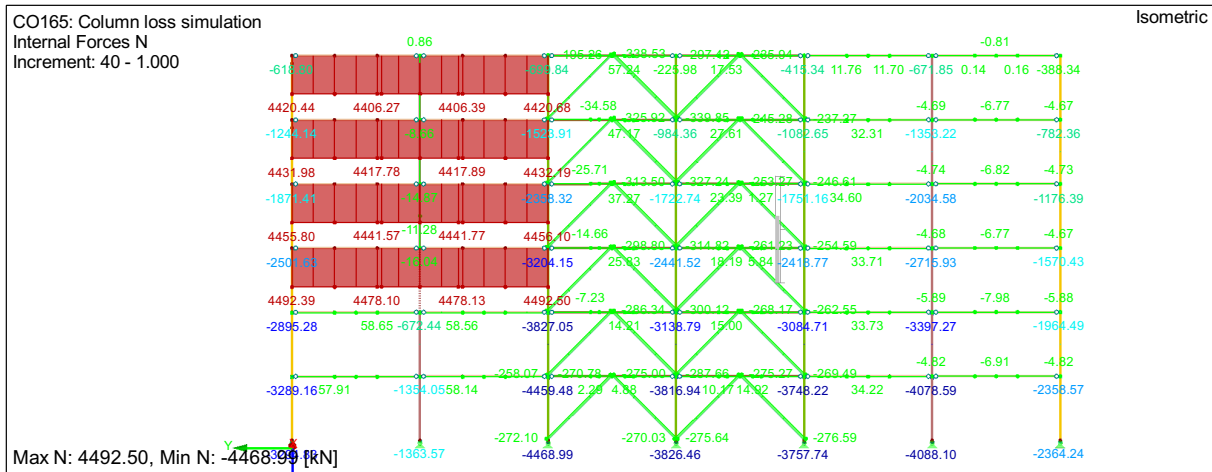


Figure 87. Normal internal forces in IPE600 frame after column loss (scenario 3)

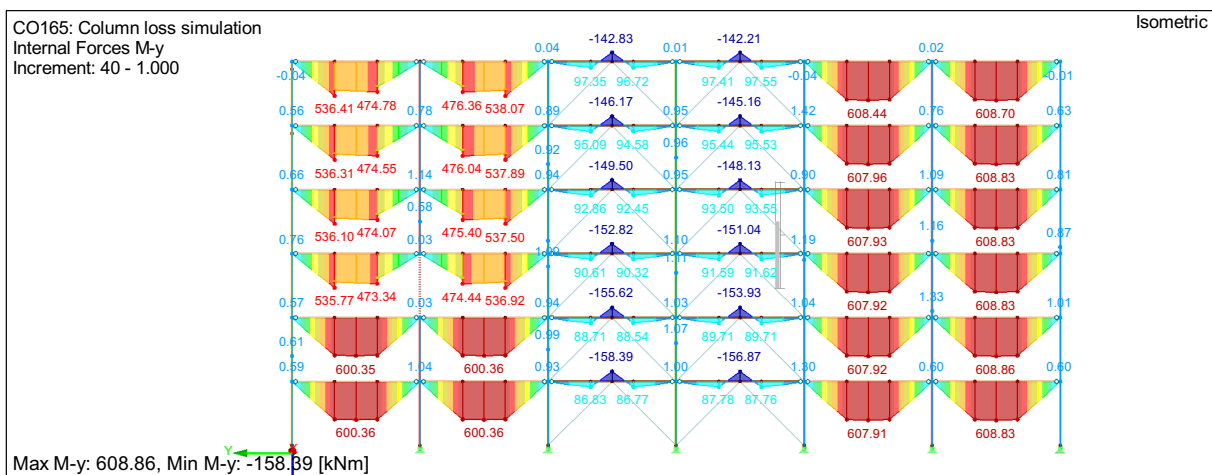


Figure 88. Bending moments in IPE600 frame after column loss (scenario 3)

From these results, it appears that 2D membrane effects develop for scenarios 1 and 3 (internal column loss) while only 1D membrane effects appears for scenario 2 (facade column loss). Note that a corner column loss could not work as no membrane forces (with simple joints at least) could develop. Corner columns should then be designed as key elements if robustness requirements for these columns are required.

Results of the column loss scenarios in the directly affected part are summarized in the Table 40.

Table 40. Internal forces in members/joints after column loss

Scenario	Member	Joint	Tensile force (kN)	Moment (kNm)
1	IPE550	B1/B3	1741	274
	IPE600	C2/C3	4565	536
2	IPE500	A1s/A2	1620	195
3	IPE550	B1/B3	1715	275
	IPE600	C2/C3	4493	537

5.3.2.4 Verifications of members / joints

- **Scenario 1** : Inner column loss at floor 0

The verification procedure is automatically performed within RSTAB using the STEEL EC3 module. Results from scenario 1 are summarized in the Table 41. Member verifications (scenario 1).

Table 41. Member verifications (scenario 1)

Member	Section	Axial force (kN)	Moment (kNm)	UF
Columns Y-facades	HEB 340	-2910	0	0.66
Columns X-facades	HEB 360	-3763	0	0.81
Inner columns	HEM 300	-4887	0	0.60
Inner X-beams	IPE550	1736	274	0.58
Inner Y-beams	IPE600	4562	536	1.15

Detailed members verifications are given in the Annex A.3.7.

Due to the missing column, compression forces in neighbour columns are increased. However, in this worked example, these forces stay lower than the design compression forces from ULS, so that no redesign of columns is required.

The IPE550 members were required due to SLS requirements (limitation of the deflection), so that in this case, the resistance of these members is still sufficient in case of a column loss.

The IPE600 are not sufficient for the high tensile forces. The exceedance is about 15%. From an engineering point of view, we expect that due to the development of plastic hinges, the real tensile force in these profiles should be lower than the value obtained from the elastic analysis, so that the IPE600 might be sufficient. On the contrary, the tensile force in the IPE550 would then be larger. In any case, the design was performed elastically and from this point of view, a cross-section change is required.

This will lead to a modification of tensile forces in joints, so that joints verification will be performed after the redesign of the structure members. However, it can already be stated that the fin plates designed for ULS won't be resistant enough to withstand those high tensile forces.

- **Scenario 2** : Facade column loss at floor 0

For scenario 2, member verifications are summarized in the following table.

Table 42. Member verifications (scenario 2)

Member	Section	Axial force (kN)	Moment (kNm)	UF
Columns Y-facades	HEB 340	-2473	15	0.58
Columns X-facades	HEB 360	-3521	14	0.77
Inner columns	HEM 300	-5383	3	0.69
Beams X-facades	IPE500	1615	195	0.59

Detailed members verifications are given in Annex A.3.8.

All verifications are fulfilled. Similar conclusions can be drawn from this scenario.

The joints verifications for the tensile forces are summarized in the following table.

Table 43. Joints verifications (scenario 2)

Position s = strong axis w = weak axis	Tying force (kN)	Failure mode	UF
A1s / A2s	1620	Fin plate in bearing	3.71

The detailed verification is given in A.3.9 and briefly presented in Figure 89.

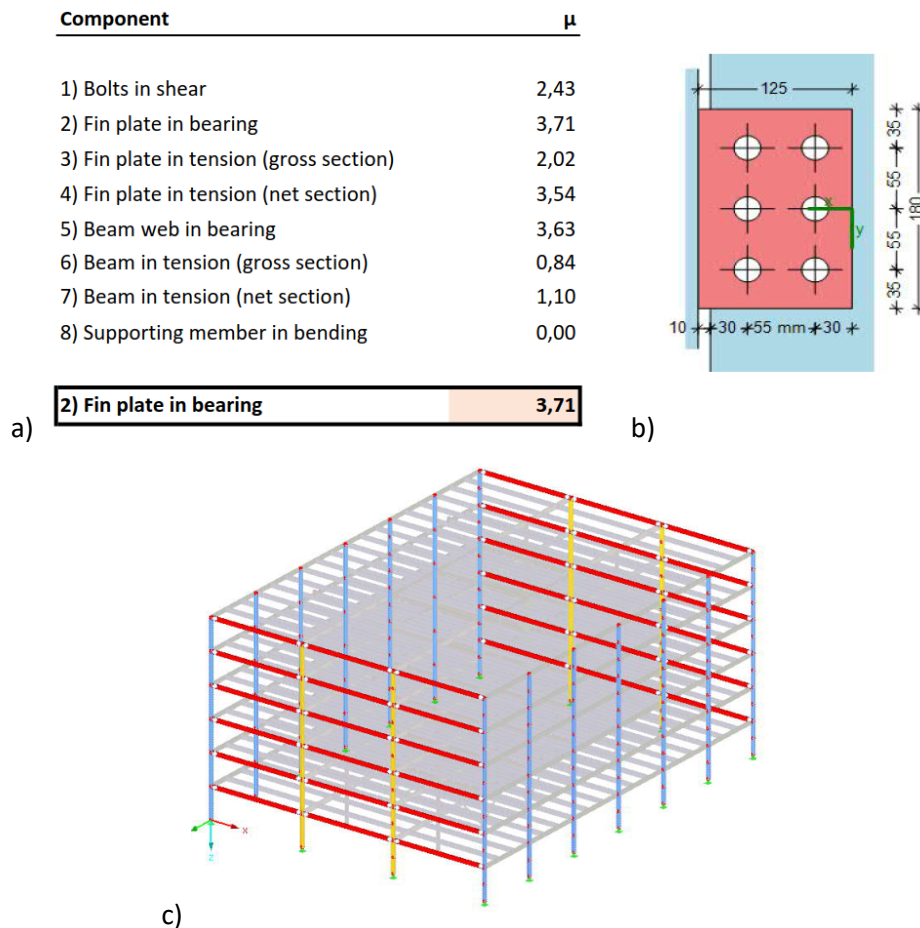


Figure 89. Connection A1s / A2s: a) capacity ratios for components of connection; b) connection geometry; c) location in the structure

The verification is not fulfilled and joints A1s/A2s need to be redesigned.

- **Scenario 3** : Inner column loss above column splice

It appears that for this structure, the loss of an internal column above a column splice doesn't lead to tying forces in vertical ties, but in tensile forces in horizontal ties. These tensile forces are in the same order of magnitude that in scenario 1 so that scenario 3 won't be investigated further in the following.

5.3.2.5 Redesign of the structure

- **Scenario 1** : Inner column loss at floor 0

Due to the section change of the IPE600, the internal force distribution will be modified. In the following, the column loss scenario 1 was simulated again by replacing all IPE600 members with IPE750x137. This leads to the following modified tensile forces in horizontal ties and compression forces in columns as well as modified utilization factors:

Table 44. Redesign members verifications

Member	Section	Axial force (kN)	Moment (kNm)	UF
Columns Y-facades	HEB 340	-2862	0	0.65
Columns X-facades	HEB 360	-3827	0	0.82
Inner columns	HEM 300	-4941	0	0.61
Inner X-beams	IPE550	1658	276	0.56
Inner Y-beams	IPE750x137	4850	565	1.03

Detailed members verifications are given in Annex A.3.10.

The utilization factor of the IPE750x137 is exceeded by 3%. This exceedance can be considered as acceptable.

Due to the cross-section change, inner Y-beams now have a larger axial stiffness, so that the tensile forces from membrane effects in those members are larger, too. In the same way, the tensile forces in the inner X-beams (IPE550) are now smaller. Alternatively, it has been tried to modify the IPE550 members for IPE600 members, in order to reduce the tensile force in the inner Y-beams. However, the positive effect for inner Y-beams was neglectable, so that changing to IPE750x137 for inner Y-beams with an elastic analysis is the only solution we retain here.

Joints verifications with modified tying forces are summarized in the following table.

Table 45. Joints verifications (scenario 1)

Position s = strong axis w = weak axis	Tensile force (kN)	Failure mode	UF
B1 / B3	1662	Fin plate in bearing	3.80
C2w	4852	Column web in bending	11.20
C3w	4852	Fin plate in tension (net)	6.17

Detailed verifications are shown in the following. The main results are presented from Figure 90 to Figure 92, while the detailed analysis is presented in annexes A.3.11 to A.3.13.

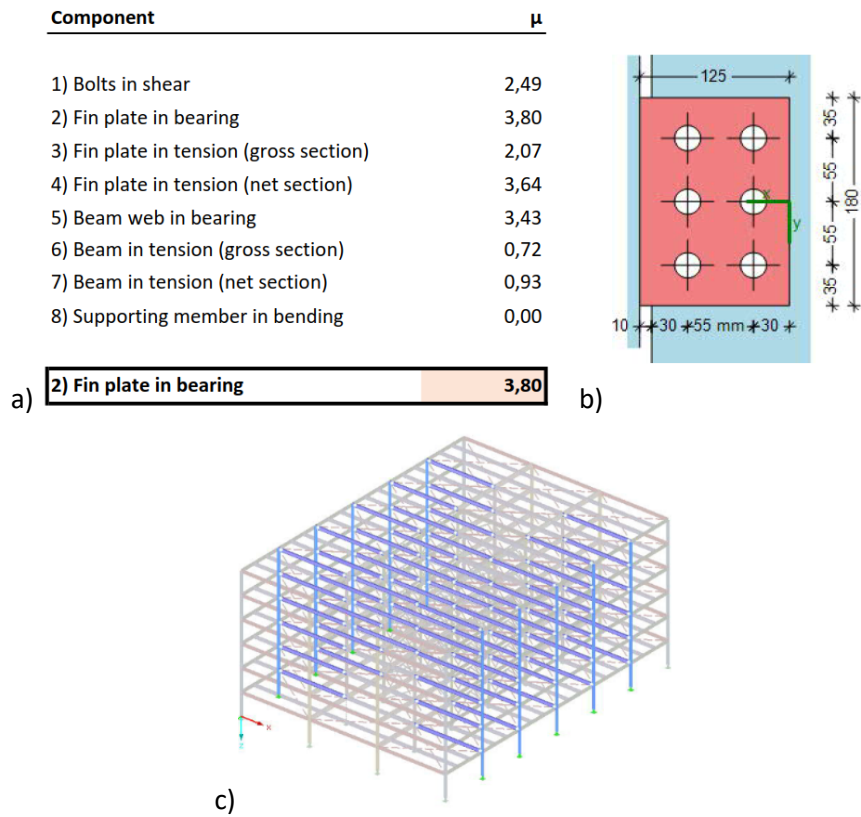


Figure 90. Connection B1 / B3: a) capacity ratios for components of connection; b) connection geometry; c) location in the structure

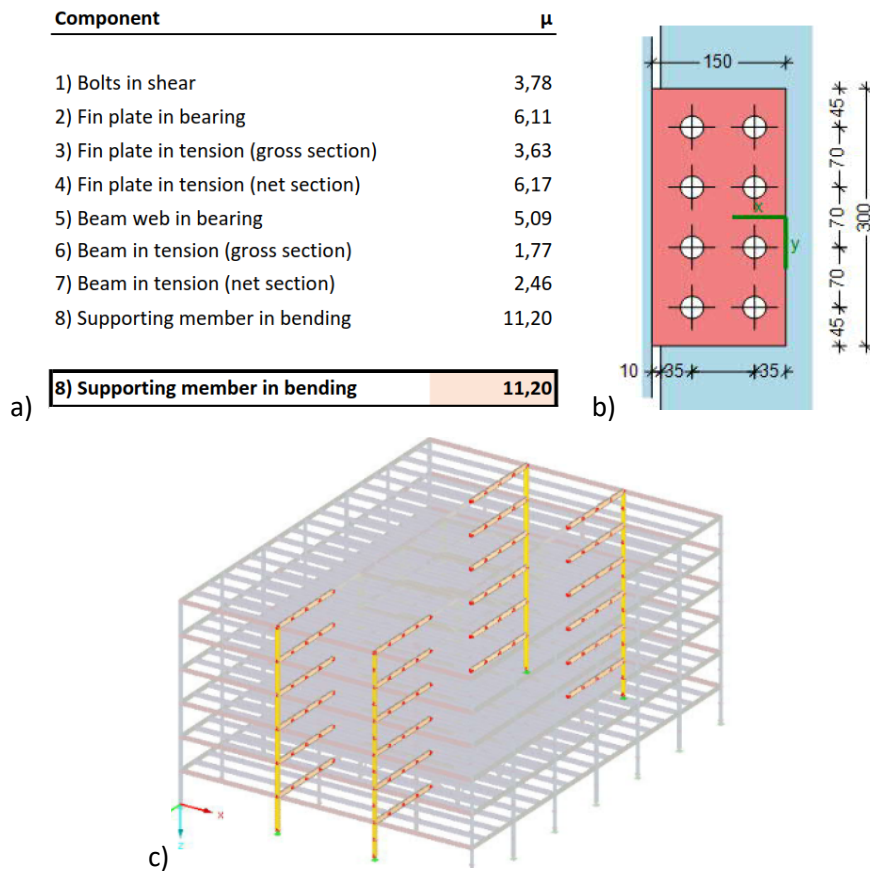


Figure 91. Connection C2w: a) capacity ratios for components of connection; b) connection geometry; c) location in the structure

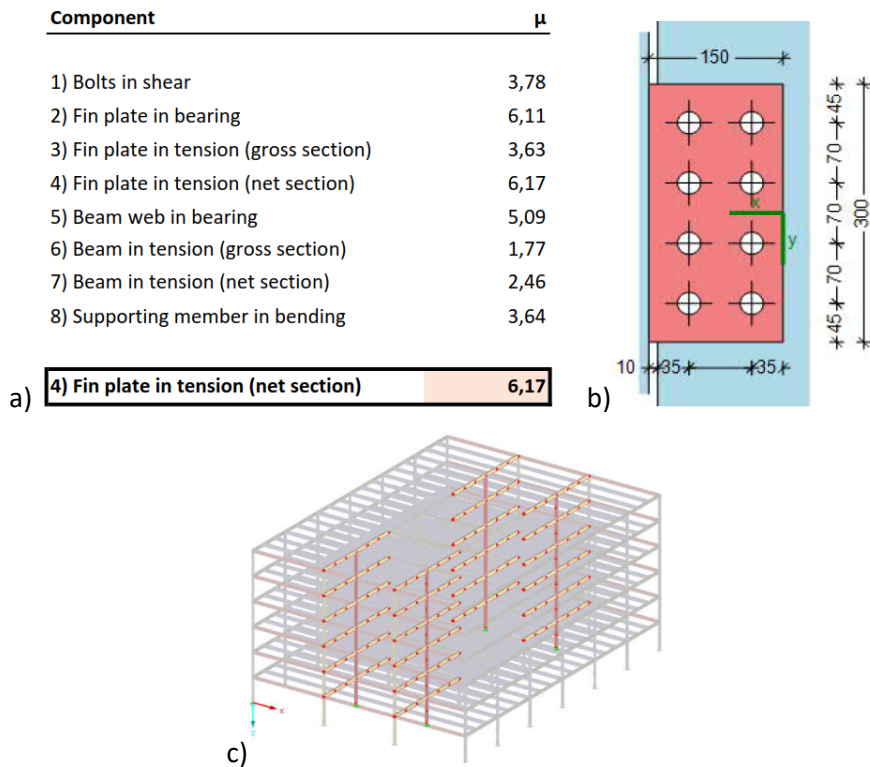


Figure 92. Connection C3w: a) capacity ratios for components of connection; b) connection geometry; c) location in the structure

Note: The slight difference in joint tying forces in Table 45 and tying forces for member verifications from Table 44 is due to the fact that member verifications are performed at mid-span where the moment is at its maximal value.

Redesigned joint **B1/B3** requires the following :2 added bolts, M27 instead of M24, additional welded web plate to the beam, modified fin plate geometry and thickness (25 mm) as well as thicker weld for ductility requirements (15 mm).

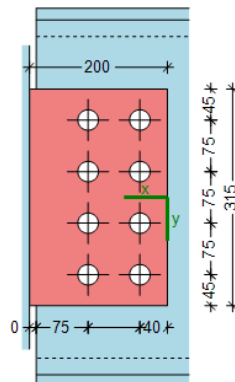


Figure 93. Redesigned joint B1/B3 to fulfill tying forces verifications according to the numerical approach

Table 46. Redesigned joints verifications (scenario 2)

Position s = strong axis w = weak axis	Tensile force (kN)	Failure mode	UF
B1 / B3	1662	Bolts in shear	1.00
C2w / C3w	4852	Not feasible	

This leads to an utilization factor of 1.00 with bolts in shear as failure mode. Welded web plates to the beam are preferred to changing the beam cross-section in order to reduce the weight and thus the cost of the structure. The verification is illustrated in Figure 94, with details given in Annex A.3.11.

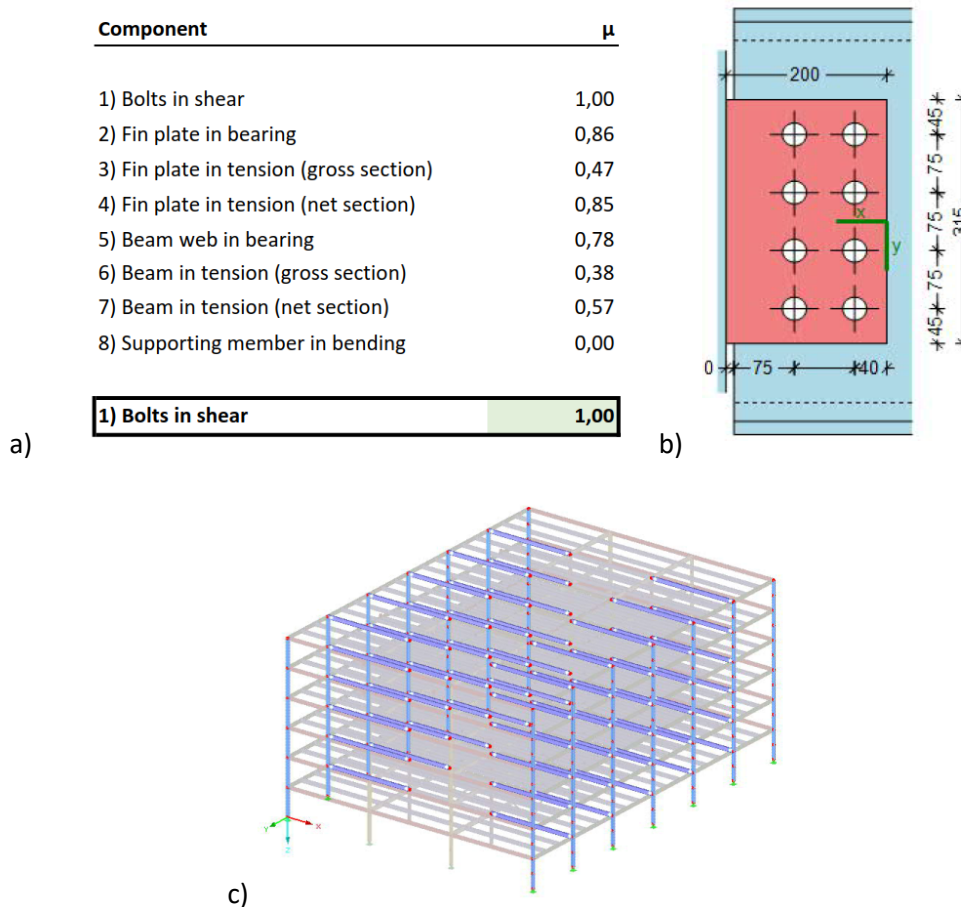


Figure 94. Connection B1 /B3: a) capacity ratios for components of connection; b) connection geometry; c) location in the structure

For joints **C2w** and **C3w** (see Annexes A.3.12 and A.3.13), no reasonable redesign could be found. For C2w, even a welded 40 mm column web plate would still not be sufficient to sufficiently reinforce the component column web in bending. And for both joints, 14 M36 10.9 bolts would be required to fulfil the verification of bolts in shear, however this would be not feasible geometrically speaking due to the limited beam height and required bolts and pitch distances, together with an impossible verification of the net section of the beam. Changing the beam cross-section would also lead to an unreasonable solution in terms of beam height and overall weight. Even by taking into account the plasticity in the numerical analysis, the tensile force would be of the same order of magnitude.

An alternative could be to use pinned header plate joints. This would solve the problem of lack of beam net section resistance as there won't be holes in the beam web anymore. However, the number of required bolts would still be unreasonable and column flanges should also be greatly reinforced to withstand high bending moments in column flanges.

It appears that pinned joints are not a reasonable choice to ensure sufficient robustness to this structure. Another suitable approach might be to replace pinned joints with semi-rigid joints (partial strength). This alternative is discussed by applying the analytical method in 5.3.3.2.

- **Scenario 2** : Facade column loss at floor 0

In this scenario, no member redesign is needed. However, IPE500 beam-to-column joints (A1s and A2s) have to be redesigned.

Joints verifications for tying forces are illustrated in the following.

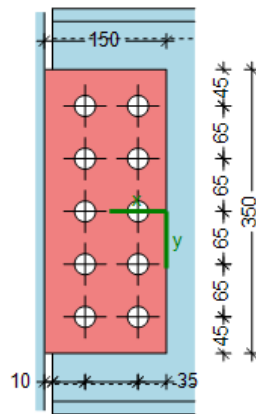


Figure 95. Redesigned joint A1s / A2s to fulfill tying forces verifications according to the numerical approach

Redesigned joint **A1s / A2s** requires the following :4 added bolts, M24 instead of M20, additional welded web plate to the beam, modified fin plate geometry and thickness (20 mm) as well as thicker weld for ductility requirements (12 mm).

Table 47. Redesigned joints verifications (scenario 2)

Position s = strong axis w = weak axis	Tensile force (kN)	Failure mode	UF
A1s / A2s	1620	Bolts in shear	1.01

The utilization factor is exceeded by 1%. This exceedance can be considered as acceptable. The redesigned solution could still be considered as feasible. The verification is illustrated in Figure 96 with details presented in A.3.15.

Component	μ
1) Bolts in shear	1,01
2) Fin plate in bearing	0,94
3) Fin plate in tension (gross section)	0,52
4) Fin plate in tension (net section)	0,92
5) Beam web in bearing	0,81
6) Beam in tension (gross section)	0,84
7) Beam in tension (net section)	0,68
8) Supporting member in bending	0,00

a) 1) Bolts in shear	1,01
-----------------------------	-------------

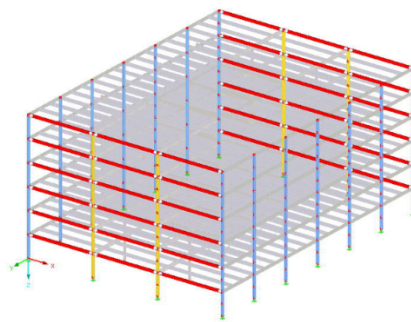
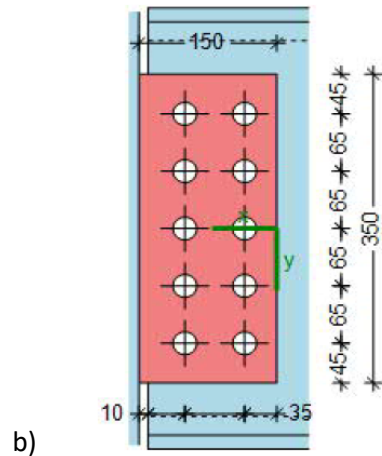


Figure 96. Connection A1s / A2s: a) capacity ratios for components of connection; b) connection geometry; c) location in the structure

5.3.3 ALPM : Analytical approach

5.3.3.1 Structure with simple joints

Analytical approaches are applied here for the column loss **scenario 1** (see 5.3.2.1).

The procedure consists of solving the system of 4 equations as shown in Figure 97.

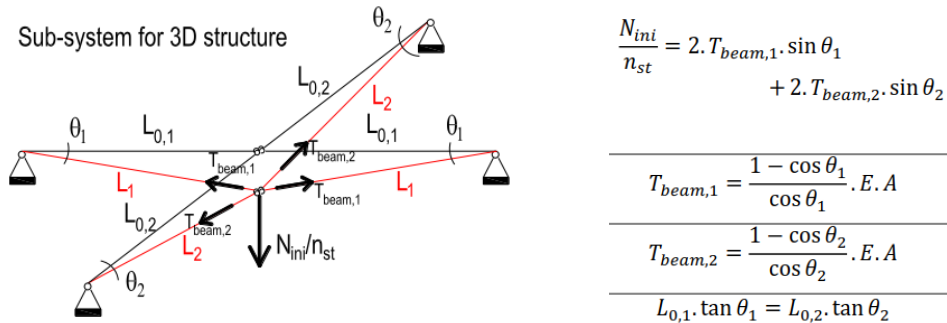


Figure 97. Equation system of the analytical approach for simple joints

Parameters are summarized in Table 48.

Table 48. Input parameters for the analytical approach with simple joints

N_{ini}	n_{st}	E	A_1	$L_{0,1}$	A_2	$L_{0,2}$
4078.51 kN	6	210000 MPa	134 cm ²	12 m	156 cm ²	8 m

Beam with index 1 is the IPE550, while beam with index 2 is the IPE600. The initial force in the column N_{ini} is taken from the numerical approach by considering the accidental load case combination as defined in 5.3.

By reworking the equation system and embedding values from the above table, the first equation can be written as follow for $x = \theta_2$:

$$17866.67 \tan(x) (1 - \cos(\tan^{-1}(0.67 \tan(x)))) + 31200 \tan(x) (1 - \cos(x)) - 3.24 = 0$$

The solution to this equation is $x = \theta_2 = 0.05485$ rad. All four unknowns are summarized in the following table.

Table 49. Solution of the equation system for the analytical approach in scenario 1

θ_1	θ_2	$T_{beam,1}$	$T_{beam,2}$
0.03659 rad	0.05485 rad	1884 kN	4934 kN

The tensile forces due to membrane effects in IPE550 and IPE600 beams are respectively 1884 kN and 4934 kN. With the numerical approach, we had respectively 1741 kN and 4565 kN, see Table 40. The tension forces obtained with the analytical approach are approximately 8% higher than the values from the numerical approach. However, it is known that the analytical approach overestimates the tensile forces, so that the order of magnitude here is coherent and validates the tensile forces obtained with the numerical approach.

The same conclusions as in the numerical approach in term of needs of redesign of the structure for robustness can then be drawn from these analytical results.

Notice that the contribution of the slab has been neglected in the above calculation. In the next section, this contribution will be assessed.

5.3.3.2 Structure with partial-strength joints

As stated above, partial-strength joints might be a good alternative to pinned joints to increase the robustness of the structure. In order to investigate this, main beam-to-column joints will be replaced by flush end plate joints as illustrated in the following.

All these joints have M24 10.9 bolts and 15 mm thick end plates.

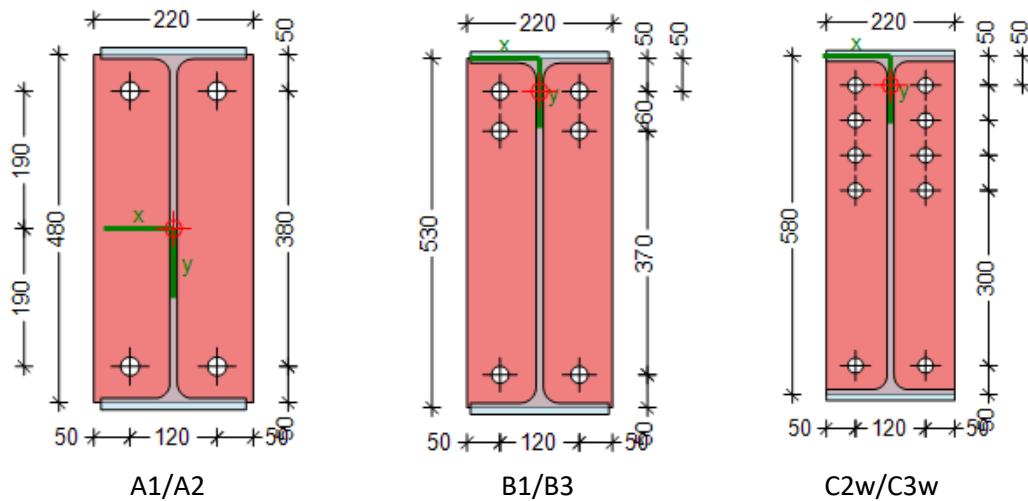


Figure 98. Alternative partial-strength flush end plate joints for the analytical approach

These semi-rigid joints have been designed to withstand the ULS shear forces from the initial design by considering the possible N-V interaction in bolts on the safe side.

Note that for beam-to-column joints bolted on the weak axis of the column (through the column web), a welded part is needed to rebuild a “strong axis” typed joint, as exemplary illustrated in Figure 99.

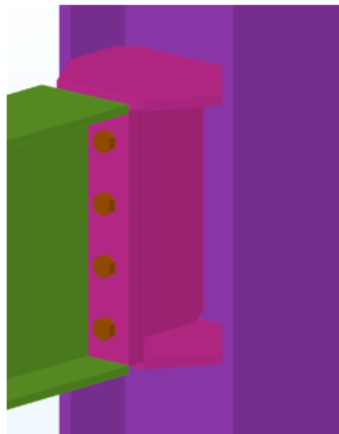


Figure 99. Welded part for weak axis flush end plate joints (bolt pattern not representative)

The simplified analytical method with partial-strength joints takes following effects into account:

- Contribution of the plastic mechanism of beams
- Contribution of the slab
- Contribution of the arch effect

If the sum of the above contributions is not sufficient, larger deformations develop and membrane effects in the beams are activated similarly as in the simple joint example. As this requires greater

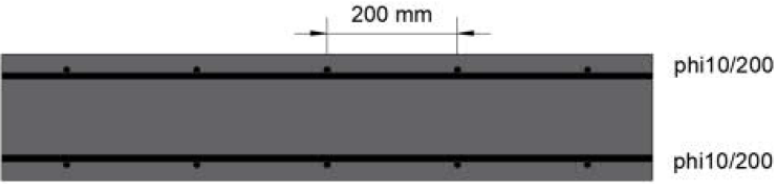
rotational capacity for the joints, we will here perform the robustness design alternatively by optimizing the three above contributions in order not to require membrane effects.

5.3.3.2.1 Contribution of the slab

The slab is designed to fulfil SLS/ULS requirements. The steel reinforcement is defined by the minimal constructive reinforcement according to DIN EN 1992-1 Chap. 9. The detailed design is given in the following.

Analytical approach : ULS design of the slab

Properties



Class	C30/37	Dead load	5 kN/m ²
Thickness	20 cm	Live load	3 kN/m ²
Cover	20 mm	<i>Note: Snow loads are neglected (no combinations with live loads)</i>	
f_{ck}	30 MPa	q_{Ed}	11,3 kN/m ² ULS Load
f_{yk}	500 MPa		
A_{sx}	3,925 cm ² /m		
A_{sy}	3,925 cm ² /m		
Bar diameter	10 mm		

ULS design

For the design, we consider a 1 m wide section spanning in 1 direction (beam behaviour)

A_s	3,925 cm ²	Reinforcement
f_{yd}	434,8 MPa	Design value of the reinforcement yield stress
f_{cd}	17,0 MPa	Design value of concrete resistance
z	15,75 cm	Leverarm
M_{Rd}	26,88 kNm/m	Design bending resistance

Note: Due to the secondary beams, the span of the slab is small (2.66 m) so that the ULS design is not relevant.

Stress block verification (crushing of concrete)

x	12,55 mm	Height of concrete zone at yielding
σ_c	13,6 MPa	Compressive stress in concrete at yielding

Bending resistance governed by rebars yielding (ductile failure mode)

Minimal reinforcement (constructive rule acc. To DIN EN 1992-1 Chap. 9)

f_{ctm}	2,832 N/mm ²	
f_{yk}	500 N/mm ²	
d	175 mm	
$A_{s,min}$	2,577 cm ² /m	Minimal required reinforcement

The required reinforcement is governed by the constructive minimal reinforcement.

After the column loss according to the investigated scenario 1, the static system of the concrete slab without accounting for any restraints coming from the inner beams as at this point no membrane effect could develop (they occur first when larger deformations could develop) becomes as illustrated in Figure 100.

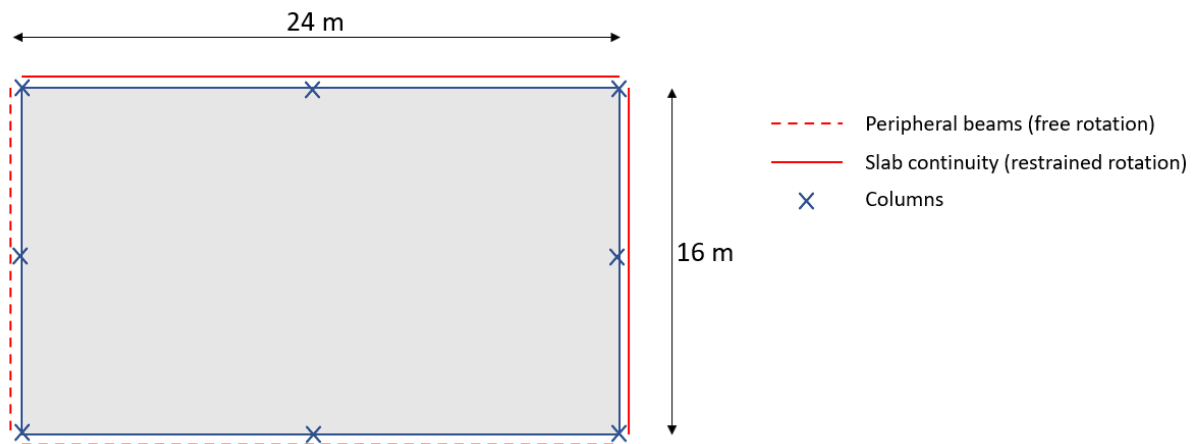


Figure 100. Statical system of the concrete slab after column loss

The accidental loading ($1 \times G + 0.5 \times Q$) of 6.5 kN/m^2 (by neglecting facade loads) creates large bending moments for which the slab was not designed, see Figure 101.

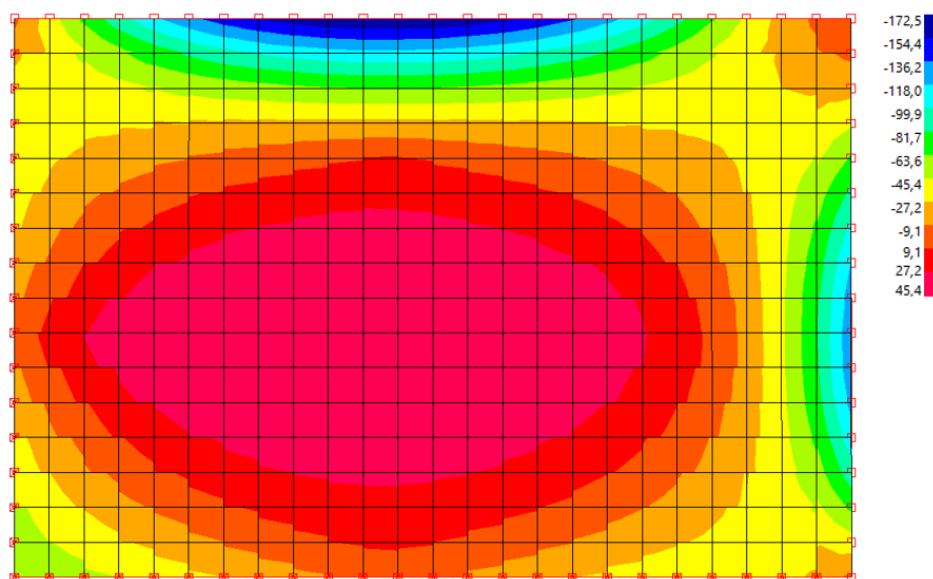


Figure 101. Accidental bending moment in the concrete slab after column loss ($M_{Ed} = -172.5 \text{ kNm}$)

Consequently, the concrete slab won't be sufficient by itself to ensure the robustness of the structure. However, together with other effects as listed above, the slab can still contribute to ensure robustness. This contribution is expressed as the vertical point force P_{slab} (where the column is lost) needed for a plastic mechanism to develop. As the failure mode of the slab is ductile (yielding of the steel reinforcement), the slab will be able to maintain the plastic moment along yielding lines.

The plastic mechanism is obtained according to the Johanssen method. Two failure patterns were investigated : a non-circular and a circular one. Both are illustrated in the following figures.

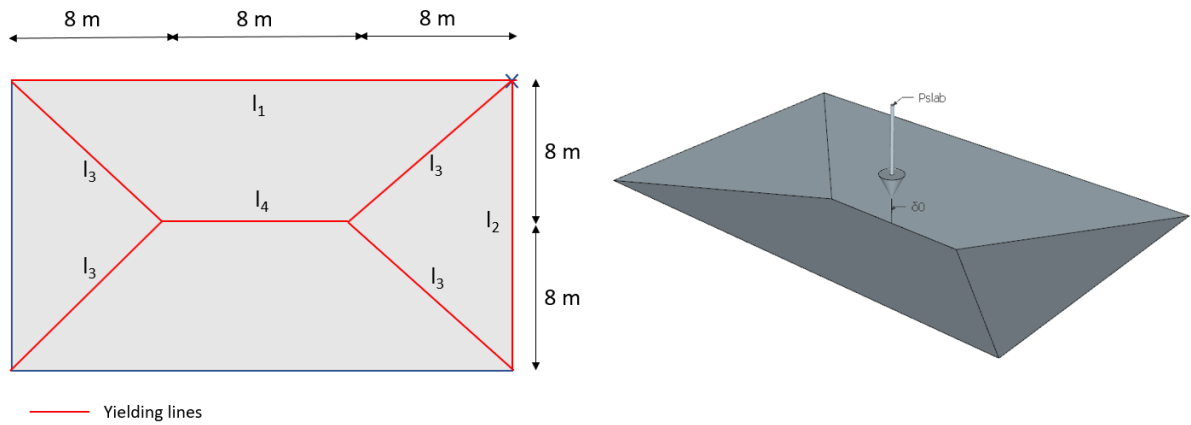


Figure 102. Non-circular plastic mechanism pattern

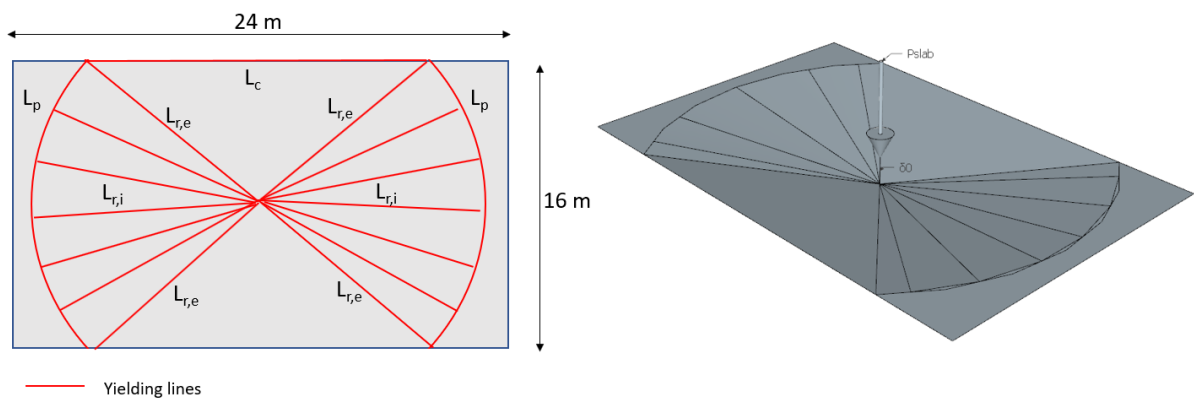


Figure 103. Circular plastic mechanism pattern

Using the virtual works principle, we obtain following forces:

- **Non-circular pattern: 313.6 kN**

Detailed calculation:

Work of external forces $W = P_{slab} \cdot \delta_0$

Work of internal forces $U = M_{Pl} [kN.m/m] \cdot l_{lines} [m] \cdot \theta [rad]$

$M_{pl,Rd,slab}$ 26,9 kNm/m

Moment resistance of the slab

$$U = M_{Pl} \cdot 24 \cdot \frac{\delta_0}{8} + M_{Pl} \cdot 16 \cdot \frac{\delta_0}{8} + 4 \cdot M_{Pl} \cdot \sqrt{8^2 + 8^2} \cdot \frac{\delta_0}{8} + M_{Pl} \cdot 8 \cdot \frac{\delta_0}{8}$$

U/δ_0 313,6 kNm

$P_{slab,nc}$ 313,6 kN by equalling W and U

- **Circular pattern: 330.4 kN**

Detailed calculation:

Work of external forces $W = P_{slab} \cdot \delta_0$

Work of internal forces $U = M_{Pl} \cdot \delta_0 \cdot \left(2\varphi + 4 \cdot \cot\left(\frac{\varphi}{2}\right) \right) + 2 \cdot \varphi \cdot M_{Pl} \cdot \delta_0 + M_{Pl} \cdot 2 \cdot \cot\left(\frac{\varphi}{2}\right) \cdot \delta_0$

see the Master Thesis of Maxime Vermeylen for a detailed explanation of this equation.

$\varphi = 90,0$ deg angle minimising the mechanism resistance

$$P_{slab,cone} = M_{Pl} \cdot (\pi + 4) + \pi \cdot M_{Pl} + M_{Pl} \cdot 2$$

$$= 330,42 \text{ kN} \quad \text{by equalling W and U}$$

The value of $N_{pl,slab}$ is given by the minimum of both above values, i.e. 313.6 kN

More details about the derivation of these values from the plastic mechanisms are found in the detailed calculation and in the Master Thesis of Maxime Vermeylen (Vermeylen 2021).

5.3.3.2.2 Contribution of the steel beam mechanism

Due to the use of partial-strength joints, we can compute the vertical force associated to the development of a plastic beam mechanism s due to the formation of plastic hinges in the joints.

As we have partial-strength joints in both directions, this force is given by the following equation (adapted from the 1D version), see Figure 104 for the illustrated mechanism.

$$N_{pl} = \frac{2 \cdot M_{pl,Rd,1}^- + 2 \cdot M_{pl,Rd,1}^+}{L_{0,1}} + \frac{2 \cdot M_{pl,Rd,2}^- + 2 \cdot M_{pl,Rd,2}^+}{L_{0,2}}$$

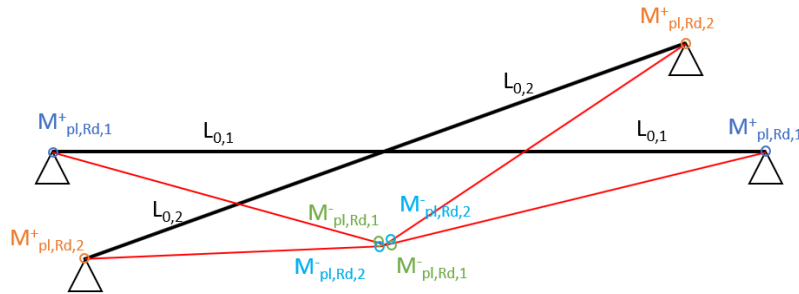


Figure 104. Plastic beam mechanism developing in the beams with partial-strength joints

Sagging and hogging moment resistances are given in the Table 50 with detailed calculations provided in Annex A.3.16.

Table 50. Additional input parameters for the analytical approach with partial-strength joints

Joint B1/B3		Joint C2/C3	
$M_{pl,Rd,1}^+$ (hogging)	$M_{pl,Rd,1}^-$ (sagging)	$M_{pl,Rd,2}^+$ (hogging)	$M_{pl,Rd,2}^-$ (sagging)
306.1 kNm	224.7 kNm	416.6 kNm	305.6 kNm

The detailed determination of the moment resistance of the above joints is given in the following. Notice that 2 load cases (one with a positive moment and one with a negative one) are defined in order to derive both sagging and hogging moment resistances.

Beam parameters are given below:

Beam 1	IPE550	Beam 2	IPE600
A_1	13400 mm ²	A_2	15600 mm ²
$L_{0,1}$	12000 mm	$L_{0,2}$	8000 mm

From these values, we can obtain the force N_{pl} using the above formula which equals 269.0 kN

5.3.3.2.3 Contribution of the arch effect

In analogy to previous sections, we calculate here the vertical point force P_{arch} needed to overcome the arch effect.

The arch effect is only activable if the compression resistance of any activated component of the platform system once the above mechanism has developed is not governing, in other words if the failure mode of the platform is not a component (i.e. a joint or a beam) in compression. In such conditions, an arch effect can be mobilised within the beams of the directly affected part, as soon as the plastic mechanism has formed. The following table summarizes the failures modes of concerned joints.

Table 51. Failure modes of the partial-strength joints

Joint	Sagging / hogging	Failure mode
B1/B3	hogging (+)	Column web in compression
B1/B3	sagging (-)	Column web in compression
C2/C3	hogging (+)	Column web in compression
C2/C3	sagging (-)	Column web in compression

As all joints fail in compression, no arch effect can be activated, so that $P_{arch} = 0$ kN.

5.3.3.2.4 Verification of the structure with partial-strength joints

Contribution from the slab, the beam mechanism and the arch effect can be cumulated as they as their activation requires limited deformation capacities. The total resistance is then:

$$N = N_{slab} + N_{pl} + N_{arch} = 313.6 + 269.0 + 0.0 = 582.6 \text{ kN}$$

The vertical action applied when the column is lost equals the vertical tying force in internal columns (for scenario 1) and has been estimated to 694.2 kN (see 5.3.1.1). As the resistance of all the above contributions together is lower that the vertical tying force, the structure cannot be assumed as robust.

This means that significant vertical displacements of the directly affected part will develop with the apparition of membrane forces $N_{membrane}$ in the beams. Such membrane forces cannot be cumulated with the previous contributions as they disappear once large deformations are reached.

The contribution $N_{membrane}$ requires the adoption of advanced design methods due to M-N interaction in the joints. This contribution would require significant deformation capacities at the level of the partial-strength joints. In such situation, the required levels of deformation capacities are not achievable in most of the cases, so that this contribution won't be assessed here.

As already stated earlier, ductile joints (ductile joint failure modes) are required for the assumption of plastic hinges formations in joints. The failure mode of joints is here column web in compression under bending moments. As this component is not considered as ductile, these joints need to be redesigned. This will be assessed with the robustness redesign in the next part.

5.3.3.2.5 Redesign of the structure with partial-strength joints

Before performing the redesign, it has to be noted that in a consistent way, the use of semi-rigid joints would modify the internal forces distribution in the structure. We could expect smaller beam

deflections at SLS so that smaller beam cross-sections could be used, but we should expect bending moments in columns so that larger column cross-sections might be required. However for usual buildings, the column cross-sections don't need to be upgraded due to the additional restraint coming from the beam-to-column joint stiffnesses. In the framework of this worked example, the steel structure has been kept as it is (designed with internal forces with the simple joint modelling). Modelling semi-rigid joints as hinges is still a valid assumption if these joints have enough ductility and rotation capacity to form plastic hinges at ULS in order to reach the same internal forces distribution as with pinned joints.

There are several ways of achieving the robustness requirements, such as:

- Modify the slab design to increase the contribution from the slab mechanism
- Strengthen the joints in one or both directions to increase the contribution of the beam mechanism
- Reinforce compression components to activate the arch effect

In order to show the contribution of the arch effect in practice, we mainly chose here to modify the joints C2/C3 as shown in the following figure.

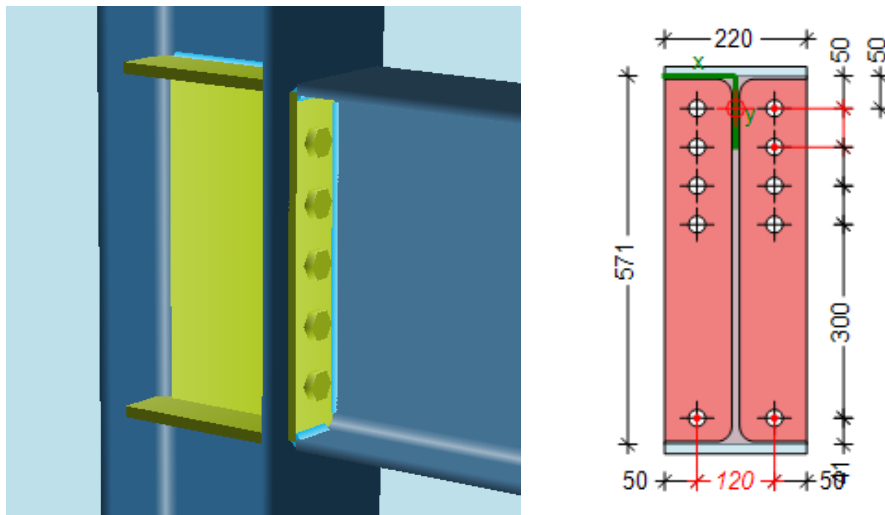


Figure 105. Redesign of joint C2w/C3w to fulfill robustness requirements

Changes are as follows:

- Column stiffeners (same thickness as beam flanges)
- Web stiffener
- Adapted bolt pattern
- Flange welds changed from 6 to 7 mm

Column and web stiffeners are needed to activate the arch effect (see below). Note that specific rules from the EN 1993-1-8 have to be fulfilled in order to take web plates into account in the joint verification. As hogging and sagging bending moments play a role in the beam mechanism as well as in the arch effect, the unsymmetrical bolt pattern has been modified to a symmetrical one. M27 bolts (instead of M24) have been chosen to still fulfill the ULS shear force verification. Finally, the flange welds have been increased for ductility issues.

Modifications of the B1/B3 joint are needed to increase the contribution of the beam mechanism and reach the robustness requirements.

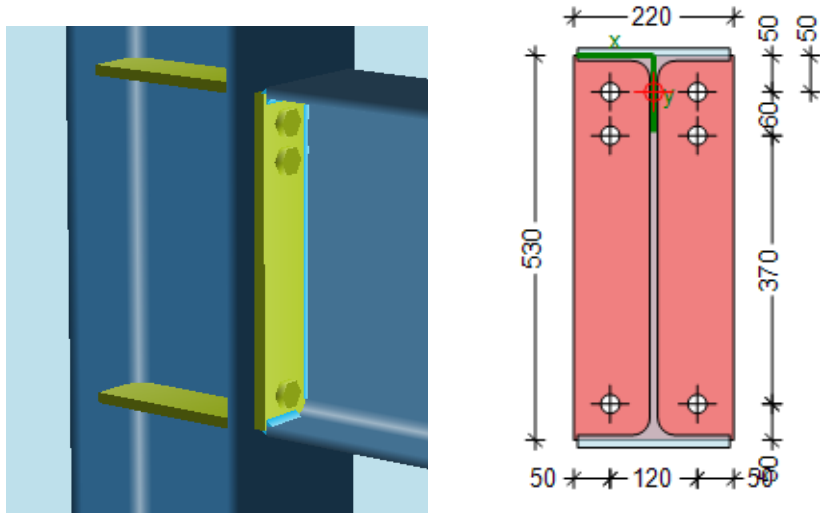


Figure 106. Redesign of joint B1/B3 to fulfill robustness requirements

Changes are as follows:

- Column stiffeners (same thickness as beam flanges)
- End plate thickness changed from 15 to 20 mm
- Flange welds changed from 6 to 7 mm

Changes in this joint allow to increase the bending moment resistance of the joint and thus the beam mechanism. The bolt pattern remains unchanged.

a) Contribution of the slab

As no changes have been made to the slab, the contribution of this component remains unchanged ($N_{slab} = 313.6$ kN).

b) Contribution of the beam mechanism

The sagging and hogging bending moment resistances of the redesigned joints are given in Table 52.

Table 52. Bending moment resistances of the redesigned joints B1/B3 and C2/C3

Joint B1/B3		Joint C2/C3	
$M_{pl,Rd,1}^+$ (hogging)	$M_{pl,Rd,1}^-$ (sagging)	$M_{pl,Rd,2}^+$ (hogging)	$M_{pl,Rd,2}^-$ (sagging)
368.9 kNm	285.4 kNm	451.3 kNm	451.3 kNm
CWS	CWS	EPB	EPB

From these values, we can obtain the force N_{pl} which equals now 334.7 kN.

The detailed determination of the moment resistance of the above joints is given in Annex.

c) Contribution of the arch effect

In the framework of this example, we consider only the arch effect coming from the short frame (IPE600 with C2/C3 joints), as illustrated in two dimensions in the Figure 107.

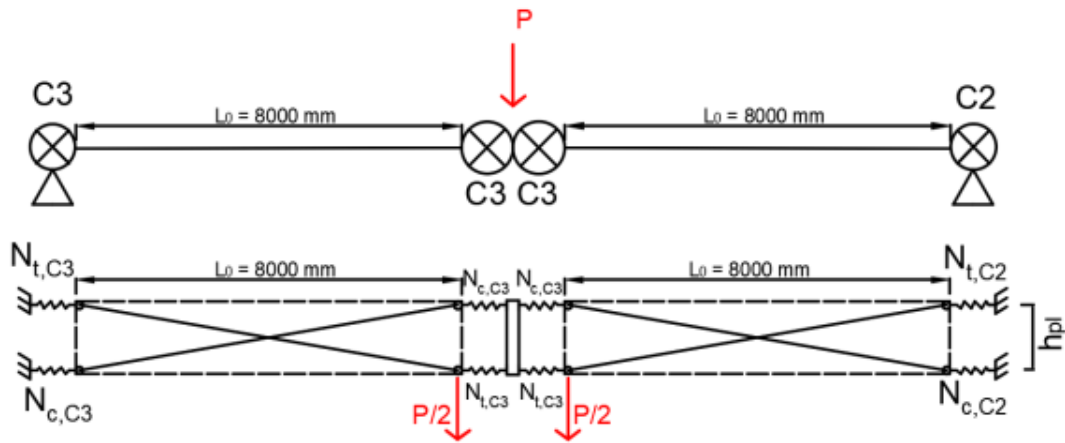
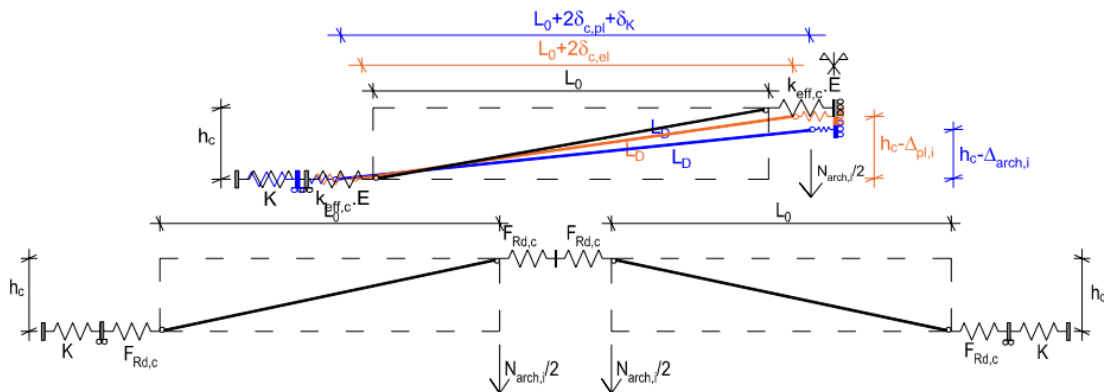


Figure 107. Model applied for the arch effect

Indeed, there will be no contribution coming from the other direction as the failure mode of the joints B1/B3 is column web in shear. This means that once the moment resistance of these joints is reached, there is no way to increase the tension forces in the rows to contribute to an extra arch effect.

For the redesigned joint C2/C3, the failure mode is end plate in bending. Notice that since the joint is now symmetrical, values for hogging and sagging are identical. A detailed calculation of the arch effect is illustrated in the following. A similar calculation can also be found in the Master Thesis of Maxime Vermeulen (Vermeulen 2021) for other input parameters.

Analytical approach : Arch effect with redesigned partial strength joints



$P_{pl,beam}$	334,7 kN	Load needed to activate the beam mechanism
L_0	8000 mm	Length of the beam
E	210000 MPa	Young Modulus
I_y	92080 cm ⁴	Moment of inertia of the beam
Δ_{beam}	36,9 mm	Vertical displ. of the beam due to the mechanism
η	2 [-]	acc. to Table 5.2 of EN 1993-1-8
M_{Rd+}	451,3 kNm	Positive moment resistance (hogging)
S_{jt}	114000 kNm/rad	Positive rotational stiffness
θ_+	0,00792 rad	Rotation of the joint due to the mechanism

M_{Rd}	451,3 kNm	Negative moment resistance (sagging)
S_j	114000 kNm/rad	Negative rotational stiffness
θ	0,00792 rad	Rotation of the joint due to the mechanism

θ 0,00792 rad Minimal value governing

Δ_{joints} 63,3 mm Rotation of the joint due to the mechanism

Δ 100,3 mm Total vertical displacement due to the mechanism

Bolt rows Nr. Force

1	430,2 kN	Tension force in bolt row 1
2	317,3 kN	Tension force in bolt row 2
3	200,3 kN	Tension force in bolt row 3
4	200,3 kN	Tension force in bolt row 4
5	221,3 kN	Tension force in bolt row 5
Ft	1369,4 kN	Sum of tension forces in bolt rows

Stiffness coefficients

k_7	$+\infty$ mm	Beam flange in compression
k_1	9,461 mm	Column web in shear
k_2	$+\infty$ mm	Column web in compression

$k_{eff,c}$ 9,461 mm Effective compression stiffness

$\Delta_{c,el}$ 0,689 mm Compression shortening of the joint

h_{Beam}	600 mm	Beam height
t_f	19 mm	Flange thickness
h_c	581 mm	Lever arm
L_D	8017,0 mm	Length of arch rod when mechanism forms

$F_{Rd,c}$ 1783 kN Compression resistance of the joint (column web in shear)

$\Delta_{c,pl}$ 0,897 mm Compression shortening once arch resistance is reached

$\cos(\theta)$ 0,998

θ 0,062 rad Inclination of the arch rod (stiffness of IAP = diaphragm)

N_{arch} 51,0 kN Contribution of the arch effect

Resistance of the arch rod (buckling resistance acc. To DIN EN 1993-1-1)

L_b	16 m	Buckling length (safe approach)
I_z	3387 cm ⁴	Moment of inertia (buckling along weak axis)
N_{cr}	274,2 kN	Critical load (Euler)
A	15600,0 mm ²	Cross section
f_y	355 MPa	Elastic limit
N_{plRd}	5538,0 kN	Plastic resistance of the arch rod
α	0,34	Imperfection coefficient (buckling curve b)
λ	4,49	
ψ	11,3	
χ	0,046	
N_{bRd}	231,7 kN	Buckling resistance

Note that the compression resistance of the joint is governed by the component column web in shear.

Following further assumptions have been made:

- Since the IAP is made of diaphragms, its lateral displacement has been neglected.
- Since joints C2 and C3 are similar, they have been considered as identical in terms of stiffness and resistance.

From these values, we can obtain the force N_{arch} which equals 51.0 kN

This contribution can be cumulated to the ones coming from the beam and slab plastic mechanisms as the activation of this arch effect required limited deformation capacities.

By cumulating all of the above contributions, the total resistance is now:

$$N = N_{slab} + N_{pl} + N_{arch} = 313.6 + 334.7 + 51.0 = 699.3 \text{ kN}$$

The resistance is now greater than the vertical tying force of 694.2 kN, so that the redesigned structure can now be assumed as robust.

5.3.4 Segmentation (prescriptive approach)

If the alternative load path method is not an option because redesign requirements are too expensive, the segmentation method might be an alternative solution to ensure a sufficient robustness, depending on the project requirements.

In the current case of a horizontal low-rise building, a weak segmentation border strategy could be chosen. The ULS designed pinned fin plate joints of the structure are not able to withstand the large tensile forces from membrane effects, as it has already been seen with both analytical and numerical approaches. These joints will then act as “fuses” so that in case of a column loss, the building will collapse in full height, but the damage will be limited horizontally. In addition to this, as these joints are ductile, they help creating large deformations before collapse of the directly affected zone.

5.4 Final design outputs and remarks

From this worked example, several conclusions can be drawn:

- Tying forces according to the prescriptive approach are much smaller than the values obtained with both analytical and numerical approaches. The prescriptive approach is then considered as unsafe for the design of robust steel structures.
- The full numerical approach is quite complex and requires some good finite element knowledge.
- The analytical method is a good alternative to the full numerical approach for practitioners and provides results close to the ones obtained with the full numerical approach.
- The need of reinforcement driven by robustness requirements is more related to joints than to members.
- Pinned joints (especially fin plates) are not the best solution for robust steel structures. The use of partial-strength joints allows to delay the apparition of membrane effects and thus tends to lower tensile forces in ties.
- Another key of robustness structures is ductility and capacity of deformation. This avoids brittle failure and optimizes the postcritical behaviour of the structure in case of an exceptional event.

6 Composite Structure in Non-Seismic area (AM)

6.1 Description of the design and main outputs

In the scope of this analysis, two different designs were considered:

- Office building with composite beams and steel columns;
- Office building with composite beams and composite columns.

The design of the composite structure was developed using the software SCIA® (version 2019) and considering standard IPE sections for the beams, combined with a cofraplus floor system, HD sections for the columns and tubular elements for the bracing system.

- Beams.
 - Perimeter beams – IPE450.
 - Interior beams.
 - X direction – IPE360.
 - Y direction – IPE500.
 - Inner core beams – IPE500.
- Columns.
 - Perimeter columns – HD360x162.
 - Inner columns – HD400x216.
- Bracing system.
 - CHS 219.1x5.0.
- Floor system.
 - Cofraplus 60 (0.88 mm) – 130 mm slab thickness.

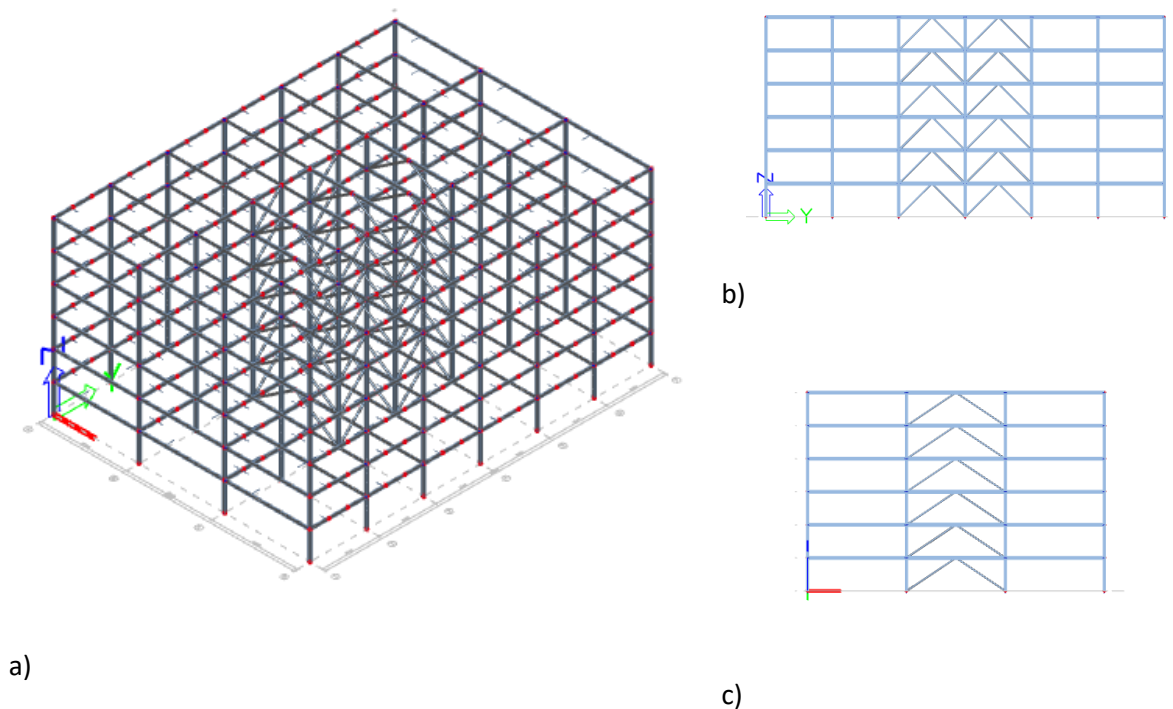


Figure 108. Structural view: a) 3D view; b) Y-Z side view; c) X-Z side view.

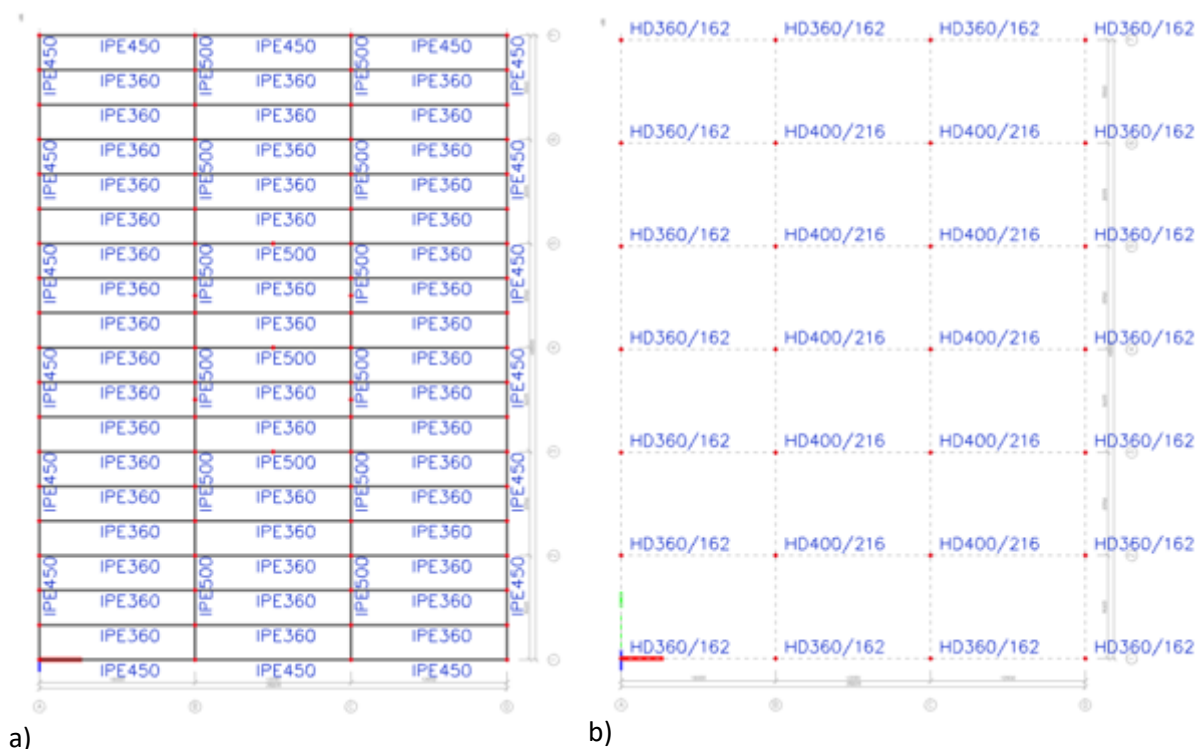


Figure 109. Plan view: a) beams; b) columns.

A set of load combinations was defined in accordance with EN 1990 considering the construction stage:

- SLS - Char - Construction Stage / SLS - Char - Final Stage / ULS - Set B - Construction Stage / ULS - Set B - Final Stage.

The connections were defined as pinned and the bottom supports for the columns fixed. The composite design was made with SCIA® composite design module and using the Eurocode (EN 1994 - 1-1:2004) with the respective Luxembourgish National Annex. "Nelson studs d=19mm, h=100 mm" were used in a single row and a longitudinal and transversal reinforcement of $\phi 12//100$ applied on the slab.

The output of the design check was the following (in terms of utility factors):

Table 53. Utility factors.

Element	Type	Section	Utility		Critical design (ULS / SLS)
			ULS	SLS	
Beams	Perimeter beams	IPE 450	0.93	0.8	- Final Stage - Crushing concrete flange. - Final Stage - Deflection
	Interior beams	IPE 500	0.96	0.86	- Final Stage - Bending - Final Stage - Deflection
		IPE 360	0.95	0.98	- Final Stage - Bending - Final Stage - Deflection
Columns	Perimeter columns	HD 360x162	0.61	-	- Final Stage - Bending and axial compression
	Interior columns	HD 400x216	0.78	-	- Final Stage - Bending and axial compression
Bracing system	Circular hollow sections	CHS219.1x5.0	0.71	-	- Final Stage - Bending and axial compression

The global arrangement of the office building with composite columns was based on the previously design, replacing only the vertical steel elements by circular composite columns.

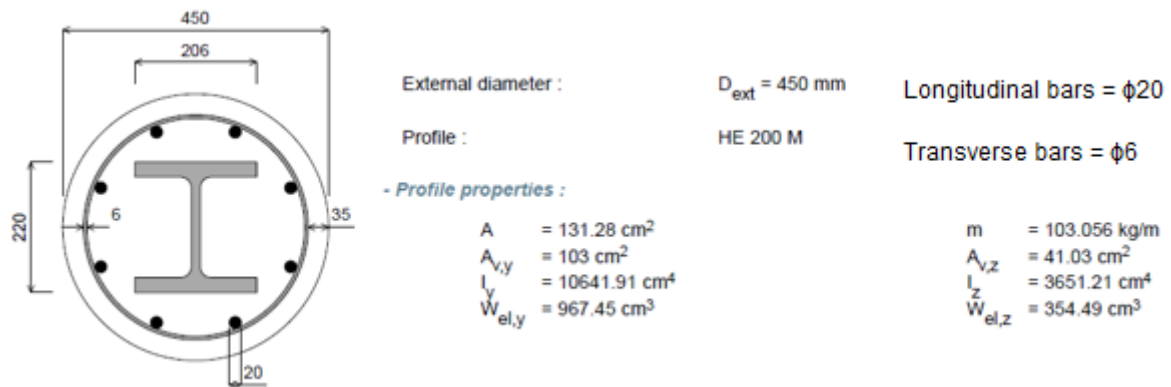
The design of these columns was made considering the loads from the previous SCIA® design and using ArcelorMittal's software A3C® as a pre-design approach, according to the following process:

- Check of the critical load combinations for the design of the perimeter and interior steel columns;
- Extract of the loads for each load case corresponding to the critical load combination;
- Input of the loads and respective combinations in A3C®;
- Pre-design of the composite sections.

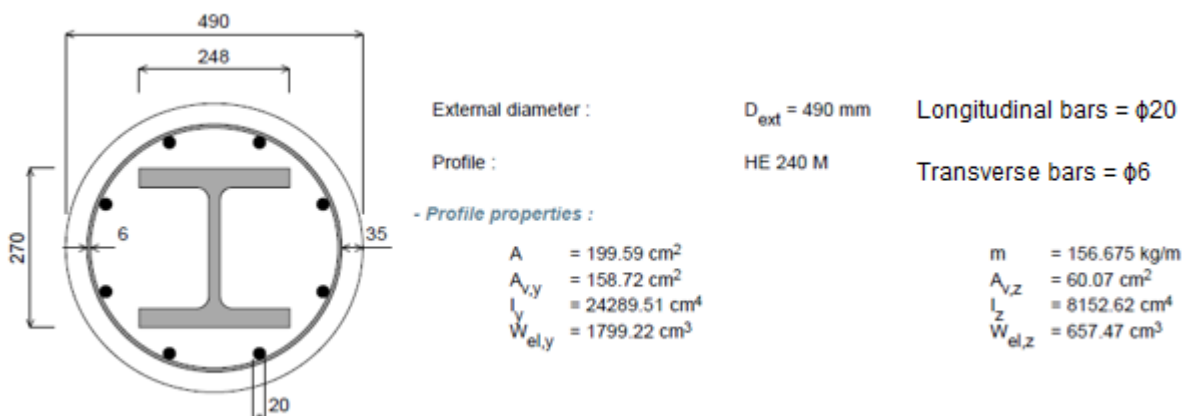
Note that the composite columns were pre-designed in order to have similar capacity as the steel columns (similar utility factors). In A3C®, the self-weight of the vertical steel elements was removed and replaced by the weight of the pre-designed composite columns (however this value represents a small percentage of the total load).

Based on the previous process the following composite columns were defined:

- Perimeter columns (**Maximum utility factor = 0.63**)



- Interior columns (**Maximum utility factor = 0.78**)



6.1.1 Connections

Two different types of connections were calculated:

- Header plate;
- Fin plate.

A comparison between header plate and fin plate connections was performed for the joints of the perimeter beams (IPE450) and internal beams (IPE360) to the columns (HD360x162).

The summary of the results for the joints may be found in the Table 54.

Table 54. Verifications of joints at ULS, CS-NS

Position	Connection type	Shear resistance (kN)	Moment resistance (kNm)	Failure mode	UF
Perimeter	Header plate	289.38	-	Shear resistance of bolt group	0.73
	Fin plate	297.96	-	Shear resistance of bolt Group	0.71
Internal	Header plate	289.38	-	Shear resistance of bolt group	0.64
	Fin plate	265.89	-	Bolt bearing in supported beam web	0.70

6.2 Verifications for identified actions

6.2.1 Impact

The equivalent static approach method is applied for the impact analysis. According to the flow of traffic, a total of four different situations are assumed for pre-selected columns located at the ground floor of the building, as illustrated in Figure 112.

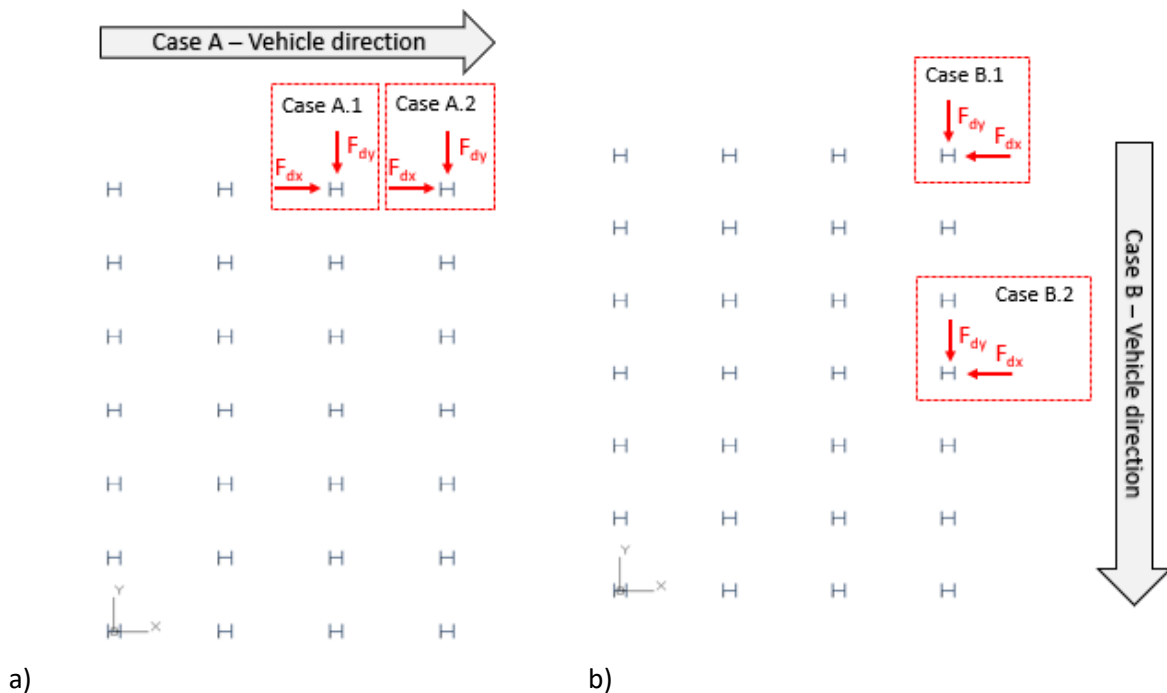


Figure 112. Plan view at ground floor level, columns assumed for impact analysis: a) case A; b) case B.

In the equivalent static load approach prescribed in EN 1991-1-7:2006, the impact load is replaced by an equivalent static force that accounts for effects of the load in the structure (including dynamic effects). The most common situation in buildings is the impact of a vehicle in one of the supporting columns.

The loads applied in the columns are derived from the Table 55 and Table 56 taken from EN 1993-1-7:2006.

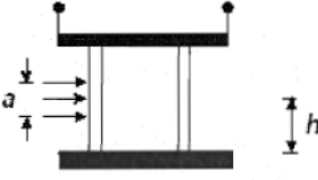
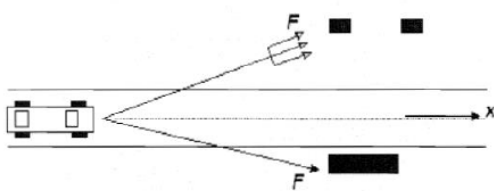
Table 55. Equivalent static design forces due to vehicle impact on members supporting structures over or adjacent to roadways – table 4.1 of (EN 1991-1-7, 2006).

Category of traffic	Force F_{dx}^a [kN]	Force F_{dy}^a [kN]
Motorways and country national and main roads	1000	500
Country roads in rural area	750	375
Roads in urban area	500	250
Courtyards and parking garages with access to:		
- Cars	50	25
- Lorries ^b	150	75

^a x = direction of the normal travel, y = perpendicular to the direction of normal travel
^b The term "lorry" refers to vehicles with maximum gross weight greater than 3,5 tonnes

Table 56. Recommended position of the equivalent static due to vehicle impact on supporting members in accordance with (EN 1991-1-7, 2006).

Vehicle type	Height h (Figure 45)	Application area a (Figure 45)
Lorry	Between 0,5 m and 1,5 m	height – 0,5 m width – 1,5 m or member width (the smallest)
Car	0,5 m	height – 0,25 m width – 1,5 m or member width (the smallest)

The position (height h and area a) of the force in the column depends on the type of vehicle (car or lorry), while the magnitude of the force F is dependent of the type of road where the vehicle is traveling, i.e. the maximum velocity that it can achieve.

According to the Table 55 and assuming "country roads in rural area" the loads to be applied for the four scenarios previously mentioned can be defined.

Table 57. Impact forces for linear static analysis.

Case	F_{dx} (kN)	F_{dy} (kN)
A.1	750	375
A.2	750	375
B.1	375	750
B.2	375	750

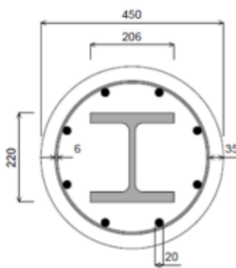
A linear elastic analysis is made on the full 3D model using the software SCIA® structural design code for standard steel columns by applying the forces from Table 57. Composite columns are calculated using the software A3C®.

The cross sections of the members are those resulted from the initial design and the acceptance criteria are given in terms of utilization factor (U.F.) for accidental combinations only.

Table 58. Linear static analysis results for impact on steel columns.

Case	Section	Loading		Bottom support	Utility	
		F _{dx} (kN)	F _{dy} (kN)		S355	S460
A.1	HD 360x162	750	375	Fixed	1.30	0.91
				Hinged	1.50	1.05
A.2	HD 360x162	750	375	Fixed	1.08	0.78
				Hinged	1.23	0.92
B.1	HD 360x162	375	750	Fixed	1.29	0.98
				Hinged	1.54	1.17
B.2	HD 360x162	375	750	Fixed	1.45	1.10
				Hinged	1.72	1.30

Table 59. Linear static analysis results for impact on composite columns.



Steel section - HE200M
Concrete class – C30/37
Rebar (A500) – ϕ 20 mm / ϕ 6 mm

Case	Loading		Upper and Bottom supports	Utility S355
	F _{dx} (kN)	F _{dy} (kN)		
A.1	750	375	Hinged	2.63
A.2	750	375	Hinged	2.04
B.1	375	750	Hinged	2.25
B.2	375	750	Hinged	2.34

Standard steel columns

The results show that the S355 columns will surpass the yield strength for both pinned and fixed conditions with utility factors up to 1.72.

The same example is made considering S460 and the results show a considerable improvement when compared with S355.

Composite steel columns

Regarding composite columns the utilisation factors are substantially higher. This is mainly related with the pre-design of the sections and supporting conditions. The columns were pre-designed considering the same capacity as the steel columns and pinned supports at both extremities (the steel cross sections used for the composite elements are substantially smaller).

When an impact load is applied (considering an equivalent static approach), the element will be subjected to bending which will be taken for the most part by the steel profile when it comes to the composite section (approximately 65% to 70%). Due to this, the composite columns show a higher utility factor for impact analysis.

It is concluded that for the non-composite steel columns if the standard design is made considering around 60% to 65% utility, the columns can still be able to sustain the impact load (static approach), assuming that the bottom connections remain fixed. It is reminded that using smaller loads associated with different road types, the behaviour of the columns will be better. Note that the conclusions are obtained for a simplified static analysis.

For the sections that are failing using this approach, a capacity assessment with more sophisticated approaches should be made.

As shown previously, the main improvement that can be made is by increasing the steel grade to S460, by doing so the columns have a better behaviour for the majority of cases.

In order to improve the design and response to the impact load, a set of changes could be implemented:

- Orientate the columns (according to their cross-sections's strong axis) to maximize the resistance to impact;
- Increase the size of the sections;
- Design the end-connections of the columns with higher stiffness and resistance (i.e., fixed (rigid) column bases);
- Use of composite columns, to achieve an optimum solution in terms of size, used grade of steel, used concrete;
- More advanced approaches may be used to assess more accurately the capacity.

6.2.2 Blast

The blast analysis is made by applying the SDOF method to evaluate the out-of-plane deflection demand, when compared with the capacity of the column.

The column considered in the analysis is a perimeter column located in the middle of the longest façade of the building, as illustrated in Figure 113.

As scenario, it is assumed a car placed at a standoff distance of 20m from the column with an explosive charge equal to 100kg of TNT. The burst defined as a free-air burst with a free height from the ground floor of 1m.

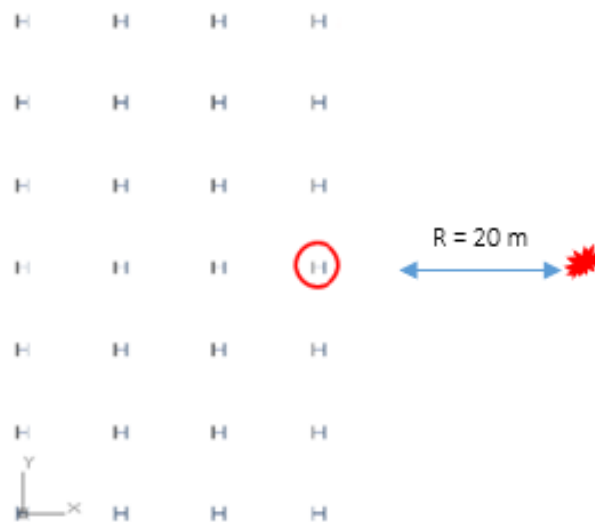


Figure 113. Plan view of the ground floor, column under blast load.

An explosion scenario is defined first, including the expected charge weight (W), type of explosion, and distance to the building (R). The first step in calculating the peak dynamic pressure consists in obtaining the scaled distance (Z), distance from blast source (R_h) and angle of incidence (α_i) according to the previously defined scenario.

TNT equivalent mass of the explosive charge	$W = 100kg$
Standoff distance	$R = 20m$
Height of the blast	$H_c = 1m$

Scaled distance	$Z = \frac{R}{W^{\frac{1}{3}}} = \frac{20}{100^{\frac{1}{3}}} = 4.309 \frac{m}{kg^{\frac{1}{3}}}$
Distance from blast source	$R_h = \sqrt{R^2 + H_c^2} = \sqrt{20^2 + 1^2} = 20.025m$
Angle of incidence	$\alpha_i = \tan^{-1}\left(\frac{H_c}{W^{\frac{1}{3}}}\right) = \tan^{-1}\left(\frac{1}{100^{\frac{1}{3}}}\right) = 12.158^\circ$

By using the previous values, the data necessary to define the pressures and additional parameters can be obtained directly from the web site <https://unsafeguard.org/un-safeguard/kingery-bulmash> and/or from Figure 138 (DoD 2014).

Incident pressure	$P_{so} = 56.44kPa$
Incident impulse	$I_s = 313.71kPa.ms$
Reflected pressure	$P_r = 137.37kPa$
Reflected impulse	$I_r = 688.09kPa.ms$
Time of arrival	$t_a = 30.29ms.W^{\frac{1}{3}} = 140.59ms$
Positive phase duration	$t_0 = 16.49ms$
Blast wavelength	$b_w = 0.4 \frac{m}{kg^{\frac{1}{3}}}$
Shock front velocity	$U = 413.93 \frac{m}{s}$

Note! The difference between using the UN SaferGuard website and Figure 138 is in the scaling of the parameters. Using the web site, the values are already scaled ($W^{1/3}$). Only the wavelength was obtained from the chart and it needed to be scaled. In case the chart is used, the values for the time intervals, impulses and wavelength need to be scaled (multiplied with $W^{1/3}$).

Considering the incident pressure defined previously (P_{so}), the sound velocity (C_r) and the peak dynamic pressure (q) can be obtained using Figure 139 and Figure 140.

Sound velocity	$C_r = 0.38 \frac{m}{ms}$
Peak dynamic pressure	$q = 8.5kPa$

Afterwards the fictitious reduced time intervals need to be computed. This process is necessary since the blast wave and formulation was initially defined for an infinite surface.

Fictitious positive phase duration	$t_{0f} = 2 \frac{I_s}{P_{so}} = 2 \times \frac{313.71}{56.44} = 11.12ms$
Fictitious duration for the reflected wave	$t_{rf} = 2 \frac{I_r}{P_r} = 2 \times \frac{688.09}{137.37} = 10.02ms$
Height of the element	$h_s = 4m$
Width of the wall	$w_s = 4m$

Drag coefficient	$C_D = 1$
Smallest dimensions (height versus wall)	$s_d = \min\left(h_s, \frac{w_s}{2}\right) = \min\left(4, \frac{4}{2}\right) = 2m$
Largest dimension (height versus wall)	$l_d = \max\left(h_s, \frac{w_s}{2}\right) = \max\left(4, \frac{4}{2}\right) = 4m$
Ratio (smallest / largest)	$r_{s,l} = \frac{s_d}{l_d} = \frac{2}{4} = 0.5$
Clearing time	$t_c = \frac{4s_d}{(1 + r_{s,l})C_r} = \frac{4 \times 2}{(1 + 0.5) \times 0.38} = 14.04ms$
Peak pressure acting on the wall	$P = P_{so} + q \cdot C_D = 56.44 + 8.5 \times 1 = 64.94kPa$

Single degree of freedom approach (SDOF)

For simple structures, a rigorous dynamic analysis can be performed to evaluate the response. For practical design purposes however, approximations need to be made to allow the design with reasonable accuracy.

In order to compute the ductility demand of the column subjected to the reflected pressure calculated previously, an equivalent SDOF system of the column can be used. The first step consists in calculating the uniformly distributed load (F_d) and point load (F_p) generated by the blast on the column.

Reflected pressure	$P_r = 137.37kPa$
Height of the column	$h_c = 4m$
Width of the panel in front of the column	$w_p = 5m$
Fictitious duration of the reflected wave	$t_{rf} = 10.02ms$
Selfweight of the column (Steel ; Composite)	$G_c = (1.834 ; 4.721) \frac{kN}{m}$
Distributed load from the blast on the column	$F_d = P_r w_p = 137.37 \times 5 = 686.85 \frac{kN}{m}$
Point load from the blast on the column	$F_p = F_d h_c = 686.85 \times 4 = 2747.4kN$

A first assumption of $t_d/T = 2/3$ (relation between reflected wave duration and period) is defined such that a DLF may be considered. Then, a maximum moment corresponding to the load may be obtained according to Figure 145.

Dynamic load factor	$DLF = 1.45$
---------------------	--------------

The maximum moment corresponding to the load considering the DLF may be calculated, together with the different properties of the sections from Table 66.

Loading factor	$K_L = 0.64$
Mass factor	$K_M = 0.50$

Steel column

Plastic section modulus $W_{pl.c} = 3162cm^3$

Second moment of area $I_c = 51890cm^4$

Composite column

Stiffness $E \cdot I_{eff} = 44350.87kN \cdot m^2$

Maximum resistant moment $M_{Ra.cp} = 632.85kN \cdot m$

Dynamic increase factor $DIF = 1.2$

Steel yield strength $f_y = 355MPa$

Steel elastic modulus $E = 210GPa$

Column stiffness
(Steel ; Composite)

$$K_c = \left(\frac{384E \cdot I_c}{5h_c^3} ; \frac{384E \cdot I_{eff}}{5h_c^3} \right)$$
$$= \left(\frac{384 \times 210 \times 10^6 \times 51890 \times 10^{-8}}{5 \times 4^3} ; \right)$$
$$= \left(; \frac{384 \times 44350.87}{5 \times 4^3} \right)$$
$$= (130762.8 ; 53221.04) \frac{kN}{m}$$

Maximum resistant moment
(Steel ; Composite)

$$M_{Ra} = (W_{pl.c} \cdot f_y \cdot DIF ; M_{Ra.cp} \cdot DIF)$$
$$= (3162 \times 10^{-6} \times 355 \times 10^3 \times 1.2 ; 632.85 \times 1.2)$$
$$= (1347.01 ; 759.42)kN \cdot m$$

Maximum applied moment

$$M_{max} = \frac{F_p \cdot h_c}{8} DLF = \frac{2747.4 \times 4}{8} \times 1.45$$
$$= 1991.87kN \cdot m$$

Effective mass
(Steel ; Composite)

$$M_e = \frac{G_c \cdot h_c \cdot K_M}{g} = \frac{(1.834 ; 4.721) \times 4 \times 0.50}{9.81}$$
$$= (374.03 ; 962.82)kg$$

Effective stiffness
(Steel ; Composite)

$$K_e = K_c \cdot K_L = (130762.8 ; 53221.04) \times 0.64$$
$$= (83688.19 ; 34061.47) \frac{kN}{m}$$

Natural period of vibration
(Steel ; Composite)

$$T_c = 2\pi \sqrt{\frac{M_e}{K_e}} = 2 \times \pi \sqrt{\frac{(374.03 ; 962.82)}{(83688.19 ; 34061.47)}} \times 10^3$$
$$= (13.28 ; 33.41)ms$$

Ratio
(Steel ; Composite)

$$\frac{t_{rf}}{T_c} = \frac{10.02}{(13.28 ; 33.41)} = (0.75 ; 0.30)$$

The new determined ratio allows for a second, more precise iteration. After the maximum resistance is determined.

Second interaction $DLF = (1.30 ; 1.80)$

(Steel ; Composite)

$$M_{max} = \frac{F_p \cdot h_c}{8} DLF = \frac{2747.4 \times 4}{8} \times (1.30 ; 1.80)$$

(Steel ; Composite) $= (1785.81 ; 2472.66) kN.m$

$$R_m = \frac{8(2M_{Rd})}{h_c} = \frac{8 \times 2 \times (1347.01 ; 759.42)}{4}$$

(Steel; Composite) $= (5388.05 ; 3037.68) kN$

$$V_m = 0.39R_m + 0.11F_p + G_c \cdot h_c \cdot 0.5$$

Dynamic reaction $= 0.39 \times (5388.05 ; 3037.68) + 0.11 \times 2747.4$
(Steel; Composite) $+ (1.834 ; 4.721) \times 4 \times 0.5$
 $= (2407.22 ; 1496.36) kN$

$$\frac{R_m}{F_p} = \frac{(5388.05 ; 3037.68)}{2747.4} = (1.96 ; 1.11)$$

(Steel; Composite)

The ratio between the maximum resistance and the point load is used to determine the ductility demand, using Figure 141.

$$\mu_1 = (0.80 ; 0.95) (X_M / X_E)$$

Ratios
(Steel; Composite) $\mu_2 = (0.55 ; 1.2) (t_m / T)$

$$\chi_e = \frac{R_m}{K_e} = \frac{(5388.05 ; 3037.7)}{(83688.19 ; 34061.47)}$$

Yield displacement
(Steel; Composite) $= (64.38 ; 89.18) mm$

$$\chi_M = \mu_1 \times \chi_e = (0.80 ; 0.95) \times (64.38 ; 89.18)$$

Maximum displacement
(Steel; Composite) $= (51.51 ; 84.72) mm$

$$t_m = \mu_2 \times T_c = (0.55 ; 1.2) \times (13.28 ; 33.41)$$

Maximum response time
(Steel; Composite) $= (7.331 ; 40.09) ms$

P-I diagrams may be used to evaluate the performance of a structural system or component, based on several damage limits, see Figure 146 and Figure 147

Based on Figure 146 and Figure 147, the damage can be defined according to the impulse and pressure previously calculated.

$$\mu_{max} = 1 \quad \text{Compression -> Beam -column with compact section -> B1}$$

$$\frac{\mu_1}{\mu_{max}} = (0.80 ; 0.95)$$

Check
(Steel ; Composite)

According to the results, the steel and composite columns do not surpass the maximum response limits and both elements are able to withstand the blast load. The verification for superficial damage (class B1) was fulfilled.

6.2.3 Localised fire

The accidental fire situations are represented by localised fires. Models are given in the Annex C of Eurocode 1 (EN 1991-1-2:2002) to represent the thermal impact from a localised fire which is defined by a circular basis (with diameter D) and a flame length L_f . The flame length can be obtained through the following formula (EN1991-1-2:2002 equation C.1) with D being the diameter of the fire basis in (m) and Q the rate of heat release of the fire in (W).

$$L_f = -1.02D + 0.0148Q^{2/5}$$

The gas temperature θ_z in the plume along the symmetrical vertical flame axis is given by the following equation (in $^{\circ}\text{C}$):

$$\theta_{(z)} = 20 + 0.25Q_c^{2/3}(z - z_0)^{-4/3} \leq 900$$

With Q_c the convective part of the rate of heat release ($=0.8Q$), z the height along the flame axis (m) and H the distance between the fire source and the ceiling (m) as demonstrated in the following figure:

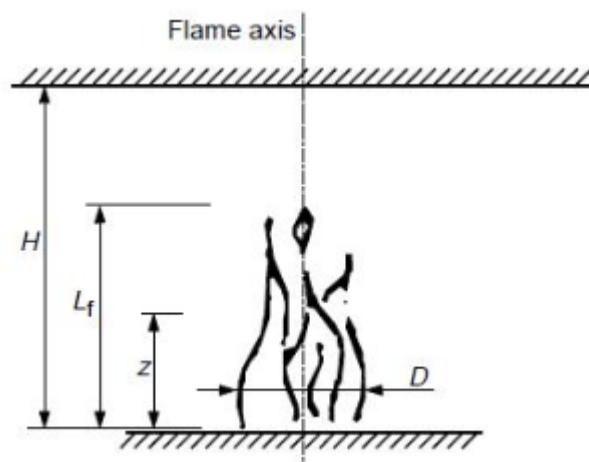


Figure 114. Idealised fire.

The rate of heat release of a fire Q can be assessed while applying the procedure described in the Annex E of Eurocode 1 (EN 1991-1-2:2002).

Three parameters are governing the evolution of the rate of heat release with time: the fire growth rate t_α (s), the fire load density $q_{f,d}$ (MJ/m^2) and the rate of heat release density RHR_f (kW/m^2).

Annex E of Eurocode 1 provides values for these parameters for given occupancies. Based on this, four scenarios are defined, starting from a baseline scenario considering the values for an office building.

The three other scenarios assume “exaggerated values”: either for the rate of heat release (a double value of $500 \text{ kW}/\text{m}^2$) or for the fire load density and the fire growth rate (values for the “commercial area” occupancy, which are more severe than for office building).

Then, two realistic fire basis diameters are considered: 1 (m) and 2 (m). For all scenarios, a safe-sided assumption is made, considering that the localised fire is placed just next to the column, i.e. there is a null distance between the exterior of the fire circular basis and the column.

Indeed, the bigger the distance between the fire and the column, the lower the heat fluxes and the resulting steel temperatures. The four scenarios are described in Figure 115. For each scenario, the software OZone[®] is used, applying the LOCAFI (Brasseur et al. 2017) model as well as the equations from EN1991-1-2:2002, to evaluate the steel temperatures of a bare steel column made of a hot rolled profile HEB340 (as an example).

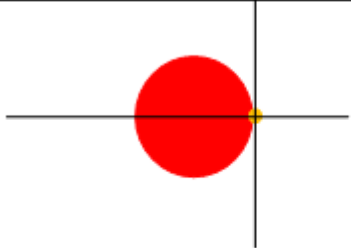
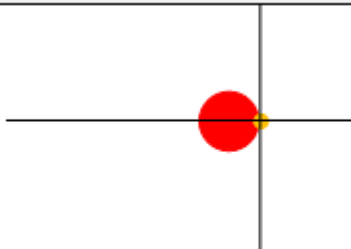
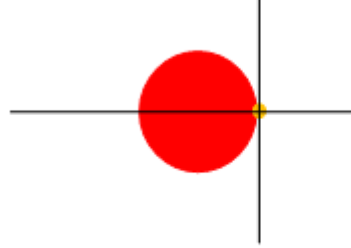
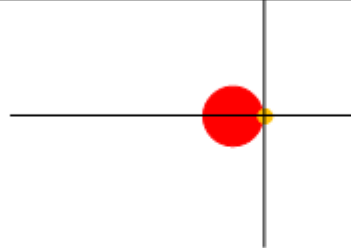
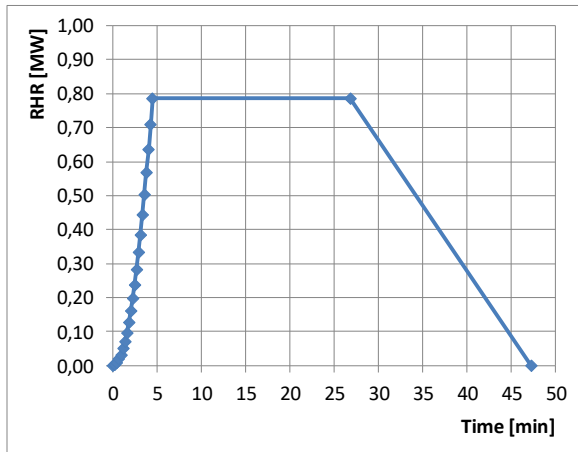
Scenario A			
	Diameter of the fire basis	2 m	
	Rate of Heat Release density	250 kW/m ² (office building EN 1991-1-2)	
	Fire load density	511 MJ/m ² (office building EN 1991-1-2)	
	Fire growth rate	300 sec (office building EN 1991-1-2)	
Scenario B			
	Diameter of the fire basis	1 m	
	Rate of Heat Release density	500 kW/m ²	
	Fire load density	511 MJ/m ² (office building EN 1991-1-2)	
	Fire growth rate	300 sec (office building EN 1991-1-2)	
Scenario C			
	Diameter of the fire basis	2 m	
	Rate of Heat Release density	250 kW/m ² (commercial area EN 1991-1-2)	
	Fire load density	730 MJ/m ² (commercial area EN 1991-1-2)	
	Fire growth rate	150 sec (commercial area EN 1991-1-2)	
Scenario D			
	Diameter of the fire basis	1 m	
	Rate of Heat Release density	500 kW/m ²	
	Fire load density	730 MJ/m ² (commercial area EN 1991-1-2)	
	Fire growth rate	150 sec (commercial area EN 1991-1-2)	

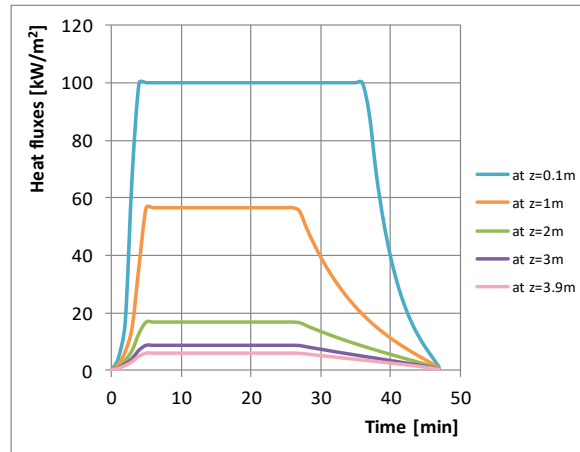
Figure 115. Scenarios A, B, C and D.

The graphs below provide the evolution of the following parameters, as a function of time:

- The rate of heat release of the fire;
- The heat fluxes for different heights;
- The steel temperatures in the column for different heights.

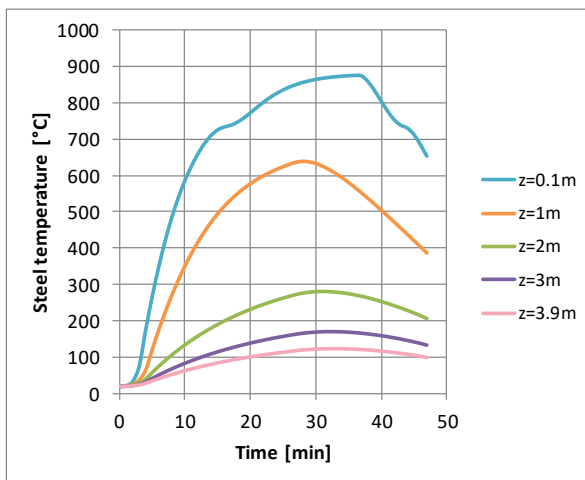


a)

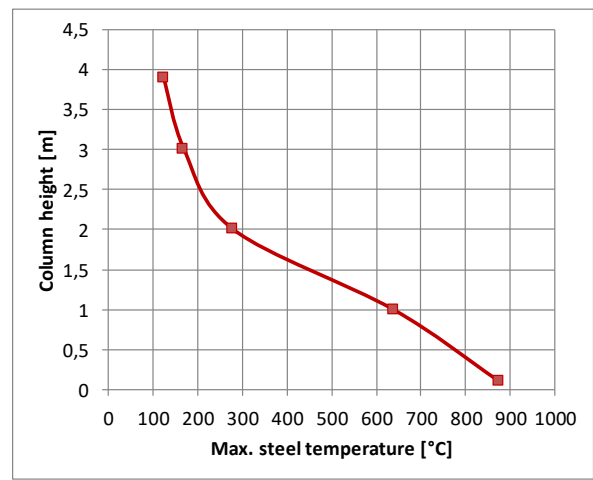


b)

Figure 116. Scenario A: a) Rate of heat release density vs time; b) Heat fluxes vs time.

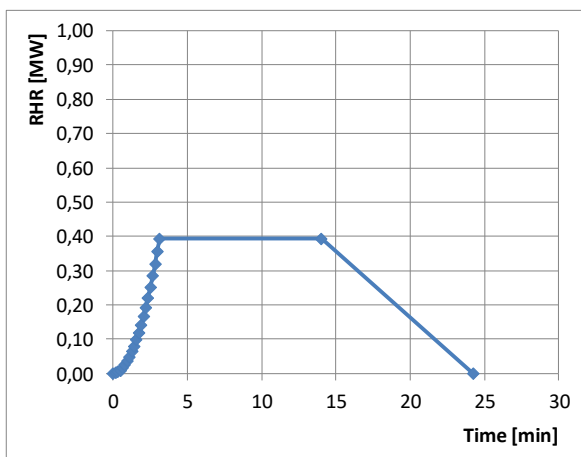


a)

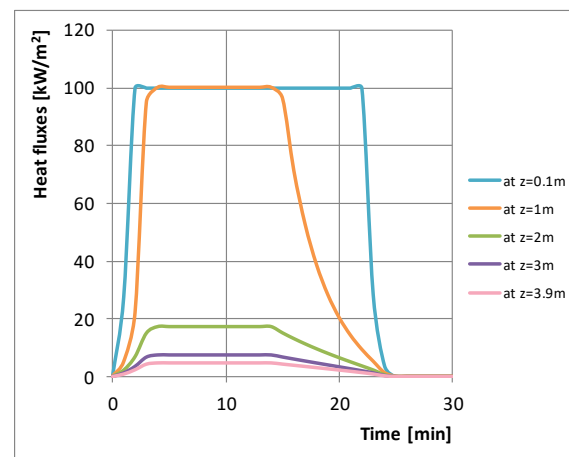


b)

Figure 117. Scenario A: a) Steel temperature vs time; b) Column height vs max. steel temperature.

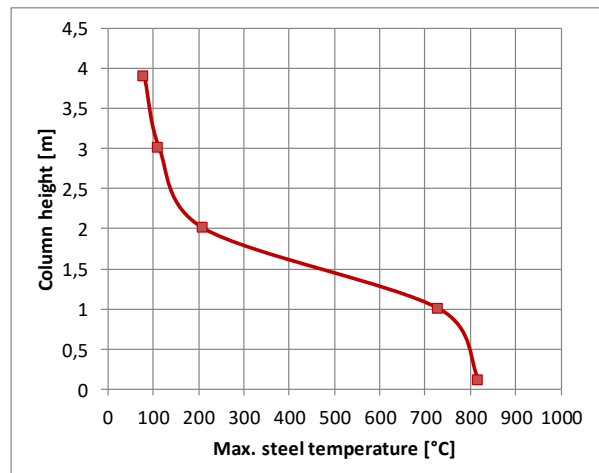
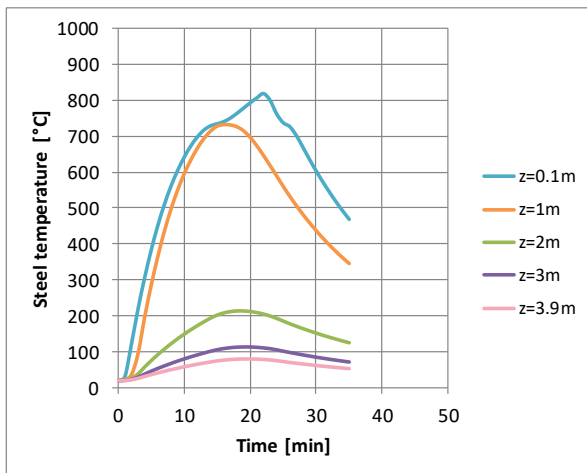


a)



b)

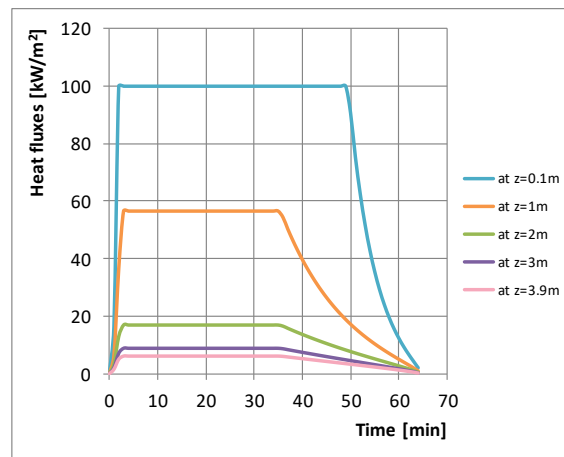
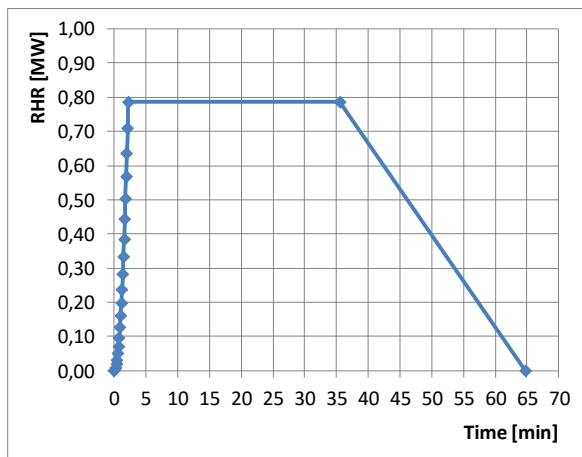
Figure 118. Scenario B: a) Rate of heat release density vs time; b) Heat fluxes vs time.



a)

b)

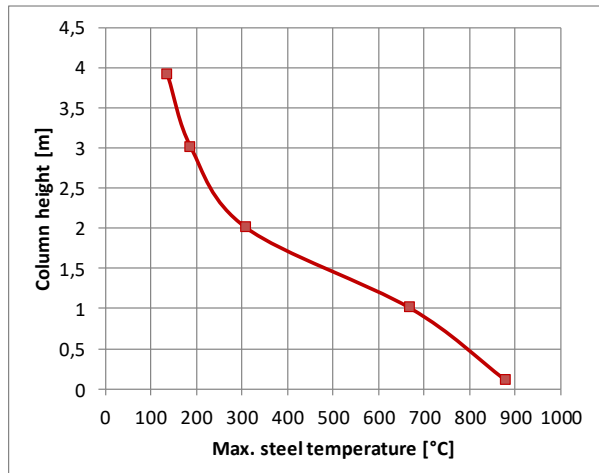
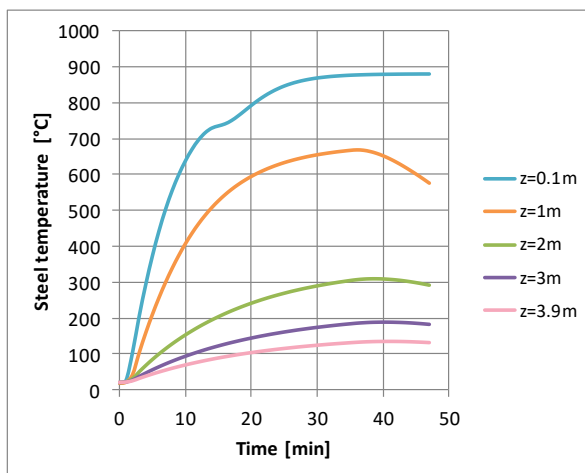
Figure 119. Scenario B: a) Steel temperature vs time; b) Column height vs max. steel temperature.



a)

b)

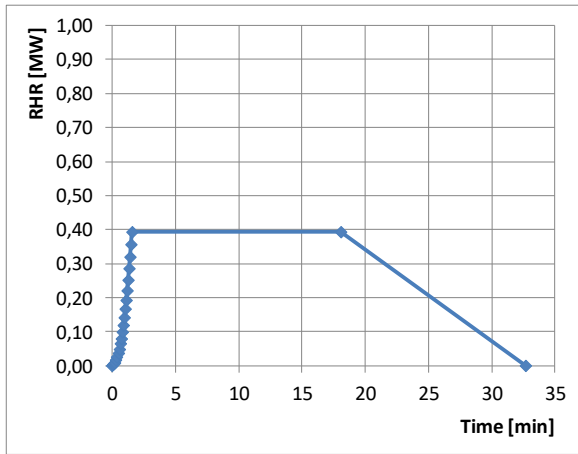
Figure 120. Scenario C: a) Rate of heat release density vs time; b) Heat fluxes vs time.



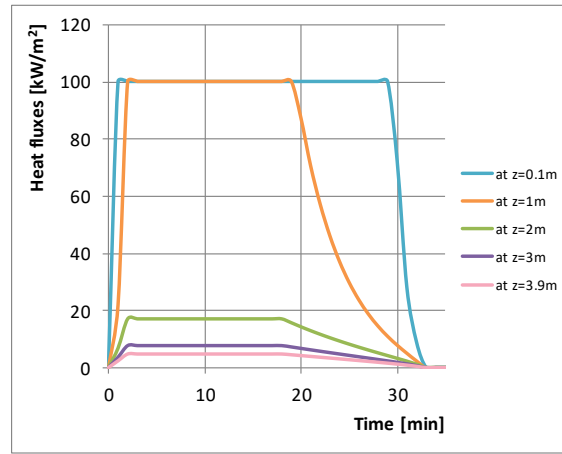
a)

b)

Figure 121. Scenario C: a) Steel temperature vs time; b) Column height vs max. steel temperature.

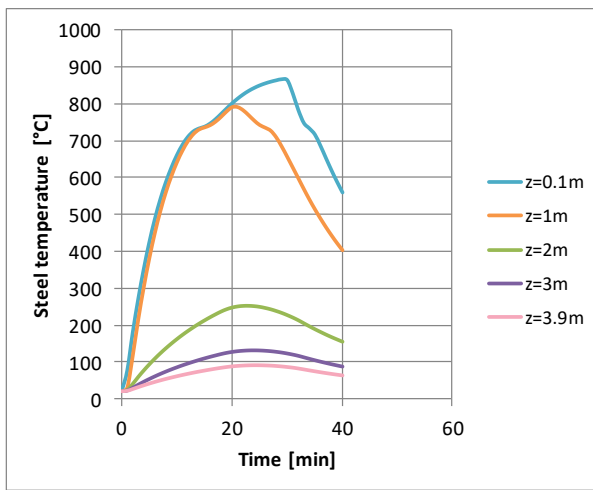


a)

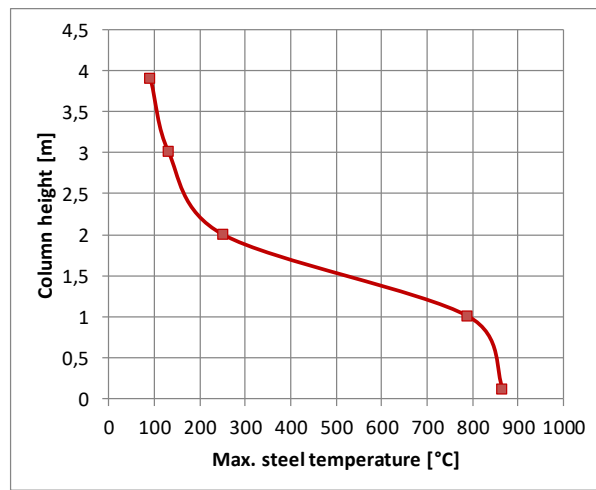


b)

Figure 122. Scenario D: a) Rate of heat release density vs time; b) Heat fluxes vs time.



a)



b)

Figure 123. Scenario D: a) Steel temperature vs time; b) Column height vs max. steel temperature.

The maximum steel temperatures along the height of the column are compared on a common graph for each scenario.

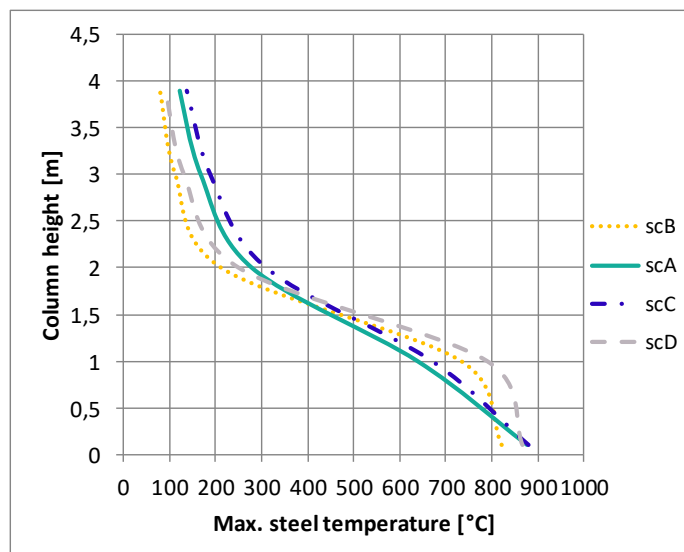


Figure 124. Comparison between scenarios - Column height vs Max. steel temperature.

This comparison highlights that, although different assumptions are made to characterize the localised fire, the same trend and order of magnitude are achieved. Significant steel temperatures are obtained at the bottom of the column and can cause buckling or a local plastic failure. In order to avoid fire damage, fire protection can be used instead of designing the structural elements for specific fire resistance or increase the size of the section.

6.3 Verifications for unidentified actions

6.3.1 ALPM

6.3.1.1 Prescriptive method

The tying force method is an indirect design process that is assumed to provide a minimum level of structural robustness and resistance to progressive/disproportionate collapse. The method ensures that a minimum level of continuity, ductility and strength is achieved between the different structural members by means of horizontal and vertical ties, resulting in an enhanced overall structural integrity.

In this example the calculations are made for the beams connected to the middle column located at the middle of the longest façade of the building.

According to EN 1991-1-7:2006, for framed structures, the minimum tensile forces to be resisted by an effective horizontal tying can be estimated using the following calculations.

Horizontal tying

Permanent action	$g_k = 5 \frac{kN}{m^2}$
Variable action	$q_k = 3 \frac{kN}{m^2}$
Office floor loading factor	$\Psi = 0.5$
Spacing between ties	$s = 12m$
Span of the tie	$L = 8m$
Design tensile load for internal ties	$T_i = \max[0.8(g_k + \Psi \cdot q_k)s \cdot L, 75kN]$ $= \max[0.8(5 + 0.5 \times 3)12 \times 8, 75kN]$ $= 499.2 kN$
Design tensile load for perimeter ties	$T_p = \max[0.4(g_k + \Psi \cdot q_k)s \cdot L, 75kN]$ $= \max[0.4(5 + 0.5 \times 3)12 \times 8, 75kN]$ $= 249.6 kN$
Area on internal beams (IP360)	$A_{s,i} = 7270mm^2$
Area on perimeter beams (IP450)	$A_{s,p} = 9880mm^2$
Plastic resistance of the internal beams	$N_{pl,i} = A_{s,i} \cdot f_y = 7270 \times 10^{-6} \times 355 \times 10^3$ $= 2580.85kN$
Plastic resistance of the perimeter beams	$N_{pl,p} = A_{s,p} \cdot f_y = 9880 \times 10^{-6} \times 355 \times 10^3$ $= 3507.4kN$
Utility check – Internal beams	$U_i = \frac{T_i}{N_{pl,i}} = \frac{499.2}{2580.85} = 0.19$

Utility check – Perimeter beams

$$U_p = \frac{T_p}{N_{pl,p}} = \frac{249.6}{3507.4} = 0.07$$

The calculations show that the beams are able to sustain the tensile loads defined in the standards.

Vertical tying (Force calculation example)

Distance between columns in x direction $d_x = 12m$

Distance between column in y direction $d_y = 8m$

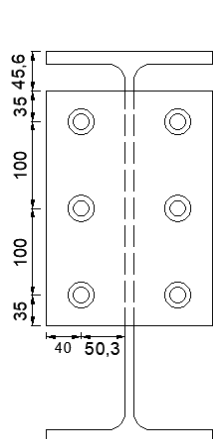
Required vertical tie resistance

$$T_p = (g_k + \Psi \cdot q_k) \cdot d_x \cdot d_y = (5 + 0.5 \times 3)12 \times 8 = 624kN$$

Connections

The design of the connections is calculated based on spreadsheets and the resistance should also be able to accommodate the tensile loads defined previously (tying forces). A set of specific checks is made in order to arrive at the tying resistance of the joint.

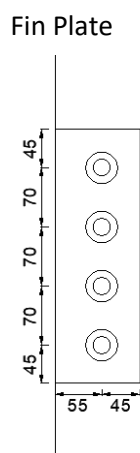
Two different examples are made for the beam column connections (header plate / fin plate).



Header Plate

Bolt Type:
M16 8.8 (6 bolts)

Plate:
Thick. $t_p = 10mm$
Height $h_p = 270mm$
Width $b_p = 190mm$
Weld $a_w = 2X6mm$



Bolt Type:
M20 8.8 (4 bolts)

Plate:
Thick. $t_p = 10mm$
Height $h_p = 300mm$
Width $b_p = 100mm$
Weld $a_w = 2X6mm$

The verification of the connections mentioned above is made according the prescriptions presented in the document “Design Manual Annex A.5 – Resistance of joints under tension”.

Bolts in tension $N_{u1} = 602.88kN$ Bolts in shear $N_{u1} = 376.32kN$

Header Plate in bending $N_{u2} = 271.17kN$ Fin plate in bearing $N_{u2} = 512.73kN$

Supporting member in tension $N_{u3} = 383.08kN$ Fin plate in tension: Gross $N_{u2} = 1128.00kN$

Beam web in tensions $N_{u4} = 954.29kN$ Fin plate in tension: Net $N_{u4} = 717.41kN$

Tying resistance of the $N_u = 271.17kN$ joint

Beam web in bearing $N_{u5} = 481.96kN$

Beam web in tension: $N_{u6} = 1060.32kN$
Gross

Beam web in tension: $N_{u7} = 674.36N$
Net

Supporting member in $N_{u8} = 350.99N$
bending

Tying resistance of the $N_u = 350.99kN$ joint

Utility check

$$U = \frac{T_p}{N_u} = 0.92$$

Utility check

$$U = \frac{T_p}{N_u} = 0.71$$

It can be observed that the joints were computed assuming pinned connections, i.e., neglecting the possible composite actions which could develop at the level of these joints. This is considered as a safe approach if ductility is guarantee which is the case here. In fact, the rebars at the level of the joints can act as tying elements if the rebar arrangement is continuous throughout the building floor and their contribution could be then simply added to the joint resistance.

Table 60. Utility factors.

Summary of results			
Type	ULS Utility	Tying Utility	Remarks
Header Plate	0.73	0.92	Bolt Group / Header plate in bending
Fin Plate	0.71	0.71	Bolt group / Support member in bending

It is possible to conclude for the current example that using a connection targeted for a basic design with 70% utility, is an adequate approach when making the pre-design in order to comply with the tying requirements.

6.3.1.2 Full numerical analysis

The objective of this analysis is to evaluate the behaviour of the composite building in case of accidental situation (column removal). The calculations are made by using the software SAFIR®, which is a special purpose computer program for the analysis of structures under ambient and elevated temperature conditions.

The program is based on the Finite Element Method (FEM) and can be used to study the behaviour of three-dimensional structures. Note that all the calculations of this study are made under ambient temperature conditions, using the standard steel columns building design (composite columns are not considered).

The behaviour of the building is studied for different accidental situations where certain column lost scenarios are defined:

- Corner column (C1);
- Façade column (C2);
- Center core column (C5).

For each of the scenario mentioned above, 4 simulations are made by removing the columns at different levels of the building: level 0, 1, 3 and 5.

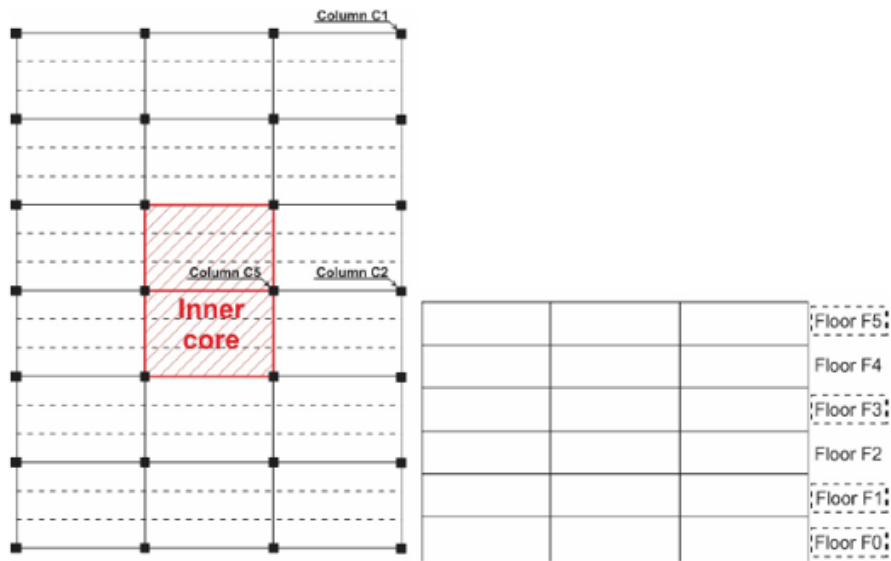


Figure 125. Columns and floors considered for the analysis.

A total of 12 scenarios for column lost are assumed and the following figures show the different SAFIR models.

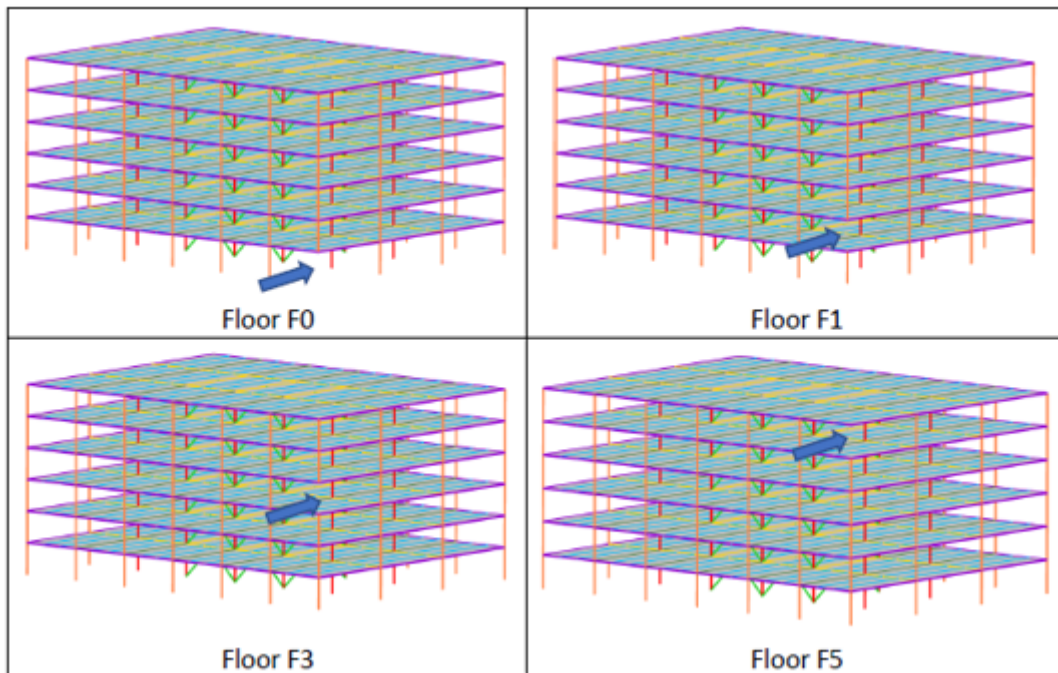


Figure 126. Column loss - C1.

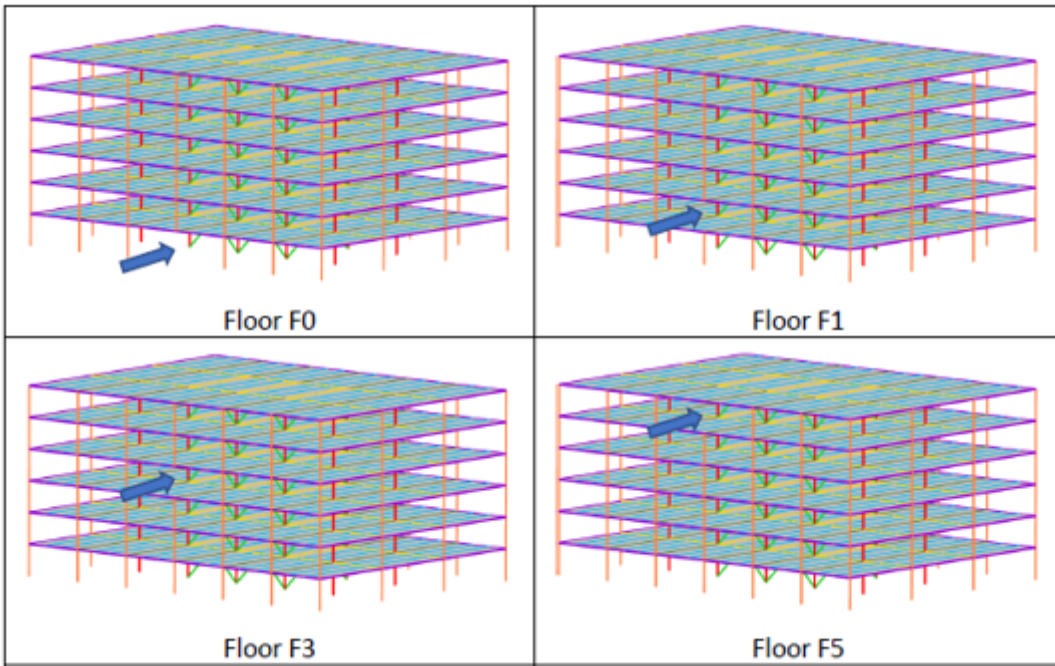


Figure 127. Column loss – C2.

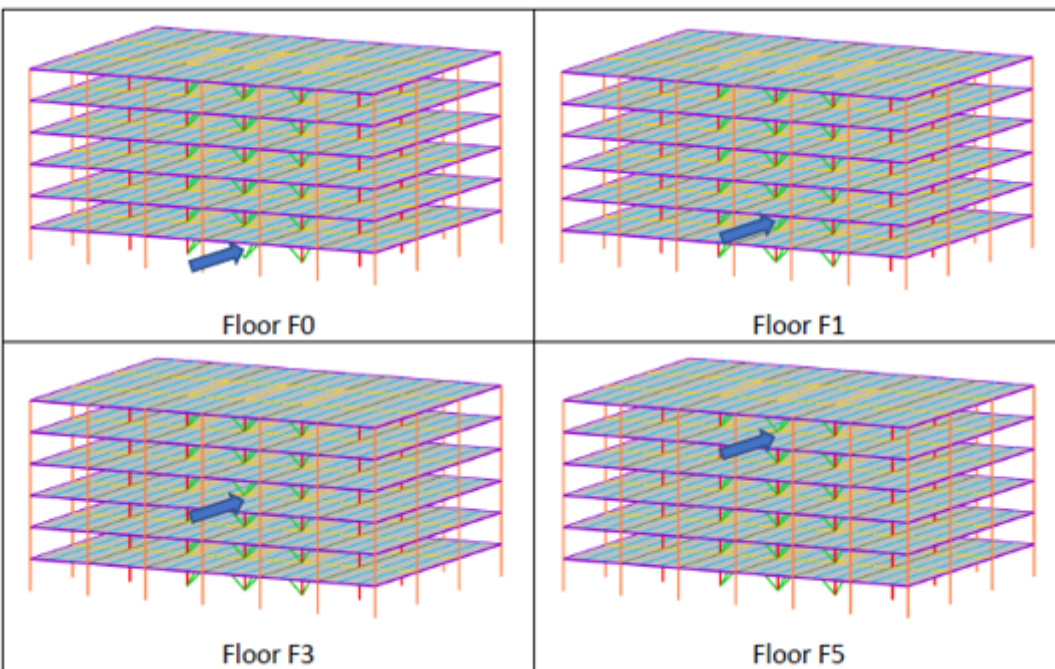


Figure 128. Column loss – C5.

A total of 20 simulations are made and divided into 2 different groups according to the connections between the beams / columns along the vertical alignment where the columns are removed:

- 12 simulations with all pinned beam-to-column connections;
- 8 simulations with rigid beam-to-column connections.

In the cases where the column C1 is removed, two different assumptions are defined:

- All pinned beam-to-column connections;
- Rigid beam-to-column connection at the corner and above where the column is removed.

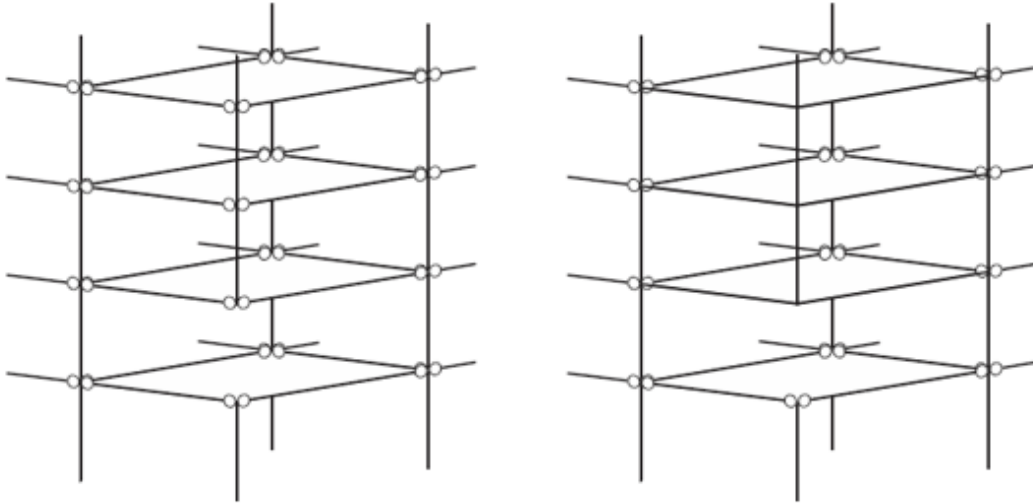


Figure 129. C1 "Pinned connections" (Left) / C1 "Rigid connections" (Right).

In the cases where the column C2 is removed, two different assumptions are defined:

- All pinned beam-to-column connections;
- Rigid beam-to-column connection where the column is removed.

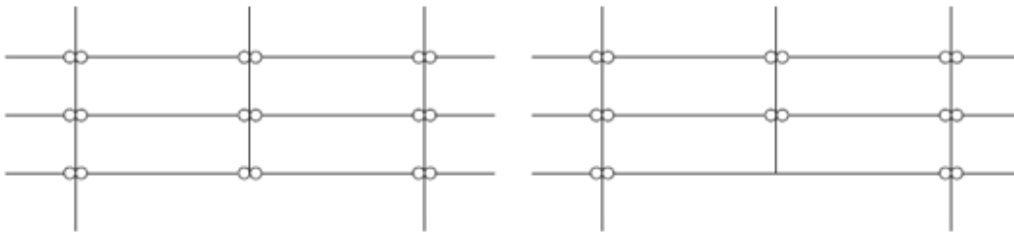


Figure 130. C2 "Pinned connections" (Left) / C2 "Rigid connections" (Right).

The output of the SAFIR® calculations are summarized in Table 61, that shows the maximum vertical displacement at the location of the column loss.

Table 61. Maximum vertical displacement

Max. Vertical disp. (m)	Floor	All pinned connections	Rigid connections
C1 Corner Column	F0	1.340	0.081
	F1	1.340	0.083
	F3	1.320	0.088
	F5	1.380	0.720
C2 Façade Column	F0	0.670	0.610
	F1	0.670	0.600
	F3	0.670	0.550
	F5	0.670	0.250
C5 Center core Column	F0	0.016	-
	F1	0.017	
	F3	0.018	
	F5	0.018	

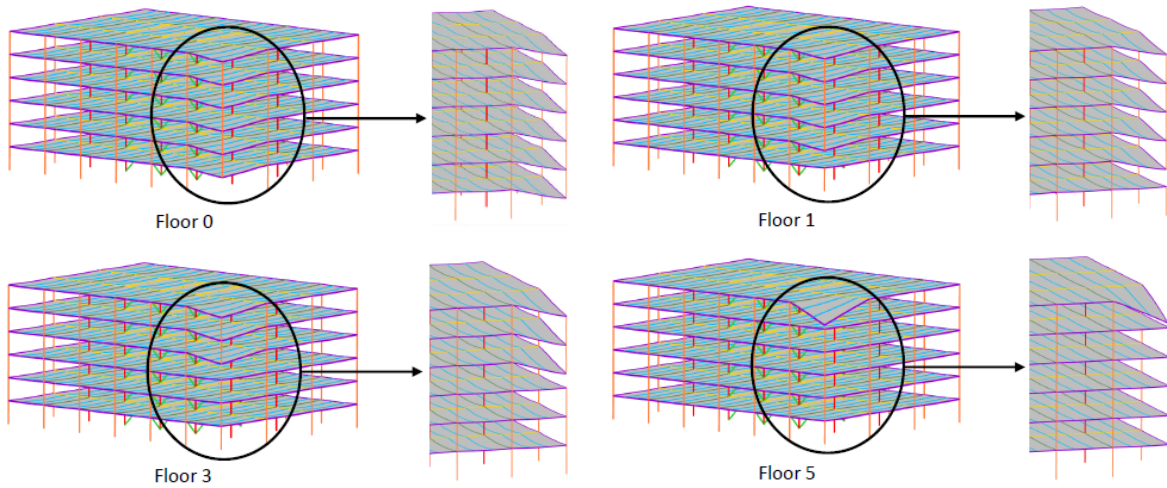


Figure 131. Global view of the structure - Losing corner column C1 (Rigid connection).

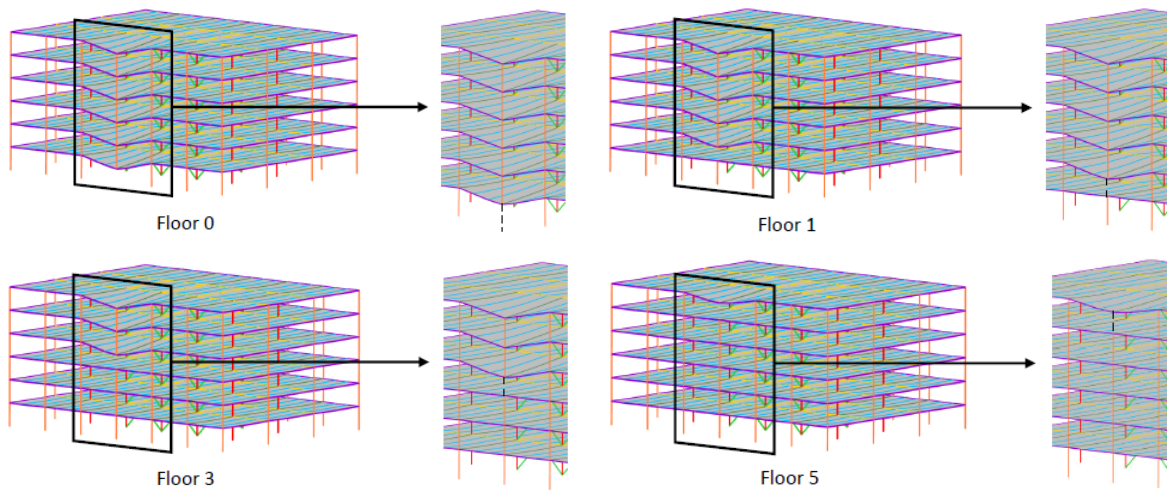


Figure 132. Global view of the structure - Losing corner column C2 (Pinned connection).

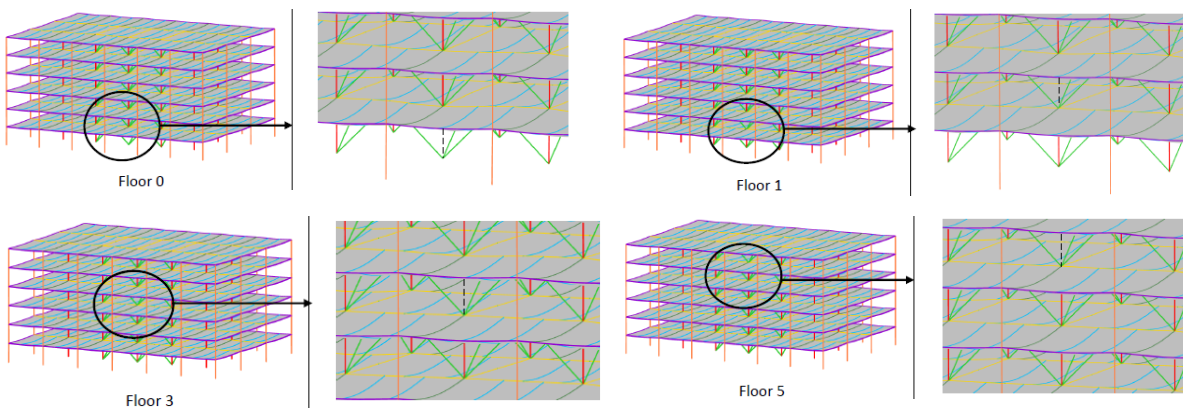
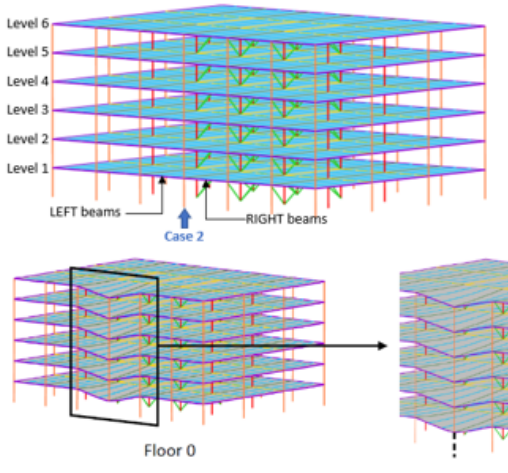


Figure 133. Global view of the structure - Losing corner column C5 (Pinned connection).

Considering the removal of column C2 at ground level (F0) the following forces are obtained for the left and right beams at all the levels.

Table 62. Maximum vertical displacement for case 2

Maximum Beam Axial Forces (Case 2)		Pinned connections	
		Left Beam (kN)	Right Beam (kN)
Floor 0	Level 1	1381.6	1381.2
	Level 2	1327.6	1326.8
	Level 3	1340.4	1339.5
	Level 4	1338.2	1337.4
	Level 5	1337.6	1336.7
	Level 6	1332.5	1331.7



Important to note that the forces presented are substantially higher than the forces calculated by the tying method. The IPE 450 perimeter beams are still able to accommodate these axial loads, but the connections would need to be redesigned.

Loss of column C1:

- For the loss of the corner column C1, the structure shows very high vertical displacement (approximately 1.35m), as the only contribution in resisting the gravity loads is provided by the cantilevered concrete slab (beams have pinned ends);
- Robustness behaviour can be improved by:
 - Reinforcing the beam-column joints along the vertical alignment of the columns (pinned -> semi-rigid -> rigid). The use of semi-rigid/rigid joints provides additional flexural capacity;
 - Improving the cantilever capacity of the slab (additional reinforcement at the corners of the building).

Loss of columns C2 and C5:

- The displacements are much smaller than for the corner column loss and the load is distributed through the floors (Table 62);
- These column loss scenarios do not lead to progressive collapse of the structure, but only to localised damage;
- Lateral displacements in columns adjacent to the lost column are small indicating the loads are relatively uniformly redistributed on all floors above the missing column.

6.3.2 Key element

A key element consists in a primary structural member (or group of members), which in case of failure will lead to further damage that compromises the stability of the global structure. Once these elements have been identified, they must be verified to withstand the internal forces developed with the damage scenario.

According to EN 1991-1-7:2006, the accidental design load to be considered in order to verify key elements is 34 kN/m² applied in any direction. For the scope of the study specific columns are identified (as an example) as key elements and the verifications made accordingly.

For columns, an accidental load equal to 34 kN/m² should be applied over a width that represents the components attached to the column after the accidental action. In addition, the accidental loading in the other direction of the column should also be considered as a separate case.

In this analysis 3 different columns are verified in a similar approach as for the impact analysis.

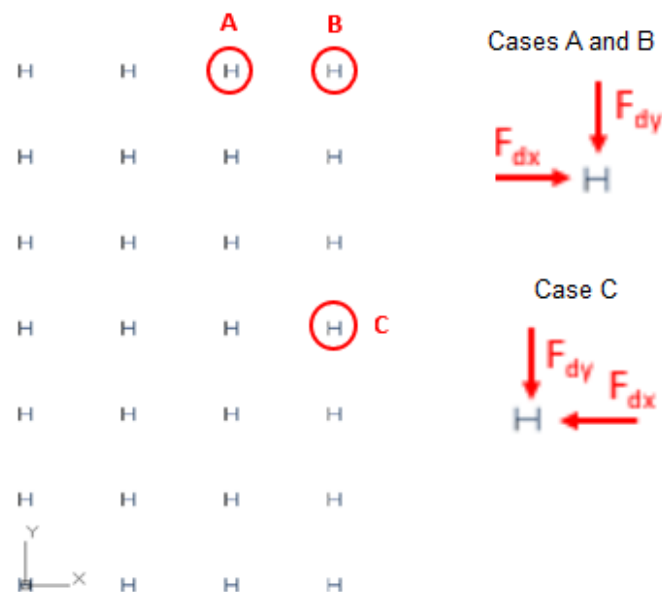


Figure 134. Plan view of the ground floor, columns defined as key elements.

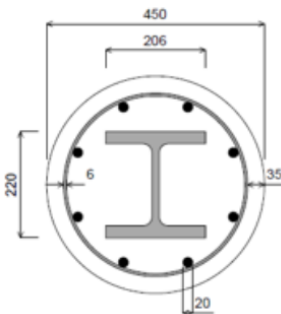
Point loads are calculated and applied directly in the SCIA® model (steel columns model) at the center of each proposed column (A, B and C) in both axis individually, considering the accidental combination. Regarding the composite columns, the approach is similar as for impact analysis, using the software A3C®.

Accidental load	$A_d = 34 \frac{kN}{m^2}$
Length of the column	$l_c = 4m$
Height of the column (Steel; Composite)	$h_c = (364 ; 450)mm$
Width of the column (Steel; Composite)	$b_c = (371 ; 450)mm$
Width of the attached object in front of the column	$w_p = 5m$
Point load (panel width)	$F_p = A_d \cdot w_p \cdot l_c = 34 \times 5 \times 4 = 680kN$
Point load (section height) (Steel; Composite)	$F_{s,h} = A_d \cdot h_c \cdot l_c = (34 \times 364 \times 10^{-3} \times 4 ; 34 \times 450 \times 10^{-3} \times 4) = (49.5 ; 61.2)kN$
Point load (section width) (Steel; Composite)	$F_{s,w} = A_d \cdot b_c \cdot l_c = (34 \times 371 \times 10^{-3} \times 4 ; 34 \times 450 \times 10^{-3} \times 4) = (50.46 ; 61.2)kN$

Table 63. Summary of results for the key element method (columns).

Case	Section	Loading		Bottom support	Utility		Lateral deflection S355 (mm)
		F _{dx} (kN)	F _{dy} (kN)		S355	S460	
A.1	HD 360x162	50.46	0	Fixed	0.39	0.28	0.7
				Hinged	0.39	0.28	0.8
A.2	HD 360x162	0	680	Fixed	1.03	0.82	-
				Hinged	1.25	1.00	-
B.1	HD 360x162	50.46	0	Fixed	0.22	0.16	0.7
				Hinged	0.23	0.17	0.8
B.2	HD 360x162	0	680	Fixed	0.95	0.75	9.1
				Hinged	1.14	0.92	-
C.1	HD 360x162	680	0	Fixed	0.68	0.54	5.0
				Hinged	0.83	0.65	8.1
C.2	HD 360x162	0	49.5	Fixed	0.40	0.29	1.4
				Hinged	0.42	0.31	1.4

Table 64. Summary of results for impact analysis - Composite columns.



Steel section - HE200M
 Concrete class – C30/37
 Rebar (A500) – ϕ 20 mm / ϕ 6 mm

Case	Loading		Upper & Bottom supports	Utility S355
	F _{dx} (kN)	F _{dy} (kN)		
A.1	61.2	0	Hinged	0.42
A.2	0	680	Hinged	2.29
B.1	61.2	0	Hinged	0.24
B.2	0	680	Hinged	1.84
C.1	680	0	Hinged	1.34
C.2	0	61.2	Hinged	0.40

For standard steel sections the results show that using fixed supports the resistance does not surpass the yield strength (1.03 can be admissible), however with hinged supports for cases A.2 and B.2 this limit is surpassed.

Regarding composite columns the utilisation factors are considerably higher as explained previously for the impact analysis.

Overall, it is concluded that for non-composite steel columns the standard design is able to sustain the developed loads, when the lower connection of the column is fixed. The composite columns however show worst results due to the fact that the main contribution for the resistance will be the steel element which is substantially smaller than the one used for the standard steel design.

Note that the forces applied in the columns according to the key element method are lower than the ones applied for impact and blast verifications.

According to Table 63, the main improvement that can be made is increasing the steel grade to S460, by doing so the utility factors are all below or equal to 1.0 for standard steel sections.

In order to improve the design and response, a set of other changes could be implemented:

- Increase the size of the sections;
- Design considering more advantageous boundary condition for the connections;
- Combination of the previous for composite columns, to achieve an optimum ratio (size / grade of steel / concrete).

6.4 Final design outputs and remarks

The robustness analysis of building construction can be a complex and detailed process. The current study for a composite building was developed using simple design examples to demonstrate basic approaches that could be used to evaluate the behaviour of steel composite buildings when subjected to an accidental loading case.

The impact analysis was evaluated through simplified methods presented in EN 1991-1-7:2006. It was shown that for the non-composite steel columns if the standard design is made considering around 60% to 65% utility, the columns could still be able to sustain the impact load, assuming that the bottom connections will be fixed (reinforced to deal with the impact load). For the cases that are not verified using the equivalent static approach, a more detail analysis should be made. In order to improve the design and response to the impact load a set of changes could be implemented, such as: increase of the steel grade to S460 and/or increase of the section size.

The blast analysis is a more complex process when compared to the impact. For the current analysis the SDOF method was applied by assuming a blast scenario with respective blast parameters and wave design pressure, and columns verified.

A set of fire scenarios were defined based on certain assumptions and occupancies. These scenarios were made by varying the fire diameter, fire load density, growth rate and rate of heat. Based on the output results, even though different assumptions were used, the same trend and order of magnitude are obtained for the maximum steel temperatures. Concluding that the steel temperatures present at the bottom of the column can cause buckling or local plastic failure. In order to avoid fire damage, fire protection can be used instead of designing the structural elements for specific fire resistance or increase the size of the section.

The prescriptive method consists in an indirect approach that provides a certain level of robustness and resistance to progressive collapse. In the current study the tying forces were calculated and compared with the existing elements and connections. For the current design the beams were sufficient to sustain the loads prescribed in EN 1991-1-7:2006.

In order to evaluate the complete building when subjected to column loss, a full numerical analysis was made using the software SAFIR®. A set of scenarios was calculated, by removing certain columns at different floors. With this analysis it is concluded that the corner column can be the critical element in the building and in order to improve the robustness, the connections in this area should be reinforced and/or by adding extra continuous reinforcements in the slab. For the remaining cases, the displacements presented were relatively smaller, with the columns located at the sides of the elements removed sustain very small lateral displacements. Meaning that when for example the column in the ground floor is removed the loads are redistributed in the same manner on all the floors above, thus the same range of displacements for the different floors is achieved.

The key element method is an approach that consists in identifying the main elements throughout the building that are critical load paths. This method can be applied using simplified formulation and showed that for the current design, the columns are adequate with just a couple of exceptions.

7 Explicit modelling of accidental actions (identified threat) vs. notional column removal (unidentified threat)

Notional column removal is a useful approach to evaluate the robustness and the capacity of the building structure to resist the progressive collapse following an unspecified accidental action. It is also considered a very conservative approach, as the total loss of a column from an accidental action is an unlikely event. To evaluate to which extent the notional column removal can model the loss of a column due to an accidental action, the structure is analysed for two extreme events that can cause heavy local damage, i.e., near field blast and car impact, respectively. The column under investigation is a first story perimeter column (column D4) of the steel structure SS/S. The analysis is done using a full nonlinear dynamic approach.

For blast analysis, the charge was placed at small distance from the structure to concentrate the damage in a reduced area of the column, then incremented up to an almost complete fracture of the column. Note that, a full removal was not possible without causing significant damages to adjacent members. For the impact analysis, the speed of the car was limited to 90 km/h, then the impact mass was incremented up to the initiation of column buckling. The assumptions used in the analyses are summarised below:

- Notional column removal: instantaneous column removal (removal time 0.0001 sec)
- Car impact: 11.5 tons vehicle with 90 km/h speed at an impact point at 1.5 m elevation (impact on weak axis)
- Near field blast: 12 kg TNT at 0.5m distance and 2.0 m from the ground (weak axis exposed)

Note: For the calculation of the blast pressure, the reflected pressure was evaluated considering infinite surface and infinite column rigidity.

The gravity loads on the floors are calculated using the equation:

$$DL + 0.5 \times LL$$

where:

DL - permanent load (see Table 4)

LL - live load (see Table 4 for SS/S structure).

The vertical displacement at the top of the column D4 for each type of analysis is plotted in Figure 135. In case of notional column removal, the progressive collapse is prevented, and the maximum vertical displacement reaches 146 mm.

For the blast analysis, the column web is completely removed due to shear, but the flanges are still in place, even heavily deformed (see Figure 136). In this case, the maximum vertical displacement is 63 mm, with the curve showing small effects of structural renounce in comparison to the notional column removal. As the column flanges do not instantly buckle, they provide significant residual capacity to limit the dynamic effect, thus resulting in smaller displacements and plastic deformations.

For the impact analysis, in the first phases (0 - ii) there is a strong load-structure interaction. During this stage, the axial force changes from compression (- 1160 kN) to tension (+ 1838 kN) due to the development of the catenary effect in the column, which pulls down the upper part of the structure. Even the impacting body eventually bounces back, the additional downward force caused by the impact leads to the development of progressive collapse (see Figure 137).

As a conclusion, the design using the explicit modelling of the accidental action could give different results compared with the notional column removal. However, considering the variability of the accidental loading conditions (e.g., position, intensity, duration, single or cascading hazard), the notional column removal remains an efficient approach for robustness design/assessment of the steel and composite building frame structures.

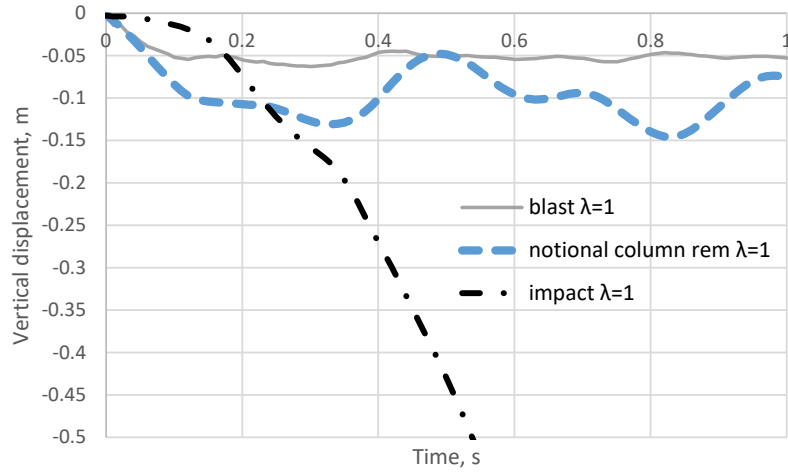


Figure 135 Structural response for notional column removal vs blast and impact loading

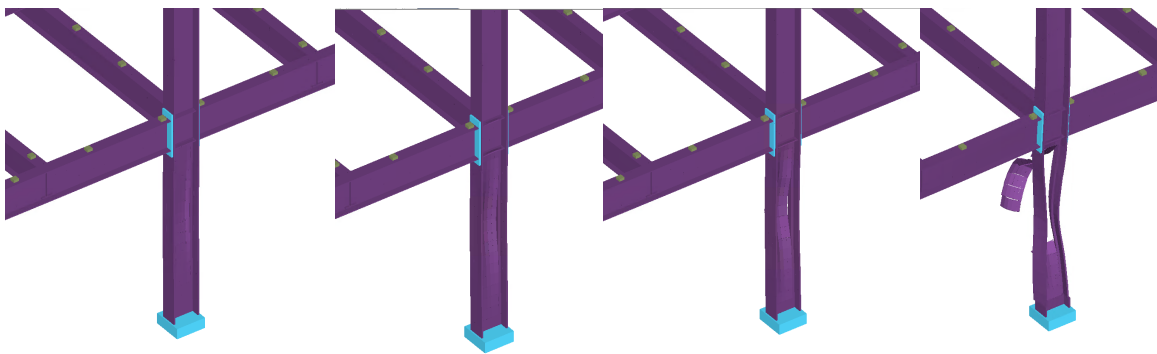


Figure 136 Deformation phases of D4 column under direct blast

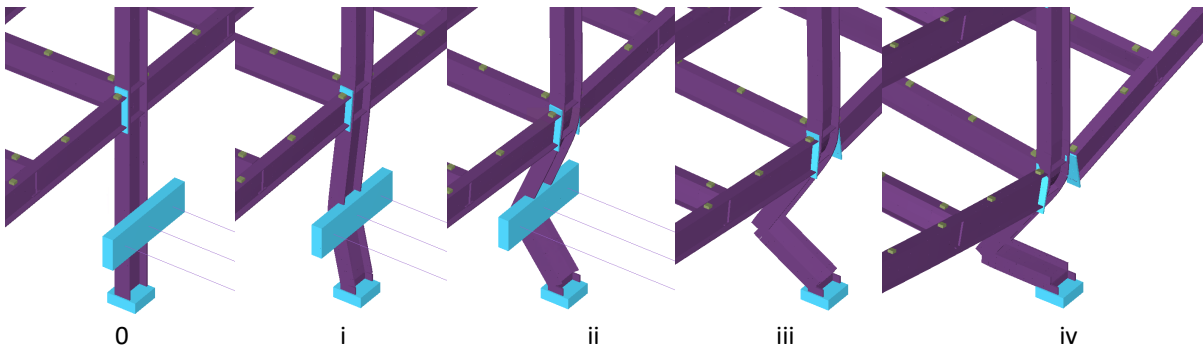


Figure 137 Deformation phases of D4 column under car impact

8 Remarks and conclusions

The structural robustness is a measure of the capacity to “withstand events like fire, explosions, impact or the consequences of human error, without being damaged to an extent disproportionate to the original cause” (EN1991-1-7). If the event (or threat) can be identified and modeled, the robustness may be demonstrated using several analysis methods, each with different level of sophistication (elastic/plastic, static/dynamic). However, as the events can be considered “abnormal”, their identification and modelling can be difficult to accomplish, which may have serious consequences (local/global damage, fatalities). Therefore, the hazard and robustness design/assessment can be decoupled by assuming notional actions (e.g., key element design using a load of 34 kPa) or notional initial damage. In case of building frame structures, the most critical local damage results from the loss of a column, as it can trigger the partial or total collapse of the building. So, by limiting the propagation of damage and preventing the progressive collapse, the structure becomes insensitive to local damage, i.e., robust structure. In this respect, a robust structure is generally able to develop alternative load paths by means of continuity, strength, and ductility. While the successful application of the threat dependent approaches (i.e., design against identified accidental actions) is mainly linked to local strengthening, the application of the threat independent approaches (i.e., design against unidentified accidental actions) does not necessarily result in an over-design, but in the activation of latent resisting mechanisms that are not usually exploited to withstand normal loads (Adam, 2018).

In the following, the main conclusions and recommendations are given, focusing mainly on the importance of the design assumptions (i.e., non-seismic vs seismic), level of approximation and complexity (simplified vs. advanced methods).

8.1 Structures in non-seismic area

The application of different accidental design scenarios against non-seismically designed structures showed that the initial design requirements (strength, stiffness) but also constructional measures, like orientation of columns against facades or joint detailing, have large impact on the robustness and capacity to resist progressive collapse. From the worked example, several conclusions can be drawn:

- Whenever possible, the adoption of seismic design principles improves the robustness and the progressive collapse resistance.
- Tying forces according to the prescriptive approach are much smaller than the values obtained with both analytical and numerical approaches. The prescriptive approach can therefore be unsafe for the design of robust steel / composite structures.
- The full numerical approach provides a better evaluation of the response but can be quite complex and therefore requires higher levels of expertise and knowledge.
- The analytical method is a good alternative to the full numerical approach for practitioners and can provide results close to the ones obtained with the full numerical approach.
- The need of reinforcement driven by robustness requirements is more related to joints than to members.
- For what concerns the joints, it has been demonstrated that their behaviour strongly influences the global response of the structure. Accordingly, it is important to respect the design recommendations provided in Section 2.2.3 of the design manual, which allow to guarantee a minimum level of ductility or of deformation capacity to the structural joints
- Pinned joints (especially fin plates) are not the best solution for robust steel structures. The use of partial-strength joints allows to delay the development of membrane effects and thus tends to lower the tensile forces in ties.

8.2 Structures in seismic area

The worked examples presented in this document showed that the seismic general principles (e.g., regularity in plan and elevation, continuity at joints), requirements in terms of lateral strength and stiffness, local and global ductility, but also the hierarchy of members and connections, make the steel and composite building structures more robust against accidental loading events. Stronger columns offer direct protection against impact and explosion, while minimum flexural requirements and ductility at beam-to-column joints provide higher capacity and load redistribution capacity after the loss of a column.

However, the results also indicated that some loading scenarios can still lead to significant damage and partial progressive collapse, for example when local damage affects areas designed for gravity loads only (i.e., beams with pinned end connections), as they do not follow the seismic requirements (no flexural capacity, limited axial capacity due to weak connections). In such cases, the use of stronger beam-to-column connections or the composite action between steel beams and concrete slab provide additional redistribution capacity and considerably reduces the local damage and the risk of progressive collapse.

8.3 Simplified vs. advanced approaches

For both families of strategies, i.e., design against identified or unidentified threats, the worked examples showed that the adoption of more advanced methods allows for a better and more accurate capture of the actual response of the structure and, in some cases, can limit or even avoid the need for strengthening measures.

The results also indicated that some loading scenarios can still lead to significant damage and partial progressive collapse, for example in frames equipped with simple joints subjected to a column loss scenario. In such cases, the use of partial-strength beam-to-column joints is seen as a good alternative as it does not prevent the designer to still use simple methods of analysis considering the joints as pinned (if the ductility of the joints is guaranteed through the use of the recommendations of Section 2.2.3) while profiting from the extra resistance provided by the joints in case of exceptional events.

Considering the application of the alternative load path method, it has been clearly highlighted that the level of tensile loads obtained using the prescriptive method as recommended in EN 1991-1-7 are much smaller than the ones obtained through more sophisticated methods that imply explicit column loss simulations. This confirms that the prescriptive method is not aimed at predicting the loads associated to a column loss scenario but at ensuring a minimum level of continuity in the structure.

It also means that the use of the prescriptive method is not sufficient to guarantee that the structure will survive to a column loss scenario. To achieve this objective, the analytical or numerical methods proposed within the present design manual have to be employed in the design process.

A.1 Definition of structural blast loads

A.1.1 Charts to determine the blast parameters

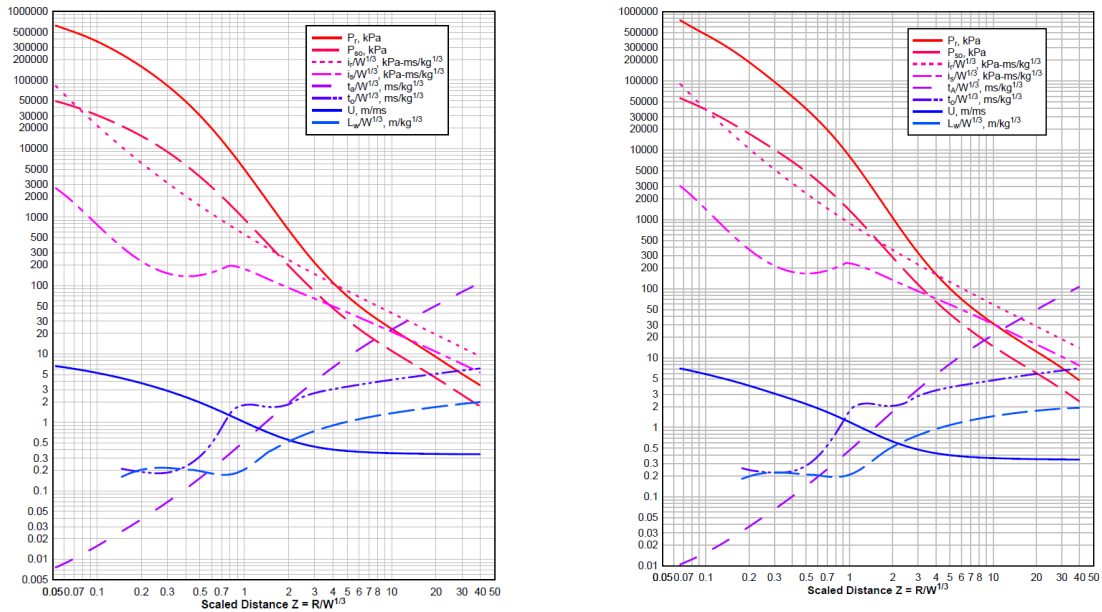


Figure 138. Parameters of positive phase of shock spherical wave of TNT charges from free-air bursts (left) and surface bursts (right) (modified from (DoD 2014))

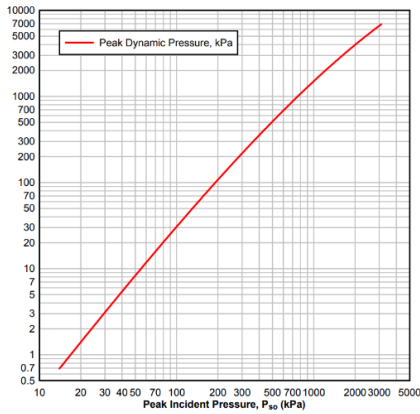


Figure 139. Variation of peak dynamic pressure q_0 versus peak incident pressure (modified from (DoD 2014))

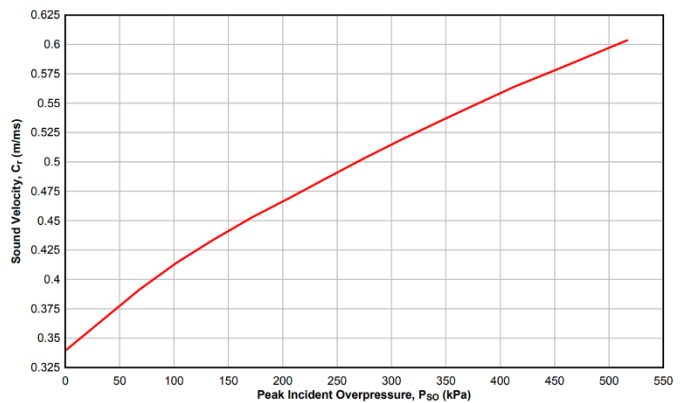


Figure 140. Sound velocity in reflected overpressure region (modified from (DoD 2014))

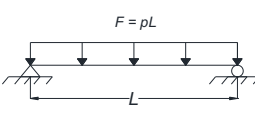
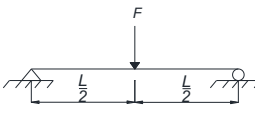
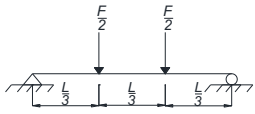
A.2 Tabular tools for response estimation SDOF systems

To determine the response of the SDOF system with elasto-plastic behaviour, the required ductility μ , given by the ratio γ_m/γ_e , as a function of t_d/T_n is presented in chart form, as a family of curves R_m/F_m .

A.2.1 Transformation factors for Beams and One-way Slabs

To determine the response of the SDOF system with elasto-plastic behaviour, the ultimate resistance R_m , loading factors (K_L), mass factors (K_M), load mass factors (K_{LM}), spring constant (k) and dynamic reactions ((K_{LM}) ,) can be determined for beams and one-way slabs from the following table.

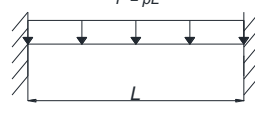
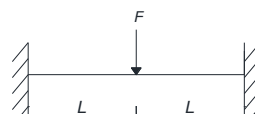
Table 65. Transformation Factors for Beams and One-way Slabs - simply supported beam (Biggs 1964)

Loading diagram	Strain range	Loading factor K_L	Mass factor K_M		Load-mass factor K_{LM}		Maximum resistance R_m	Spring constant k	Dynamic reaction V
			Concentrated mass*	Uniform mass	Concentrated mass*	Uniform mass			
	Elastic	0.64	...	0.50	...	0.78	$\frac{8M_P}{L}$	$\frac{384EI}{5L^3}$	$0.39R+0.11F$
	Plastic	0.50	...	0.33	...	0.66	$\frac{8M_P}{L}$	0	$0.38R_m+0.12F$
	Elastic	1.0	1.0	0.49	1.0	0.49	$\frac{4M_P}{L}$	$\frac{48EI}{L^3}$	$0.78R-0.28F$
	Plastic	1.0	1.0	0.33	1.0	0.33	$\frac{4M_P}{L}$	0	$0.75R_m-0.25F$
	Elastic	0.87	0.76	0.52	0.87	0.60	$\frac{6M_P}{L}$	$\frac{56.4EI}{L^3}$	$0.525R-0.025F$
	Plastic	1.0	1.0	0.56	1.0	0.56	$\frac{6M_P}{L}$	0	$0.52R_m-0.02F$

* Equal parts of the concentrated mass are lumped at each concentrated load.

Source: "Design of Structures to Resist the Effects of Atomic Weapons", U.S Army Corps of Engineers Manual EM 1110-345-415, 1957.

Table 66. Transformation Factors for Beams and One-way Slabs double fixed beam (Biggs 1964)

Loading diagram	Strain range	Loading factor K_L	Mass factor K_M		Load-mass factor K_{LM}		Maximum resistance R_m	Spring constant k	Effective spring constant k_E	Dynamic reaction V
			Concentrated mass*	Uniform mass	Concentrated mass*	Uniform mass				
	Elastic	0.53	...	0.41	...	0.77	$\frac{12M_{Ps}}{L}$	$\frac{384EI}{L^3}$...	$0.36R+0.14F$
	Elastic - plastic	0.64	...	0.50	...	0.78	$\frac{8}{L}(M_{Ps} + M_{Pm})$	$\frac{384EI}{5L^3}$	$\frac{307EI}{L^3}$	$0.39R+0.11F$
	Plastic	0.50	...	0.33	...	0.66	$\frac{8}{L}(M_{Ps} + M_{Pm})$	0	...	$0.38R_m+0.12F$
	Elastic	1.0	1.0	0.37	1.0	0.37	$\frac{4}{L}(M_{Ps} + M_{Pm})$	$\frac{192EI}{L^3}$...	$0.71R-0.21F$
	Plastic	1.0	1.0	0.33	1.0	0.33	$\frac{4}{L}(M_{Ps} + M_{Pm})$	0	...	$0.75R_m-0.25F$

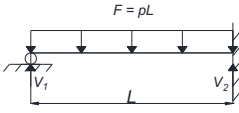
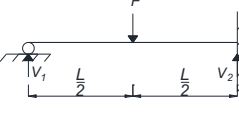
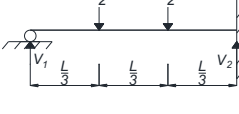
M_{Ps} – ultimate moment capacity at support

M_{Pm} – ultimate moment capacity at midspan

* Concentrated mass is lumped at the concentrated load.

Source: "Design of Structures to Resist the Effects of Atomic Weapons", U.S Army Corps of Engineers Manual EM 1110-345-415, 1957.

Table 67. Transformation Factors for Beams and One-way Slabs simply supported and fixed beam (Biggs 1964)

Loading diagram	Strain range	Load factor K_L	Mass factor K_M		Load-mass factor K_{LM}		Maximum resistance R_m	Spring constant k	Effective spring constant k_E	Dynamic reaction V
			Concentr. mass*	Uniform mass	Concentr. mass*	Uniform mass				
	Elastic	0.58	...	0.45	...	0.78	$\frac{8M_{Ps}}{L}$	$\frac{185EI}{L^3}$	$\frac{160EI}{L^3}$	$V_1 = 0.26R + 0.12F$ $V_2 = 0.43R + 0.19F$
	Elastic-plastic	0.64	...	0.50	...	0.78	$\frac{4}{L}(M_{Ps} + 2M_{Pm})$	$\frac{384EI}{5L^3}$		$V = 0.39R + 0.11F \pm M_{Ps}/L$
	Plastic	0.50	...	0.33	...	0.66	$\frac{4}{L}(M_{Ps} + 2M_{Pm})$	0		$V = 0.38R_m + 0.12F \pm M_{Ps}/L$
	Elastic	1.0	1.0	0.43	1.0	0.43	$\frac{16M_{Ps}}{3L}$	$\frac{107EI}{L^3}$	$\frac{106EI}{L^3}$	$V_1 = 0.25R + 0.07F$ $V_2 = 0.54R + 0.14F$
	Elastic-plastic	1.0	1.0	0.49	1.0	0.49	$\frac{2}{L}(M_{Ps} + 2M_{Pm})$	$\frac{48EI}{L^3}$		$V = 0.78R - 0.28F \pm M_{Ps}/L$
	Plastic	1.0	1.0	0.33	1.0	0.33	$\frac{2}{L}(M_{Ps} + 2M_{Pm})$	0		$V = 0.75R_m - 0.25F \pm M_{Ps}/L$
	Elastic	0.81	0.67	0.45	0.83	0.55	$\frac{6M_{Ps}}{3L}$	$\frac{132EI}{L^3}$	$\frac{122EI}{L^3}$	$V_1 = 0.17R + 0.17F$ $V_2 = 0.33R + 0.33F$
	Elastic-plastic	0.87	0.76	0.52	0.87	0.60	$\frac{2}{L}(M_{Ps} + 3M_{Pm})$	$\frac{56EI}{L^3}$		$V = 0.525R - 0.025F \pm M_{Ps}/L$
	Plastic	1.0	1.0	0.56	1.0	0.56	$\frac{2}{L}(M_{Ps} + 3M_{Pm})$...		$V = 0.52R_m - 0.02F \pm M_{Ps}/L$

M_{Ps} – ultimate bending capacity at support
 M_{Pm} – ultimate bending capacity at midspan
 * Equal parts of the concentrated mass are lumped at each concentrated load.
 Source: "Design of Structures to Resist the Effects of Atomic Weapons", U.S Army Corps of Engineers Manual EM 1110-345-415, 1957.

A.2.2 Maximum deflection and maximum response time of elasto-plastic SDOF systems

To determine the response of the SDOF system with elasto-plastic behaviour, the required ductility μ , given by the ratio γ_m/γ_e , as a function of t_d/T_n is presented in chart form, as a family of curves R_m/F_m .

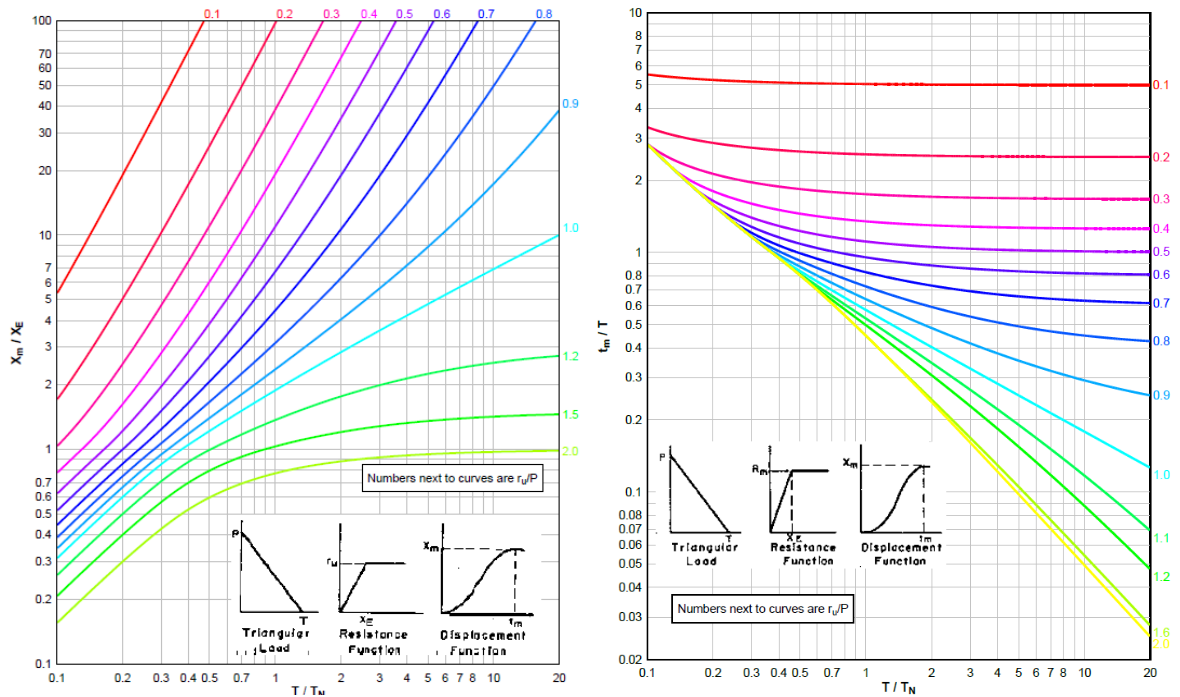


Figure 141. Maximum deflection (a) and maximum response time (b) of elasto-plastic SDOF system for triangular load (DoD 2014)

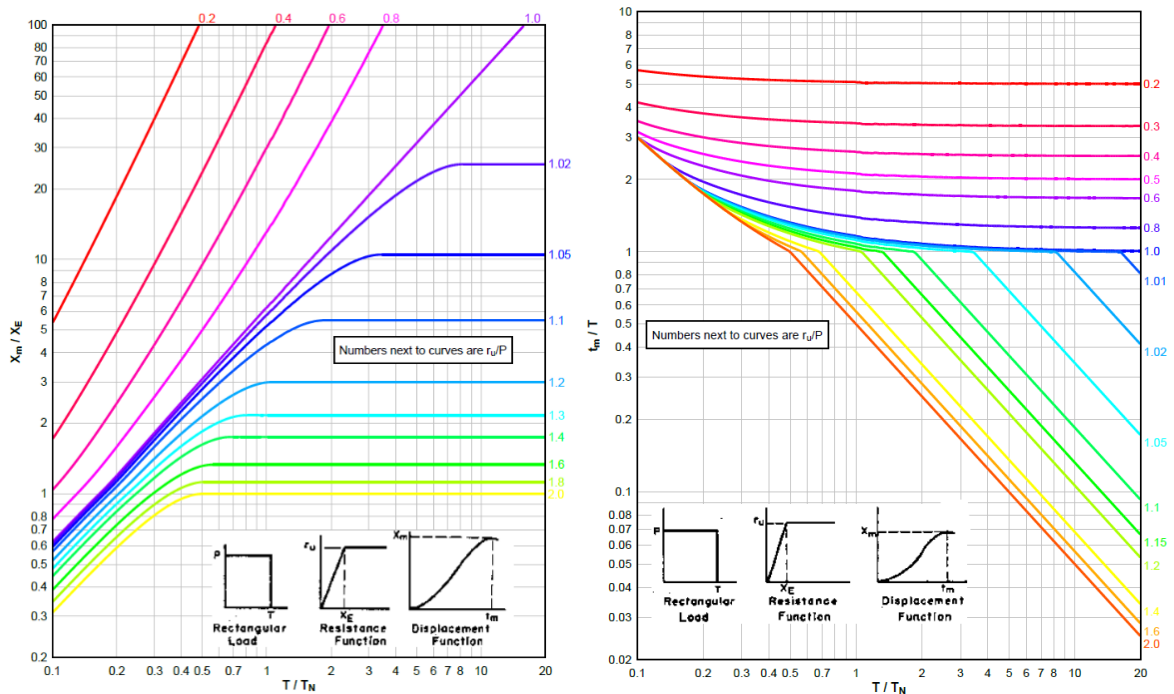


Figure 142. Maximum deflection (a) and maximum response time (b) of elasto-plastic SDOF system for rectangular load (DoD 2014)

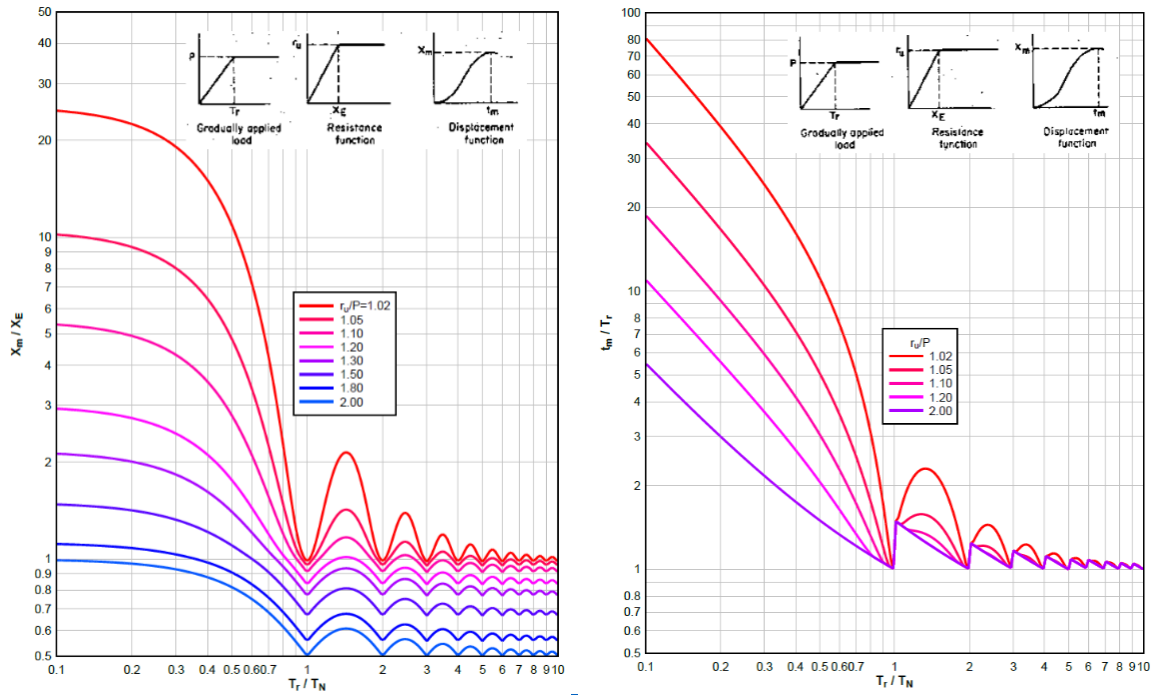


Figure 143. Maximum deflection (a) and maximum response time (b) of elasto-plastic SDOF system for gradually applied load (DoD 2014)

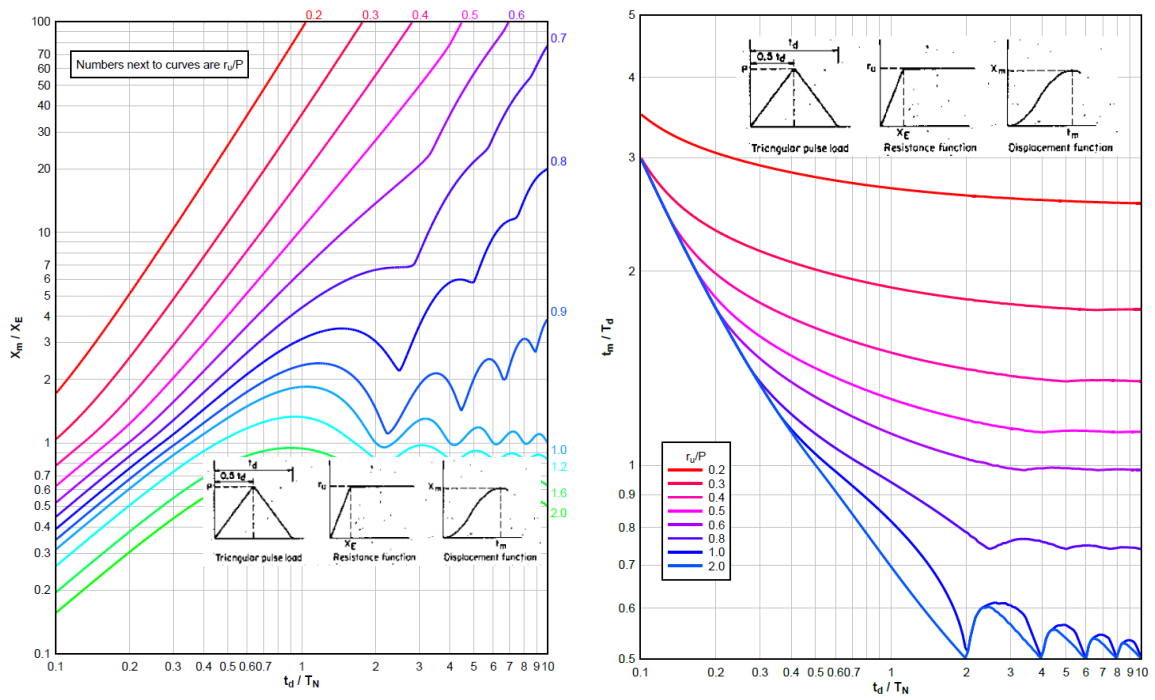


Figure 144. Maximum deflection (a) and maximum response time (b) of elasto-plastic SDOF system for triangular pulse load (DoD 2014)

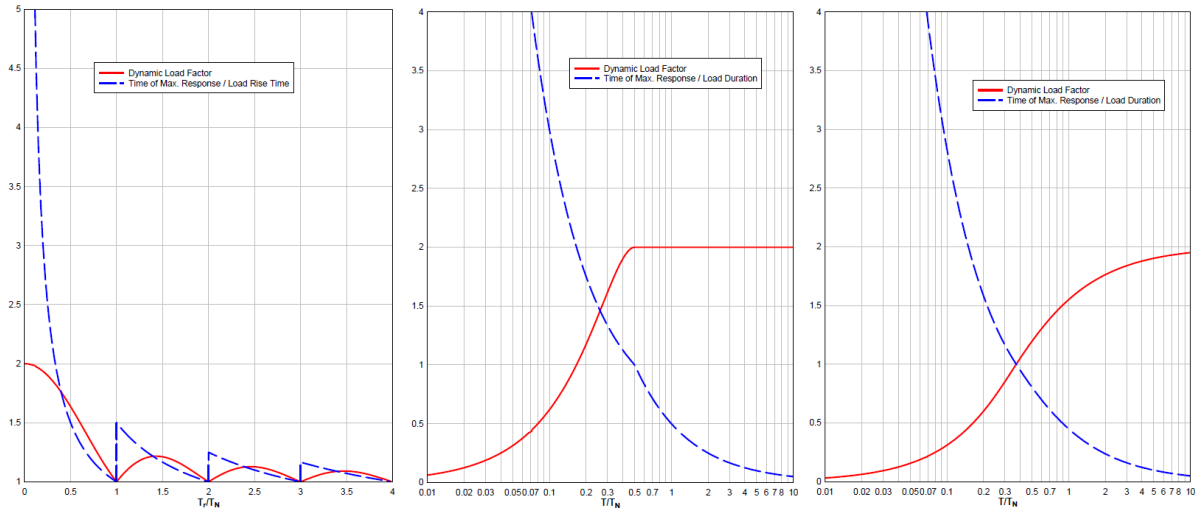


Figure 145. Maximum Response of elastic, one-degree-of-freedom system for gradually applied load (a), for rectangular load (b) and for triangular load (c)

A.2.3 Pressure-impulse charts for deformations

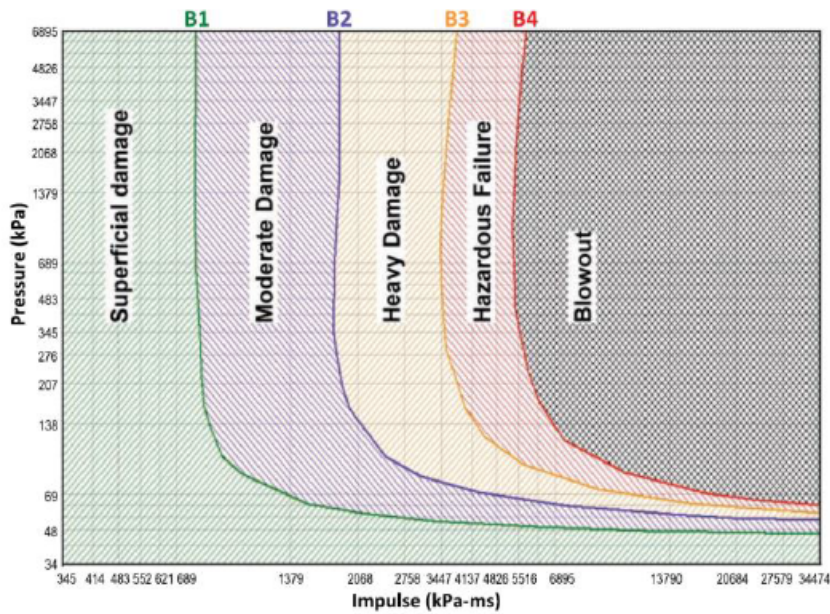


Figure 146. Pressure-Impulse relationships for deformations corresponding to damage limits (B1 to B4) (CSA S850 2012)

Element type		B1		B2		B3		B4	
		μ_{max}	θ_{max}	μ_{max}	θ_{max}	μ_{max}	θ_{max}	μ_{max}	θ_{max}
Flexure	Beam with compact section†	1	—	3	3°	12	10°	25	20°
	Beam with noncompact section †,‡	0.7	—	0.85	3°	1	—	1.2	—
	Plate bent about weak axis	4	1°	8	2°	20	6°	40	12°
Compression	Beam-column with compact section†,§	1	—	3	3°	3	3°	3	3°
	Beam-column with noncompact section †,§	0.7	—	0.85	3°	0.85	3°	0.85	3°
	Column (axial failure)**	0.9	—	1.3	—	2	—	3	—

* Where a dash (—) is shown, the corresponding parameter is not applicable as a response limit.
† Limiting width-to-thickness ratios for compact and noncompact sections are defined in CSA S16.
‡ These response limits are applicable for flexural evaluation of existing elements that satisfy the design requirements of Clauses 6 through 8 but do not satisfy the detailing requirements in Clause 9, and shall not be used for design of new elements.
§ If a shear plane through the anchor bolts connecting the column base plate to the foundation exists, the response limit for superficial damage shall apply, using the shear capacity of this connection, rather than the element flexural capacity, as the ultimate resistance for analysis.
** Ductility ratio is based on axial deformation, rather than flexural deformation.
Note: Adapted from PDC-TR 06-08

Figure 147. Response limits for hot-rolled structural steel (CSA S850 2012)

A.3 Detailed calculation of SS/NS structure

A.3.1 Joint B1

Resistance to tying forces

B-1 strong axis (IPE 550 to HEB 340)

Loads	$V_{z,Ad}$	100 kN	(RSTAB)	
	N_T	499,2 kN	(prescriptive method acc. to EN 1991-1-7)	
safety factor	γ_{Mu}	1,10		
column		HEB 340	h 340 mm	
	f_y	355 N/mm ²	b 300 mm	
	f_u	490 N/mm ²	t_w 12 mm	
			t_f 21,5 mm	
beam		IPE 550	h 550 mm	
	f_y	355 N/mm ²	b 210 mm	
	f_u	490 N/mm ²	t_w 11,1 mm	
			t_f 17,2 mm	
			h_w 467 mm	
fin plate	S355	f_y	355 N/mm ²	h 180 mm
		f_u	490 N/mm ²	b 125 mm
				t 10 mm
				gap 10 mm

bolts 10.9

f_{ub}	1000 N/mm ²	d	20 mm
α_v	0,5	d_o	22 mm
		A_s	2,45 cm ²

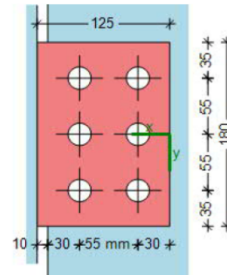
bolt pattern

columns	n_2	2	rows	n_1	3
vertical pitch	p_1	55 mm	hor. Pitch	p_2	55 mm
n Bolts	n	6	vert. edge	e_1	35 mm
			hor. edge	e_2	30 mm

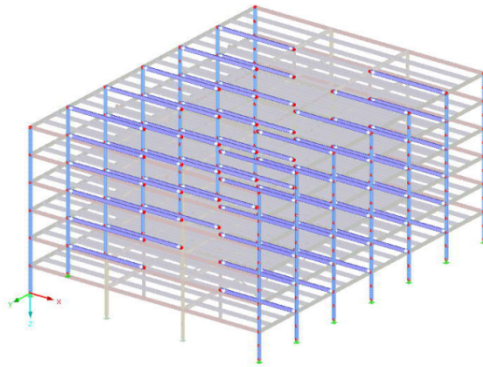
weld a 6 mm

Component μ

1) Bolts in shear	0,76
2) Fin plate in bearing	1,16
3) Fin plate in tension (gross section)	0,62
4) Fin plate in tension (net section)	1,09
5) Beam web in bearing	1,04
6) Beam in tension (gross section)	0,22
7) Beam in tension (net section)	0,28
8) Supporting member in bending	0,00



2) Fin plate in bearing 1,16



Notice: Ductility and plastic redistribution allowance already verified with COP

1) Bolts in shear

A_s	2,45 cm ²
n	6
α_v	0,5
f_{ub}	1000 N/mm ²
$F_{v,Rd}$	111,4 kN
$N_{U,1}$	668,2 kN
N_{Ed}	499,2 kN
V_{Ed}	100 kN
F_{Ed}	509,1 kN
μ	0,76

2) Fin plate in bearing

d_0	22 mm		
e_1	35 mm	N_{Ed}	499,2 kN
e_2	30 mm	V_{Ed}	100 kN
p_1	55 mm	μ	1,16
p_2	55 mm		

Vertical direction

α_b	0,53
k_1	1,80
$F_{y,b,Rd}$	85,0 kN
$N_{u,2,y}$	510,2 kN

Horizontal direction

α_b	0,45
k_1	1,80
$F_{y,b,Rd}$	72,9 kN
$N_{u,2,y}$	437,4 kN

3) Fin plate in tension (gross section)

t_p	10 mm
h_p	180 mm
f_{up}	490 mm
$N_{u,3}$	801,8 kN
N_{Ed}	499,2 kN
μ	0,62

4) Fin plate in tension (net section)

d_0	22 mm
$A_{net,p}$	1140 mm ²
$N_{u,4}$	457,0 kN
N_{Ed}	499,2 kN
μ	1,09

5) Beam web in bearing

d_0	22 mm		
e_1	- mm	N_{Ed}	499,2 kN
e_{2b}	30 mm	V_{Ed}	100 kN
p_1	55 mm	μ	1,04
p_2	55 mm		

Vertical direction

α_b	0,58
k_1	1,80
$F_{y,b,Rd}$	103,8 kN
$N_{u,2,y}$	623,0 kN

Horizontal direction

α_b	0,45
k_1	1,80
$F_{y,b,Rd}$	80,91 kN
$N_{u,2,y}$	485,46 kN

6) Beam in tension (gross section)

t_w	11,1 mm
h_w	467 mm
f_u	490 mm
$N_{u,6}$	2309,1 kN
N_{Ed}	499,2 kN
μ	0,22

7) Beam in tension (net section)

d_0	22 mm
$A_{net,p}$	4451,1 mm ²
$N_{u,7}$	1784,5 kN
N_{Ed}	499,2 kN
μ	0,28

8) Supporting member in bending

$N_{u,8}$	∞ kN
-----------	-------------

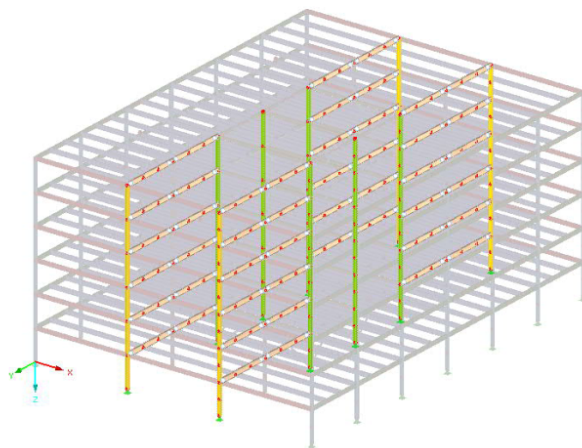
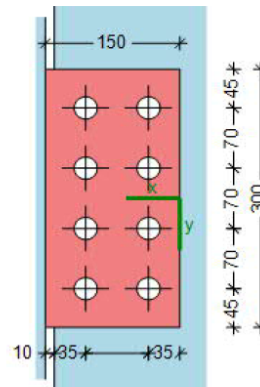
A.3.2 Joint C2w

Resistance to tying forces

C-2 weak axis (IPE 600 to HEB 360)

Loads	$V_{z,Ad}$	238 kN	(RSTAB)
	N_T	499,2 kN	(prescriptive method acc. to EN 1991-1-7)
safety factor	γ_{Mu}	1,10	
column	HEB 360		
	f_y	355 N/mm ²	h 360 mm
	f_u	490 N/mm ²	b 300 mm
	h_w	261 mm	t_w 12,5 mm
			t_f 22,5 mm
beam	IPE 600		
	f_y	355 N/mm ²	h 600 mm
	f_u	490 N/mm ²	b 220 mm
			t_w 12 mm
			t_f 19 mm
			h_w 514 mm
fin plate	S355		
	f_y	355 N/mm ²	h 300 mm
	f_u	490 N/mm ²	b 150 mm
			t 10 mm
			gap 10 mm
bolts	10.9		
	f_{ub}	1000 N/mm ²	d 24 mm
	α_v	0,5	d_o 26 mm
			A_s 3,53 cm ²
bolt pattern			
columns	n_2	2	rows n_1 4
vertical pitch	p_1	70 mm	hor. Pitch p_2 70 mm
n Bolts	n	8	vert. edge e_1 45 mm
			hor. edge e_2 35 mm
weld	a	6 mm	

Component	μ
1) Bolts in shear	0,43
2) Fin plate in bearing	0,67
3) Fin plate in tension (gross section)	0,37
4) Fin plate in tension (net section)	0,64
5) Beam web in bearing	0,55
6) Beam in tension (gross section)	0,18
7) Beam in tension (net section)	0,25
8) Supporting member in bending	1,15



Notice: Ductility and plastic redistribution allowance already verified with COP

1) Bolts in shear	
A_s	3,53 cm ²
n	8
α_v	0,5
f_{ub}	1000 N/mm ²
$F_{v,Rd}$	160,5 kN
$N_{U,1}$	1283,6 kN
N_{Ed}	499,2 kN
V_{Ed}	238 kN
F_{Ed}	553,0 kN
μ	0,43

2) Fin plate in bearing

d_0	26 mm		
e_1	45 mm	N_{Ed}	499,2 kN
e_2	35 mm	V_{Ed}	238 kN
p_1	70 mm	μ	0,67
p_2	70 mm		

Vertical direction

α_b	0,58
k_1	2,07
$F_{y,b,Rd}$	127,6 kN
$N_{u,2,y}$	1021,0 kN

Horizontal direction

α_b	0,45
k_1	2,07
$F_{y,b,Rd}$	99,3 kN
$N_{u,2,y}$	794,1 kN

3) Fin plate in tension (gross section)

t_p	10 mm
h_p	300 mm
f_{up}	490 mm
$N_{u,3}$	1336,4 kN
N_{Ed}	499,2 kN
μ	0,37

4) Fin plate in tension (net section)

d_0	26 mm
$A_{net,p}$	1960 mm ²
$N_{u,4}$	785,8 kN
N_{Ed}	499,2 kN
μ	0,64

5) Beam web in bearing

d_0	26 mm		
e_1	- mm	N_{Ed}	499,2 kN
e_{2b}	35 mm	V_{Ed}	238 kN
p_1	70 mm	μ	0,55
p_2	70 mm		

Vertical direction

α_b	0,65
k_1	2,07
$F_{y,b,Rd}$	171,9 kN
$N_{u,2,y}$	1375,0 kN

Horizontal direction

α_b	0,45
k_1	2,07
$F_{y,b,Rd}$	119,12 kN
$N_{u,2,y}$	952,95 kN

6) Beam in tension (gross section)

t_w	12 mm
h_w	514 mm
f_u	490 MPa
$N_{u,6}$	2747,6 kN
N_{Ed}	499,2 kN
μ	0,18

7) Beam in tension (net section)

d_o	26 mm
$A_{net,p}$	4920 mm ²
$N_{u,7}$	1972,5 kN
N_{Ed}	499,2 kN
μ	0,25

8) Supporting member in bending

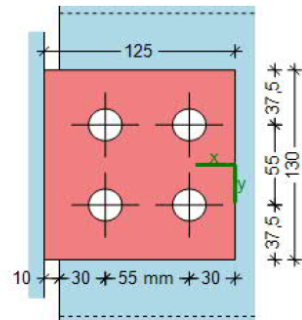
k_m	1
f_u	490 MPa
t_w	12,5 mm
h_p	300 mm
d_c	261 mm
t_p	10 mm
$N_{u,8}$	433,0 kN
N_{Ed}	499,2 kN
μ	1,15

$$N_{u,8} = k_m \cdot f_{u,c} \cdot t_{w,c}^2 \cdot \left[\frac{2 \cdot h_p}{d_c} + 4 \cdot \sqrt{1 - \frac{t_p}{d_c}} \right] / \gamma_{Mu}$$

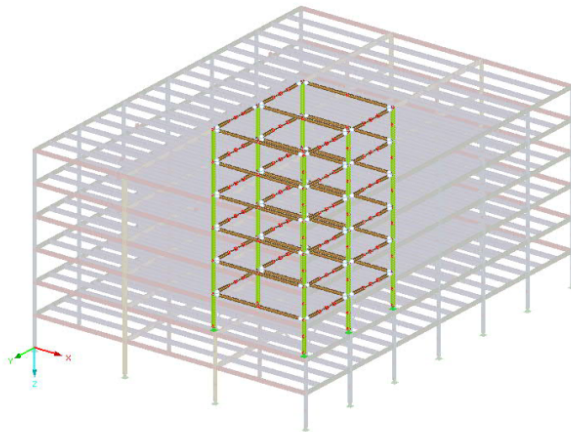
A.3.3 Joint D3s

Resistance to tying forces		D-3 strong axis (HEA 300 to HEM 300)	
Loads	$V_{z,Ad}$	40 kN	(RSTAB)
	N_T	499,2 kN	(prescriptive method acc. to EN 1991-1-7)
safety factor	γ_{Mu}	1,10	
column		HEM 300	h 340 mm
	f_y	355 N/mm ²	b 310 mm
	f_u	490 N/mm ²	t_w 21 mm
			t_f 39 mm
beam		HEA 300	h 290 mm
	f_y	355 N/mm ²	b 300 mm
	f_u	490 N/mm ²	t_w 8,5 mm
			t_f 14 mm
			h_w 208 mm
fin plate	S355	f_y 355 N/mm ²	h 180 mm
		f_u 490 N/mm ²	b 125 mm
			t 10 mm
			gap 10 mm
bolts	10.9	f_{ub} 1000 N/mm ²	d 20 mm
		α_v 0,5	d_o 22 mm
			A_s 2,45 cm ²
bolt pattern	columns	n_2 2	rows n_1 2
	vertical pitch	p_1 55 mm	hor. Pitch p_2 55 mm
	n Bolts	n 4	vert. edge e_1 37,5 mm
			hor. edge e_2 30 mm
weld	a	6 mm	

Component	μ
1) Bolts in shear	1,12
2) Fin plate in bearing	1,72
3) Fin plate in tension (gross section)	0,62
4) Fin plate in tension (net section)	0,92
5) Beam web in bearing	2,02
6) Beam in tension (gross section)	0,63
7) Beam in tension (net section)	0,89
8) Supporting member in bending	0,00



5) Beam web in bearing	2,02
-------------------------------	-------------



Notice: Ductility and plastic redistribution allowance already verified with COP

1) Bolts in shear

A_s	2,45 cm ²
n	4
α_v	0,5
f_{ub}	1000 N/mm ²
$F_{V,Rd}$	111,4 kN
$N_{U,1}$	445,5 kN
N_{Ed}	499,2 kN
V_{Ed}	40 kN
F_{Ed}	500,8 kN
μ	1,12

2) Fin plate in bearing

d_0	22 mm		
e_1	37,5 mm	N_{Ed}	499,2 kN
e_2	30 mm	V_{Ed}	40 kN
p_1	55 mm	μ	1,72
p_2	55 mm		

Vertical direction

α_b	0,57
k_1	1,80
$F_{y,b,Rd}$	91,1 kN
$N_{u,2,y}$	364,5 kN

Horizontal direction

α_b	0,45
k_1	1,80
$F_{y,b,Rd}$	72,9 kN
$N_{u,2,y}$	291,6 kN

3) Fin plate in tension (gross section)

t_p	10 mm
h_p	180 mm
f_{up}	490 mm
$N_{u,3}$	801,8 kN
N_{Ed}	499,2 kN
μ	0,62

4) Fin plate in tension (net section)

d_0	22 mm
$A_{net,p}$	1360 mm ²
$N_{u,4}$	545,2 kN
N_{Ed}	499,2 kN
μ	0,92

5) Beam web in bearing

d_0	22 mm		
e_1	- mm	N_{Ed}	499,2 kN
e_{2b}	30 mm	V_{Ed}	40 kN
p_1	55 mm	μ	2,02
p_2	55 mm		

Vertical direction

α_b	0,58
k_1	1,80
$F_{y,b,Rd}$	79,5 kN
$N_{u,2,y}$	318,1 kN

Horizontal direction

α_b	0,45
k_1	1,80
$F_{y,b,Rd}$	61,96 kN
$N_{u,2,y}$	247,83 kN

6) Beam in tension (gross section)

t_w	8,5 mm
h_w	208 mm
f_u	490 mm
$N_{u,6}$	787,6 kN
N_{Ed}	499,2 kN
μ	0,63

7) Beam in tension (net section)

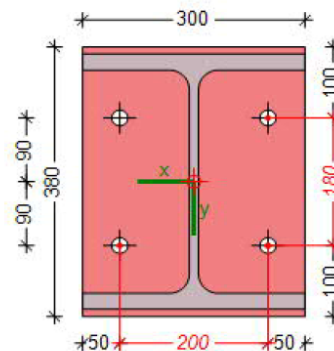
d_0	22 mm
$A_{net,p}$	1394 mm ²
$N_{u,7}$	558,9 kN
N_{Ed}	499,2 kN
μ	0,89

8) Supporting member in bending

$N_{u,8}$	∞ kN
-----------	-------------

A.3.4 Joint 3-3 (column splice):

Resistance to tying forces		3-3 HEM 300 internal column	
Loads	N_T	694,2 kN	(prescriptive method acc. to EN 1991-1-7)
safety factor	γ_{M2}	1,25	
column	HEM 300	f_y 355 N/mm ²	f_u 490 N/mm ²
		h 340 mm	b 310 mm
		t_w 21 mm	t_f 39 mm
		r 27 mm	d 208 mm
plate	S355	f_y 355 N/mm ²	f_u 490 N/mm ²
		h 360 mm	b 310 mm
		t 15 mm	
bolts	10.9	f_{ub} 1000 N/mm ²	α_v 0,5
		d 20 mm	d_o 22 mm
		A_s 2,45 cm ²	
bolt pattern			
columns	n_2	2	rows n_1 2
vertical pitch	p_1	180 mm	hor. Pitch p_2 200 mm
n Bolts	n	4	vert. edge e_1 90 mm
			hor. edge e_2 55 mm
weld	a_r	6 mm	a_w 6 mm



Rows resistances from COP

Bolt row 1	End plate in bending	$F_{EPB,1,Rd}$	286 kN
	Beam web in tension	$F_{BWT,1,Rd}$	3729 kN
	End plate in bending (2)	$F_{EPB,1,Rd}$	286 kN
	Beam web in tension (2)	$F_{BWT,1,Rd}$	3729 kN
	Effective tension resistance	$F_{T1,Rd}$	286 kN
	Lever arm	h_1	240,5 mm
Bolt row 2	End plate in bending	$F_{EPB,2,Rd}$	286 kN
	Beam web in tension	$F_{BWT,2,Rd}$	3729 kN
	End plate in bending (2)	$F_{EPB,2,Rd}$	286 kN
	Beam web in tension (2)	$F_{BWT,2,Rd}$	3729 kN
	Effective tension resistance	$F_{T2,Rd}$	222,3 kN
	Lever arm	h_2	60,5 mm

1) Rows resistance

The total tension resistance of the joint (no bending force applied) is equal to the sum of the contribution of each bolt row.

$$F_{T,Rd} = 508,3 \text{ kN}$$

$$F_{Ed} = 694,2 \text{ kN}$$

$$\mu = 1,37$$

Ductility and plastic redistribution allowance already considered by COP.

Note that this result is on the safe side as COP uses f_y for plate bending. For robustness scenarios (exceptional load case combination), we could use f_u .

2) Welds resistance

a_f	6 mm	
a_w	6 mm	
l_{wf}	545 mm	Total weld length of one flange
l_{ww}	416 mm	Total weld length of the web
A_{wf}	3270 mm ²	Total weld area of one flange
A_{wf}	2496 mm ²	Total weld area of the web
A_w	9036 mm ²	Total weld area
f_u	490 N/mm ²	
β_w	0,9	
$F_{w,Rd}$	2272,3 kN	
F_{Ed}	694,2 kN	
μ	0,31	

1) Rows resistance using f_u

As the total tension resistance of the joint is defined by the group resistance of both rows (end plate in bending), we can optimize the calculation using f_u and γ_{M2} instead of f_y and γ_{M0} for this component in the following.

Results from COP:

2.1.3.1.1.5.6 End plate in bending (2) / Group 1 to 2

Effective length in mode 1	$L_{eff,1}$	=	780,7 mm
Effective length in mode 2	$L_{eff,2}$	=	780,7 mm
Edge distance	n	=	55 mm EN1993-1-8 Tbl. 6.2

L_{eff1}	780,7 mm	t_p	15 mm
L_{eff2}	780,7 mm	γ_{M2}	1,25
n	55 mm	f_{up}	490 MPa
m	82,7 mm		

Resistance of the plate in bending

$M_{pl,1,Rd}$	17214435 Nmm
$M_{pl,2,Rd}$	17214435 Nmm

Resistance of the bolts in tension

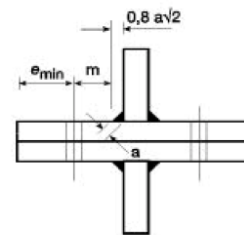
n_{Bolts}	4
f_{ub}	1000 MPa
A_s	2,45 cm ²
ΣF_{TRd}	705,6 kN (for n bolts)

T-stub modes (using Method 1 acc. To EN 1993-1-8 Tab. 6.2)

$F_{T1,Rd}$	832,5 kN	Mode 1
$F_{T2,Rd}$	531,8 kN	Mode 2
$F_{T3,Rd}$	705,6 kN	Mode 3
$F_{T,Rd}$	531,8 kN	

Optimized verification

F_{Ed}	694,2 kN
μ	1,31



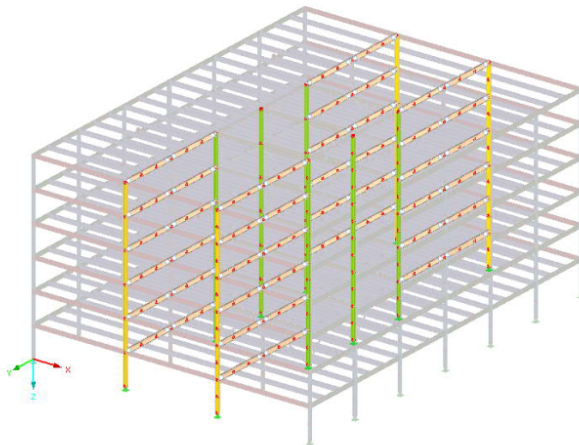
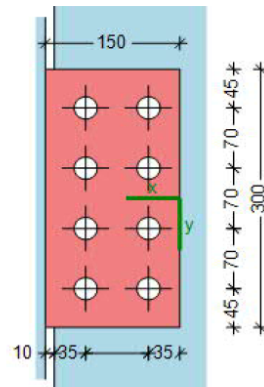
A.3.5 Joint C2w - redesigned

Resistance to tying forces

C-2 weak axis (IPE 600 to HEB 360)

Loads	$V_{z,Ad}$	238 kN	(RSTAB)
	N_T	499,2 kN	(prescriptive method acc. to EN 1991-1-7)
safety factor	γ_{Mu}	1,10	
column		HEB 360	
	f_y	355 N/mm ²	h 360 mm
	f_u	490 N/mm ²	b 300 mm
	h_w	261 mm	t_w 12,5 mm
			t_f 22,5 mm
	t_p	10 mm	welded web plate
beam		IPE 600	
	f_y	355 N/mm ²	h 600 mm
	f_u	490 N/mm ²	b 220 mm
			t_w 12 mm
			t_f 19 mm
			h_w 514 mm
fin plate	S355		
	f_y	355 N/mm ²	h 300 mm
	f_u	490 N/mm ²	b 150 mm
			t 10 mm
			gap 10 mm
bolts	10.9		
	f_{ub}	1000 N/mm ²	d 24 mm
	α_v	0,5	d_o 26 mm
			A_s 3,53 cm ²
bolt pattern			
columns	n_2	2	rows n_1 4
vertical pitch	p_1	70 mm	hor. Pitch p_2 70 mm
n Bolts	n	8	vert. edge e_1 45 mm
			hor. edge e_2 35 mm
weld	a	6 mm	

Component	μ
1) Bolts in shear	0,43
2) Fin plate in bearing	0,67
3) Fin plate in tension (gross section)	0,37
4) Fin plate in tension (net section)	0,64
5) Beam web in bearing	0,55
6) Beam in tension (gross section)	0,18
7) Beam in tension (net section)	0,25
8) Supporting member in bending	0,88
8) Supporting member in bending	0,88



Notice: Ductility and plastic redistribution allowance already verified with COP

1) Bolts in shear

A_s	3,53 cm ²
n	8
α_v	0,5
f_{ub}	1000 N/mm ²
$F_{v,Rd}$	160,5 kN
$N_{U,1}$	1283,6 kN
N_{Ed}	499,2 kN
V_{Ed}	238 kN
F_{Ed}	553,0 kN
μ	0,43

2) Fin plate in bearing

d_0	26 mm		
e_1	45 mm	N_{Ed}	499,2 kN
e_2	35 mm	V_{Ed}	238 kN
p_1	70 mm	μ	0,67
p_2	70 mm		

Vertical direction

α_b	0,58
k_1	2,07
$F_{y,b,Rd}$	127,6 kN
$N_{u,2,y}$	1021,0 kN

Horizontal direction

α_b	0,45
k_1	2,07
$F_{y,b,Rd}$	99,3 kN
$N_{u,2,y}$	794,1 kN

3) Fin plate in tension (gross section)

t_p	10 mm
h_p	300 mm
f_{up}	490 mm
$N_{u,3}$	1336,4 kN
N_{Ed}	499,2 kN
μ	0,37

4) Fin plate in tension (net section)

d_0	26 mm
$A_{net,p}$	1960 mm ²
$N_{u,4}$	785,8 kN
N_{Ed}	499,2 kN
μ	0,64

5) Beam web in bearing

d_0	26 mm		
e_1	- mm	N_{Ed}	499,2 kN
e_{2b}	35 mm	V_{Ed}	238 kN
p_1	70 mm	μ	0,55
p_2	70 mm		

Vertical direction

α_b	0,65
k_1	2,07
$F_{y,b,Rd}$	171,9 kN
$N_{u,2,y}$	1375,0 kN

Horizontal direction

α_b	0,45
k_1	2,07
$F_{y,b,Rd}$	119,12 kN
$N_{u,2,y}$	952,95 kN

6) Beam in tension (gross section)

t_w	12 mm
h_w	514 mm
f_u	490 MPa
$N_{u,6}$	2747,6 kN
N_{Ed}	499,2 kN
μ	0,18

7) Beam in tension (net section)

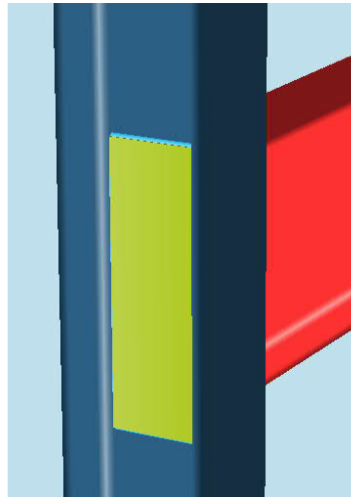
d_o	26 mm
$A_{net,p}$	4920 mm ²
$N_{u,7}$	1972,5 kN
N_{Ed}	499,2 kN
μ	0,25

8) Supporting member in bending

k_m	1
f_u	490 MPa
$t_{w,eq}$	14,3 mm
h_p	300 mm
d_c	261 mm
t_p	10 mm
$N_{u,8}$	570,5 kN
N_{Ed}	499,2 kN
μ	0,88

equivalent web thickness

$$N_{u,8} = k_m \cdot f_{u,c} \cdot t_{w,c}^2 \cdot \left[\frac{2 \cdot h_p}{d_c} + 4 \cdot \sqrt{1 - \frac{t_p}{d_c}} \right] / \gamma_{Mu}$$

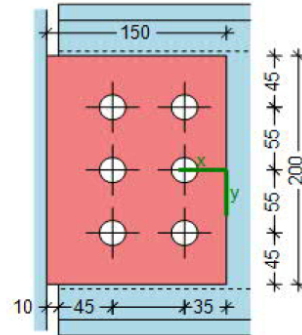


A.3.6 Joint D3s – redesigned

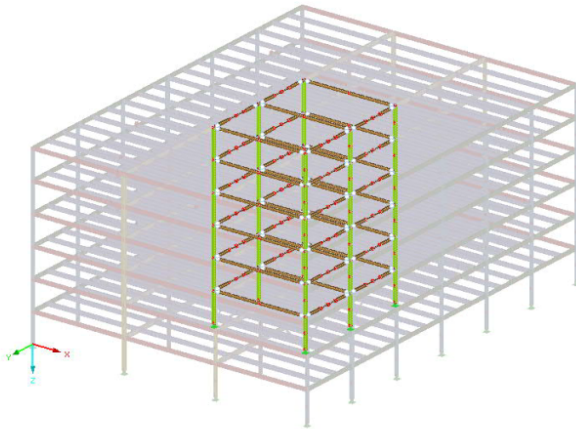
Resistance to tying forces		D-3 strong axis (HEA 300 to HEM 300)				
Loads	$V_{z,Ad}$	40 kN	(RSTAB)			
	N_T	499,2 kN	(prescriptive method acc. to EN 1991-1-7)			
safety factor	γ_{Mu}	1,10				
column		HEM 300	h 340 mm			
	f_y	355 N/mm ²	b 310 mm			
	f_u	490 N/mm ²	t_w 21 mm			
			t_f 39 mm			
beam		HEA 300	h 290 mm			
	f_y	355 N/mm ²	b 300 mm			
	f_u	490 N/mm ²	t_w 8,5 mm			
			t_f 14 mm			
			h_w 208 mm			
fin plate	S355	f_y	355 N/mm ²	h 200 mm		
		f_u	490 N/mm ²	b 150 mm		
			t 10 mm			
			gap	10 mm		
bolts	10.9	f_{ub}	1000 N/mm ²	d 20 mm		
		α_v	0,5	d_o 22 mm		
				A_s 2,45 cm ²		
bolt pattern	columns	n_2	2	rows	n_1	3
	vertical pitch	p_1	55 mm	hor. Pitch	p_2	60 mm
	n Bolts	n	6	vert. edge	e_1	45 mm
				hor. edge	e_2	35 mm
weld	a	6 mm				

Component	μ
-----------	-------

1) Bolts in shear	0,75
2) Fin plate in bearing	0,98
3) Fin plate in tension (gross section)	0,56
4) Fin plate in tension (net section)	0,93
5) Beam web in bearing	0,93
6) Beam in tension (gross section)	0,63
7) Beam in tension (net section)	1,03
8) Supporting member in bending	0,00



7) Beam in tension (net section)	1,03
---	-------------



Notice: Ductility and plastic redistribution allowance already verified with COP

1) Bolts in shear

A_s	2,45 cm ²
n	6
α_v	0,5
f_{ub}	1000 N/mm ²
$F_{V,Rd}$	111,4 kN
$N_{U,1}$	668,2 kN
N_{Ed}	499,2 kN
V_{Ed}	40 kN
F_{Ed}	500,8 kN
μ	0,75

2) Fin plate in bearing

d_0	22 mm		
e_1	45 mm	N_{Ed}	499,2 kN
e_2	35 mm	V_{Ed}	40 kN
p_1	55 mm	μ	0,98
p_2	60 mm		

Vertical direction

α_b	0,58
k_1	2,12
$F_{y,b,Rd}$	110,1 kN
$N_{u,2,y}$	660,5 kN

Horizontal direction

α_b	0,53
k_1	1,80
$F_{y,b,Rd}$	85,0 kN
$N_{u,2,y}$	510,2 kN

3) Fin plate in tension (gross section)

t_p	10 mm
h_p	200 mm
f_{up}	490 mm
$N_{u,3}$	890,9 kN
N_{Ed}	499,2 kN
μ	0,56

4) Fin plate in tension (net section)

d_0	22 mm
$A_{net,p}$	1340 mm ²
$N_{u,4}$	537,2 kN
N_{Ed}	499,2 kN
μ	0,93

5) Beam web in bearing

d_0	22 mm		
e_1	- mm	N_{Ed}	499,2 kN
e_{2b}	45 mm	V_{Ed}	40 kN
p_1	55 mm	μ	0,93
p_2	60 mm		

Vertical direction

α_b	0,58
k_1	1,80
$F_{y,b,Rd}$	79,5 kN
$N_{u,2,y}$	477,1 kN

Horizontal direction

α_b	0,66
k_1	1,80
$F_{y,b,Rd}$	89,84 kN
$N_{u,2,y}$	539,04 kN

6) Beam in tension (gross section)

t_w	8,5 mm
h_w	208 mm
f_u	490 mm
$N_{u,6}$	787,6 kN
N_{Ed}	499,2 kN
μ	0,63

7) Beam in tension (net section)

d_0	22 mm
$A_{net,p}$	1207 mm ²
$N_{u,7}$	483,9 kN
N_{Ed}	499,2 kN
μ	1,03

3%-Exceedance could be accepted. If not, go to HEB300 or add web plates locally, depending on the most economical option.

8) Supporting member in bending

$N_{u,8}$	∞ kN
-----------	-------------

A.3.7 Indirect affected columns verification - numerical approach (scenario 1)

■ Design by Cross-Section

Sect. No.	Member No.	Location x [m]	LC/CO/RC	Design		Equation No.	Description
1	HEB 340 - column long facade 25	0.00	CO165	0.66	≤ 1	ST312)	Stability analysis - Flexural buckling about z-axis acc. to 6.3.1.1 and 6.3.1.2
Design Internal Forces							
	Axial Force					N_{Ed}	-2910.15 kN
	Shear Force					$V_{y,Ed}$	-0.06 kN
	Shear Force					$V_{z,Ed}$	0.22 kN
	Torsional Moment					T_{Ed}	0.00 kNm
	Moment					$M_{y,Ed}$	0.00 kNm
	Moment					$M_{z,Ed}$	0.00 kNm
Design Ratio							
	Modulus of Elasticity					E	21000.00 kN/cm ²
	Moment of Inertia					I_z	9690.00 cm ⁴
	Effective Member Length					$L_{cr,z}$	4.00 m
	Elastic Flexural Buckling Force					$N_{cr,z}$	12552.30 kN
	Cross-Sectional Area					A	170.90 cm ²
	Yield Strength					f_y	35.50 kN/cm ²
	Slenderness					λ_{z}	0.695
	Axial Force (Compression)					N_{Ed}	2910.15 kN
	Criterion $N_{Ed} / N_{cr,z}$					$\eta_{N,cr}$	0.232
	Buckling Curve					BC_z	c
	Imperfection Factor					α_z	0.490
	Auxiliary Factor					Φ_z	0.863
	Reduction Factor					χ_z	0.728
	Partial Factor					γ_{M1}	1.000
	Flexural Buckling Resistance					$N_{b,z,Rd}$	4414.58 kN
	Design Ratio					η	0.66
Design Formula							
	$N_{Ed} / N_{b,z,Rd} = 0.66 \leq 1$ (6.46)						
2	HEB 360 - column short facade 7	0.00	CO165	0.81	≤ 1	ST312)	Stability analysis - Flexural buckling about z-axis acc. to 6.3.1.1 and 6.3.1.2
Design Internal Forces							
	Axial Force					N_{Ed}	-3763.03 kN
	Shear Force					$V_{y,Ed}$	-0.07 kN
	Shear Force					$V_{z,Ed}$	0.27 kN
	Torsional Moment					T_{Ed}	0.00 kNm
	Moment					$M_{y,Ed}$	0.00 kNm
	Moment					$M_{z,Ed}$	0.00 kNm
Design Ratio							
	Modulus of Elasticity					E	21000.00 kN/cm ²
	Moment of Inertia					I_z	10140.00 cm ⁴
	Effective Member Length					$L_{cr,z}$	4.00 m
	Elastic Flexural Buckling Force					$N_{cr,z}$	13135.20 kN
	Cross-Sectional Area					A	180.60 cm ²
	Yield Strength					f_y	35.50 kN/cm ²
	Slenderness					λ_{z}	0.699
	Axial Force (Compression)					N_{Ed}	3763.03 kN
	Criterion $N_{Ed} / N_{cr,z}$					$\eta_{N,cr}$	0.286
	Buckling Curve					BC_z	c
	Imperfection Factor					α_z	0.490
	Auxiliary Factor					Φ_z	0.866
	Reduction Factor					χ_z	0.726
	Partial Factor					γ_{M1}	1.000
	Flexural Buckling Resistance					$N_{b,z,Rd}$	4651.59 kN
	Design Ratio					η	0.81
Design Formula							
	$N_{Ed} / N_{b,z,Rd} = 0.81 \leq 1$ (6.46)						
3	HEM 300 - inner column 37	0.00	CO165	0.59	≤ 1	ST312)	Stability analysis - Flexural buckling about z-axis acc. to 6.3.1.1 and 6.3.1.2

Design by Cross-Section

Sect. No.	Member No.	Location x [m]	LC/CO/ RC	Design	Equation No.	Description
Design Internal Forces						
					N_{Ed}	-4754.39 kN
					$V_{y,Ed}$	-0.10 kN
					$V_{z,Ed}$	0.40 kN
					T_{Ed}	0.00 kNm
					$M_{y,Ed}$	0.00 kNm
					$M_{z,Ed}$	0.00 kNm
Design Ratio						
					E	21000.00 kN/cm ²
					I_z	19400.00 cm ⁴
					$L_{cr,z}$	4.00 m
					$N_{cr,z}$	25130.50 kN
					A	303.10 cm ²
					f_y	35.50 kN/cm ²
					λ_{z}	0.654
					N_{Ed}	4754.39 kN
					$\eta_{N,cr}$	0.189
					BC_z	c
					α_z	0.490
					Φ_z	0.825
					χ_z	0.753
					γ_{M1}	1.000
					$N_{b,z,Rd}$	8099.38 kN
					η	0.59
Design Formula						
						$N_{Ed} / N_{b,z,Rd} = 0.59 \leq 1$ (6.46)
4	HEM 300 - inner core column					
	55	0.00	CO165	0.60	≤ 1	ST312) Stability analysis - Flexural buckling about z-axis acc. to 6.3.1.1 and 6.3.1.2
Design Internal Forces						
					N_{Ed}	-4887.57 kN
					$V_{y,Ed}$	-0.09 kN
					$V_{z,Ed}$	0.39 kN
					T_{Ed}	0.00 kNm
					$M_{y,Ed}$	0.00 kNm
					$M_{z,Ed}$	0.00 kNm
Design Ratio						
					E	21000.00 kN/cm ²
					I_z	19400.00 cm ⁴
					$L_{cr,z}$	4.00 m
					$N_{cr,z}$	25130.50 kN
					A	303.10 cm ²
					f_y	35.50 kN/cm ²
					λ_{z}	0.654
					N_{Ed}	4887.57 kN
					$\eta_{N,cr}$	0.194
					BC_z	c
					α_z	0.490
					Φ_z	0.825
					χ_z	0.753
					γ_{M1}	1.000
					$N_{b,z,Rd}$	8099.38 kN
					η	0.60
Design Formula						
						$N_{Ed} / N_{b,z,Rd} = 0.60 \leq 1$ (6.46)
6	IPE 550 - inner beam X					
	5054	6.00	CO165	0.58	≤ 1	CS181) Cross-section check - Bending, shear and axial force acc. to 6.2.9.1
Design Internal Forces						
					N_{Ed}	1736.40 kN
					$V_{y,Ed}$	0.00 kN

■ Design by Cross-Section

Sect. No.	Member No.	Location x [m]	LC/CO/ RC	Design	Equation No.	Description
					$V_{z,Ed}$	0.00 kN
					T_{Ed}	0.03 kNm
					$M_{y,Ed}$	273.97 kNm
					$M_{z,Ed}$	0.00 kNm
					Design Ratio	
					Moment $M_{y,Ed}$	273.97 kNm
					Yield Strength f_y	35.50 kN/cm ²
					Partial Factor γ_{M0}	1.000
					Moment Resistance $M_{pl,y,Rd}$	989.39 kNm
					Shear Force $V_{z,Ed}$	0.00 kN
					Effective Shear Area $A_{v,z}$	72.33 cm ²
					Shear Force Resistance $V_{pl,z,Rd}$	1482.37 kN
					Criterion $V_{z,Ed} / V_{pl,z,Rd}$	0.000
					Axial Force N_{Ed}	1736.40 kN
					Cross-Sectional Area A	134.40 cm ²
					Axial Force Resistance $N_{pl,Rd}$	4771.20 kN
					Web Heights h_w	515.6 mm
					Web Thickness t_w	11.1 mm
					Criterion 1 n	0.364
					Criterion 2 n_w	0.855
					Flange Width b	210.0 mm
					Flange Thickness t_f	17.2 mm
					Factor a	0.463
					Moment Resistance $M_{N,pl,y,Rd}$	818.62 kNm
					Design Component for M_y η_{My}	0.33
					Design Ratio η	0.58
					Design Formula	
					$M_{y,Ed} / M_{N,y,Rd} = 0.58 \leq 1$ (6.31)	
9	IPE 600 - inner beam Y					
	2023	0.00	CO165	1.15	> 1	CS181) Cross-section check - Bending, shear and axial force acc. to 6.2.9.1
					Design Internal Forces	
					Axial Force N_{Ed}	4562.56 kN
					Shear Force $V_{y,Ed}$	0.00 kN
					Shear Force $V_{z,Ed}$	-199.08 kN
					Torsional Moment T_{Ed}	0.11 kNm
					Moment $M_{y,Ed}$	535.74 kNm
					Moment $M_{z,Ed}$	0.00 kNm
					Design Ratio	
					Moment $M_{y,Ed}$	535.74 kNm
					Yield Strength f_y	35.50 kN/cm ²
					Partial Factor γ_{M0}	1.000
					Moment Resistance $M_{pl,y,Rd}$	1246.76 kNm
					Shear Force $V_{z,Ed}$	199.08 kN
					Effective Shear Area $A_{v,z}$	83.80 cm ²
					Shear Force Resistance $V_{pl,z,Rd}$	1717.56 kN
					Criterion $V_{z,Ed} / V_{pl,z,Rd}$	0.116
					Axial Force N_{Ed}	4562.56 kN
					Cross-Sectional Area A	156.00 cm ²
					Axial Force Resistance $N_{pl,Rd}$	5538.00 kN
					Web Heights h_w	562.0 mm
					Web Thickness t_w	12.0 mm
					Criterion 1 n	0.824
					Criterion 2 n_w	1.906
					Flange Width b	220.0 mm
					Flange Thickness t_f	19.0 mm
					Factor a	0.464
					Moment Resistance $M_{N,pl,y,Rd}$	285.96 kNm
					Design Component for M_y η_{My}	1.87
					Design Ratio η	1.15
					Design Formula	
					$M_{y,Ed} / M_{N,y,Rd} = 1.15 > 1$ (6.31)	

A.3.8 A1s/ A2 connection verification - numerical approach (scenario 1)

■ Design by Cross-Section

Sect. No.	Member No.	Location x [m]	LC/CO/ RC	Design		Equation No.	Description
1	HEB 340 - column long facade	1	2.00	CO165	0.58	≤ 1	ST364) Stability analysis - Bending and compression acc. to 6.3.3, Method 2
Design Internal Forces							
	Axial Force					N_{Ed}	-2472.97 kN
	Shear Force					$V_{y,Ed}$	0.14 kN
	Shear Force					$V_{z,Ed}$	3.80 kN
	Torsional Moment					T_{Ed}	0.00 kNm
	Moment					$M_{y,Ed}$	7.94 kNm
	Moment					$M_{z,Ed}$	-0.33 kNm
Design Ratio							
	Elastic Critical Load for Torsional Buckling					$N_{cr,T}$	19380.70 kN
	Slenderness					$\lambda_{,T}$	0.560
	Buckling Curve					BC_z	c
	Imperfection Factor					α_z	0.490
	Auxiliary Factor					Φ_T	0.745
	Reduction Factor					χ_T	0.809
	Modulus of Elasticity					E	21000.00 kN/cm ²
	Moment of Inertia					I_y	36660.00 cm ⁴
	Effective Member Length					$L_{cr,y}$	4.00 m
	Elastic Flexural Buckling Force					$N_{cr,y}$	47488.80 kN
	Cross-Sectional Area					A	170.90 cm ²
	Yield Strength					f_y	35.50 kN/cm ²
	Slenderness					$\lambda_{,y}$	0.357
	Buckling Curve					BC_y	b
	Imperfection Factor					α_y	0.340
	Auxiliary Factor					Φ_y	0.591
	Reduction Factor					χ_y	0.943
	Moment of Inertia					I_z	9690.00 cm ⁴
	Effective Member Length					$L_{cr,z}$	4.00 m
	Elastic Flexural Buckling Force					$N_{cr,z}$	12552.30 kN
	Slenderness					$\lambda_{,z}$	0.695
	Buckling Curve					BC_z	c
	Imperfection Factor					α_z	0.490
	Auxiliary Factor					Φ_z	0.863
	Reduction Factor					χ_z	0.728
	Section Height					h	340.0 mm
	Section Width					b	300.0 mm
	Criterion					h/b	1.13
	Buckling Curve					BC_{LT}	b
	Imperfection Factor					α_{LT}	0.340
	Shear Modulus					G	8076.92 kN/cm ²
	Length Factor					k_z	1.000
	Length Factor					k_w	1.000
	Length					L	4.00 m
	Warping Constant of Cross-Section					I_w	2454000.00 cm ⁶
	Torsional Constant					I_t	257.20 cm ⁴
	Elastic Critical Moment for Lateral-Torsional Buckling					M_{cr}	5395.01 kNm
	Section Modulus					W_y	2408.00 cm ³
	Slenderness					$\lambda_{,LT}$	0.398
	Parameter					$\lambda_{,LT,0}$	0.400
	Parameter					β	0.750
	Auxiliary Factor					Φ_{LT}	0.559
	Reduction Factor					χ_{LT}	1.000
	Correction Factor					k_c	0.860
	Modification Factor					f	0.953
	Reduction Factor					$\chi_{LT,mod}$	1.000
	Structure type about y-axis					Type	Non-sway
	Moment Distribution					Diagr M_y	3) Max in Span
	Moment Factor					ψ_y	0.000
	Moment					$M_{h,y}$	0.20 kNm
	Moment					$M_{s,y}$	0.84 kNm
	Ratio $M_{h,y} / M_{s,y}$					$\alpha_{h,y}$	0.237
	Load Type					Load z	Sing. Load

Design by Cross-Section

Sect. No.	Member No.	Location x [m]	LC/CO/ RC	Design	Equation No.	Description
					BC_{LT}	b
					α_{LT}	0.340
					G	8076.92 kN/cm ²
					k_z	1.000
					k_w	1.000
					L	4.00 m
					I_w	4386000.00 cm ⁶
					I_t	1408.00 cm ⁴
					M_{cr}	17179.30 kNm
					W_y	4078.00 cm ³
					$\lambda_{c,LT}$	0.290
					$\lambda_{c,LT,0}$	0.400
					β	0.750
					Φ_{LT}	0.513
					χ_{LT}	1.000
					k_c	0.632
					f	0.912
					$\chi_{LT,mod}$	1.000
					Type	Non-sway
					Diagr M_y	2) Max on Edge
					ψ_y	0.000
					$M_{h,y}$	-0.78 kNm
					$M_{s,y}$	0.56 kNm
					$\alpha_{s,y} / M_{h,y}$	-0.717
					Load z	Sing. Load
					C_{my}	0.573
					Type	Non-sway
					Diagr M_z	3) Max in Span
					ψ_z	0.000
					$M_{h,z}$	0.23 kNm
					$M_{s,z}$	0.35 kNm
					$\alpha_{h,z} / M_{s,z}$	0.659
					Load y	Sing. Load
					C_{mz}	0.966
					Diagr $M_{y,LT}$	2) Max on Edge
					$\psi_{y,LT}$	0.000
					$M_{h,y,LT}$	-0.78 kNm
					$M_{s,y,LT}$	0.56 kNm
					$\alpha_{s,y,LT} / M_{h,y,LT}$	-0.717
					Load z	Sing. Load
					$C_{m,LT}$	0.573
					Component	Torsion. Weak
					k_{yy}	0.627
					k_{yz}	0.852
					k_{zy}	0.865
					k_{zz}	1.421
					N_{Ed}	5383.44 kN
					A_g	303.10 cm ²
					N_{Rk}	10760.10 kN
					γ_{M1}	1.000
					η_{Ny}	0.53
					η_{Nz}	0.66
					$M_{y,Ed}$	2.76 kNm
					W_y	4078.00 cm ³
					$M_{y,Rk}$	1447.69 kNm
					$\eta_{My,lim}$	0.010
					$\eta_{Mpl,y,Rd}$	0.002
					η_{My}	0.00
					$M_{z,Ed}$	12.09 kNm
					W_z	1913.00 cm ³
					$M_{z,Rk}$	679.12 kNm
					η_{Mz}	0.02
					η_1	0.55

■ Design by Cross-Section

Sect. No.	Member No.	Location x [m]	LC/CO/ RC	Design	Equation No.	Description
					C_{my}	0.924
					Type	Non-sway
					Diagr M_z	3) Max in Span
					ψ_z	0.001
					$M_{h,z}$	0.00 kNm
					$M_{s,z}$	-0.11 kNm
					$\alpha_{h,z}$	0.004
					Load y	Sing. Load
					C_{mz}	0.900
					Diagr $M_{y,LT}$	3) Max in Span
					$\psi_{y,LT}$	0.000
					$M_{h,y,LT}$	0.20 kNm
					$M_{s,y,LT}$	0.84 kNm
					$\alpha_{h,y,LT}$	0.237
					Load z	Sing. Load
					C_{mLT}	0.924
					Component	Torsion. Weak
					k_{yy}	0.987
					k_{yz}	0.779
					k_{zy}	0.942
					k_{zz}	1.299
					N_{Ed}	2472.97 kN
					A_i	170.90 cm ²
					N_{Rk}	6066.95 kN
					γ_{M1}	1.000
					η_{Ny}	0.43
					η_{Nz}	0.56
					$M_{y,Ed}$	14.86 kNm
					W_y	2408.00 cm ³
					$M_{y,Rk}$	854.84 kNm
					η_{My}	0.02
					$M_{z,Ed}$	0.50 kNm
					W_z	985.70 cm ³
					$M_{z,Rk}$	349.92 kNm
					$\eta_{Mz,lim}$	0.010
					$\eta_{Mpl,z,Rd}$	0.001
					η_{Mz}	0.00
					η_1	0.45
					η_2	0.58
					Design Formula	
					$N_{Ed} / (\chi_y N_{Rk} / \gamma_{M1}) + k_{yy} M_{y,Ed} / (\chi_{LT} M_{y,Rk} / \gamma_{M1}) + k_{yz} M_{z,Ed} / (M_{z,Rk} / \gamma_{M1}) = 0.45 \leq 1$ (6.61)	
					$N_{Ed} / (\chi_z N_{Rk} / \gamma_{M1}) + k_{zy} M_{y,Ed} / (\chi_{LT} M_{y,Rk} / \gamma_{M1}) + k_{zz} M_{z,Ed} / (M_{z,Rk} / \gamma_{M1}) = 0.58 \leq 1$ (6.62)	
2	HEB 360 - column short facade					
	10103	0.00	CO165	0.77	≤ 1	ST364) Stability analysis - Bending and compression acc. to 6.3.3, Method 2
						Design Internal Forces
					N_{Ed}	-3520.96 kN
					$V_{y,Ed}$	-0.53 kN
					$V_{z,Ed}$	-3.58 kN
					T_{Ed}	0.00 kNm
					$M_{y,Ed}$	-7.53 kNm
					$M_{z,Ed}$	1.37 kNm
						Design Ratio
					$N_{cr,T}$	20647.60 kN
					$\lambda_{z,T}$	0.557
					BC_z	c
					α_z	0.490
					ϕ_T	0.743
					χ_T	0.810
					E	21000.00 kN/cm ²
					I_y	43190.00 cm ⁴
					$L_{cr,y}$	4.00 m

■ Design by Cross-Section

Sect. No.	Member No.	Location x [m]	LC/CO/ RC	Design	Equation No.	Description	
					η_2	0.69	
						Design Formula $N_{Ed} / (\chi_y N_{Rk} / \gamma_{M1}) + k_{yy} M_{y,Ed} / (\chi_{LT} M_{y,Rk} / \gamma_{M1}) + k_{yz} M_{z,Ed} / (M_{z,Rk} / \gamma_{M1}) = 0.55 \leq 1$ (6.61) $N_{Ed} / (\chi_z N_{Rk} / \gamma_{M1}) + k_{zy} M_{y,Ed} / (\chi_{LT} M_{y,Rk} / \gamma_{M1}) + k_{zz} M_{z,Ed} / (M_{z,Rk} / \gamma_{M1}) = 0.69 \leq 1$ (6.62)	
5	IPE 500 - beam short facade	5000	6.00	CO165	0.59	≤ 1	CS181) Cross-section check - Bending, shear and axial force acc. to 6.2.9.1
						Design Internal Forces Axial Force N_{Ed} 1615.53 kN Shear Force $V_{y,Ed}$ 0.00 kN Shear Force $V_{z,Ed}$ 0.00 kN Torsional Moment T_{Ed} 0.00 kNm Moment $M_{y,Ed}$ 194.13 kNm Moment $M_{z,Ed}$ 0.00 kNm Design Ratio Moment $M_{y,Ed}$ 194.13 kNm Yield Strength f_y 35.50 kN/cm ² Partial Factor γ_{M0} 1.000 Moment Resistance $M_{pl,y,Rd}$ 778.87 kNm Shear Force $V_{z,Ed}$ 0.00 kN Effective Shear Area $A_{v,z}$ 59.85 cm ² Shear Force Resistance $V_{pl,z,Rd}$ 1226.72 kN Criterion $V_{z,Ed} / V_{pl,z,Rd}$ v_z 0.000 Axial Force N_{Ed} 1615.53 kN Cross-Sectional Area A 115.50 cm ² Axial Force Resistance $N_{pl,Rd}$ 4100.25 kN Web Heights h_w 468.0 mm Web Thickness t_w 10.2 mm Criterion 1 n 0.394 Criterion 2 n_w 0.953 Flange Width b 200.0 mm Flange Thickness t_f 16.0 mm Factor a 0.446 Moment Resistance $M_{N,pl,y,Rd}$ 607.41 kNm Design Component for M_y η_{My} 0.32 Design Ratio η 0.59 Design Formula $M_{y,Ed} / M_{N,y,Rd} = 0.59 \leq 1$ (6.31)	

■ Design by Cross-Section

Sect. No.	Member No.	Location x [m]	LC/CO/ RC	Design	Equation No.	Description
					k_{zy}	0.907
					k_{zz}	1.443
					N_{Ed}	3520.96 kN
					A_i	180.60 cm ²
					N_{Rk}	6411.30 kN
					γ_{M1}	1.000
					η_{Ny}	0.58
					η_{Nz}	0.76
					$M_{y,Ed}$	13.91 kNm
					W_y	2683.00 cm ³
					$M_{y,Rk}$	952.47 kNm
					η_{My}	0.01
					$M_{z,Ed}$	1.88 kNm
					W_z	1032.00 cm ³
					$M_{z,Rk}$	366.36 kNm
					$\eta_{Mz,lim}$	0.010
					$\eta_{Mplz,Rd}$	0.005
					η_{Mz}	0.00
					Design 1	0.59
					Design 2	0.77
					Design Formula	
					$N_{Ed} / (\chi_y N_{Rk} / \gamma_{M1}) + k_{zy} M_{y,Ed} / (\chi_{LT} M_{y,Rk} / \gamma_{M1}) + k_{zz} M_{z,Ed} / (M_{z,Rk} / \gamma_{M1}) = 0.59 \leq 1$ (6.61)	
					$N_{Ed} / (\chi_z N_{Rk} / \gamma_{M1}) + k_{zy} M_{y,Ed} / (\chi_{LT} M_{y,Rk} / \gamma_{M1}) + k_{zz} M_{z,Ed} / (M_{z,Rk} / \gamma_{M1}) = 0.77 \leq 1$ (6.62)	
3	HEM 300 - inner column					
	31	1.20	CO165	0.69	≤ 1	ST364
						Stability analysis - Bending and compression acc. to 6.3.3, Method 2
					Design Internal Forces	
					N_{Ed}	-5383.44 kN
					$V_{y,Ed}$	-4.02 kN
					$V_{z,Ed}$	-0.75 kN
					T_{Ed}	0.00 kNm
					$M_{y,Ed}$	-0.92 kNm
					$M_{z,Ed}$	5.15 kNm
					Design Ratio	
					$N_{cr,T}$	65763.70 kN
					λ_{T}	4.04
					BC_z	c
					α_z	0.490
					Φ_T	0.632
					Reduction Factor	0.895
					χ_T	
					E	21000.00 kN/cm ²
					I_y	59200.00 cm ⁴
					Effective Member Length	4.00 m
					$N_{cr,y}$	76686.80 kN
					Cross-Sectional Area	A
					f_y	303.10 cm ²
					Yield Strength	35.50 kN/cm ²
					λ_{-y}	0.375
					Buckling Curve	BC_y
					α_y	b
					Imperfection Factor	0.340
					Auxiliary Factor	Φ_y
					Reduction Factor	0.600
					χ_y	0.936
					Moment of Inertia	I_z
					Effective Member Length	19400.00 cm ⁴
					$N_{cr,z}$	4.00 m
					Elastic Flexural Buckling Force	25130.50 kN
					Slenderness	λ_{-z}
					Buckling Curve	0.654
					BC_z	c
					Imperfection Factor	α_z
					Auxiliary Factor	0.490
					Reduction Factor	Φ_z
					χ_z	0.825
					Section Height	0.753
					h	340.0 mm
					Section Width	b
					Criterion	310.0 mm
					h/b	1.10

Design by Cross-Section

Sect. No.	Member No.	Location x [m]	LC/CO/ RC	Design	Equation No.	Description
					$N_{cr,y}$	55947.70 kN
					A	180.60 cm ²
					f_y	35.50 kN/cm ²
					λ_{-y}	0.339
					BC _y	b
					α_y	0.340
					Φ_y	0.581
					χ_y	0.950
					I_z	10140.00 cm ⁴
					$L_{-cr,z}$	4.00 m
					$N_{cr,z}$	13135.20 kN
					λ_{-z}	0.699
					BC _z	c
					α_z	0.490
					Φ_z	0.866
					χ_z	0.726
					h	360.0 mm
					b	300.0 mm
					h/b	1.20
					BC _{LT}	b
					α_{LT}	0.340
					G	8076.92 kN/cm ²
					k_z	1.000
					k_w	1.000
					L	4.00 m
					I_w	2883000.00 cm ⁶
					I_t	292.50 cm ⁴
					M_{cr}	6483.03 kNm
					W_y	2683.00 cm ³
					λ_{-LT}	0.383
					$\lambda_{-LT,0}$	0.400
					β	0.750
					Φ_{LT}	0.552
					χ_{LT}	1.000
					k_c	0.860
					f	0.954
					$\chi_{LT,mod}$	1.000
					Type	Non-sway
					Diagr M _y	3) Max in Span
					Ψ_y	0.000
					M _{h,y}	-0.17 kNm
					M _{s,y}	0.20 kNm
					$\alpha_{h,y}$	-0.811
					Load z	Sing. Load
					C _{my}	0.819
					Type	Non-sway
					Diagr M _z	3) Max in Span
					Ψ_z	0.005
					M _{h,z}	0.00 kNm
					M _{s,z}	0.10 kNm
					$\alpha_{h,z}$	0.002
					Load y	Sing. Load
					C _{mz}	0.900
					Diagr M _{y,LT}	3) Max in Span
					$\Psi_{y,LT}$	0.000
					M _{h,y,LT}	-0.17 kNm
					M _{s,y,LT}	0.20 kNm
					$\alpha_{h,y,LT}$	-0.811
					Load z	Sing. Load
					C _{mLT}	0.819
					Component	Torsion. Weak
					k_{yy}	0.885
					k_{yz}	0.866

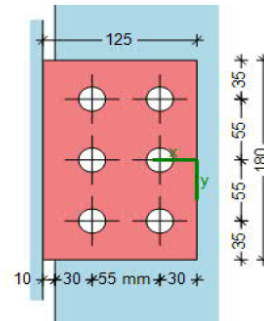
A.3.9 A1s/ A2 connection verification - numerical approach (scenario 1)

Resistance to tying forces

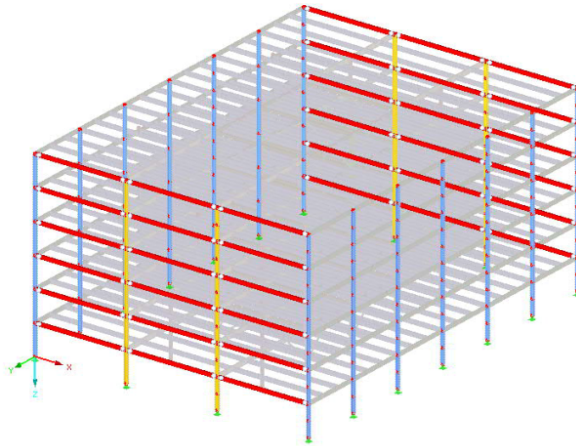
A-1 strong axis (IPE 500 to HEB 340)

Loads	$V_{z,Ad}$	63 kN	(numerical approach)
	N_T	1620 kN	(numerical approach)
safety factor	γ_{Mu}	1,10	
column		HEB 340	
	f_y	355 N/mm ²	h 340 mm
	f_u	490 N/mm ²	b 300 mm
			t_w 12 mm
			t_f 21,5 mm
beam		IPE 500	
	f_y	355 N/mm ²	h 500 mm
	f_u	490 N/mm ²	b 200 mm
			t_w 10,2 mm
			t_f 16 mm
			h_w 426 mm
fin plate	S355		
	f_y	355 N/mm ²	h 180 mm
	f_u	490 N/mm ²	b 125 mm
			t 10 mm
			gap 10 mm
bolts	10.9		
	f_{ub}	1000 N/mm ²	d 20 mm
	α_v	0,5	d_o 22 mm
			A_s 2,45 cm ²
bolt pattern			
columns	n_2	2	rows n_1 3
vertical pitch	p_1	55 mm	hor. Pitch p_2 55 mm
n Bolts	n	6	vert. edge e_1 35 mm
			hor. edge e_2 30 mm
weld	a	6 mm	

Component	μ
1) Bolts in shear	2,43
2) Fin plate in bearing	3,71
3) Fin plate in tension (gross section)	2,02
4) Fin plate in tension (net section)	3,54
5) Beam web in bearing	3,63
6) Beam in tension (gross section)	0,84
7) Beam in tension (net section)	1,10
8) Supporting member in bending	0,00



2) Fin plate in bearing 3,71



Notice: Ductility and plastic redistribution allowance already verified with COP

1) Bolts in shear

A_s	2,45 cm ²
n	6
α_v	0,5
f_{ub}	1000 N/mm ²
$F_{V,Rd}$	111,4 kN
$N_{U,1}$	668,2 kN
N_{Ed}	1620,0 kN
V_{Ed}	63 kN
F_{Ed}	1621,2 kN
μ	2,43

2) Fin plate in bearing

d_0	22 mm		
e_1	35 mm	N_{Ed}	1620,0 kN
e_2	30 mm	V_{Ed}	63 kN
p_1	55 mm	μ	3,71
p_2	55 mm		

Vertical direction

α_b	0,53
k_1	1,80
$F_{y,b,Rd}$	85,0 kN
$N_{u,2,y}$	510,2 kN

Horizontal direction

α_b	0,45
k_1	1,80
$F_{y,b,Rd}$	72,9 kN
$N_{u,2,y}$	437,4 kN

3) Fin plate in tension (gross section)

t_p	10 mm
h_p	180 mm
f_{up}	490 mm
$N_{u,3}$	801,8 kN
N_{Ed}	1620 kN
μ	2,02

4) Fin plate in tension (net section)

d_0	22 mm
$A_{net,p}$	1140 mm ²
$N_{u,4}$	457,0 kN
N_{Ed}	1620 kN
μ	3,54

5) Beam web in bearing

d_0	22 mm		
e_1	- mm	N_{Ed}	1620 kN
e_{2b}	30 mm	V_{Ed}	63 kN
p_1	55 mm	μ	3,63
p_2	55 mm		

Vertical direction

α_b	0,58
k_1	1,80
$F_{y,b,Rd}$	95,4 kN
$N_{u,2,y}$	572,5 kN

Horizontal direction

α_b	0,45
k_1	1,80
$F_{y,b,Rd}$	74,35 kN
$N_{u,2,y}$	446,10 kN

6) Beam in tension (gross section)

t_w	10,2 mm
h_w	426 mm
f_u	490 mm
$N_{u,6}$	1935,6 kN
N_{Ed}	1620 kN
μ	0,84

7) Beam in tension (net section)

d_0	22 mm
$A_{net,p}$	3672 mm ²
$N_{u,7}$	1472,1 kN
N_{Ed}	1620 kN
μ	1,10

8) Supporting member in bending

$N_{u,8}$	∞ kN
-----------	-------------

A.3.10 Redesign column verifications – numerical model – scenario 1

Design by Cross-Section

Sect. No.	Member No.	Location x [m]	LC/CO/ RC	Design		Equation No.	Description
1	HEB 340 - column long facade						
	25	0.00	CO165	0.65	≤ 1	ST312)	Stability analysis - Flexural buckling about z-axis acc. to 6.3.1.1 and 6.3.1.2
Design Internal Forces							
	Axial Force					N_{Ed}	-2862.38 kN
	Shear Force					$V_{y,Ed}$	-0.06 kN
	Shear Force					$V_{z,Ed}$	0.23 kN
	Torsional Moment					T_{Ed}	0.00 kNm
	Moment					$M_{y,Ed}$	0.00 kNm
	Moment					$M_{z,Ed}$	0.00 kNm
Design Ratio							
	Modulus of Elasticity					E	21000.00 kN/cm ²
	Moment of Inertia					I_z	9690.00 cm ⁴
	Effective Member Length					$L_{cr,z}$	4.00 m
	Elastic Flexural Buckling Force					$N_{cr,z}$	12552.30 kN
	Cross-Sectional Area					A	170.90 cm ²
	Yield Strength					f_y	35.50 kN/cm ²
	Slenderness					λ_{z}	0.695
	Axial Force (Compression)					N_{Ed}	2862.38 kN
	Criterion $N_{Ed} / N_{cr,z}$					$\eta_{N,cr}$	0.228
	Buckling Curve					BC_z	c
	Imperfection Factor					α_z	0.490
	Auxiliary Factor					Φ_z	0.863
	Reduction Factor					χ_z	0.728
	Partial Factor					γ_{M1}	1.000
	Flexural Buckling Resistance					$N_{b,z,Rd}$	4414.58 kN
	Design Ratio					η	0.65
Design Formula							
	$N_{Ed} / N_{b,z,Rd} = 0.65 \leq 1$ (6.46)						
2	HEB 360 - column short facade						
	7	0.00	CO165	0.82	≤ 1	ST312)	Stability analysis - Flexural buckling about z-axis acc. to 6.3.1.1 and 6.3.1.2
Design Internal Forces							
	Axial Force					N_{Ed}	-3827.77 kN
	Shear Force					$V_{y,Ed}$	-0.07 kN
	Shear Force					$V_{z,Ed}$	0.28 kN
	Torsional Moment					T_{Ed}	0.00 kNm
	Moment					$M_{y,Ed}$	0.00 kNm
	Moment					$M_{z,Ed}$	0.00 kNm
Design Ratio							
	Modulus of Elasticity					E	21000.00 kN/cm ²
	Moment of Inertia					I_z	10140.00 cm ⁴
	Effective Member Length					$L_{cr,z}$	4.00 m
	Elastic Flexural Buckling Force					$N_{cr,z}$	13135.20 kN
	Cross-Sectional Area					A	180.60 cm ²
	Yield Strength					f_y	35.50 kN/cm ²
	Slenderness					λ_{z}	0.699
	Axial Force (Compression)					N_{Ed}	3827.77 kN
	Criterion $N_{Ed} / N_{cr,z}$					$\eta_{N,cr}$	0.291
	Buckling Curve					BC_z	c
	Imperfection Factor					α_z	0.490
	Auxiliary Factor					Φ_z	0.866
	Reduction Factor					χ_z	0.726
	Partial Factor					γ_{M1}	1.000
	Flexural Buckling Resistance					$N_{b,z,Rd}$	4651.59 kN
	Design Ratio					η	0.82
Design Formula							
	$N_{Ed} / N_{b,z,Rd} = 0.82 \leq 1$ (6.46)						
3	HEM 300 - inner column						
	37	0.00	CO165	0.58	≤ 1	ST312)	Stability analysis - Flexural buckling about z-axis acc. to 6.3.1.1 and 6.3.1.2

Design by Cross-Section

Sect. No.	Member No.	Location x [m]	LC/CO/ RC	Design	Equation No.	Description
						Design Internal Forces
					N_{Ed}	-4714.10 kN
					$V_{y,Ed}$	-0.10 kN
					$V_{z,Ed}$	0.41 kN
					T_{Ed}	0.00 kNm
					$M_{y,Ed}$	0.00 kNm
					$M_{z,Ed}$	0.00 kNm
						Design Ratio
					E	21000.00 kN/cm ²
					I_z	19400.00 cm ⁴
					$L_{cr,z}$	4.00 m
					$N_{cr,z}$	25130.50 kN
					A	303.10 cm ²
					f_y	35.50 kN/cm ²
					λ_{z}	0.654
					N_{Ed}	4714.10 kN
					Criterion $N_{Ed} / N_{cr,z}$	0.188
					Buckling Curve	BC _z c
					Imperfection Factor	α_z 0.490
					Auxiliary Factor	Φ_z 0.825
					Reduction Factor	χ_z 0.753
					Partial Factor	γ_{M1} 1.000
					Flexural Buckling Resistance	$N_{b,z,Rd}$ 8099.38 kN
					Design Ratio	η 0.58
						Design Formula
						$N_{Ed} / N_{b,z,Rd} = 0.58 \leq 1$ (6.46)
4	HEM 300 - inner core column					
	55	0.00	CO165	0.61	≤ 1	ST312) Stability analysis - Flexural buckling about z-axis acc. to 6.3.1.1 and 6.3.1.2
						Design Internal Forces
					N_{Ed}	-4941.80 kN
					$V_{y,Ed}$	-0.09 kN
					$V_{z,Ed}$	0.40 kN
					T_{Ed}	0.00 kNm
					$M_{y,Ed}$	0.00 kNm
					$M_{z,Ed}$	0.00 kNm
						Design Ratio
					E	21000.00 kN/cm ²
					I_z	19400.00 cm ⁴
					$L_{cr,z}$	4.00 m
					$N_{cr,z}$	25130.50 kN
					A	303.10 cm ²
					f_y	35.50 kN/cm ²
					λ_{z}	0.654
					N_{Ed}	4941.80 kN
					Criterion $N_{Ed} / N_{cr,z}$	0.197
					Buckling Curve	BC _z c
					Imperfection Factor	α_z 0.490
					Auxiliary Factor	Φ_z 0.825
					Reduction Factor	χ_z 0.753
					Partial Factor	γ_{M1} 1.000
					Flexural Buckling Resistance	$N_{b,z,Rd}$ 8099.38 kN
					Design Ratio	η 0.61
						Design Formula
						$N_{Ed} / N_{b,z,Rd} = 0.61 \leq 1$ (6.46)
6	IPE 550 - inner beam X					
	5054	6.00	CO165	0.56	≤ 1	CS181) Cross-section check - Bending, shear and axial force acc. to 6.2.9.1
						Design Internal Forces
					N_{Ed}	1658.01 kN
					$V_{y,Ed}$	0.00 kN

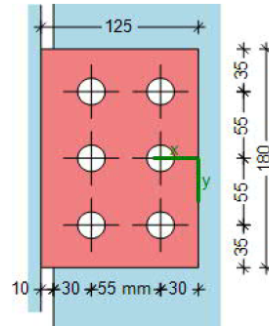
Design by Cross-Section

Sect. No.	Member No.	Location x [m]	LC/CO/ RC	Design	Equation No.	Description
					$V_{z,Ed}$	0.00 kN
					T_{Ed}	0.03 kNm
					$M_{y,Ed}$	275.96 kNm
					$M_{z,Ed}$	0.00 kNm
					Design Ratio	
					Moment $M_{y,Ed}$	275.96 kNm
					Yield Strength f_y	35.50 kN/cm ²
					Partial Factor γ_{M0}	1.000
					Moment Resistance $M_{pl,y,Rd}$	989.39 kNm
					Shear Force $V_{z,Ed}$	0.00 kN
					Effective Shear Area $A_{v,z}$	72.33 cm ²
					Shear Force Resistance $V_{pl,z,Rd}$	1482.37 kN
					Criterion $V_{z,Ed} / V_{pl,z,Rd}$	0.000
					Axial Force N_{Ed}	1658.01 kN
					Cross-Sectional Area A	134.40 cm ²
					Axial Force Resistance $N_{pl,Rd}$	4771.20 kN
					Web Heights h_w	515.6 mm
					Web Thickness t_w	11.1 mm
					Criterion 1 n	0.348
					Criterion 2 n_w	0.816
					Flange Width b	210.0 mm
					Flange Thickness t_f	17.2 mm
					Factor a	0.463
					Moment Resistance $M_{N,pl,y,Rd}$	839.77 kNm
					Design Component for M_y η_{My}	0.33
					Design Ratio η	0.56
					Design Formula	
					$M_{y,Ed} / M_{N,y,Rd} = 0.56 \leq 1$ (6.31)	
9	IPE 750x137 - inner beam Y					
	2023	0.00	CO165	1.03	> 1	CS181) Cross-section check - Bending, shear and axial force acc. to 6.2.9.1
					Design Internal Forces	
					Axial Force N_{Ed}	4849.97 kN
					Shear Force $V_{y,Ed}$	0.00 kN
					Shear Force $V_{z,Ed}$	-205.71 kN
					Torsional Moment T_{Ed}	0.10 kNm
					Moment $M_{y,Ed}$	564.52 kNm
					Moment $M_{z,Ed}$	0.00 kNm
					Design Ratio	
					Moment $M_{y,Ed}$	564.52 kNm
					Yield Strength f_y	35.50 kN/cm ²
					Partial Factor γ_{M0}	1.000
					Moment Resistance $M_{pl,y,Rd}$	1725.30 kNm
					Shear Force $V_{z,Ed}$	205.71 kN
					Effective Shear Area $A_{v,z}$	99.22 cm ²
					Shear Force Resistance $V_{pl,z,Rd}$	2033.65 kN
					Criterion $V_{z,Ed} / V_{pl,z,Rd}$	0.101
					Axial Force N_{Ed}	4849.97 kN
					Cross-Sectional Area A	174.60 cm ²
					Axial Force Resistance $N_{pl,Rd}$	6198.30 kN
					Web Heights h_w	719.0 mm
					Web Thickness t_w	11.5 mm
					Criterion 1 n	0.782
					Criterion 2 n_w	1.652
					Flange Width b	263.0 mm
					Flange Thickness t_f	17.0 mm
					Factor a	0.488
					Moment Resistance $M_{N,pl,y,Rd}$	496.39 kNm
					Design Component for M_y η_{My}	1.14
					Design Ratio η	1.03
					Design Formula	
					$M_{y,Ed} / M_{N,y,Rd} = 1.03 > 1$ (6.31)	

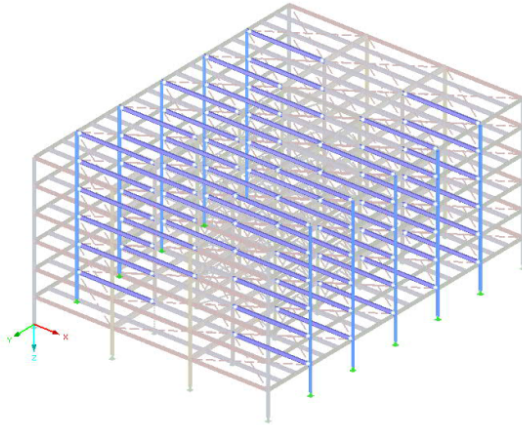
A.3.11 B1/ B3 connection verification - numerical approach ()

Resistance to tying forces		B-1 strong axis (IPE 550 to HEB 340)			
Loads	$V_{z,Ad}$	85 kN	(numerical approach)		
	N_T	1662 kN	(numerical approach)		
safety factor	γ_{Mu}	1,10			
column		HEB 340	h	340 mm	
	f_y	355 N/mm ²	b	300 mm	
	f_u	490 N/mm ²	t_w	12 mm	
			t_f	21,5 mm	
beam		IPE 550	h	550 mm	
	f_y	355 N/mm ²	b	210 mm	
	f_u	490 N/mm ²	t_w	11,1 mm	
			t_f	17,2 mm	
			h_w	467 mm	
fin plate	S355		h	180 mm	
		f_y	355 N/mm ²	b	125 mm
		f_u	490 N/mm ²	t	10 mm
			gap	10 mm	
bolts	10.9		d	20 mm	
		f_{ub}	1000 N/mm ²	d_o	22 mm
		α_v	0,5	A_s	2,45 cm ²
bolt pattern					
columns	n_2	2	rows	n_1	3
vertical pitch	p_1	55 mm	hor. Pitch	p_2	55 mm
n Bolts	n	6	vert. edge	e_1	35 mm
			hor. edge	e_2	30 mm
weld	a	6 mm			

Component	μ
1) Bolts in shear	2,49
2) Fin plate in bearing	3,80
3) Fin plate in tension (gross section)	2,07
4) Fin plate in tension (net section)	3,64
5) Beam web in bearing	3,43
6) Beam in tension (gross section)	0,72
7) Beam in tension (net section)	0,93
8) Supporting member in bending	0,00



2) Fin plate in bearing	3,80
--------------------------------	-------------



Notice: Ductility and plastic redistribution allowance already verified with COP

1) Bolts in shear

A_s	2,45 cm ²
n	6
α_v	0,5
f_{ub}	1000 N/mm ²
$F_{V,Rd}$	111,4 kN
$N_{U,1}$	668,2 kN
N_{Ed}	1662,0 kN
V_{Ed}	85 kN
F_{Ed}	1664,2 kN
μ	2,49

2) Fin plate in bearing

d_0	22 mm		
e_1	35 mm	N_{Ed}	1662,0 kN
e_2	30 mm	V_{Ed}	85 kN
p_1	55 mm	μ	3,80
p_2	55 mm		

Vertical direction

α_b	0,53
k_1	1,80
$F_{y,b,Rd}$	85,0 kN
$N_{u,2,y}$	510,2 kN

Horizontal direction

α_b	0,45
k_1	1,80
$F_{y,b,Rd}$	72,9 kN
$N_{u,2,y}$	437,4 kN

3) Fin plate in tension (gross section)

t_p	10 mm
h_p	180 mm
f_{up}	490 mm
$N_{u,3}$	801,8 kN
N_{Ed}	1662 kN
μ	2,07

4) Fin plate in tension (net section)

d_0	22 mm
$A_{net,p}$	1140 mm ²
$N_{u,4}$	457,0 kN
N_{Ed}	1662 kN
μ	3,64

5) Beam web in bearing

d_0	22 mm		
e_1	- mm	N_{Ed}	1662 kN
e_{2b}	30 mm	V_{Ed}	85 kN
p_1	55 mm	μ	3,43
p_2	55 mm		

Vertical direction

α_b	0,58
k_1	1,80
$F_{y,b,Rd}$	103,8 kN
$N_{u,2,y}$	623,0 kN

Horizontal direction

α_b	0,45
k_1	1,80
$F_{y,b,Rd}$	80,91 kN
$N_{u,2,y}$	485,46 kN

6) Beam in tension (gross section)

t_w	11,1 mm
h_w	467 mm
f_u	490 mm
$N_{u,6}$	2309,1 kN
N_{Ed}	1662 kN
μ	0,72

7) Beam in tension (net section)

d_0	22 mm
$A_{net,p}$	4451,1 mm ²
$N_{u,7}$	1784,5 kN
N_{Ed}	1662 kN
μ	0,93

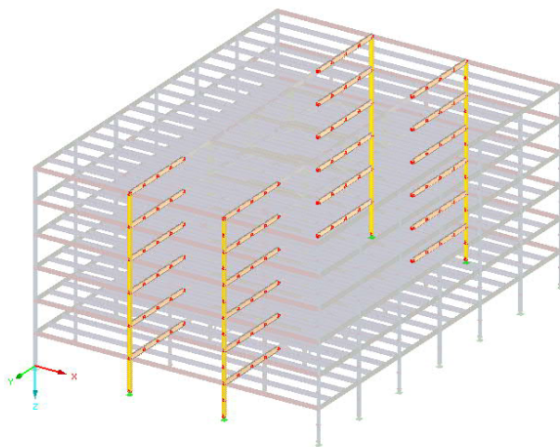
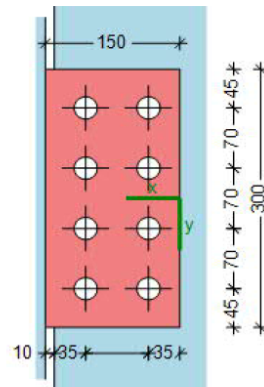
8) Supporting member in bending

$N_{u,8}$	∞ kN
-----------	-------------

A.3.12 C2w connection verification - numerical approach (scenario1)

Resistance to tying forces		C-2 weak axis (IPE 600 to HEB 360)				
Loads	$V_{z,Ad}$	221 kN	(numerical approach)			
	N_T	4852 kN	(numerical approach)			
safety factor	γ_{Mu}	1,10				
column		HEB 360	h	360 mm		
	f_y	355 N/mm ²	b	300 mm		
	f_u	490 N/mm ²	t_w	12,5 mm		
	h_w	261 mm	t_f	22,5 mm		
beam		IPE 600	h	600 mm		
	f_y	355 N/mm ²	b	220 mm		
	f_u	490 N/mm ²	t_w	12 mm		
			t_f	19 mm		
			h_w	514 mm		
fin plate	S355	f_y	355 N/mm ²	h	300 mm	
		f_u	490 N/mm ²	b	150 mm	
			t	10 mm		
			gap	10 mm		
bolts	10.9	f_{ub}	1000 N/mm ²	d	24 mm	
		α_v	0,5	d_o	26 mm	
				A_s	3,53 cm ²	
bolt pattern	columns	n_2	2	rows	n_1	4
	vertical pitch	p_1	70 mm	hor. Pitch	p_2	70 mm
	n Bolts	n	8	vert. edge	e_1	45 mm
				hor. edge	e_2	35 mm
weld	a	6 mm				

Component	μ
1) Bolts in shear	3,78
2) Fin plate in bearing	6,11
3) Fin plate in tension (gross section)	3,63
4) Fin plate in tension (net section)	6,17
5) Beam web in bearing	5,09
6) Beam in tension (gross section)	1,77
7) Beam in tension (net section)	2,46
8) Supporting member in bending	11,20
8) Supporting member in bending	11,20



Notice: Ductility and plastic redistribution allowance already verified with COP

1) Bolts in shear	
A_s	3,53 cm ²
n	8
α_v	0,5
f_{ub}	1000 N/mm ²
$F_{v,Rd}$	160,5 kN
$N_{U,1}$	1283,6 kN
N_{Ed}	4852,0 kN
V_{Ed}	221 kN
F_{Ed}	4857,0 kN
μ	3,78

2) Fin plate in bearing

d_0	26 mm		
e_1	45 mm	N_{Ed}	4852,0 kN
e_2	35 mm	V_{Ed}	221 kN
p_1	70 mm	μ	6,11
p_2	70 mm		

Vertical direction

α_b	0,58
k_1	2,07
$F_{y,b,Rd}$	127,6 kN
$N_{u,2,y}$	1021,0 kN

Horizontal direction

α_b	0,45
k_1	2,07
$F_{y,b,Rd}$	99,3 kN
$N_{u,2,y}$	794,1 kN

3) Fin plate in tension (gross section)

t_p	10 mm
h_p	300 mm
f_{up}	490 mm
$N_{u,3}$	1336,4 kN
N_{Ed}	4852 kN
μ	3,63

4) Fin plate in tension (net section)

d_0	26 mm
$A_{net,p}$	1960 mm ²
$N_{u,4}$	785,8 kN
N_{Ed}	4852 kN
μ	6,17

5) Beam web in bearing

d_0	26 mm		
e_1	- mm	N_{Ed}	4852 kN
e_{2b}	35 mm	V_{Ed}	221 kN
p_1	70 mm	μ	5,09
p_2	70 mm		

Vertical direction

α_b	0,65
k_1	2,07
$F_{y,b,Rd}$	171,9 kN
$N_{u,2,y}$	1375,0 kN

Horizontal direction

α_b	0,45
k_1	2,07
$F_{y,b,Rd}$	119,12 kN
$N_{u,2,y}$	952,95 kN

6) Beam in tension (gross section)

t_w	12 mm
h_w	514 mm
f_u	490 MPa
$N_{u,6}$	2747,6 kN
N_{Ed}	4852 kN
μ	1,77

7) Beam in tension (net section)

d_o	26 mm
$A_{net,p}$	4920 mm ²
$N_{u,7}$	1972,5 kN
N_{Ed}	4852 kN
μ	2,46

8) Supporting member in bending

k_m	1
f_u	490 MPa
t_w	12,5 mm
h_p	300 mm
d_c	261 mm
t_p	10 mm
$N_{u,8}$	433,0 kN
N_{Ed}	4852 kN
μ	11,20

$$N_{u,8} = k_m \cdot f_{u,c} \cdot t_{w,c}^2 \cdot \left[\frac{2 \cdot h_p}{d_c} + 4 \cdot \sqrt{1 - \frac{t_p}{d_c}} \right] / \gamma_{Mu}$$

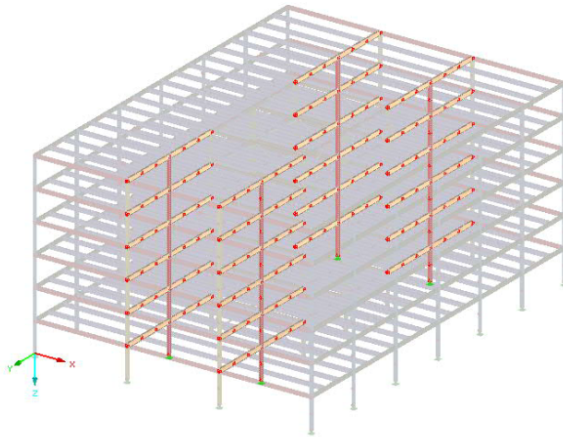
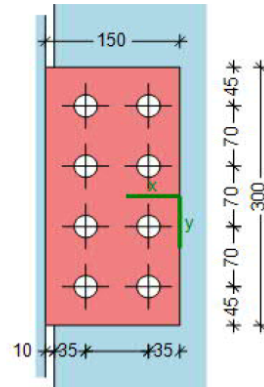
A.3.13 C3w connection verification - numerical approach (scenario1)

Resistance to tying forces

C-3 weak axis (IPE 600 to HEM 300)

Loads	$V_{z,Ad}$	221 kN	(numerical approach)
	N_T	4852 kN	(numerical approach)
safety factor	γ_{Mu}	1,10	
column		HEM 300	
	f_y	355 N/mm ²	h 340 mm
	f_u	490 N/mm ²	b 310 mm
	h_w	208 mm	t_w 21 mm
			t_f 39 mm
beam		IPE 600	
	f_y	355 N/mm ²	h 600 mm
	f_u	490 N/mm ²	b 220 mm
			t_w 12 mm
			t_f 19 mm
		h_w 514 mm	
fin plate	S355		
	f_y	355 N/mm ²	h 300 mm
	f_u	490 N/mm ²	b 150 mm
			t 10 mm
			gap 10 mm
bolts	10.9		
	f_{ub}	1000 N/mm ²	d 24 mm
	α_v	0,5	d_o 26 mm
			A_s 3,53 cm ²
bolt pattern	columns	n_2 2	rows n_1 4
	vertical pitch	p_1 70 mm	hor. Pitch p_2 70 mm
	n Bolts	n 8	vert. edge e_1 45 mm
			hor. edge e_2 35 mm
	weld	a 6 mm	

Component	μ
1) Bolts in shear	3,78
2) Fin plate in bearing	6,11
3) Fin plate in tension (gross section)	3,63
4) Fin plate in tension (net section)	6,17
5) Beam web in bearing	5,09
6) Beam in tension (gross section)	1,77
7) Beam in tension (net section)	2,46
8) Supporting member in bending	3,64
4) Fin plate in tension (net section)	6,17



Notice: Ductility and plastic redistribution allowance already verified with COP

1) Bolts in shear	
A_s	3,53 cm ²
n	8
α_v	0,5
f_{ub}	1000 N/mm ²
$F_{v,Rd}$	160,5 kN
$N_{U,1}$	1283,6 kN
N_{Ed}	4852,0 kN
V_{Ed}	221 kN
F_{Ed}	4857,0 kN
μ	3,78

2) Fin plate in bearing

d_0	26 mm		
e_1	45 mm	N_{Ed}	4852,0 kN
e_2	35 mm	V_{Ed}	221 kN
p_1	70 mm	μ	6,11
p_2	70 mm		

Vertical direction

α_b	0,58
k_1	2,07
$F_{y,b,Rd}$	127,6 kN
$N_{u,2,y}$	1021,0 kN

Horizontal direction

α_b	0,45
k_1	2,07
$F_{y,b,Rd}$	99,3 kN
$N_{u,2,y}$	794,1 kN

3) Fin plate in tension (gross section)

t_p	10 mm
h_p	300 mm
f_{up}	490 mm
$N_{u,3}$	1336,4 kN
N_{Ed}	4852 kN
μ	3,63

4) Fin plate in tension (net section)

d_0	26 mm
$A_{net,p}$	1960 mm ²
$N_{u,4}$	785,8 kN
N_{Ed}	4852 kN
μ	6,17

5) Beam web in bearing

d_0	26 mm		
e_1	- mm	N_{Ed}	4852 kN
e_{2b}	35 mm	V_{Ed}	221 kN
p_1	70 mm	μ	5,09
p_2	70 mm		

Vertical direction

α_b	0,65
k_1	2,07
$F_{y,b,Rd}$	171,9 kN
$N_{u,2,y}$	1375,0 kN

Horizontal direction

α_b	0,45
k_1	2,07
$F_{y,b,Rd}$	119,12 kN
$N_{u,2,y}$	952,95 kN

6) Beam in tension (gross section)

t_w	12 mm
h_w	514 mm
f_u	490 MPa
$N_{u,6}$	2747,6 kN
N_{Ed}	4852 kN
μ	1,77

7) Beam in tension (net section)

d_o	26 mm
$A_{net,p}$	4920 mm ²
$N_{u,7}$	1972,5 kN
N_{Ed}	4852 kN
μ	2,46

8) Supporting member in bending

k_m	1
f_u	490 MPa
t_w	21 mm
h_p	300 mm
d_c	208 mm
t_p	10 mm
$N_{u,8}$	1333,3 kN
N_{Ed}	4852 kN
μ	3,64

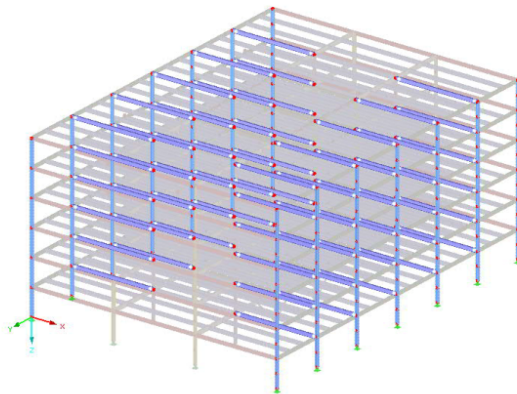
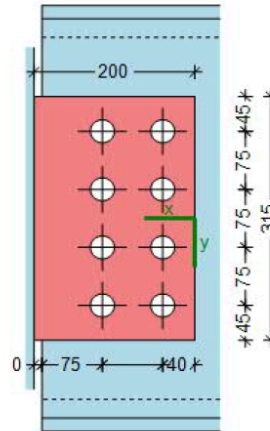
(not relevant as double sided joint config.)

A.3.14 Modified C3w connection verification - numerical approach

Resistance to tying forces		B-1 strong axis (IPE 550 to HEB 340)				
Loads	$V_{z,Ad}$	85 kN	(numerical approach)			
	N_T	1662 kN	(numerical approach)			
safety factor	γ_{Mu}	1,10				
column		HEB 340	h	340 mm		
	f_y	355 N/mm ²	b	300 mm		
	f_u	490 N/mm ²	t_w	12 mm		
			t_f	21,5 mm		
beam		IPE 550	h	550 mm		
	f_y	355 N/mm ²	b	210 mm		
	f_u	490 N/mm ²	t_w	11,1 mm		
			$t_{w,add}$	10 mm		
			t_f	17,2 mm		
			h_w	467 mm		
fin plate	S355	f_y	355 N/mm ²	h	315 mm	
		f_u	490 N/mm ²	b	200 mm	
			t	25 mm		
			gap	10 mm		
bolts	10.9	f_{ub}	1000 N/mm ²	d	27 mm	
		α_v	0,5	d_o	30 mm	
				A_s	4,59 cm ²	
bolt pattern	columns	n_2	2	rows	n_1	4
	vertical pitch	p_1	75 mm	hor. Pitch	p_2	75 mm
	n Bolts	n	8	vert. edge	e_1	45 mm
				hor. edge	e_2	40 mm
weld		a	15 mm			

Component	μ
1) Bolts in shear	1,00
2) Fin plate in bearing	0,86
3) Fin plate in tension (gross section)	0,47
4) Fin plate in tension (net section)	0,85
5) Beam web in bearing	0,78
6) Beam in tension (gross section)	0,38
7) Beam in tension (net section)	0,57
8) Supporting member in bending	0,00

1) Bolts in shear 1,00



Notice: Ductility and plastic redistribution allowance already verified with COP

1) Bolts in shear

A_s	4,59 cm ²
n	8
α_v	0,5
f_{ub}	1000 N/mm ²
$F_{V,Rd}$	208,6 kN
$N_{U,1}$	1669,1 kN
N_{Ed}	1662,0 kN
V_{Ed}	85 kN
F_{Ed}	1664,2 kN
μ	1,00

2) Fin plate in bearing

d_0	30 mm		
e_1	45 mm	N_{Ed}	1662,0 kN
e_2	40 mm	V_{Ed}	85 kN
p_1	75 mm	μ	0,86
p_2	75 mm		

Vertical direction

α_b	0,50
k_1	1,80
$F_{y,b,Rd}$	270,6 kN
$N_{u,2,y}$	2164,9 kN

Horizontal direction

α_b	0,44
k_1	1,80
$F_{y,b,Rd}$	240,5 kN
$N_{u,2,y}$	1924,4 kN

3) Fin plate in tension (gross section)

t_p	25 mm
h_p	315 mm
f_{up}	490 mm
$N_{u,3}$	3508,0 kN
N_{Ed}	1662 kN
μ	0,47

4) Fin plate in tension (net section)

d_0	30 mm
$A_{net,p}$	4875 mm ²
$N_{u,4}$	1954,4 kN
N_{Ed}	1662 kN
μ	0,85

5) Beam web in bearing

d_0	30 mm		
e_1	- mm	N_{Ed}	1662 kN
e_{2b}	75 mm	V_{Ed}	85 kN
p_1	75 mm	μ	0,78
p_2	75 mm		

Vertical direction

α_b	0,58
k_1	1,80
$F_{y,b,Rd}$	266,5 kN
$N_{u,2,y}$	2131,7 kN

Horizontal direction

α_b	0,58
k_1	1,80
$F_{y,b,Rd}$	266,46 kN
$N_{u,2,y}$	2131,71 kN

6) Beam in tension (gross section)

t_w	21,1 mm
h_w	467 mm
f_u	490 mm
$N_{u,6}$	4389,4 kN
N_{Ed}	1662 kN
μ	0,38

7) Beam in tension (net section)

d_0	30 mm
$A_{net,p}$	7321,7 mm ²
$N_{u,7}$	2935,3 kN
N_{Ed}	1662 kN
μ	0,57

8) Supporting member in bending

$N_{u,8}$	∞ kN
-----------	-------------

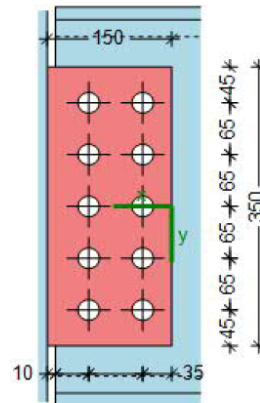
A.3.15 A1s/ A2 connection verification - numerical approach (scenario 2)

Resistance to tying forces

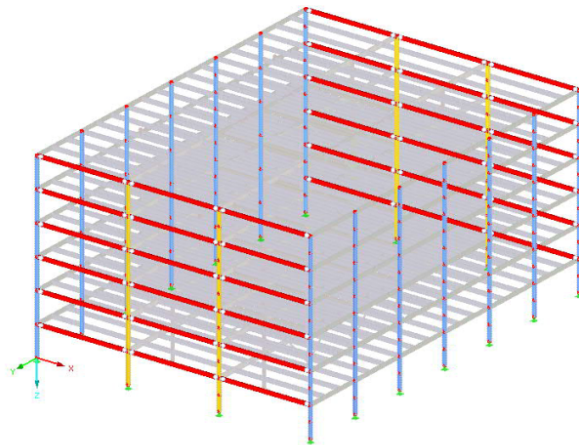
A-1 strong axis (IPE 500 to HEB 340)

Loads	$V_{z,Ad}$	63 kN	(numerical approach)
	N_T	1620 kN	(numerical approach)
safety factor	γ_{Mu}	1,10	
column		HEB 340	
	f_y	355 N/mm ²	h 340 mm
	f_u	490 N/mm ²	b 300 mm
			t_w 12 mm
			t_f 21,5 mm
beam		IPE 500	h 500 mm
	f_y	355 N/mm ²	b 200 mm
	f_u	490 N/mm ²	t_w 10,2 mm
			$t_{w,add}$ 10 mm
			t_f 16 mm
			h_w 426 mm
fin plate	S355		
	f_y	355 N/mm ²	h 350 mm
	f_u	490 N/mm ²	b 150 mm
			t 20 mm
			gap 10 mm
bolts	10.9		
	f_{ub}	1000 N/mm ²	d 24 mm
	α_v	0,5	d_o 26 mm
			A_s 3,53 cm ²
bolt pattern			
columns	n_2	2	rows n_1 5
vertical pitch	p_1	65 mm	hor. Pitch p_2 65 mm
n Bolts	n	10	vert. edge e_1 45 mm
			hor. edge e_2 35 mm
weld	a	12 mm	

Component	μ
1) Bolts in shear	1,01
2) Fin plate in bearing	0,94
3) Fin plate in tension (gross section)	0,52
4) Fin plate in tension (net section)	0,92
5) Beam web in bearing	0,81
6) Beam in tension (gross section)	0,84
7) Beam in tension (net section)	0,68
8) Supporting member in bending	0,00



1) Bolts in shear	1,01
--------------------------	-------------



Notice: Ductility and plastic redistribution allowance already verified with COP

1) Bolts in shear

A_s	3,53 cm ²
n	10
α_v	0,5
f_{ub}	1000 N/mm ²
$F_{v,Rd}$	160,5 kN
$N_{U,1}$	1604,5 kN
N_{Ed}	1620,0 kN
V_{Ed}	63 kN
F_{Ed}	1621,2 kN
μ	1,01

1%-Exceedance in exceptional LCC could be accepted.

2) Fin plate in bearing

d_0	26 mm		
e_1	45 mm	N_{Ed}	1620,0 kN
e_2	35 mm	V_{Ed}	63 kN
p_1	65 mm	μ	0,94
p_2	65 mm		

Vertical direction

α_b	0,58
k_1	1,80
$F_{y,b,Rd}$	222,0 kN
$N_{u,2,y}$	2220,4 kN

Horizontal direction

α_b	0,45
k_1	1,80
$F_{y,b,Rd}$	172,7 kN
$N_{u,2,y}$	1727,0 kN

3) Fin plate in tension (gross section)

t_p	20 mm
h_p	350 mm
f_{up}	490 mm
$N_{u,3}$	3118,2 kN
N_{Ed}	1620 kN
μ	0,52

4) Fin plate in tension (net section)

d_0	26 mm
$A_{net,p}$	4400 mm ²
$N_{u,4}$	1764,0 kN
N_{Ed}	1620 kN
μ	0,92

5) Beam web in bearing

d_0	26 mm		
e_1	- mm	N_{Ed}	1620 kN
e_{2b}	40 mm	V_{Ed}	63 kN
p_1	65 mm	μ	0,81
p_2	65 mm		

Vertical direction

α_b	0,58
k_1	1,80
$F_{y,b,Rd}$	226,8 kN
$N_{u,2,y}$	2267,5 kN

Horizontal direction

α_b	0,51
k_1	1,80
$F_{y,b,Rd}$	199,34 kN
$N_{u,2,y}$	1993,44 kN

6) Beam in tension (gross section)

t_w	10,2 mm
h_w	426 mm
f_u	490 mm
$N_{u,6}$	1935,6 kN
N_{Ed}	1620 kN
μ	0,84

7) Beam in tension (net section)

d_0	26 mm
$A_{net,p}$	5979,2 mm ²
$N_{u,7}$	2397,1 kN
N_{Ed}	1620 kN
μ	0,68

8) Supporting member in bending

$N_{u,8}$	∞ kN
-----------	-------------

A.3.16 Moment verification for connections (analytical approach)

A.3.16.1 Joint B1/B3

Table 4: Component assembly for hogging moment

Global	Beam flange in compression	$F_{BFC,Rd}$	1857 kN	k_7	$+\infty$ mm
	Column web in shear	$F_{CWS,Rd}$	1035 kN	k_1	5,007 mm
	Column web in compression	$F_{CWC,Rd}$	809,9 kN	k_2	9,443 mm
	Compression resistance	$F_{c,Rd}$	809,9 kN		
Bolts	Bolts in tension	$F_{t,Rd}$	254,2 kN	k_{10}	9,614 mm
Bolt row 1	End plate in bending	$F_{EPB,1,Rd}$	375,6 kN	k_5	4,935 mm
	Beam web in tension	$F_{BWT,1,Rd}$	1195 kN	k_8	$+\infty$ mm
	Column web in tension	$F_{CWT,1,Rd}$	888 kN	k_3	5,221 mm
	Column flange in bending	$F_{CFB,1,Rd}$	508,3 kN	k_4	39,72 mm
	Effective tension resistance	$F_{t1,Rd}$	375,6 kN		
	Lever arm	h_1	481,4 mm		
Bolt row 2	End plate in bending	$F_{EPB,2,Rd}$	359,1 kN	k_5	3,932 mm
	Beam web in tension	$F_{BWT,2,Rd}$	1033 kN	k_8	$+\infty$ mm
	Column web in tension	$F_{CWT,2,Rd}$	888 kN	k_3	5,221 mm
	Column flange in bending	$F_{CFB,2,Rd}$	508,3 kN	k_4	39,72 mm
	Effective tension resistance	$F_{t2,Rd}$	278,3 kN		
	Lever arm	h_2	421,4 mm		
Bolt row 3	End plate in bending	$F_{EPB,3,Rd}$	375,6 kN	k_5	7,402 mm
	Beam web in tension	$F_{BWT,3,Rd}$	1195 kN	k_8	$+\infty$ mm
	Column web in tension	$F_{CWT,3,Rd}$	888 kN	k_3	7,037 mm
	Column flange in bending	$F_{CFB,3,Rd}$	508,3 kN	k_4	53,54 mm
	Effective tension resistance	$F_{t3,Rd}$	156 kN		
	Lever arm	h_3	51,4 mm		

The effective tension resistance considers reduction due to bolt group effects, global components and possible lack of ductility (see EN 1993-1-8, 6.2.7.2 (5)-(9)).

Plastic moment resistance

$$M_{pl,Rd} = 306,1 \text{ kNm}$$

Elastic moment resistance

$$M_{el,Rd} = 204,1 \text{ kNm}$$

Initial rotational stiffness

$$S_{j,ini} = 6,987 \cdot 10^4 \text{ kNm/rad}$$

Rotational stiffness

$$S_{j,ini} / \eta = 3,494 \cdot 10^4 \text{ kNm/rad}$$

Table 7: Component assembly for sagging moment

Global	Beam flange in compression	$F_{BFC,Rd}$	1857 kN	k_7	$+\infty$ mm
	Column web in shear	$F_{CWS,Rd}$	1035 kN	k_1	5,259 mm
	Column web in compression	$F_{CWC,Rd}$	809,9 kN	k_2	9,443 mm
	Compression resistance	$F_{c,Rd}$	809,9 kN		
Bolts	Bolts in tension	$F_{t,Rd}$	254,2 kN	k_{10}	9,614 mm
Bolt row 1	End plate in bending	$F_{EPB,1,Rd}$	375,6 kN	k_5	7,402 mm
	Beam web in tension	$F_{BWT,1,Rd}$	1195 kN	k_8	$+\infty$ mm
	Column web in tension	$F_{CWT,1,Rd}$	888 kN	k_3	7,037 mm
	Column flange in bending	$F_{CFB,1,Rd}$	508,3 kN	k_4	53,54 mm
	Effective tension resistance	$F_{t1,Rd}$	375,6 kN		
	Lever arm	h_1	481,4 mm		
Bolt row 2	End plate in bending	$F_{EPB,2,Rd}$	359,1 kN	k_5	3,932 mm
	Beam web in tension	$F_{BWT,2,Rd}$	1033 kN	k_8	$+\infty$ mm
	Column web in tension	$F_{CWT,2,Rd}$	888 kN	k_3	5,221 mm
	Column flange in bending	$F_{CFB,2,Rd}$	508,3 kN	k_4	39,72 mm
	Effective tension resistance	$F_{t2,Rd}$	359,1 kN		
	Lever arm	h_2	111,4 mm		
Bolt row 3	End plate in bending	$F_{EPB,3,Rd}$	375,6 kN	k_5	4,935 mm
	Beam web in tension	$F_{BWT,3,Rd}$	1195 kN	k_8	$+\infty$ mm
	Column web in tension	$F_{CWT,3,Rd}$	888 kN	k_3	5,221 mm
	Column flange in bending	$F_{CFB,3,Rd}$	508,3 kN	k_4	39,72 mm
	Effective tension resistance	$F_{t3,Rd}$	75,24 kN		
	Lever arm	h_3	51,4 mm		

The effective tension resistance considers reduction due to bolt group effects, global components and possible lack of ductility (see EN 1993-1-8, 6.2.7.2 (5)-(9)).

Plastic moment resistance

$$M_{pl,Rd} = 224,7 \text{ kNm}$$

Elastic moment resistance

$$M_{el,Rd} = 149,8 \text{ kNm}$$

Initial rotational stiffness

$$S_{j,ini} = 6,083 \cdot 10^4 \text{ kNm/rad}$$

Rotational stiffness

$$S_{j,ini} / \eta = 3,041 \cdot 10^4 \text{ kNm/rad}$$

A.3.16.2 Joint C2 / C3

2.1.3.1.2.1 Loadcase 2 (Negative)

Table 4: Component assembly for hogging moment

Global	Beam flange in compression	$F_{BFC,Rd}$	2146 kN	k_7	$+\infty$ mm
	Column web in shear	$F_{CWS,Rd}$	1118 kN	k_1	5,282 mm
	Column web in compression	$F_{CWC,Rd}$	863,6 kN	k_2	9,386 mm
	Compression resistance	$F_{c,Rd}$	863,6 kN		
Bolts	Bolts in tension	$F_{t,Rd}$	254,2 kN	k_{10}	9,453 mm
Bolt row 1	End plate in bending	$F_{EPB,1,Rd}$	379,6 kN	k_5	5,387 mm
	Beam web in tension	$F_{BWT,1,Rd}$	1271 kN	k_8	$+\infty$ mm
	Column web in tension	$F_{CWT,1,Rd}$	930,7 kN	k_3	5,047 mm
	Column flange in bending	$F_{CFB,1,Rd}$	508,3 kN	k_4	46,44 mm
	Effective tension resistance	$F_{t1,Rd}$	379,6 kN		
	Lever arm	h_1	530,5 mm		
Bolt row 2	End plate in bending	$F_{EPB,2,Rd}$	362,4 kN	k_5	1,613 mm
	Beam web in tension	$F_{BWT,2,Rd}$	1090 kN	k_8	$+\infty$ mm
	Column web in tension	$F_{CWT,2,Rd}$	930,7 kN	k_3	2,011 mm
	Column flange in bending	$F_{CFB,2,Rd}$	508,3 kN	k_4	18,51 mm
	Effective tension resistance	$F_{t2,Rd}$	282,8 kN		
	Lever arm	h_2	470,5 mm		
Bolt row 3	End plate in bending	$F_{EPB,3,Rd}$	362,4 kN	k_5	1,613 mm
	Beam web in tension	$F_{BWT,3,Rd}$	1090 kN	k_8	$+\infty$ mm
	Column web in tension	$F_{CWT,3,Rd}$	930,7 kN	k_3	2,011 mm
	Column flange in bending	$F_{CFB,3,Rd}$	508,3 kN	k_4	18,51 mm
	Effective tension resistance	$F_{t3,Rd}$	194,1 kN		
	Lever arm	h_3	410,5 mm		
Bolt row 4	End plate in bending	$F_{EPB,4,Rd}$	362,4 kN	k_5	4,246 mm
	Beam web in tension	$F_{BWT,4,Rd}$	1090 kN	k_8	$+\infty$ mm
	Column web in tension	$F_{CWT,4,Rd}$	930,7 kN	k_3	5,047 mm
	Column flange in bending	$F_{CFB,4,Rd}$	508,3 kN	k_4	46,44 mm
	Effective tension resistance	$F_{t4,Rd}$	7,093 kN		
	Lever arm	h_4	350,5 mm		
Bolt row 5	End plate in bending	$F_{EPB,5,Rd}$	379,6 kN	k_5	8,02 mm
	Beam web in tension	$F_{BWT,5,Rd}$	1271 kN	k_8	$+\infty$ mm
	Column web in tension	$F_{CWT,5,Rd}$	930,7 kN	k_3	6,772 mm
	Column flange in bending	$F_{CFB,5,Rd}$	508,3 kN	k_4	62,32 mm
	Effective tension resistance	$F_{t5,Rd}$	0 kN		
<i>Continuation on next page...</i>					
	Lever arm	h_5	50,5 mm		

The effective tension resistance considers reduction due to bolt group effects, global components and possible lack of ductility (see EN 1993-1-8, 6.2.7.2 (5)-(9)).

Plastic moment resistance

$$M_{pl,Rd} = 416,6 \text{ kNm}$$

Elastic moment resistance

$$M_{el,Rd} = 277,7 \text{ kNm}$$

Initial rotational stiffness

$$S_{j,ini} = 8,462 \cdot 10^4 \text{ kNm/rad}$$

Rotational stiffness

$$S_{j,ini} / \eta = 4,231 \cdot 10^4 \text{ kNm/rad}$$

2.1.3.3.2.1 Loadcase 1 (Default loadcase)

Table 6: Component assembly for sagging moment

Global	Beam flange in compression	$F_{BFC,Rd}$	2146 kN	k_7	$+\infty$ mm
	Column web in shear	$F_{CWS,Rd}$	1118 kN	k_1	5,649 mm
	Column web in compression	$F_{CWC,Rd}$	863,6 kN	k_2	9,386 mm
	Compression resistance	$F_{c,Rd}$	863,6 kN		
Bolts	Bolts in tension	$F_{t,Rd}$	254,2 kN	k_{10}	9,453 mm
Bolt row 1	End plate in bending	$F_{EPB,1,Rd}$	379,6 kN	k_5	8,02 mm
	Beam web in tension	$F_{BWT,1,Rd}$	1271 kN	k_8	$+\infty$ mm
	Column web in tension	$F_{CWT,1,Rd}$	930,7 kN	k_3	6,772 mm
	Column flange in bending	$F_{CFB,1,Rd}$	508,3 kN	k_4	62,32 mm
	Effective tension resistance	$F_{t1,Rd}$	379,6 kN		
	Lever arm	h_1	530,5 mm		
Bolt row 2	End plate in bending	$F_{EPB,2,Rd}$	362,4 kN	k_5	4,246 mm
	Beam web in tension	$F_{BWT,2,Rd}$	1090 kN	k_8	$+\infty$ mm
	Column web in tension	$F_{CWT,2,Rd}$	930,7 kN	k_3	5,047 mm
	Column flange in bending	$F_{CFB,2,Rd}$	508,3 kN	k_4	46,44 mm
	Effective tension resistance	$F_{t2,Rd}$	362,4 kN		
	Lever arm	h_2	230,5 mm		
Bolt row 3	End plate in bending	$F_{EPB,3,Rd}$	362,4 kN	k_5	1,613 mm
	Beam web in tension	$F_{BWT,3,Rd}$	1090 kN	k_8	$+\infty$ mm
	Column web in tension	$F_{CWT,3,Rd}$	930,7 kN	k_3	2,011 mm
	Column flange in bending	$F_{CFB,3,Rd}$	508,3 kN	k_4	18,51 mm
	Effective tension resistance	$F_{t3,Rd}$	121,6 kN		
	Lever arm	h_3	170,5 mm		
Bolt row 4	End plate in bending	$F_{EPB,4,Rd}$	362,4 kN	k_5	1,613 mm
	Beam web in tension	$F_{BWT,4,Rd}$	1090 kN	k_8	$+\infty$ mm
	Column web in tension	$F_{CWT,4,Rd}$	930,7 kN	k_3	2,011 mm
	Column flange in bending	$F_{CFB,4,Rd}$	508,3 kN	k_4	18,51 mm
	Effective tension resistance	$F_{t4,Rd}$	0 kN		
	Lever arm	h_4	110,5 mm		
Bolt row 5	End plate in bending	$F_{EPB,5,Rd}$	379,6 kN	k_5	5,387 mm
	Beam web in tension	$F_{BWT,5,Rd}$	1271 kN	k_8	$+\infty$ mm
	Column web in tension	$F_{CWT,5,Rd}$	930,7 kN	k_3	5,047 mm
	Column flange in bending	$F_{CFB,5,Rd}$	508,3 kN	k_4	46,44 mm
	Effective tension resistance	$F_{t5,Rd}$	0 kN		

Continuation on next page...

Table 6: Component assembly for sagging moment

	Lever arm	h_5	50,5 mm	
--	-----------	-------	---------	--

The effective tension resistance considers reduction due to bolt group effects, global components and possible lack of ductility (see EN 1993-1-8, 6.2.7.2 (5)-(9)).

Plastic moment resistance

$$M_{pl,Rd} = 305,6 \text{ kNm}$$

Elastic moment resistance

$$M_{el,Rd} = 203,8 \text{ kNm}$$

Initial rotational stiffness

$$S_{j,ini} = 7,269 \cdot 10^4 \text{ kNm/rad}$$

Rotational stiffness

$$S_{j,ini} / \eta = 3,635 \cdot 10^4 \text{ kNm/rad}$$

A.3.1 Moment verification for redesigned connections (analytical approach)

A.3.1.1 Joint B1/B3:

Table 5: Component assembly for hogging moment

Global	Beam flange in compression	$F_{BFC,Rd}$	1857 kN	k_7	$+\infty$ mm
	Column web in shear	$F_{CWS,Rd}$	1095 kN	k_1	4,983 mm
	Column web in compression	$F_{CWC,Rd}$	$+\infty$ kN	k_2	$+\infty$ mm
	Compression resistance	$F_{c,Rd}$	1095 kN		
Bolts	Bolts in tension	$F_{t,Rd}$	254,2 kN	k_{10}	8,86 mm
Bolt row 1	End plate in bending	$F_{EPB,1,Rd}$	471,4 kN	k_5	11,82 mm
	Beam web in tension	$F_{BWT,1,Rd}$	1204 kN	k_8	$+\infty$ mm
	Column web in tension	$F_{CWT,1,Rd}$	946,2 kN	k_3	5,593 mm
	Column flange in bending	$F_{CFB,1,Rd}$	508,3 kN	k_4	42,55 mm
	Effective tension resistance	$F_{t1,Rd}$	471,4 kN		
	Lever arm	h_1	481,4 mm		
Bolt row 2	End plate in bending	$F_{EPB,2,Rd}$	440,7 kN	k_5	9,321 mm
	Beam web in tension	$F_{BWT,2,Rd}$	1033 kN	k_8	$+\infty$ mm
	Column web in tension	$F_{CWT,2,Rd}$	888 kN	k_3	5,221 mm
	Column flange in bending	$F_{CFB,2,Rd}$	508,3 kN	k_4	39,72 mm
	Effective tension resistance	$F_{t2,Rd}$	297 kN		
	Lever arm	h_2	421,4 mm		
Bolt row 3	End plate in bending	$F_{EPB,3,Rd}$	471,4 kN	k_5	17,67 mm
	Beam web in tension	$F_{BWT,3,Rd}$	1204 kN	k_8	$+\infty$ mm
	Column web in tension	$F_{CWT,3,Rd}$	946,2 kN	k_3	7,037 mm
	Column flange in bending	$F_{CFB,3,Rd}$	508,3 kN	k_4	53,54 mm
	Effective tension resistance	$F_{t3,Rd}$	326,6 kN		
	Lever arm	h_3	51,4 mm		

The effective tension resistance considers reduction due to bolt group effects, global components and possible lack of ductility (see EN 1993-1-8, 6.2.7.2 (5)-(9)).

Plastic moment resistance

$$M_{pl,Rd} = 368,9 \text{ kNm}$$

Elastic moment resistance

$$M_{el,Rd} = 245,9 \text{ kNm}$$

Initial rotational stiffness

$$S_{j,ini} = 9,987 \cdot 10^4 \text{ kNm/rad}$$

Rotational stiffness

$$S_{j,ini} / \eta = 4,993 \cdot 10^4 \text{ kNm/rad}$$

2.1.3.3.2 Moment resistance / stiffness

2.1.3.3.2.1 Loadcase 2 (Negative)

Table 8: Component assembly for sagging moment

Global	Beam flange in compression	$F_{BFC,Rd}$	1857 kN	k_7	$+\infty$ mm
	Column web in shear	$F_{CWS,Rd}$	1095 kN	k_1	5,327 mm
	Column web in compression	$F_{CWC,Rd}$	$+\infty$ kN	k_2	$+\infty$ mm
	Compression resistance	$F_{c,Rd}$	1095 kN		
Bolts	Bolts in tension	$F_{t,Rd}$	254,2 kN	k_{10}	8,86 mm
Bolt row 1	End plate in bending	$F_{EPB,1,Rd}$	471,4 kN	k_5	17,67 mm
	Beam web in tension	$F_{BWT,1,Rd}$	1204 kN	k_8	$+\infty$ mm
	Column web in tension	$F_{CWT,1,Rd}$	946,2 kN	k_3	7,037 mm
	Column flange in bending	$F_{CFB,1,Rd}$	508,3 kN	k_4	53,54 mm
	Effective tension resistance	$F_{t1,Rd}$	471,4 kN		
	Lever arm	h_1	481,4 mm		
Bolt row 2	End plate in bending	$F_{EPB,2,Rd}$	440,7 kN	k_5	9,321 mm
	Beam web in tension	$F_{BWT,2,Rd}$	1033 kN	k_8	$+\infty$ mm
	Column web in tension	$F_{CWT,2,Rd}$	888 kN	k_3	5,221 mm
	Column flange in bending	$F_{CFB,2,Rd}$	508,3 kN	k_4	39,72 mm
	Effective tension resistance	$F_{t2,Rd}$	440,7 kN		
	Lever arm	h_2	111,4 mm		
Bolt row 3	End plate in bending	$F_{EPB,3,Rd}$	471,4 kN	k_5	11,82 mm
	Beam web in tension	$F_{BWT,3,Rd}$	1204 kN	k_8	$+\infty$ mm
	Column web in tension	$F_{CWT,3,Rd}$	946,2 kN	k_3	5,593 mm
	Column flange in bending	$F_{CFB,3,Rd}$	508,3 kN	k_4	42,55 mm
	Effective tension resistance	$F_{t3,Rd}$	183 kN		
	Lever arm	h_3	51,4 mm		

The effective tension resistance considers reduction due to bolt group effects, global components and possible lack of ductility (see EN 1993-1-8, 6.2.7.2 (5)-(9)).

Plastic moment resistance

$$M_{pl,Rd} = 285,4 \text{ kNm}$$

Elastic moment resistance

$$M_{el,Rd} = 190,3 \text{ kNm}$$

Initial rotational stiffness

$$S_{j,ini} = 8,301 \cdot 10^4 \text{ kNm/rad}$$

Rotational stiffness

$$S_{j,ini} / \eta = 4,15 \cdot 10^4 \text{ kNm/rad}$$

A.3.1.2 Joint C2/C3:

2.1.3.1.2.2 Loadcase 3 (Positive)

Table 5: Component assembly for hogging moment

Global	Beam flange in compression	$F_{BFC,Rd}$	2146 kN	k_7	$+\infty$ mm
	Column web in shear	$F_{CWS,Rd}$	1783 kN	k_1	9,461 mm
	Column web in compression	$F_{CWC,Rd}$	$+\infty$ kN	k_2	$+\infty$ mm
	Compression resistance	$F_{c,Rd}$	1783 kN		
Bolts	Bolts in tension	F_{LRd}	330,5 kN	k_{10}	11,68 mm
Bolt row 1	End plate in bending	$F_{EPB,1,Rd}$	430,2 kN	k_5	4,434 mm
	Beam web in tension	$F_{BWT,1,Rd}$	1164 kN	k_8	$+\infty$ mm
	Column web in tension	$F_{CWT,1,Rd}$	1451 kN	k_3	8,939 mm
	Column flange in bending	$F_{CFB,1,Rd}$	657,4 kN	k_4	43,81 mm
	Effective tension resistance	$F_{t1,Rd}$	430,2 kN		
	Lever arm	h_1	490,5 mm		
Bolt row 2	End plate in bending	$F_{EPB,2,Rd}$	425,9 kN	k_5	2,311 mm
	Beam web in tension	$F_{BWT,2,Rd}$	1119 kN	k_8	$+\infty$ mm
	Column web in tension	$F_{CWT,2,Rd}$	1435 kN	k_3	5,029 mm
	Column flange in bending	$F_{CFB,2,Rd}$	653 kN	k_4	24,64 mm
	Effective tension resistance	$F_{t2,Rd}$	317,3 kN		
	Lever arm	h_2	390,5 mm		
Bolt row 3	End plate in bending	$F_{EPB,3,Rd}$	425,9 kN	k_5	2,311 mm
	Beam web in tension	$F_{BWT,3,Rd}$	1119 kN	k_8	$+\infty$ mm
	Column web in tension	$F_{CWT,3,Rd}$	1435 kN	k_3	5,029 mm
	Column flange in bending	$F_{CFB,3,Rd}$	653 kN	k_4	24,64 mm
	Effective tension resistance	$F_{t3,Rd}$	200,3 kN		
	Lever arm	h_3	290,5 mm		
Bolt row 4	End plate in bending	$F_{EPB,4,Rd}$	425,9 kN	k_5	2,311 mm
	Beam web in tension	$F_{BWT,4,Rd}$	1119 kN	k_8	$+\infty$ mm
	Column web in tension	$F_{CWT,4,Rd}$	1435 kN	k_3	5,029 mm
	Column flange in bending	$F_{CFB,4,Rd}$	653 kN	k_4	24,64 mm
	Effective tension resistance	$F_{t4,Rd}$	200,3 kN		
	Lever arm	h_4	190,5 mm		
Bolt row 5	End plate in bending	$F_{EPB,5,Rd}$	430,2 kN	k_5	4,434 mm
	Beam web in tension	$F_{BWT,5,Rd}$	1164 kN	k_8	$+\infty$ mm
	Column web in tension	$F_{CWT,5,Rd}$	1451 kN	k_3	8,939 mm
	Column flange in bending	$F_{CFB,5,Rd}$	657,4 kN	k_4	43,81 mm
	Effective tension resistance	$F_{t5,Rd}$	221,3 kN		
	Lever arm	h_5	90,5 mm		

The effective tension resistance considers reduction due to bolt group effects, global components and possible lack of ductility (see EN 1993-1-8, 6.2.7.2 (5)-(9)).

Plastic moment resistance

$$M_{pl,Rd} = 451,3 \text{ kNm}$$

Elastic moment resistance

$$M_{el,Rd} = 300,8 \text{ kNm}$$

Initial rotational stiffness

$$S_{j,ini} = 1,14 \cdot 10^5 \text{ kNm/rad}$$

Rotational stiffness

$$S_{j,ini} / \eta = 5,698 \cdot 10^4 \text{ kNm/rad}$$

2.1.3.3.2 Moment resistance / stiffness

2.1.3.3.2.1 Loadcase 2 (Negative)

Table 8: Component assembly for sagging moment

Global	Beam flange in compression	$F_{BFC,Rd}$	2146 kN	k_7	$+\infty$ mm
	Column web in shear	$F_{CWS,Rd}$	1783 kN	k_1	9,461 mm
	Column web in compression	$F_{CWC,Rd}$	$+\infty$ kN	k_2	$+\infty$ mm
	Compression resistance	$F_{c,Rd}$	1783 kN		
Bolts	Bolts in tension	$F_{t,Rd}$	330,5 kN	k_{10}	11,68 mm
Bolt row 1	End plate in bending	$F_{EPB,1,Rd}$	430,2 kN	k_5	4,434 mm
	Beam web in tension	$F_{BWT,1,Rd}$	1164 kN	k_8	$+\infty$ mm
	Column web in tension	$F_{CWT,1,Rd}$	1451 kN	k_3	8,939 mm
	Column flange in bending	$F_{CFB,1,Rd}$	657,4 kN	k_4	43,81 mm
	Effective tension resistance	$F_{t,1,Rd}$	430,2 kN		
	Lever arm	h_1	490,5 mm		
Bolt row 2	End plate in bending	$F_{EPB,2,Rd}$	425,9 kN	k_5	2,311 mm
	Beam web in tension	$F_{BWT,2,Rd}$	1119 kN	k_8	$+\infty$ mm
	Column web in tension	$F_{CWT,2,Rd}$	1435 kN	k_3	5,029 mm
	Column flange in bending	$F_{CFB,2,Rd}$	653 kN	k_4	24,64 mm
	Effective tension resistance	$F_{t,2,Rd}$	317,3 kN		
	Lever arm	h_2	390,5 mm		
Bolt row 3	End plate in bending	$F_{EPB,3,Rd}$	425,9 kN	k_5	2,311 mm
	Beam web in tension	$F_{BWT,3,Rd}$	1119 kN	k_8	$+\infty$ mm
	Column web in tension	$F_{CWT,3,Rd}$	1435 kN	k_3	5,029 mm
	Column flange in bending	$F_{CFB,3,Rd}$	653 kN	k_4	24,64 mm
	Effective tension resistance	$F_{t,3,Rd}$	200,3 kN		
	Lever arm	h_3	290,5 mm		
Bolt row 4	End plate in bending	$F_{EPB,4,Rd}$	425,9 kN	k_5	2,311 mm
	Beam web in tension	$F_{BWT,4,Rd}$	1119 kN	k_8	$+\infty$ mm
	Column web in tension	$F_{CWT,4,Rd}$	1435 kN	k_3	5,029 mm
	Column flange in bending	$F_{CFB,4,Rd}$	653 kN	k_4	24,64 mm
	Effective tension resistance	$F_{t,4,Rd}$	200,3 kN		
	Lever arm	h_4	190,5 mm		
Bolt row 5	End plate in bending	$F_{EPB,5,Rd}$	430,2 kN	k_5	4,434 mm
	Beam web in tension	$F_{BWT,5,Rd}$	1164 kN	k_8	$+\infty$ mm
	Column web in tension	$F_{CWT,5,Rd}$	1451 kN	k_3	8,939 mm
	Column flange in bending	$F_{CFB,5,Rd}$	657,4 kN	k_4	43,81 mm
	Effective tension resistance	$F_{t,5,Rd}$	221,3 kN		

Continuation on next page...

	Lever arm	h_5	90,5 mm		
--	-----------	-------	---------	--	--

The effective tension resistance considers reduction due to bolt group effects, global components and possible lack of ductility (see EN 1993-1-8, 6.2.7.2 (5)-(9)).

Plastic moment resistance

$$M_{pl,Rd} = 451,3 \text{ kNm}$$

Elastic moment resistance

$$M_{el,Rd} = 300,8 \text{ kNm}$$

Initial rotational stiffness

$$S_{j,ini} = 1,14 \cdot 10^5 \text{ kNm/rad}$$

Rotational stiffness

$$S_{j,ini} / \eta = 5,698 \cdot 10^4 \text{ kNm/rad}$$

References

- Applied Science International. 2021. "Extreme Loading for Structures Theoretical Manual, Version 8."
- Biggs, John M. 1964. *Introduction to Structural Dynamics*. McGraw-Hill College.
- Bjerketvedt, Dag, Jan Roar Bakke, and Kees van Wingerden. 1997. "Gas Explosion Handbook." *Journal of Hazardous Materials, Gas Explosions Handbook*, 52 (1): 1–150. [https://doi.org/10.1016/S0304-3894\(97\)81620-2](https://doi.org/10.1016/S0304-3894(97)81620-2).
- Brasseur, M., R. Zaharia, R. Obiala, J. M. Franssen, F. Hanus, B. Zhao, D. Pintea, et al. 2017. *Temperature Assessment of a Vertical Steel Member Subjected to Localised Fire (LOCAFI)*. LU: Publications Office of the European Union. <https://data.europa.eu/doi/10.2777/67601>.
- CEB. 1988. "Concrete Structures under Impact and Impulsive Loading (CEB-Bulletin d'information, NO. 187)." *Dubrovnik (Croatia): Comité Euro-International Du Beton*.
- CSA S850. 2012. *Design And Assessment Of Buildings Subjected To Blast Loads*.
- Dinu, Florea, Ioan Marginean, Dan Dubina, Ahmed Khalil, and Emiliano De Iuliis. 2018. "Factors Affecting the Response of Steel Columns to Close-in Detonations." In , 873–80. Editorial Universitat Politècnica de València.
- Dinu, Florea, Ioan Marginean, Dan Dubina, Ioan Petran, Mircea Pastrav, Andreea Sigauan, and Adrian Ciutina. 2016. "Experimental Testing of 3D Steel Frame with Composite Beams under Column Loss." In *The International Colloquium on Stability and Ductility of Steel Structures*, 691–98. ECCS – European Convention for Constructional Steelwork.
- DoD. 2008. "UFC 3-340-02: Unified Facilities Criteria: Structures to Resist the Effects of Accidental Explosions." Washington (DC), US: United States Department of Defense.
- DoD. 2014. "UFC 3-340-02: Unified Facilities Criteria: Structures to Resist the Effects of Accidental Explosions (2008)- with Change 2." Washington (DC), US: United States Department of Defense.
- Dubina, Dan, Ioan Marginean, and Florea Dinu. 2019. "Impact Modelling for Progressive Collapse Assessment of Selective Rack Systems." *Thin-Walled Structures* 143 (October): 106201. <https://doi.org/10.1016/j.tws.2019.106201>.
- ECCS TC 10. 2009. *European Recommendations for the Design of Simple Joints in Steel Structures*. European Convention for Constructional Steelwork 126. Brussels: ECCS.
- EN 1991-1-7. 2006. *Eurocode 1 - Actions on Structures - Part 1-7: General Actions - Accidental Actions*. Brussels: European Committee for Standardisation.
- Izzuddin, B. A., A. G. Vlassis, A. Y. Elghazouli, and D. A. Nethercot. 2008. "Progressive Collapse of Multi-Storey Buildings Due to Sudden Column Loss — Part I: Simplified Assessment Framework." *Engineering Structures* 30 (5): 1308–18. <https://doi.org/10.1016/j.engstruct.2007.07.011>.
- Landolfo, Raffaele, Mario D'Aniello, Silvia Costanzo, Roberto Tartaglia, Jean-François Demonceau, Jean-Pierre Jaspard, Aurel Stratan, et al. 2018. "Equaljoints PLUS Volume with Information Brochures for 4 Seismically Qualified Joints," 124.
- RFCS. 2017. *INNOSEIS Valorization of Innovative Anti-Seismic Devices*.
- Tagel-Din, Hatem, and Kimiro Meguro. 2000. "Applied Element Method for Simulation of Nonlinear Materials: Theory and Application for RC Structures." *Structural Eng./Earthquake Eng., JSCE* 17 (2).
- Vermeulen, Maxime. 2021. "Robustness of Steel Structures - Study of the Applicability of Innovative Methods on Real Structures." MSc, Université de Liège. <https://matheo.uliege.be/handle/2268.2/11550>.